RECEPTOR MODELLING STUDIES OF AIRBORNE PARTICULATE MATTER IN THE UNITED KINGDOM AND INDIA

by

PALLAVI PANT

Submitted to the University of Birmingham in partial fulfilment for the degree of Doctor of Philosophy

Division of Environmental Health and Risk Management
School of Geography, Earth and Environmental Studies
College of Life and Environmental Sciences
University of Birmingham
Edgbaston, Birmingham
B15 2TT
United Kingdom

September 2014

ABSTRACT

Research described in this thesis was conducted in the United Kingdom and India, and although the overall subject was source apportionment of traffic emissions, specific objectives as well as research design were different in each case. In the UK, composite $PM_{2.5}$ traffic profiles were derived from ambient measurement data (London and Birmingham), and sensitivity of a chemical mass balance (CMB) model to various traffic profiles was tested. In New Delhi (India), ambient $PM_{2.5}$ samples were collected at a high-traffic location and characterized for a suite of elemental and organic markers. PM_{10} road dust was characterized in Birmingham and New Delhi, and detailed chemical source profiles were prepared for both cities.

Two composite $PM_{2.5}$ traffic profiles determined in the UK were found to be similar, although lower uncertainties were observed for a tunnel profile compared to a twin-site profile. This has important implications in future attempts at preparation of source profiles using ambient data, as higher profile uncertainties can introduce error in the receptor models. Upon testing with a CMB model, the UK-based, the composite $PM_{2.5}$ traffic profile was found to quantify the traffic contribution consistently, and independent estimates of traffic contribution were found to correlate well with the CMB output.

PM_{10} road dust loadings ($\mu g/m^2$) were found to be higher in New Delhi while the concentrations for individual species ($\mu g/g$) such as Cu, Zn and Sn were higher at a traffic tunnel in Birmingham. Crustal material was found to be the biggest contributor to the road dust in both cities while brake wear emissions were found to vary based on site type. A trimodal mass size distribution was obtained for a heavy traffic site in New Delhi with a majority of the PM mass in the fine range. Individual element size distributions were observed to vary, but crustal-associated elements were unimodal with peaks in the coarse range, while other elements such as Cu and Zn had dominant peaks in the fine range. Concentrations and size distributions of prevalent non-exhaust tracers (i.e. Cu, Sb, Ba) in ambient $PM_{2.5}$ and PM_{10} road dust indicated that these elements might not be reliable tracers for brake wear emissions in India.

Ambient $PM_{2.5}$ concentrations in New Delhi were found to exceed the air quality standards on several occasions, especially in the winter. Winter concentrations of individual tracer species were much higher, particularly for some PAHs and trace metals. Crustal material was found to be an important source in the summer, while wood burning, nitrate and chloride were found to be major source contributors in winter. The contribution of traffic emissions varied between 15-25% depending on the season.

ACKNOWLEDGEMENTS

The last four years at Birmingham have been an excellent learning experience, and it would not have been the same without the guidance and encouragement of my supervisor, Professor Roy M. Harrison. Thanks are also due to Dr. Jianxin Yin, Dr. Johanna Gietl and Dr. Zongbo Shi for the support in the laboratories and Dr. Juana Maria Delgado-Saborit for her words of encouragement. I am also indebted to Professor Judith C. Chow, Professor John G. Watson and Mr. Steve Kohl from DRI (USA), Dr. Anuradha Shukla, CRRI (India) and Dr. Sarath Guttikunda, IIT-Delhi (India)/DRI (USA) for their advice and suggestions.

This journey would not have been as fun without the company of wonderful friends in Birmingham, particularly Massimiliano Mascelloni, Barbara Macias Hernandez, Ian Keyte, Paul Sanderson and Chris Stark and in India, Rosy Nameirakpam. Thanks to the lunch group on 4th floor- I'll miss our wide-ranging discussions and rants about culture and history! Indrani, Pranav and Shipra- thanks for helping me build a home away from home. Jina- your constant motivation was a big help, and who knows, I'll even get fluent in Mandarin one day. To all others in PH and GEES, thank you for the fun times.

Many thanks to Jamie Peart, Richard Johnson and Eimear Orgill for all the help and support in organizing field visits, and conducting laboratory analysis; and to Mary Harding for advice and support on administrative matters. Thanks are also due to Dr. Stephen J. Baker for help in elemental analysis.

I would also like to acknowledge the scholarship support from the University of Birmingham and research grants from Rees Jeffreys Road Fund, UKIERI and Simon Wolff Charitable Foundation. Special thanks to AAAR, RSC and EAC for travel grants. Thanks to Amey (UK), particularly Paul Lees and CRRI (India) field staff for logistical support.

Most of all, I would like to thank my parents, Aruna and Harish Pant, my sister, Kanika and the rest of my family who were a constant source of support from several thousand miles away.

TABLE OF CONTENTS

LIST OF FIGURES

LIST OF TABLES

ABBREVIATIONS

AURN	Automatic Rural and Urban Network
BDL	Below Detection Limit
BROS	Bristol Road Observatory Site
CCN	Cloud Condensation Nuclei
CMB	Chemical Mass Balance
CNG	Compressed Natural Gas
COD	Coefficient of Divergence
COPREM	Constrained Physical Receptor Model
CPCB	Central Pollution Control Board
CPI	Carbon Preference Index
CRRI	Central Road Research Institute
DCM	Dichloromethane
DDW	Distilled Deionised Water
DPCC	Delhi Pollution Control Committee
DPF	Diesel Particulate Filter
DR	Diagnostic Ratio
DRI	Desert Research Institute
EC	Elemental Carbon
ED-XRF	Energy Dispersive X-Ray Fluorescence
EF	Enrichment Factor
EF	Emission Factor
EROS	Elms Road Observatory Site
EU	European Union
EUSAAR	European Supersites for Atmospheric Aerosol Research
FID	Flame Ionization Detector
GBD	Global Burden of Disease
GC-MS	Gas Chromatography-Mass Spectrometry
HCl	Hydrochloric Acid

HF	Hydrofluoric Acid
HDV	Heavy Duty Vehicle
IARC	International Agency for Research on Cancer
IC	Ion Chromatography
ICP-MS	Inductively Coupled Plasma Mass Spectrometry
IIT	Indian Institute of Technology
IITM	Indian Institute of Tropical Meteorology
IMPROVE	Interagency Monitoring of Protected Visual Environments
LDPE	Low Density Polyethylene
LDV	Light Duty Vehicle
LoD	Limit of Detection
LPG	Liquefied Petroleum Gas
LPM	Liters per Minute
ME	Multilinear Engine
MLR	Multi Linear Regression
MOUDI	Micro Orifice Uniform Deposition Impactor
MPIN	Modifed Pseudo-Inverse Normalized Matrix
NAAQS	National Ambient Air Quality Standards
NAO	Non Asbestos Organic
OC	Organic Carbon
OM	Organic Matter
PAH	Polycyclic Aromatic Hydrocarbon
PC	Pyrolytic Carbon
PCA	Principal Component Analysis
PFTBA	Perfluorotributylamine
PM	Particulate Matter
PMF	Positive Matrix Factorization
POC	Primary Organic Carbon
PSD	Particle Size Distribution
PTFE	Polytetrafluoroethylene
QT	Queensway Tunnel

QA/QC	Quality Assurance/ Quality Control
RAR	Reverse Aqua Regia
RD	Road Dust
RH	Relative Humidity
RM	Receptor Model
RMA	Reduced Major Axis
ROS	Reactive Oxygen Species
SA	Source Apportionment
SCE	Source Contribution Estimate
SD	Standard Deviation
SEM	Scanning Electron Microscope
SIM	Selective Ion Monitoring
SOC	Secondary Organic Carbon
SPM	Suspended Particulate Matter
TC	Total Carbon
TD-GC-MS	Thermo Desorption Gas Chromatography-Mass Spectrometry
TSP	Total Suspended Particulate
TTFA	Target Transformation Factor Analysis
TWP	Tyre Wear Particle
UCC	Upper Continental Crust
UCM	Unresolved Complex Mixture
UFP	Ultrafine Particle
UHP	Ultra High Purity
UoB	University of Birmingham
USEPA	United States Environment Protection Agency
VOC	Volatile Organic Compound
WD-XRF	Wavelength Dispersive X-Ray Fluorescence
WSOC	Water Soluble Organic Carbon

CHAPTER 1- INTRODUCTION

This chapter presents an overview of particulate matter, its sources and impacts with a focus on traffic-related PM.

This chapter is adapted from the following review articles:

[1] Pant, P. and Harrison, R.M. (2012) Critical review of receptor modelling for particulate matter: A case study of India. **Atmospheric Environment**, 49: 1-12.

[2] Pant, P. and Harrison, R.M. (2013) Estimation of the contribution of road traffic emissions to particulate matter concentrations from field measurements: A review. **Atmospheric Environment**, 77: 78-97.

Graphical Abstract

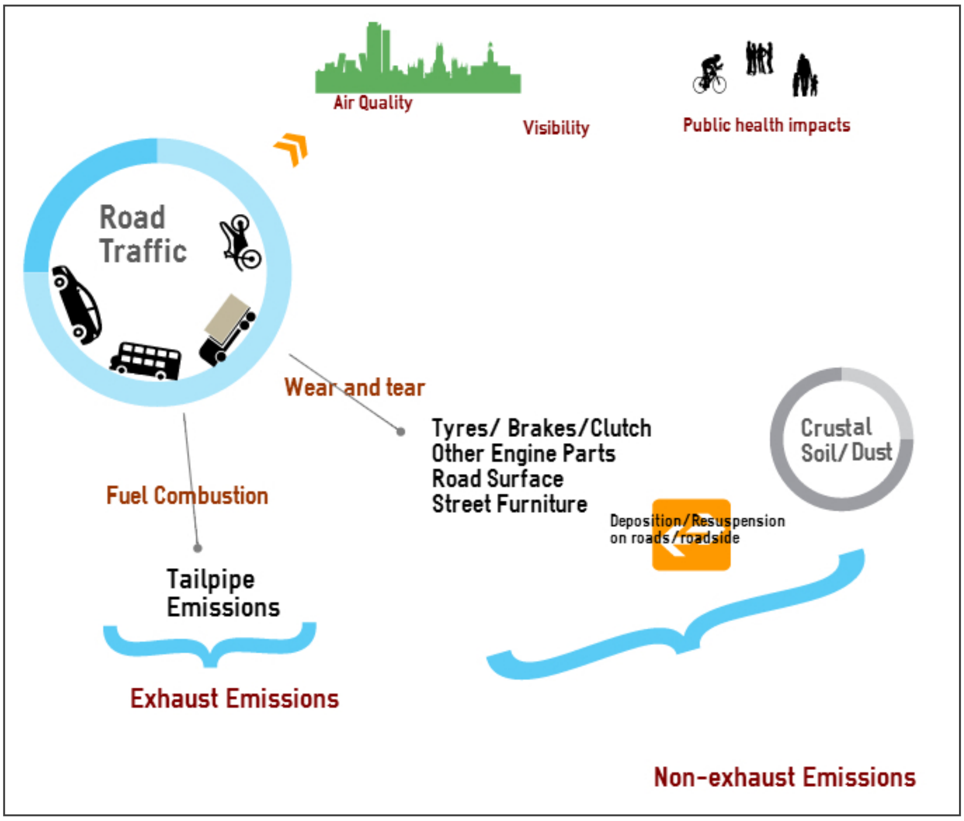

1.1 Background

Urban air quality features among the major environmental concerns in cities around the globe. A recent Global Burden of Disease (GBD) study reported air pollution to have caused 3.1 million deaths worldwide in 2010 (Lim et al., 2012). Particulate matter (PM), a group 1 carcinogen (Loomis et al., 2013), is one of the key pollutants found in the ambient air, and despite stringent pollution control programs, cities across the world often exceed the local and/or national air quality standards.

PM is defined as

> "*any non-gaseous (liquid or solid) material which, owing to its small gravitational settling rate, remains suspended in the atmosphere for appreciable time periods*" (NARSTO, 2004) and;
>
> "*can include solid particles or liquid droplets*" (Hinds, 1982).

It is generated by a range of natural (pollen and spores, crustal/mineralogical dust, sea spray, forest fires, volcanic ash, biogenic volatile organic compound (VOC) emissions) and anthropogenic sources (fossil fuel combustion, industrial and agricultural processes, biomass/wood combustion, waste incineration, construction). In addition, PM can be generated due to chemical reactions between gaseous species in the atmosphere, by condensation of gaseous species on small particles and by nucleation and/or coagulation. Primary PM typically includes all particles that are directly released into the atmosphere whereas secondary PM includes particles which are generated in the atmosphere due to gas-to-particle conversion. There is a growing body of literature focusing on mechanisms of formation of secondary PM as well as identification and quantification of secondary PM in the atmosphere (Derwent and Malcolm, 2000**;** Lim and Turpin, 2002; Fine et al., 2008; Lewandowski et al., 2008; Donahue et al., 2009; Pye and Pouliot, 2012).

In terms of chemical composition, PM includes carbonaceous species, sulphate and nitrate, trace metals, sea salt, water, crustal dust and biological material (Seinfeld and Pandis, 1998; Calvo et al., 2013). The carbonaceous species include organic, elemental and carbonate carbon and while the elemental carbon (EC) is predominantly primary, organic carbon (OC) is present in both primary and secondary forms (Seinfeld and Pankow, 2003).

Particle size is the one of the key determinants of the behaviour and impacts of PM. There are several ways to determine the particle size with aerodynamic diameter being the most commonly used metric for defining particle size. It is defined as

> "*the diameter of a sphere of unit density which has the same settling velocity as the particle*" (Hinds, 1982).

Thus, particles with different shapes and densities can have the same aerodynamic diameter. PM concentrations can be represented in terms of mass, number or volume, although mass is the most commonly used parameter for determining PM concentration. Both particle mass and number, however, are important metrics in terms of exposure assessment (Harrison et al., 2010). Particles are often described using the size distributions and such particle size distributions can be expressed in terms of mass, number or volume. A typical aerosol size distribution has four modes: nucleation (particle diameter less than 10 nm), Aitken (particle diameter between 10 and 100 nm), accumulation (particle diameter between 100 nm and 2 μm) and coarse (particle diameter more than 2 μm) (Seinfeld and Pandis, 1998). Nucleation, Aitken and accumulation mode particles are classed as fine particles with nucleation and Aitken modes comprising ultrafine particles. Particles with diameters above 1 μm are classed as coarse particles (Colbeck and Lazaridis, 2010). In simpler terms, particles with aerodynamic diameters less than 2.5 μm are classified as fine particles whereas particles with aerodynamic diameters more than 2.5 μm are classified as coarse particles. Coarse particles are often generated due to mechanical and/or abrasive processes while fine particles are typically emitted during combustion (e.g. wood, biomass, and fossil fuels), industrial processes and secondary aerosol formation. The two fractions (coarse and fine) are associated with different health effects (NARSTO, 2004; Sehlstedt et al., 2012; Clements et al., 2014). The atmospheric residence time of the different PM fractions is quite variable and ranges from minutes to weeks (Seinfeld and Pandis, 1998). Particle size distributions can be used to identify particle sources as well as to understand the health implication of different source types.

1.1.1 Impacts

There is a large body of research on the impacts of PM on human health and studies have conclusively shown that long-term exposure to PM increases mortality and morbidity and can lead to respiratory as well as cardiovascular diseases (Pope et al., 2004; Brunekreef et al., 2009; Kappos et al., 2004; Pascal et al., 2013). Particle toxicity can vary based on chemical composition and specific constituents of PM such as elements (e.g. Cu, Zn, As, Hg, Cd, Ni) and polycyclic aromatic hydrocarbons (PAHs) are particularly harmful as they can lead to generation of reactive oxygen species (ROS) which then leads to oxidative stress (Kelly, 2003; Maynard, 2004; Ayres et al., 2008; Godri et al., 2011; Stanek et al., 2011; Steenhof et al., 2011; Bell, 2012). Biological interactions of PM depend on the proportion of soluble and insoluble mass with the water-soluble mass being the one of causative factors for PM-induced oxidative stress in human body (Shafer et al., 2010). The soluble fraction of metal species can interact with the body (e.g. lung lining fluid) and typically, the mineral fraction (often derived from natural sources) has a lower solubility than the processed fraction (derived from anthropogenic sources). As a consequence, the processed fraction poses a greater health risk compared to the mineral fraction. Upon reaction with macrophages and epithelial cells, PM produces ROS, typically through the reduction of oxygen by biological reducing agents, with the catalytic assistance of redox-active chemical species (e.g. metals, OC, quinones)

(Daher et al., 2012). Oxidative stress, in turn has been linked to causing respiratory infections, cardio-pulmonary diseases and cancer (Valavadinis et al., 2008).

Several epidemiological studies have shown diesel exhaust to be linked with development of respiratory diseases and respiratory morbidity (Lloyd and Cackett, 2001). In 2012, the International Agency for Research on Cancer (IARC) classified diesel exhaust as a group 1 carcinogen (i.e. carcinogenic to humans) and in 2013, PM was also classified as a group 1 carcinogen (Benbrahim-Tallaa et al., 2012; Loomis et al., 2013).

PM also has climate effects including its direct role in light scattering and absorption (direct forcing) of sunlight and thermal radiation and the indirect role in acting as cloud condensation nuclei (CCN) (indirect forcing) (NARSTO, 2004; Prather et al., 2008; Ramanathan and Carmichael, 2008). PM can also impair visibility by scattering (e.g. SO_4^{2-}) or absorption of light by the particles (particularly dust and elemental/black carbon), and can be measured in terms of light extinction (Chow et al., 2002). A detailed account on the science of visibility as well as the role of PM is discussed in Watson (2002).

1.2 Traffic Particulate Matter

Emissions from road vehicles are of particular interest since they are emitted in the vicinity of human activity, and canyon effects can concentrate the pollutant levels, thereby increasing the threat to human health (Colville et al., 2001).

PM emissions from road vehicles include emissions from the tailpipe (exhaust emissions including fuel and lubricant combustion and fuel additives) and emissions due to wear and tear of vehicle parts such as brake, tyre and clutch and re-suspension of dust (non-exhaust emissions) (Figure 1). The particles are generated by different mechanisms and differ in physical and chemical properties (Sehlstedt et al., 2012). Non-exhaust emissions contribute mainly to the coarse mode of PM ($PM_{2.5-}$

$_{10}$) while exhaust emissions contribute predominantly to fine PM (aerodynamic diameter < 2.5 µm) (Ondov et al., 1982; Lighty et al., 2000; Abu-Allaban et al., 2003; Tervahattu et al., 2006; Thorpe et al., 2007; Kam et al., 2012) but this is far from a clear distinction. Combustion processes generate small multimodal aerosol particles which are composed of carbon (elemental and organic) and inorganic (sulphate, metal oxides) fractions and typically have large surface areas (Lighty et al., 2000; Fernandes et al., 2003; Brook et al., 2007). The physical and chemical characteristics of the emitted particles are influenced by various parameters including physical conditions during the combustion (temperature, humidity), composition of the fuel (sulphur content, cetane number, aromatic additives etc.), driving conditions (speed, load), engine age, operation and maintenance conditions (Lighty et al., 2000; Yanowitz et al., 2000; Lloyd and Cackett, 2001; Fujita et al., 2007).

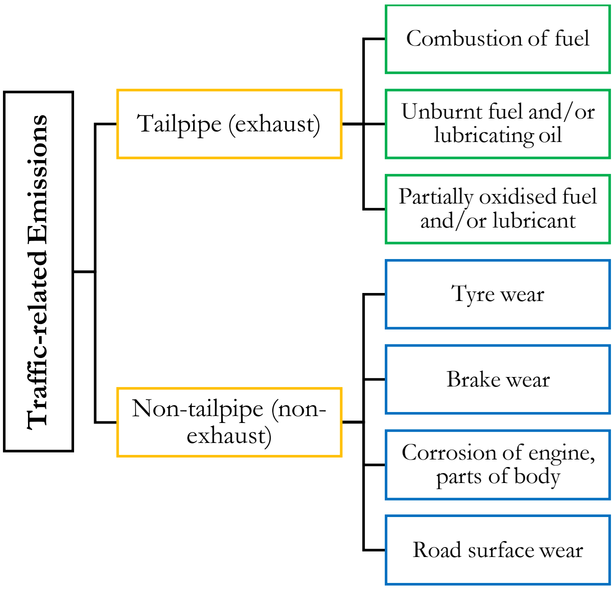

Figure 1: Sources of road traffic PM emissions

(based on Rogge et al., 1993a; Pant and Harrison, 2013)

A number of different properties of traffic emissions are studied including physical shape and structure, particle size distributions, chemical composition, and temporal and spatial variation

(Watson and Chow, 2007). Most of the research as well as policy action in the last few decades has largely focused on exhaust emissions, and stringent regulations and technological upgrades have resulted in a decline of the percentage contribution of vehicle tailpipe emissions to total ambient PM concentrations (Allen et al., 2006; Thorpe and Harrison, 2008; Mathissen et al., 2011). As a result, the contribution of non-exhaust PM is becoming more important although detailed information on non-exhaust PM emissions is relatively scarce (Amato et al., 2012a; Harrison et al., 2012a; Denier van der Gon et al., 2013). It has been shown that even with zero tailpipe emissions; traffic will continue to contribute to fine and ultrafine particles through non-exhaust emissions (Dahl et al., 2006; Kumar et al., 2013).

1.2.1 Exhaust Particulate Matter

Exhaust emissions typically include emissions due to combustion of the fuel, lubricating oil and the additives (Rogge et al., 1993a; Pulles et al., 2012). Under ideal conditions, complete combustion of the fuel (gasoline or diesel) produces carbon dioxide (CO_2) and water (H_2O). However, driving under real-world conditions results in incomplete combustion, and a complex mixture of carbonaceous material (OC and EC), trace metals, VOCs and gases are released. In some cases, unburnt fuel and lubricating oil can be released directly via the tailpipe. PM emissions from vehicles depend on the engine type and age and maintenance and contain carbon in the form of OC and EC with smaller amounts of trace metals and ions (Fraser et al., 1998; Brook et al., 2007; Robert et al., 2007a; Fulper et al., 2010; Peltier et al., 2011). Motor vehicles are an important source for carbonaceous aerosols particularly for the particles in the fine size range (aerodynamic diameter $< 2.5\ \mu m$) (El Haddad et al., 2009; Kam et al., 2012; Keuken et al., 2012) and vehicular exhaust is reported to have a bimodal distribution (Ondov et al., 1982). Emissions from diesel and gasoline vehicles are different in terms of composition as diesel engines emit both a greater mass of PM and a larger number of ultrafine particles (UFPs) compared to gasoline vehicles (Rose et al., 2006). Typical diesel PM mass concentration is 15-30 mg/m^3 compared to approximately 0.1 mg/m^3 for the gasoline engines (Lighty et al., 2000). Robert et al. (2007a, b) reported that that emission rates for ultrafine and fine particles for diesel heavy-duty vehicles (HDVs) are one order of magnitude higher than gasoline light duty vehicles (LDVs). Similarly, Chen et al. (2013) reported 4-times higher diesel emission factors (EFs) compared to gasoline EFs in a tunnel environment. Higher emissions from the high-emitting (smoker) vehicles have previously been attributed to lubricating oil (Fujita et al., 2006). Gasoline engines are known to release a higher fraction of OC while diesel engines emit more EC (Watson et al., 1994; Weingartner et al., 1997; Lloyd and Cackett, 2001; Ntziachristos et al., 2007) although Sodeman et al. (2005) demonstrated a dominance of EC in the ultrafine range in gasoline vehicles. Fraser et al. (1998) proposed the use of EC/TC (total carbon) ratio for segregating between gasoline and diesel vehicle emissions since the ratio can vary significantly between vehicle types. PM$_{2.5}$ emissions from diesel and gasoline vehicles tend to be rich in different fractions of EC and OC which correspond to the fractions desorbed at different temperature ramps during carbon analysis (Watson et al., 1994). While road traffic emissions are typically a primary source of PM, recent research has suggested that gasoline and diesel emissions are also associated with the production of secondary aerosol (Bahreini et al., 2012).

Giechaskiel et al. (2014) present a detailed review of traffic emissions' measurement techniques and advancements over the years while a detailed description of diesel particulate matter is presented in Maricq (2007). The situation in relation to exhaust emissions from traffic is constantly changing as abatement technologies develop. In particular the adoption of diesel particulate filters (DPF) is greatly reducing mass emissions.

Both trace elements and organic compounds are used as source markers for vehicle emissions. However, since the removal of lead (Pb) from gasoline, trace metals have proved far less useful as a tracer of engine exhaust (Harrison et al., 2003). Elemental markers which have been used for vehicular emissions include Cu, Mn, Fe, Zn, Ba, Sn, Ni, Mo and Sb (Lough et al., 2005; Almeida et al., 2006; Birmili et al., 2006; Dongarra et al., 2009; Fabretti et al., 2009; Gietl et al., 2010; Amato et al., 2011a, b). Metals can be emitted from various exhaust-related sources including fuel and lubricant combustion, catalytic converters, particulate filters and engine corrosion (Lough et al., 2005; Pulles et al., 2012; Sysalova et al., 2012; Varrica et al., 2012) but many of these appear most likely to arise from non-exhaust sources. Metallic emissions include Fe, Cr, Ni, Sn, Cu, Zn, Mg, Ca (diesel); Ca, P, S, Na, K, Mg, Zn (lubricating oil) and Fe, Ca, Ni, Sn, Al, Sb (engine wear, corrosion) (Lough et al., 2005; Liati et al., 2013). Metal concentrations from diesel and gasoline vehicles are reported to vary over two orders of magnitude and Ba, Cd, Zn, Sb and V in nanoparticles have been reported to be strongly associated with diesel fuel whereas Cu, Mn and Sr in the particles <0.1 μm have been found to be associated with gasoline (Lin et al., 2005; Pulles et al., 2012). Also, since several elements are emitted from multiple sources, it can be difficult to apportion the mass based solely on the trace element concentration. For example, V can be emitted from different sources including fuel oil combustion, petroleum refinery operations and the V-based selective catalytic reactors (Ondov et al., 1982; Pey et al., 2010; Shafer et al., 2012). Similarly, Zn can be emitted from vehicle tailpipe as well as from industrial processes, particularly metallurgy and waste incineration (Keuken et al., 2010) and Fe can be attributed to crustal material, fuel and coal combustion, industrial operations (e.g. steelworks) and non-exhaust vehicular sources (Ault et al., 2013; Taiwo et al., 2014). Further, the levels of trace elements emitted in the exhaust are very low, and great care is needed to distinguish them from non-exhaust traffic emissions and other sources. Different authors often attribute metals to different sources which renders precise source attribution with trace metals alone very difficult unless detailed local information on source particle composition is available (e.g. Pant and Harrison, 2012).

Organic compounds released from vehicles are particularly useful markers for conducting receptor modelling analyses since such molecular markers help in distinguishing the vehicular emissions from other sources. Molecular markers are defined as

> "*individual organic compounds which are used to define chemical fingerprints from different sources*" (Roy et al., 2011).

The most commonly used molecular markers for vehicular emissions are hopanes and steranes which are found in lubricating oil and due to their source, the distribution of hopane emissions from vehicles is suggested to be independent of fleet composition (Rogge et al., 1993a; Schauer et al., 1996; Cass, 1998; Fraser et al., 1998; Fujita et al., 2007; Lough et al., 2007; He et al., 2008; Roy et al., 2011). However, Fujita et al. (2007) reported anomalous results and noted differences in the hopane and sterane distributions between gasoline and diesel vehicles, i.e. higher abundance of lower molecular weight hopanes and steranes in diesel vehicles compared to an equal distribution of low and high molecular weight compounds in case of gasoline vehicles. Older vehicles can sometimes produce higher concentration of hopanes and steranes since older vehicles tend to use higher quantities of oil. Vehicles are also a major source of n-alkanes, and diesel engines are known to emit more n-alkanes compared to gasoline engines (Rogge et al., 1993a).

It has also been suggested that hopanes and steranes (derived from lubricating oil) and PAHs (derived from reactions at high temperature and fuel combustion) are indicative of different processes during the organic carbon formation in vehicle engines (Lee et al., 1995; Fujita et al., 2006; Riddle et al., 2007; Hanedar et al., 2008).

PAHs are formed as a result of incomplete combustion of fuel sources (e.g. wood, fossil fuels) and are emitted from a wide range of sources including vehicles, power plants, refineries, residential heaters and fireplaces (wood/coal/gas), natural gas appliances etc. (Li and Kamens, 1993; Venkataraman and Friedlander, 1994; Lee et al., 1995; Ravindra et al., 2008). A number of PAHs have been reported to be present in vehicle exhaust including benzo(e)pyrene, benzo(a)pyrene, indeno(1,2,3-cd) pyrene, coronene and benzo(ghi)perylene (Rogge et al., 1993a; Lough et al., 2007; Riddle et al., 2007). Results from tunnel studies and chassis dynamometer analyses have shown that lower molecular weight PAHs such as phenanthrene and fluoranthene are characteristic of diesel-derived aerosols whereas gasoline engines contributed more to higher molecular weight PAHs such as benzo(ghi)perylene, indeno(1,2,3-cd)pyrene and coronene (Smith and Harrison, 1996). Li and Kamens (1993) noted that while different sources can emit the same PAHs, the ratios of PAHs (referred to as diagnostic ratios) vary across sources and can be used to distinguish between sources. For example, the ratio between concentrations of indeno(1,2,3-cd) pyrene to the sum of indeno(1,2,3-cd) pyrene and benzo(ghi)perylene is also used for distinguishing between gasoline and diesel emissions and the ratio between methylphenanthrenes/phenanthrene has also been used for estimation of the contribution of traffic to PAH concentrations in ambient air (Lim et al., 1999; Chellam et al., 2005; Ancelet et al., 2011). Emission profiles for PAHs are difficult to generalize since they vary across the different vehicle classes (Miguel et al., 1998). Congener[1] profiles of PAH from road traffic have been derived from tunnel and roadside studies (e.g. Smith and Harrison, 1996; Nielsen, 1996; Mari et al., 2010). However, PAHs can be altered by atmospheric chemical reactions (photochemical degradation) and/or dilution effects, and the concentrations can vary based on season (Venkataraman and Friedlander, 1994; Lee et al., 1995). In case of PAHs, gas-particle phase partitioning also plays an important role in the ambient concentrations of the various compounds, and this can be affected by meteorological variables such as temperature, vapour pressure and humidity and compound characteristics such as molecular weight (Venkataraman and Friedlander, 1994; Lee et al., 1995). For example, at lower temperatures, PAHs tend to be present in particle-phase while at higher temperatures, gas-phase is dominant for several PAHs.

---

[1] Congeners refer to one of two or more substances related to each other by origin, structure, or function (IUPAC).

1.2.2 Non-exhaust Particulate Matter

Non-exhaust PM comprises the various emissions that do not derive from the tailpipe of a vehicle including particles generated due to brake and tyre wear, road surface abrasion, wear and tear/corrosion of other vehicle components such as the clutch, and re-suspension of road surface dusts (Table 1). Key reasons for needing to understand non-exhaust emissions include their inherent toxicity including their tendency to act as carriers of heavy metals and carcinogenic components (Adachi and Tainosho, 2004; Hjortenkrans et al., 2007; Johansson et al., 2009; Amato et al., 2011a) and their contribution to exceedances of air quality guidelines and standards (Amato et al., 2011a; Denier van der Gon, 2013). Several factors are reported to affect non-exhaust emissions including increase in vehicle speed (Chen et al., 2006; Gustafsson et al., 2008; Hussein et al., 2008; Mathissen et al., 2011).

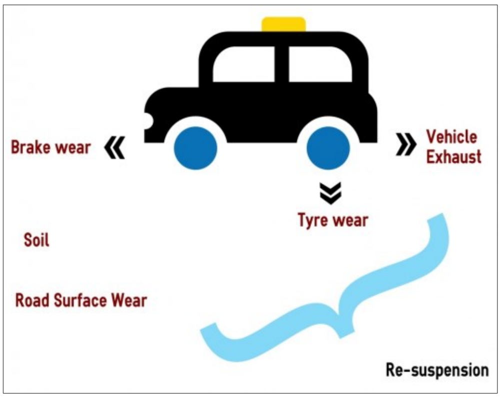

Several researchers have analysed the chemical composition of brakes (Rogge et al., 1993b; Garg et al., 2000; Blau and Meyer, 2003; Kukutschova et al., 2010, 2011) and tyres (Camatani et al., 2001; Kumata et al., 2002; Adachi and Tainosho, 2004; Councell et al., 2004; Milani et al., 2004; Aatmeeyata and Sharma, 2010; Sadiktis et al., 2012; Dall'Osto et al., 2014).

Table 1: Mechanisms for non-exhaust particle emissions

Rogge et al., 1993b; Boulter et al., 2005; Wahlin et al., 2006; Thorpe et al. 2007; Amato et al., 2009a; Gietl et al., 2010; Hays et al., 2011; Denier van der Gon, 2013)

Emission type	*Mechanism*	*Includes*
Direct	Abrasion and wear and tear Corrosion	Tyre, brake, clutch, road surface Vehicle, street furniture
Indirect	Re-suspension (due to tyre shear, wind and vehicle turbulence)	

Harrison et al. (2012a) showed that the size distributions of trace metals were indicative of particle sources and Narvaez et al. (2008) reported that although the majority of abrasion particles are in the coarse fraction, abrasion can contribute significantly to the fine fraction of PM. Road traffic was found to be a key contributor to fine/ultrafine and nano mode particles of Ba, Zn and Pb (Lin et al., 2005) and in Barcelona (Spain), 62-96% of elements including Cu, Sb, Ba, Mn and Zn were found to be present in the PM_{1-10} fraction (Perez et al., 2010). A detailed review of the nanoparticle emissions from non-exhaust sources including traffic and non-traffic sources is presented in Kumar et al. (2013). Thorpe and Harrison (2008) present a more elaborate account of sources and properties of non-exhaust emissions. Denier van der Gon et al. (2013) and Amato et al. (2014a) summarize the existing knowledge and future directions in the field.

Typical methods for characterization of road dust and non-exhaust emissions include use of brake dynamometer (Garg et al., 2000), rolling resistance testing machine (Hildemann et al., 1991), rotating drum method (Camatani et al., 2004), sweep/vacuum collection of particles followed by sieving or resuspension (Chow et al., 2003), vehicle chase and use of road dust sampler (Amato et al., 2009a) .

Non-exhaust emissions are typically characterized by trace metals (e.g. Cu, Zn, Ba, Sb, Mn) although organic markers (e.g. PAHs, n-alkanes) have been used in some cases (Lough et al., 2006; Wahlin et al., 2006; Amato et al., 2009a; Dongarra et al., 2009; Gietl et al., 2010; Oliviera et al., 2011; Kwon and Castaldi, 2012). A list of key tracers used for source characterization of non-exhaust emissions is presented in Table 2. However, emissions of trace metal markers are reported to vary with the fleet composition, with higher emissions reported for some of the elements for HDVs (Grieshop et al., 2006; Mancilla and Mendoza, 2012). In addition, the profile of trace metal concentrations in non-exhaust particulate matter is unique for every region and varies based on parameters such as traffic volume and pattern, vehicle fleet characteristics, driving and traffic patterns and climate and geology of the region (Omstedt et al., 2005; Amato et al., 2011a, b; Duong and Lee, 2011; Han et al., 2011). Another important aspect is the variability of tyre and brake composition depending on the manufacturer which makes it very difficult to ascertain fleet-wide composition other than from environmental measurements (Canepari et al., 2008; Gietl et al., 2010; Denier van der Gon et al., 2013).

Table 2: Key tracers used for non-exhaust PM

Reference	*Brake wear*	*Tyre wear*	*Re-suspension*
Adachi and Tainosho (2004)	Fe, Ba, Cu, Sb, Zr	Zn	-
Schauer et al. (2006)	Fe, Cu, Ba		-
Grieshop et al. (2006)	Cu, Sb, Ba and Ga		
Wahlin et al. (2006)	Cr, Fe, Cu, Zn, Zr, Mo, Sn, Sb, Ba and Pb	Al, Si, K, Ca, Ti, Mn, Fe, Zn and Sr (together with road dust)	
Canepari et al. (2008)	Ba, Fe, Sb, Sr	-	-
Dongarra et al. (2009)	Cu, Mo, Sb	-	
Fabretti et al. (2009)	Cu, Zn, Sb, Sn (vehicular abrasion)	-	Rb, Sr, Mn, Fe, As
Bukowiecki et al. (2010)	Fe, Cu, Zn, Zr, Mo, Sn, Sb and Ba		
Pey et al. (2010)	-	-	Fe, Ca, Sb, Sn, Cu, Zn
Perez et al. (2010)	Sb, Cu, Ni, Sn (wear of brake, tire and other parts)		Fe
Amato et al. (2011a)	Fe, Cu, Zn, Cr, Sn, Sb	OC, S, Zn	Al, Ca, Fe, V
Apeagyei et al. (2011)	Fe, Ti, Cu, Ba	Zn, Ca, W, K, Fe, Ti, Cr, Mo	-
Duong and Lee (2011)	Ni, Cu	Zn	
Ondracek et al. (2011)	Cu, Ba, Fe, Zn	-	
Sahu et al. (2011a)	Zn (brake and tyre wear)	-	
Peltier et al. (2011)	-	-	Al, Si, Ti, Fe
Harrison et al. (2012a)	Ba, Cu, Fe, Sb	Zn	Si, Al
Spada et al. (2012)		Mn, Fe, Pb, Co, Ni, Cd	
Amato et al. (2013a)	Ba, Sb, Cu, Sn, Fe	S, Zn, OC	Al, Ca, Fe, K

One of the major problems in analysis of non-exhaust PM using field data has been the difficulty in distinguishing between wear and tear emissions and road dust since the chemical composition is often very similar (Bukowiecki et al., 2010). This may, in any case, not be a clear distinction as wear emissions may deposit to the road surface, only to be re-suspended subsequently. Typically, particles generated from different sources (brake and tyre wear, mechanical abrasion of pavement upon interaction with tyres, soil) are subsequently resuspended due vehicle-induced turbulence or interaction between tyre and pavement. Resuspension strength depends on a number of factors including meteorological conditions and traffic characteristics. Gehrig et al. (2010) used mobile load simulators to compare the contributions of road abrasion and resuspension emissions, and concluded that particle emissions due to abrasion are a function of the state of the pavement whereas resuspension is normally higher, and increases with higher dust loads on the road.

In recent years, several analyses have been undertaken to test mitigation measures for road dust/non exhaust emissions. Mixed results have been obtained for the impact of street washing activities on PM and while Amato et al. (2009b) observed a reduction, albeit statistically non-significant, in the concentration of trace metals known to be contributed by non-exhaust traffic sources in Spain; Keuken et al. (2010) reported a lack of significant reduction in the non-exhaust emissions after street sweeping or washing in the Netherlands. The effect of street-washing is often short-lived and Karanasiou et al. (2014) have proposed the use of street-washing in the early hours of the morning before the traffic rush-hour, in order to derive maximum dust suppression. Based on a study in Spain, Amato et al. (2014b) concluded that the effectiveness of road dust suppressants such as $MgCl_2$ and calcium magnesium acetate (CMA) increases with higher road dust loads. A similar conclusion was presented by Barratt et al. (2012) based on tests in London, where the effect of CMA was found to be the highest in areas with high PM_{10} dust loads.

1.2.2.1 Tyre Wear

Tyre wear particles (TWPs) are generated either by shear forces between the tyre tread and the road surface or by volatilization/thermal degradation and are predominantly coarse ($PM_{2.5-10}$) with some airborne particles in the smaller size ranges (fine and ultrafine) (Rogge et al., 1993b; Kupiainen et al., 2005; Allen et al., 2006; Thorpe and Harrison, 2008; Aatmeeyata and Sharma, 2010; Sehlstedt et al., 2012). Kwak et al. (2013) estimated a 3-4 and 4-7% contribution of tyre wear to PM_{10} and $PM_{2.5}$ respectively under real-world driving conditions. Tyre wear particles are reported to be elongated with rough surfaces based on microscopic analysis (Gunawardana et al., 2011). Unimodal (70-90 nm) and bimodal (< 10 and 30-60 nm) peaks in the nano size range have been reported for tyre particles by number under low and high speed conditions respectively (Mathissen et al., 2011).

Tyre tread, a source of airborne particles, contains natural rubber copolymers such as styrene-butadiene rubber and polyisoprene rubber, and Zn is added to tyre tread as zinc oxide and organozinc compounds to facilitate the vulcanization process. Passenger car tyres in EU are known to contain nearly 1% zinc oxide, and rubber, metals and carbon black make up 47%, 16.5% and 21.5% respectively (Hildemann et al., 1991; Milani et al., 2004; Kreider et al., 2010). However, Amato et al. (2012b) reported a large amount of variability in terms of chemical composition of brake pads in Spain with high concentrations of sulphides (especially ZnS) across all brake pad types.

The key tracer components of tyre wear include n-alkanes, n-alkanoic acids, PAHs, benzothiazoles and trace metals (Rogge et al., 1993b; Reddy and Quinn, 1997; Camatani et al., 2001; Adachi and Tainosho, 2004; Boulter et al., 2005; Aatmeeyata and Sharma, 2010). Zn is reported to be nearly 1% by weight in rubber tyres (Councell et al., 2004) and tyre wear has been reported to be a significant source of Zn (Adachi and Tainosho, 2004; Hjortenkrans et al., 2007; Ondracek et al., 2011). The concentration of Zn was found to be approximately 15 times higher in tyres compared to brakes while concentrations of other heavy metals such as Cu and Ba were higher for brake materials in Massachusetts (USA) (Apaegyei et al., 2011). In Spain, Amato et al. (2012b) found high concentrations of Cu and Ba in car and motorcycle brake pads. Differences have also been observed between tyre tread composition (primarily Zn) and tyre wear (Al, Si, Ca, Fe, Zn, Ti) (Adachi and Tainosho, 2004). However, the spatial and temporal trend for Zn was found to be different from other roadside tracers in New York (USA), and a very small portion of airborne Zn concentration was attributed to tyre wear (Peltier et al., 2011). Zn is also emitted from brake wear, motor oil and other sources and cannot be used as the only tracer for tyre wear (Lough et al., 2005). Benzothiazoles are also used as markers for tyre wear, particularly benzothiazole (BT), 2-hydroxy benzothiazole (HOBT), 2-(4-morpholinyl)benzothiazole (24MoBT) and N-cyclohexyl-2-benzothiazolamine (NCBA) (Kumata et al., 2002; Allen et al., 2006; Wik and Dave, 2009). Among the PAHs, pyrene, benzo(ghi)perylene, fluoranthene and phenanthrene are known to be emitted from tyres (Boonyatumanond et al., 2007; Kwon and Castaldi, 2012). Aatmeeyata and Sharma (2010) reported that small cars tested in India emitted 378 ng of total PAH/tyre/km while in the USA, 200 μg/g of PAHs were found in tyre wear with pyrene, fluoranthene and phenanthrene being present in the highest concentrations (Rogge et al., 1993b). Tyre tread wear has also been found to contain an average of 0.53 μg/g of dibenzopyrenes, indicating that tyre dust may be a significant source of dibenzopyrenes in the environment (Sadiktis et al., 2012).

Average tread wear for tyres is reported to be between 0.006-0.009 g/km based on the road, tyre and vehicle conditions (Rogge et al., 1993b) and tyres can lose up to 10% of their mass during their lifetime (Milani et al., 2004). Speed has been reported as an influential parameter for particle mass and number concentrations for tyre wear emissions (Gustafsson et al., 2008; Mathissen et al., 2011). Other important parameters for tyre tread wear include road surface type (rough vs. smooth), vehicle type (front wheel vs. back wheel) and tyre (over or under-inflated) and driving conditions (Allen et al., 2006; Gustafsson et al., 2008). For example, asphalt surfaces have been reported to cause less tyre wear than concrete pavements and in Arizona, USA, the emission rate for tyre wear was found to be 1.4-2 times lower for asphalt pavement compared to concrete pavement (Allen et al., 2006). The type of tyre also impacts the magnitude of tyre wear emissions and studded tyres are known to cause more emissions compared with summer and friction tyres (Kupiainen et al., 2005; Gustafsson et al., 2008; Hussein et al., 2008; Schaap et al., 2009).

1.2.2.2 Brake wear

Brake wear, including abrasion of brake lining material and brake discs, caused by grinding of brake pad constituents (coarse range particles) or volatilization and condensation of brake pad materials (fine range particles), is known to release PM directly into the atmosphere and to contribute to the trace metal concentration in airborne PM, particularly less than 10 μm (Ondov et al., 1982; Garg et al., 2000; Blau and Meyer, 2003; Ingo et al., 2004; Wahlin et al., 2006). Brakes can either be disc or drum, though disc brakes are quite commonly used across vehicle types now. A variety of brake pads are used worldwide and the distinction is based on the chemical composition with metallic (steel-based), semi-metallic, low-metallic and non-asbestos organic (NAO) brake pads being the most common types. In Europe, low metallic brake pads are the most commonly used followed by the NAO brake pads. Key components of brake pads include fillers, frictional additives/modifiers, reinforcing fibres and binder (Chan and Stachowiak, 2004) and the key chemical species used include sulphides of metal, abrasives (e.g. silica), barium silicate/sulphate (particularly in brake linings) and other metallic particles (as filler material), carbon fibres and lubricant (e.g. graphite) (Ingo et al., 2004; Dongarra et al., 2009). Chan and Stachowiak (2004) present a detailed review of the chemical constituents of brake pads. Garg et al. (2000) observed an average mass median diameter (median particle diameter based on mass) of 1.49 μm for brake wear particles using tests on a brake dynamometer whereas Sanders et al. (2003) reported a mass median diameter of 6 μm for brake debris generated during urban driving conditions. Higher brake wear related emissions have been reported during rush hour. A higher number of particles are released in the braking phase as compared to the acceleration phase (Hussein et al., 2008; Mathissen et al., 2011) and various studies have corroborated this observation including Greishop et al. (2006) who reported a higher particle number concentration during rush hour where the traffic often operates in the stop-and-go mode and Abu-Allaban et al. (2003) who observed higher contribution of brake wear at freeway exit sites compared to other types of roadside sites (Abu-Allaban et al., 2003).

Passenger cars have been estimated to emit nearly 44 g/car/year brake dust (Iijima et al., 2007). Sanders et al. (2003) reported high concentrations of Fe, Ba and Cu in brake lining wear using dynamometer and track tests whereas Adachi and Tainosho (2004) reported Fe to be the most abundant metal in brake dust along with other metals such as Ba, Cu, Sb, Zr and Zn, and other studies have reported Cu, Zn, Sb and Mo to be present in brake wear emissions (Hjortenkrans et al., 2007; Dongarra et al., 2009; Kwak et al., 2013). Varrica et al. (2012) undertook a detailed study on Sb in brake dust and reported the most commonly released forms of Sb due to brake abrasion to be Sb (III) and Sb (V). However, brake pads are often found to have different composition based on the brand, particularly with respect to Cu and Sb (Hjortenkrans et al., 2007; Canepari et al., 2008; Hays et al., 2011). Polyalkylene glycol ethers are also reported to be present in brake wear particles with small concentrations of n-alkanes and n-alkanoic acids (Rogge et al., 1993b).

Iijima et al. (2007) reported a unimodal number-based distribution for brake abrasion dust with the mode at 1-2 μm while the mass-based distribution had a peak at 3-6 μm. EFs for brake wear have been reported by several studies including Garg et al. (2000) who reported a brake wear EF of 3-9 mg/km for gasoline LDVs and Abu-Allaban et al. (2003) who reported an EF of 0-80 mg/km. Wahlin et al. (2006), on the other hand, reported a Cu emission factor of 0.7± 0.2 mg/km/vehicle in Copenhagen.

Sternbeck et al. (2002) proposed the ratio of Cu: Sb (4.6 ± 2.3) as characteristic of brake wear particles although differences have been reported at various locations. Such differences can be attributed to the difference in the brake pad composition, contributions of metals from other sources and in some cases, site characteristics.

1.2.2.3 Road Surface Wear and Resuspension

Other sources that contribute to the non-exhaust emissions include corrosion of engine and vehicle parts (e.g. engine, paint, body, and chassis), street furniture, road surface, salt and grit (relevant in specific locations) and resuspended particles.

Road dust, of which crustal dust is a key component, consists of primarily coarse-sized particles derived from different sources such as traffic, industrial emissions, construction activities, coal combustion (including coal fly ash), vegetative detritus and mineralogical dust etc. (Gordon, 1980; Kupianinen et al., 2005; Bi et al., 2007; Tanner et al., 2008; Fujiwara et al., 2011). Composition of road dust shows spatial as well as temporal variation and it is often difficult to classify dust into crustal/resuspended/direct emission etc. In Monterrey (Mexico), re-suspended dust was found to be contributing nearly 20-25% to the $PM_{2.5}$ EF (Mancilla and Mendoza, 2012). The amount of re-suspended road dust particles depends on a number of factors including vehicle movement (particularly traffic speed), street maintenance, season and associated meteorological parameters (e.g. wind speed, relative humidity) and speed of traffic (Etyemezian et al., 2003; Gertler et al., 2006; Bi et al., 2007; Thorpe et al., 2007; Bhaskar and Sharma, 2008; Kaunhaniemi et al., 2011; Laidlaw et al., 2012; Majumdar et al., 2012). Nicholson (1988) presents a detailed review of the mechanisms of resuspension of road dust. Thorpe et al. (2007) reported a strong association between heavy duty traffic and re-suspension in the UK with wind speed not found to be a strong influence. In addition, precipitation was found to have no influence on the amount of re-suspension. In somewhat related research, street-washing has been reported to be ineffective for PM control based on experiments in Spain (Karanasiou et al., 2012). However, in Sweden, road wetness was found to be an important factor in the amount of re-suspension (Omstedt et al., 2005), but this appears related to road sanding and the use of studded tyres in Sweden. It is also important to note that the residence time of PM_{10} on paved roads (travel lanes) has been estimated as a few hours (Etyemezian et al., 2003). In the case of studded tyres, interaction between tyres and the road pavement can generate particles less than 0.1 μm (Gustafsson et al., 2008) and such tyres have been shown to increase PM_{10} emissions by a factor of 1.5 (Tervahattu et al., 2006). The type of pavement is another important factor for road dust emissions. Granite pavements have been reported to emit more PM compared to quartzite pavements (Kupiainen et al., 2005; Gustafsson et al., 2009) and asphalt pavement is reported to produce more particles than concrete pavement (Lee et al., 2013). Tervahattu et al. (2006) also explained the higher PM_{10} concentration attributed to use of anti-skid aggregate using the *sandpaper effect*, where the aggregates used to prevent skidding generate PM_{10} particles and lead to further particle emissions from the pavement. Mathematical models have been proposed for estimation of PM emissions due to road dust although they do not include emissions due to wear of brake/tyre materials (Omstedt et al., 2005; Ketzel et al., 2007; Berger and Denby, 2011; Kaunhaniemi et al., 2011).

Aatmeeyata et al. (2009) reported a bimodal number and mass distribution (0.3 μm and 4-5 μm) for PM_{10} generated due to surface (concrete pavement) and tyre wear. Duong and Lee (2011) reported a multi-modal distribution for road dust particles (based on weight) collected from the roadside with a majority of the particles between 180-850 μm in Ulsan, Republic of Korea. Chen et al. (2006) reported a bimodal (5-10 μm and > 30 μm) mass size distribution for road dust particles in Beijing (China).

Pristane, phytane, hopanes, steranes in addition to unresolved complex mixture (UCM) were reported in road dust particles which were found to be enriched in biogenic component by Omar et al. (2007). High concentrations of phenanthrene, fluoranthene and pyrene along with high molecular weight (4-7 ring) PAHs were reported in road dust samples from several countries in Taiwan (Fang et al., 2004; Liu et al., 2007; Han et al., 2009; Hassanien and Abdel-Latif, 2008).

Mono- (α- and β-glucose) and disaccharides (sucrose and mycose) have also been used as markers for road dust re-suspension for source apportionment (Simoneit et al., 2004a; Omar et al., 2007).

Several studies in Europe have focused on characterisation of road dust (Boulter etr al., 2005; Amato et al., 2009a; Bukowiecki et al., 2010; Pirjola et al., 2010; Amato et al., 2011a; Bardelli et al., 2011; Amato et al., 2013a). Analysis of PM_{10} road dust in Spain and Switzerland revelaed much higher dust loadings in Spain (Barcelona) and brake wear, tire wear, mineral dust (soil, construcution emissions, road wear) and motor vehicle exhaust were identified as the sources contributing to PM_{10} road dust (Amato et al., 2011a). Bardelli et al. (2011) analysed PM road dust (<63 μm) in a highway tunnel, and identifed a predominance of phylosilicates, Mn/Fe oxides and chlorides and a small organic fraction. Roads and construction sites are reported to have higher PM_{10} dust loads (Amato et al., 2011a). Sjodin et al. (2010) found road wear to be the most important source of PM_{10} emissions in streets as well as background locations in Sweden, which is probably a reflection of road sanding and use of studded tyres. Han et al. (2007) analysed suspended dust in Beijing and reported concentrations of elements such as Ca, S, Cu, Zn, Ni, Pb, and Cd to be much higher than the crustal abundances, and Cu, Zn, Ni, and Pb were attributed to traffic emissions together with coal burning. Luo et al. (2011) observed that the concentrations of trace metals contributed by vehicle exhaust and tyre abrasion, i.e. Pb, Zn and Cu have been reported to be much higher in roadside samples than the concentrations of these elements in background soils in China. Duong and Lee (2011) analysed heavy metal contamination in road dust in high traffic areas in Korea and concluded that the concentrations of heavy metals are much higher in high traffic areas in relation to a background site. Their analysis also confirmed a high degree of correlation between the concentration of heavy metals at a specific location and the traffic throughput in the area. Amato et al. (2013a) analysed PM_{10} road dust in Spain and Netherlands and demonstrated variations in the resuspension strength for the various emission sources. Significant differences were observed between source contributions in Utrecht and Barcelona- in Utrecht, tire and brake wear were found to be major contributors to RD while in Barcelona, tyre wear had the smallest contribution. Martuzevicius et al. (2011) analysed street dust and reported that it can be a major source for particle-bound PAHs together with other PM. Han et al. (2009) reported a high correlation between PAHs and OC in road dust, and traffic emissions were identified as a major contributor to PAHs in road dust using diagnostic ratio analysis and Lee et al. (1995) reported the impact of traffic emissions on road dust. Elements such as platinum, palladium and rhodium have also been reported to be present in road dust and are attributed to the catalytic converters (Prichard and Fisher, 2012). Several others studies have been conducted worldwide (Chow et al., 2003- USA; Essumang et al., 2006- Ghana; Omar et al., 2007- Malaysia; Tanner et al., 2008-China; Agarwal, 2009-India; Faiz et al., 2009- Pakistan; Han et al., 2009- China; Apaegyei et al., 2011-USA; Fujiwara et al., 2011-Argentina; Gunawardana et al., 2011- Australia). Werkenthin et al. (2014) discuss the concentrations of elements in European roadside soils while Wei and Yang (2010) present a similar discussion focused on urban and agricultural soils in China.

1.3 Receptor Modelling

The term, source apportionment (SA) describes techniques used to quantify the contribution of different sources to concentrations of atmospheric PM as well as other species (e.g. VOCs). There are three key approaches for source apportionment including use of emission inventories and dispersion models, receptor models and monitoring data (Viana et al., 2008). Dispersion models are often used for estimation of a source's impact on air quality in an area/region and use emission rates and dispersion factors together with local topography and meteorology for estimation of source impacts (Cooper and Watson, 1980; Henry et al., 1984) whereas receptor models (RMs) are used to estimate the contribution of different sources to ambient PM concentrations based on measurements and subsequent chemical analysis.

Watson and Chow (2007) describe receptor models as models that

> "*interpret measurements of physical and chemical properties taken at different times and places to infer the possible sources of excessive concentrations and to quantify the contributions from those sources*".

In other words, such models can be defined as models that utilize physico-chemical speciation data to quantify source contributions based on the principle of mass balance. RMs use the information on chemical composition at receptor sites and in source emissions to reconstruct the observed ambient concentrations and apportion the mass to different emission sources (Henry et al., 1984; Gordon, 1988; Hopke, 1991). Such models form a subset of SA techniques and apportion the pollutant concentrations based on the measured ambient air data and the knowledge about composition of the contributing sources (Henry et al., 1984). Gordon (1988) and Hopke (1991) provide a historical perspective of the development of the RMs. The key outputs of the RMs are the percentage contributions of different sources to pollutant concentration. These models have been used for identification of sources and their respective contributions to airborne particulate matter across the world (Harrison et al., 1997; Kumar et al., 2001; Larsen and Baker, 2003; Begum et al., 2004; Song et al., 2006; Chowdhury et al., 2007; Guo et al., 2009; Kong et al., 2010; Stone et al., 2010; Gu et al., 2011; Clements et al., 2014). Such models provide relevant information for development of air pollution management and control programs, validation of dispersion models and are particularly helpful in cases where complete emissions inventories are not available (Hopke, 1991; Watson et al., 2012).

RMs can be divided into two broad categories: microscopic and chemical. Microscopic methods, including optical, scanning electron microscope (SEM) and automated SEM analyses are primarily based on the analysis of morphological features of many individual particles in the ambient air (Cooper and Watson, 1980). However, they are not very feasible for large-scale use since they do not produce quantitative results in most cases. Chemical methods, on the other hand, utilize the chemical composition of airborne particles for identification and apportionment of sources of PM in the atmosphere. Each source has a characteristic emission profile, and differences among the profiles can be used for quantitative apportionment of mass to different emission sources (Friedlander, 1973). A number of receptor models are used for source apportionment including semi-qualitative methods such as enrichment factor (EF) analysis and diagnostic ratio analysis and quantitative methods such as Chemical Mass Balance (CMB) model, multivariate statistical models such as Principal Component Analysis (PCA) and Positive Matrix Factorization (PMF), Multilinear Engine (ME), Constrained Physical Receptor Model (COPREM) and UNMIX and hybrid models such as Target Transformation Factor Analysis (TTFA). A detailed classification of the receptor models is presented in Figure 2. These models have been used for regulatory purposes since they were first used in Oregon, USA in the late 1970s (Gordon, 1988).

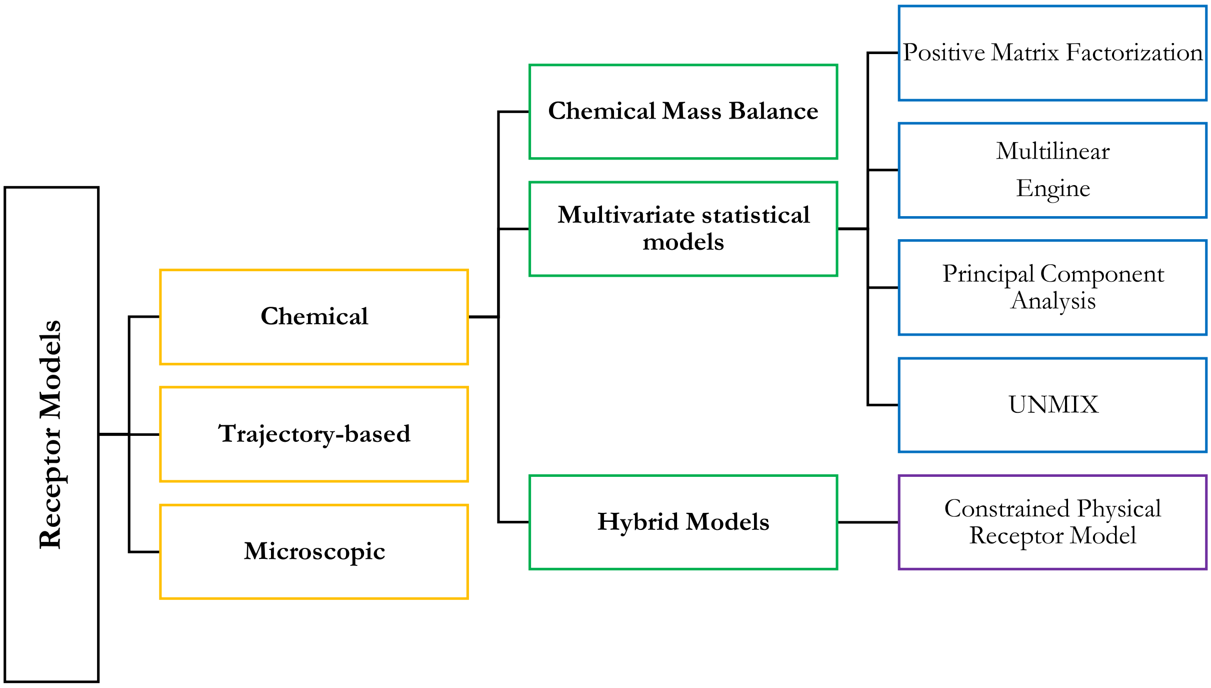

Figure 2: Types of receptor models

With the assumption that the relative concentrations of chemical species are preserved between sources and receptors, RMs use the principle of mass conservation for apportionment of PM mass to different air pollution sources. Thus, the concentration of a species measured in a particular sample can be described as (Hopke, 2003):

$$X_{ij} = \sum_{p=1}^{p} g_{ip} f_{pj} + e_{ij} \qquad (1)$$

Where
X_{ij} is the measured concentration of the jth species in the ith sample
f_{pj} is the concentration of the jth species in material emitted by the source p
g_{ip} is the contribution of the pth source to the ith sample and;
e_{ij} is the portion of the measurement that cannot be fitted by the model (i.e. residual).

Different RMs use different approaches to solve this equation, for e.g., the CMB model uses the effective-variance least squares method whereas UNMIX uses eigenvector analysis. Concentrations of trace elements (e.g. Si, Fe, Cu), ions (e.g. SO_4^{2-}), EC/OC and organic compounds (e.g. PAHs, alkanes, hopanes, alkanoic acids) are used as inputs for the models.

1.3.1 Factor Analysis Models

The multivariate models identify the emission sources based on inter-relationships between the various chemical species (Cooper and Watson, 1980; Thurston and Lioy, 1987).

There are a number of different methods based on factor analysis including PCA, PMF, UNMIX and ME. Such methods do not require a priori information about source emission characteristics and are useful in cases where relevant source profiles are not available (Hopke, 2003; Viana et al., 2008). In the simplest matrix form, the equation 2 can be represented as (Hopke, 2003):

$$X = GF' \qquad (2)$$

Where

X refers to the matrix of observed species' concentrations
G refers to the matrix of factor contributions
F refers to the matrix of factor loadings

Such methods require a substantial number (at least 50) of separate air samples and work best with a large dataset in which the number of samples far exceeds the number of analytical variables. A minimum variable to case ratio of 1:3 should be maintained in order to obtain accurate results (Thurston and Spengler, 1985). Past knowledge of source chemical profiles is used to assign factors to sources, and typically identification of six or seven different sources is a good outcome. Before PMF became widely adopted, PCA was widely used for the same purpose, but is less refined than PMF. Although both PCA and PMF are factor analysis tools, PMF is better since it has a non-negativity constraint, and unlike PCA, it does not produce negative factors. Traditionally, PMF was used with trace metal and ion data but some recent studies included organic species in the analysis (Heo et al., 2013; Jang et al., 2013). Input data plays an important role in the final results, and care has to be taken to ensure that this is of good quality and where possible uncertainties can be assigned to individual analytes.

Hybrid models such as target transformation factor analysis (TTFA) and the constrained physical receptor model (COPREM) have been designed to combine the features of CMB and factor analysis models with the aim of maximizing the advantages while minimizing the limitations of each model (Wahlin et al., 2003; Viana et al., 2008). The Multilinear Engine (ME) program also allows the use of source composition data to constrain the model, and can be used in conjunction with PMF to introduce source composition data.

1.3.2 Chemical Mass Balance Model

This model was first proposed in the 1970s (Miller et al., 1972; Friedlander, 1973) and has since been used for source apportionment studies for PM, PM-OC, PAHs and VOCs across the globe.

The CMB model uses the ambient measurement data for chemical species together with the associated uncertainty and source profiles for different sources as inputs and the output consists of estimates of contribution of each source to the total mass. There are a number of assumptions regarding the use of the model including (Gordon, 1980, 1988; Thurston and Lioy, 1987; Watson et al., 2002):

- chemical species do not react with one another and the species composition does not change between the source(s) and the receptor(s), i.e. all particles are primary
- number of species are more than the number of sources
- all of the potential sources are included the model
- source profiles are not collinear (i.e. non-similarity)
- uncertainties are random and non-correlated

However, particles can undergo physical (condensation/evaporation) and/or chemical transformations between the source and receptor (Friedlander, 1973). For example, some PAHs such as chrysene, benzo(a)pyrene and benzo(a)anthracene are known to show decay between the source and receptor while others such as indeno(123-cd)pyrene and benzo(ghi)perylene are relatively stable (Gordon, 1988).

The CMB model and the multivariate models have their own advantages and disadvantages. While the CMB model can theoretically be run with one sample, multivariate methods usually require a large number of samples (Thurston and Lioy, 1987). A comparative discussion on the two types of models is presented in Table 3.

It is important to note that while the multivariate models do not require any information on source emission composition, the CMB model requires the species abundances (in the form of source profiles) in each source as a model input. Source contribution estimates generated using the CMB model are also sensitive to the selection of fitting species (McLaren et al., 1996). Thurston and Lioy (1987) referred to multivariate models as "*hypothesis-generating models*" and CMB model as "*hypothesis-*

testing models" and recommended the use of multivariate models on chemical speciation data followed by CMB analysis for source identification and quantification.

Table 3: Comparison between CMB and multivariate models

(based on Gordon, 1980; Henry et al., 1984; Thurston and Lioy, 1987; Gordon, 1988; Harrison et al., 1997; Shrivastava et al., 2007; USEPA, 1997; Viana et al., 2008; Belis et al., 2013)

CMB Model	***Multivariate Models***
[i] A key prerequisite is detailed information about the sources/emission inventories as well as source profiles	[i] Qualitative information about the potential sources is enough, useful for areas where detailed emission inventories are not available and source profiles are not required
[ii] Only one sample is required	[ii] Require large numbers of samples
[iii] Does not apportion the secondary aerosols	[iii] Unable to account for spatial and temporal correlation between emissions (e.g. motor vehicle and road dust) or source identified may contain more than one source
[iv] Cannot take into account the time variation of the pollutant concentration or source emission	[iv] Often unable to produce a fine resolution of the sources
[v] Only non-reactive, stable tracer species can be used	[v] Some of the models allow negative contributions to sources which is physically impossible (e.g. PCA)
[vi] Near collinearity among source profiles can result in negative source contributions	[vi] Information like meteorological data, particle size etc can be incorporated in the analysis

One of the problems faced by receptor models is multicollinearity which occurs when two or more sources have similar emission profiles and it can affect the model estimates (Henry et al., 1984; Thurston and Lioy, 1987; Lowenthal et al., 1992). It can also be introduced due to meteorological factors such as wind, for e.g., for two factors that are located in the same direction from the receptor site (Gordon, 1988).

The CMB model uses the ambient measurement data for chemical species together with the associated uncertainty and source profiles for different sources as inputs, and the output consists of estimates of the contribution of each source to the total mass. Source profiles are

> "*the mass abundances, i.e. fraction of total mass of chemical species in source emissions, and such profiles are generally representative of source categories rather than individual emitters*" (Watson et al., 2002).

The model has several assumptions including non-reactivity of the chemical species and non-co-linearity of the source profiles (Watson et al., 2002). In addition, the number of species should be greater than the number of sources in order to derive results from the model. This model has been used extensively for source apportionment of PM mass (Schauer et al., 1996; Bi et al., 2007; Sheesley et al., 2007; Lambe et al., 2009; Stone et al., 2010; Yin et al., 2010; El Haddad et al., 2011; Rutter et al., 2011; Guo et al., 2012; Perrone et al., 2012; Green et al., 2013).

Since PM is composed of both inorganic (trace metals, cations and anions) and organic species, a range of source markers are used in receptor modelling studies. A summary is provided in Table 4.

Traditionally, most studies were carried out using trace elements such as Fe, Zn, Pb, Cr, Al and Ni. However, since many of the trace elements are emitted from a range of sources, it was difficult to apportion the PM to sources with a high degree of confidence (Lin et al., 2010). In addition, with removal of species such as Br and Pb from fuels, such markers cannot be used conclusively for source apportionment analyses. In the last two decades, research has focused on the identification and development of organic molecular markers for SA since they can be characteristic of sources, thus reducing the source ambiguity, and creating markers for sources which are difficult to be apportioned solely on the basis of inorganic markers.

With the idea that molecular marker compounds are emitted by specific sources and can be used to distinguish between PM sources, Schauer et al. (1996) proposed CMB modelling using organic molecular markers (hereafter referred to as CMB-MM). A number of source-specific organic molecular markers have since been proposed for use in CMB modelling. Key molecular markers include levoglucosan for wood burning, hopanes and steranes for vehicular emissions, higher n-alkanes for vegetative detritus, benzothiazoles for tyre wear and cholesterols and lactones for cooking (Rogge et al., 1993a, b, d; Schauer et al., 1996; Simoneit et al., 2004a; Lough et al., 2007; Heo et al., 2013). A detailed description of various organic markers for different sources has been compiled by Lin et al. (2010). However, it is important to be careful about the chemical stability of the organic species that are used in receptor modelling analysis.

Table 4: Marker species associated with major PM sources

Source	Key markers	References
Sea/Road Salt	Na, Cl, Mg	Harrison et al. (1996); Pey et al. (2010); Belis et al. (2013)
Mineral/Crustal Dust	Al, Ca, Si, Fe, Ti, Mg	Harrison et al. (1996); Chow et al. (2007a); Stone et al. (2010); Ondracek et al. (2011); Peltier et al. (2011)
Traffic	EC, Fe, Ba, Zn, Cu, Pb, Sn, Sb, Mo, Hopanes, Steranes, PAHs	Schauer et al. (1996); Birmili et al. (2006); Lin et al. (2010); Belis et al. (2013); Green et al. (2013)
Gasoline emissions	Coronene, Benzo[ghi]perylene, Indeno[123-cd]pyrene	Schauer et al. (1996); Chellam et al. (2005); Chow et al. (2007a); Fujita et al. (2007); Pant and Harrison (2014)
Diesel emissions	EC, fluoranthene, pyrene	Schauer et al. (1996); Chellam et al. (2005); Chow et al. (2007a); Riddle et al. (2007); Green et al. (2013); Pant and Harrison (2014)
Brake wear	Ba, Cu, Sb, Sn, Fe	Hildemann et al. (1991); Adachi and Tainosho (2004); Hjortenkrans et al. (2007); Amato et al. (2009a); Gietl et al. (2010); Ondracek et al. (2011)
Tyre wear	Zn, Benzothiazole, Organic Zn, Benzothiazolamine	Hildemann et al. (1991); Kumata et al. (2002); Adachi and Tainosho (2004); Amato et al. (2013a)
Natural gas emissions	Benzo[k]fluoranthene, Benzo[b]fluoranthene	Rogge et al. (1993c)
Ship emissions/fuel oil combustion	Ni, V	Harrison et al. (1996); Belis et al. (2013); Green et al. (2013); Cusack et al. (2013); Viana et al. (2009)
Coal combustion	Picene, BC, Sulphur , Se	Thurston and Spengler (1985); Cass (1998); Chowdhury et al. (2007); Stone et al. (2010); Davy et al. (2011)
Biomass combustion	K, Levoglucosan, Galactosan, Mannosan	Fine et al. (2001); Simoneit (2002); Lin et al. (2010); Stone et al. (2010)
Secondary Inorganic Aerosol	NH_4^+, SO_4^{2-}, NO_3^-	Harrison et al. (1996); Belis et al. (2013); Green et al. (2013); Cusack et al. (2013)
Vegetative detritus	N-alkanes (C29, C31)	Rogge et al. (1993d)
Construction	Ca, Al, Sr, Ti	Harrison et al. (2003); Chow et al. (2003); Amato et al. (2011a)
Secondary organic aerosol	Aromatic diacids, n-alkanoic acids, methylthreitrols	Schauer and Sioutas (2012)
Road surface wear	Na, Mg, Ba	Lawrence et al. (2013)

CMB model outputs are generally evaluated using several different parameters including:

[1] Goodness-of-fit parameters- R-square (r^2), chi-square (χ^2), degrees of freedom and the percent mass explained (i.e. percent of PM mass explained by the model based on measured PM). The r^2 value is calculated through linear regression between the observed and predicted values of fitting species. Values closer to 1 indicate that the source contribution estimates are predicted well and typically, 0.8-1.0 are considered acceptable. χ^2 is defined as "*the weighted sum of squares of the difference between calculated and measured values of fitting species*" (USEPA, 1997). A value of zero indicates no difference between the calculated and measured values and generally, a value less than 4 is acceptable.

[2] T-stat values- Defined as "*the ratio of the source contribution estimate and standard error*", this statistic is used to determine the significance of a particular source and a value less than 2 indicates that the source is at or below detection limit (USEPA, 1997).

[3] Calculated/Measured (C/M) ratio- Defined as the ratio between calculated and measured concentration) with acceptable values ranging between 0.75-1.5 (USEPA, 1997).

[4] Residual/Uncertainty (R/U) ratio- Defined as the ratio of signed difference between calculated and measured concentration, i.e. residual divided by standard error (uncertainty) with acceptable values ranging between -2 to +2 (USEPA, 1997).

[5] MPIN (modified pseudo inverse normalized) matrix- Refers to the diagnostic matrix which is used to identify the influential species for each source type. The matrix defines the contribution of individual fitting species in determination of the source contribution estimate and their variance. Species with values between 0.5 and 1 are classified as influential species (Chow et al., 2007a).

It is important to note that while the CMB model works well for attribution of primary organic carbon (POC) sources, it is not able to apportion secondary organic carbon (SOC), due to lack of appropriate source profiles. However, it is very difficult to generate SOC source profiles due to the complex chemistry of secondary organic aerosol formation (Bullock et al., 2008).

1.4 Traffic Particulate Matter Measurement and Analysis

Traffic emission profiles can be generated using several different methods including lab-based dynamometer studies, tunnel/roadway studies and twin-site studies (Rogge et al., 1993a; Lough et al., 2007; He et al., 2008; El Haddad et al., 2009; Yan et al., 2009). Since the twin site/tunnel/roadway measurements are carried out in the ambient environment, and for a mixed fleet, they are seen to be more representative of real-world emissions. In recent years, significant differences have been observed between laboratory-tested and real-world mixed source traffic emissions (Lighty et al., 2000; Gertler et al., 2002; Yan et al., 2009; Ancelet et al., 2011). Near roadside/kerbside, traffic tunnel and roadway/highway/freeway measurements are reported to be more realistic since they represent mixed-fleet emissions under real-world driving conditions (Steahlin et al., 1995; Phuleria et al., 2007). Table 5 presents a comparison on measurements made using dynamometers and ambient sampling. Ke et al. (2013) used an alternate approach and prepared a composite vehicular emission source profile using four different approaches including peak analysis, windless model-based regression analysis, PMF and UNMIX.

Tunnels are often used for analysis of emissions from road vehicles including estimation of emission factors and physical and chemical characterization of vehicular emissions (El-Fadel and Hashisho, 2000). Several studies have been conducted for measurement of PM emissions in roadway tunnels in different parts of the world including the USA (Fraser et al., 1998; Rogak et al., 1998; Abu-Allaban et al., 2002; Gertler et al., 2002), China (He et al., 2006; He et al., 2008), Europe (Stechmann and Dannecker, 1990; Smith and Harrison, 1996; Weingartner et al., 1997; Handler et al., 2008; El Haddad et al., 2009; Oliviera et al. 2011; Lawrence et al., 2013; Pio et al., 2013; Alves et al., 2015), New Zealand (Ancelet et al., 2011), Japan (Funasaka et al., 1998), Chile (Caceres et al., 1998), Brazil (Brito et al., 2013) and Mexico (Mancilla and Mendoza, 2012).

Use of dynamometers for preparation of source profiles limits the use since the profiles depend on the technology, fuel quality used, age and operating conditions of the vehicle (McLaren et al., 1996). On the other hand, tunnel/roadway measurements represent a mixture of the emission contributions from the vehicle fleet (Phuleria et al., 2007). However, the same has been said for the tunnel samples since the results are representative of the vehicles and driving cycles typical of the location where the sampling is conducted and cold start emissions are not included (Gertler and Pierson, 1996; Yanowitz et al., 2000). A qualitative comparison is presented in Table 5.

Table 5: Comparison between dynamometer and tunnel/roadway measurements

(Imhof et al., 2005; Phuleria et al., 2006; Phuleria et al., 2007; Handler et al., 2008; He et al., 2008; El Haddad et al., 2009; Sanchez-Ccoyllo et al., 2009; Franco et al., 2013)

Parameter	Dynamometer measurements	Ambient measurements (includes tunnels, roadways)
Test conditions	Precise and controlled conditions within laboratory; different test cycles and driving conditions can be analysed; can include cold-start emissions	Ambient environment- cannot be physically controlled; cannot include cold-start emissions Since sampling in conducted in ambient conditions, boundary conditions and dilution effects (in case of tunnel environment) However, atmospheric conditions can vary between tunnel and ambient environments
Representativeness for vehicle fleet	Low since tests are conducted on a sub-set of the in-use fleet and variations in engine type Vehicle age and maintenance and mixing of emissions from difference vehicles etc. are not accounted for. Particle aging effects are not accounted for.	High, since the measurements are made in ambient environment and for in-use mixed fleet.
Emission type accounted for	Exhaust (or non-exhaust based on experiment design)	Exhaust and non-exhaust (difficult to separate the two)

1.5 Objectives

This thesis was initially intended to focus on chemical speciation and receptor modelling of $PM_{2.5}$ in New Delhi (India). However, after one year of delays in instrument procurement and non-committal response towards sampling set-up, the Indian collaborators decided to step away from the project and it was subsequently abandoned. At this stage, the project was reformulated with the objective of improving receptor modelling of UK particulate matter. The only CMB receptor modelling study conducted in the UK (Yin et al., 2010) used USEPA SPECIATE profiles in the absence of local profiles from UK. However, while the CMB model provided an adequate fit for the data, there were uncertainties over the applicability of the North American dynamometer-based traffic profiles in the UK context. Receptor models also lacked robust and representative input data relating to non-exhaust emissions from road traffic. As a result, the following objectives were finalized:

1. Characterization of traffic aerosol ($PM_{2.5}$) in the UK and preparation of a composite traffic profile using different ambient monitoring methods (Chapters 3, 4)
2. Characterization of PM_{10} road dust and estimation of source contributions from non-exhaust sources (Chapter 5)

These research objectives also complemented other work being carried out by the group focusing on characterization of industrial and cooking emissions in the UK.

In early 2012, opportunities arose for a collaborative project in India, and the funding was approved in December 2012. As a result, a $PM_{2.5}$ speciation and receptor modelling study was undertaken in New Delhi in 2013-2014 in collaboration with Indian Institute of Technology-Delhi (India) and Desert Research Institute-Reno (USA). At the time of the sampling, further collaboration was sought with Indian Institute of Technology- Kanpur (India) and additional measurements were made for size-segregated aerosols in winter 2013.

Based on these gaps in the literature, the following additional objectives were finalized for this thesis:

3. Characterization of size-segregated aerosol and detailed chemical speciation of $PM_{2.5}$ in New Delhi, India (Chapter 6)
4. Characterization of PM_{10} road dust, and preparation of a road dust source profile (Chapter 5)

1.6 Thesis Structure

The thesis chapters are organized as follows:

Chapter 2 describes the general methods and procedures used during various sampling campaigns including the instrumentation and chemical analysis methods.

Chapter 3 describes results of a modelling study to assess the sensitivity of the CMB model to traffic profiles derived using different methods.

Chapter 4 describes results from chemical speciation of PM in Birmingham, UK and preparation of a chemical profiles for traffic emissions.

Chapter 5 presents results on chemical characterization and source estimation of PM_{10} road dust in Birmingham (UK) and New Delhi (India).

Chapter 6 describes details results from chemical speciation of PM at a heavy traffic site in New Delhi, India.

Chapter 7 describes the conclusions from the current study.

Chapter 8 provides recommendation for future work.

CHAPTER 2- MATERIALS AND METHODOLOGY

This chapter describes the various sampling campaigns and the analytical procedures.

Part of the sampling in Birmingham was carried out in collaboration with Amey (UK) while sampling in New Delhi was carried out in collaboration with Central Road Research Institute (CRRI) - New Delhi, Desert Research Institute (DRI), USA and Indian Institute of Technology (IIT)-Kanpur, India.

Graphical Abstract

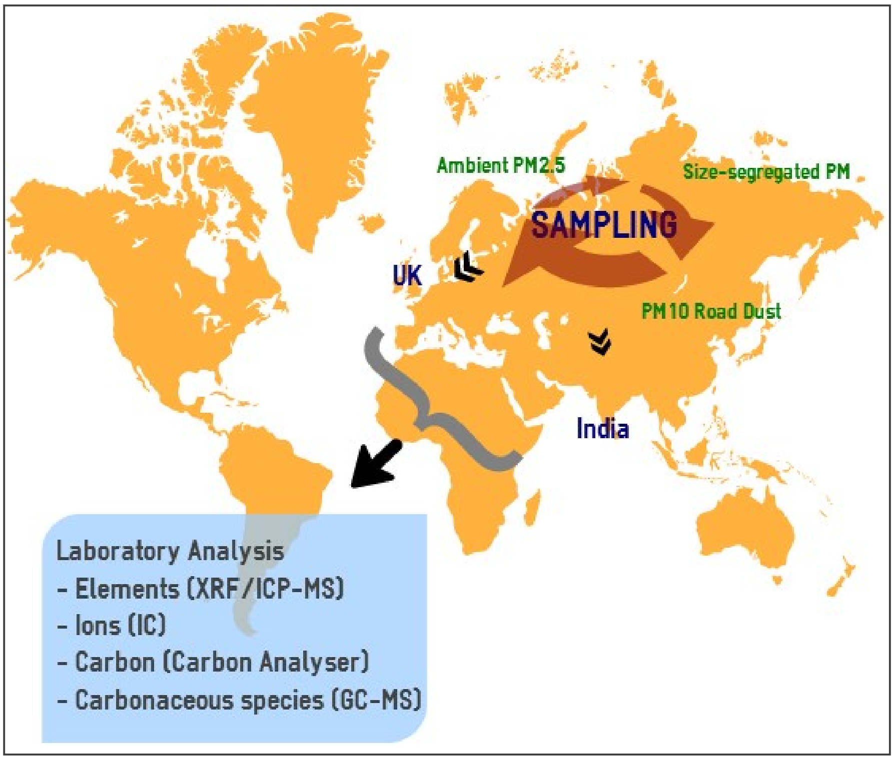

2.1 Overview

In line with the objectives of this thesis, primary data was collected via sampling in Birmingham (UK) in 2012 and 2013 and New Delhi (India) in 2013-14 for PM_x. In addition, a range of secondary datasets from Birmingham and London (UK) were used for data analysis although the sampling and chemical analysis was not completed during the PhD program. Datasets from Birmingham (2007-2008) and London (2010 and 2011) that have been used in CMB modelling analyses in Chapter 6 were collected by Dr. Jianxin Yin and Dr. Johanna Gietl as part of a DEFRA project and details of the sampling campaigns and chemical analysis are available in Yin et al. (2010), Harrison and Yin (2010), Gietl et al. (2010) and Harrison and Yin (2013). Appropriate references have also been included throughout the thesis to highlight these data sources.

The sampling campaigns and the analytical procedures are detailed in the following sections.

2.2 Sampling Instrumentation

Both ambient and road dust PM_x samples were collected in this study in United Kingdom and India. Owing to differences in availability of sampling instrumentation, different sampling equipment were deployed in India and UK for ambient PM measurements. However, road dust samples were collected using the same instrument in both countries. The following sections detail the various sampling equipment that were used during the study.

2.2.1 High Volume Sampler

The instrument uses the filtration/impaction method for collection of PM samples and the size of PM collected can be chosen based on the sampler head (Figure 3). Since the instrument uses an automated filter exchange mechanism, up to 15 filters can be loaded at a time.

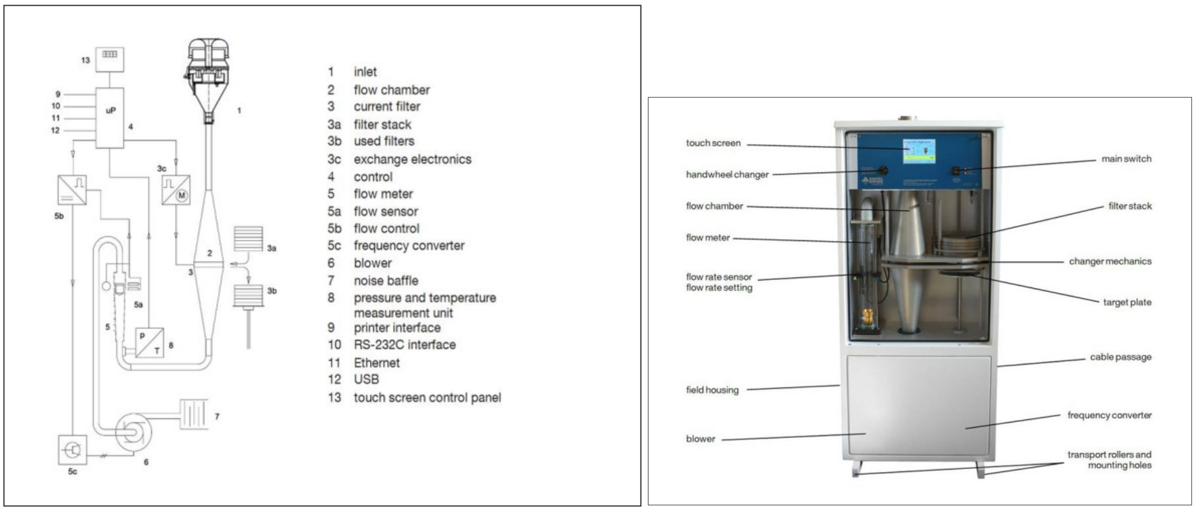

Figure 3: Layout of the high volume sampler *(Enviro Technology Services Plc, n.d.)*

2.2.2 Low Volume Sampler

In Delhi, $PM_{2.5}$ samples were collected using the Airmetrics MiniVol™ portable air samplers that operate at 5 lpm and collect $PM_{2.5}$ aerosol fraction using the principle of filtration. Use of low volume sampler was more suitable in Delhi since the area records high PM concentrations, and use of lower flow rates can help minimize clogging.

2.2.3 Micro Orifice Uniform Deposition Impactor (MOUDI)

Size-segregated aerosol samples were collected using an 8-stage micro-orifice uniform deposit impactor (MOUDI™) (MSP Corporation, Minneapolis, Minnesota, USA) in Birmingham (rotating MOUDI) and New Delhi (non-rotating MOUDI) (Figure 4). The sampler consists of a series of impaction plates with decreasing diameters and works on the principle of inertial impaction (Marple et al., 1991). Each impaction plate has micro-orifice nozzles and as the jet of air passes through each stage, particles larger than the cut size are collected on the impaction plate while particles with smaller diameters proceed to the next stage. The cut-off size can be estimated using the Stokes Number and for all practical purposes, the Stokes number with 50% collection efficiency is used to calculate the cut-off size. The rotating set-up allows even deposition of the particles across the filter. At 30 litres per minute (lpm), samples are collected in the range of 0.18-10 µm (10, 5.6, 3.2, 1.8, 1.0, 0.56, 0.32 and 0.18 µm). In the event that a flow rate of 30 lpm is not achieved, the cut points can be adjusted using the Equation 3.

$$\textbf{Corrected } D_p = D_p\sqrt{\frac{F_1}{F_2}} \qquad (3)$$

Where
D_p is nominal cut point
F_1 is nominal flow rate (30 lpm)
F_2 is recorded flow rate

Using the data obtained from MOUDI samples, a continuous mass size distribution ($dM/dlogD_p$) was obtained using the numerical inversion method described in Keywood et al. (1999). This approach has previously used in several studies (Allen et al., 2001a; Gietl et al., 2010).

Figure 4: Layout of the MOUDI sampler *(MSP Corporation, n.d.)*

2.2.4 Road Dust Sampler

For the collection of PM_{10} road dust samples, a custom-built PM_{10} dust sampler based on the specifications proposed by Amato et al. (2009a) was used (Figure 5). Particles are vacuumed off the road with the help of a vacuum pump (flow rate of 25 lpm), and upon entering the sampling chamber, heavier particles tend to settle down. Smaller particles in the air flow pass through a *Negretti* elutriation filter (based on the principle of gravitational settling) which allows particles with an average density of PM_{10} to pass through (dependent on the flow rate). These particles are subsequently deposited on a filter and can be used for chemical analysis. Each sample was collected over an area of $1m^2$ for a period of 10 minutes. Samples were collected close to the signal-controlled pedestrian crossings, and covered both the middle lane and the side lanes.

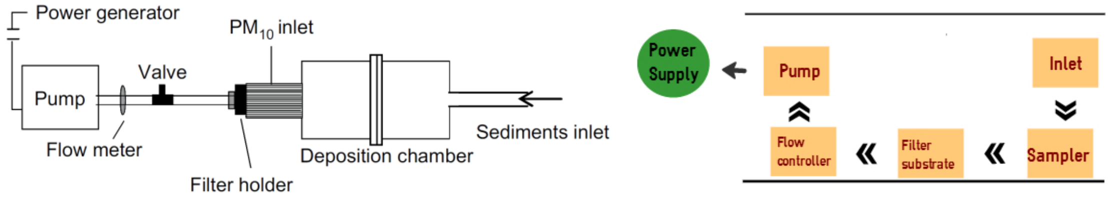

Figure 5: Road dust sampling set-up *(reproduced from Amato et al., 2009a)*

2.3 Filter Selection and Artefacts

A wide range of filters are available for chemical speciation and analysis of particulate matter. Quartz fibre filters, composed of SiO_2, can withstand high temperatures and are the most commonly used substrate for analysis of organic species (e.g. carbon, PAHs, alkanes). They are more suitable for sample collection using high volume samplers since they are less prone to clogging (Chow and Watson, 2012). Polytetrafluoroethylene (PTFE) filters were used for gravimetric analysis since they are not prone to absorption of ambient water vapour.

Sampling artefacts can occur due to adsorption and volatilization depending on ambient conditions (e.g. temperature, RH) and can vary based on filter type. Quartz filters are prone to artefacts which can be produced either by the adsorption of gas-phase organic compounds (positive) or volatilization of compounds from the filter (negative) (Hildemann et al., 1991). Examples include volatilization of NH_4NO_3 and adsportion of water vapour and gas-phase species.

High and low-volume samplers have different face velocities and previous studies have concluded that low volume samplers have larger positive artefacts (Viana et al., 2006). This is due to the fact that the adsorption of gas-phase species is inversely related to face velocity.

In the current study, no corrections were made for the artefacts.

2.4 Sampling Locations

PM sampling was conducted at four different sites in Birmingham, UK, and at one site in New Delhi, India:

- Birmingham, UK
    - *Low-traffic site* (University Ring Road South)- University campus (Chapter 5)
    - Urban background site (hereafter referred to as EROS[2]) - Located within the university campus, but not close to any major sources. (Chapters 3,4)
    - *High traffic site* (hereafter referred to as BROS[3]) – Located adjacent to the university campus, this is one of the major roads running across Birmingham. (Chapter 5)

---

[2] Elms Road Observatory Site

[3] Bristol Road Observatory Site

    - *Traffic tunnel* (hereafter referred to as QT[4]) - This road tunnel runs through the centre of Birmingham city and carries both intra- and intercity traffic. (Chapters 4, 5)
- New Delhi
    - *Heavy traffic road* (hereafter referred to as CRRI) - This site is located next to Mathura Road/National Highway 2. (Chapters 5,6)

Details about the site characteristics are presented in individual chapters.

2.5 Sampling Campaigns

Sampling was undertaken in Birmingham (UK) in 2012 and 2013 and in New Delhi (India) in 2013 and 2014 and the campaigns are summarized in Table 6.

2.5.1 Birmingham, United Kingdom

A two-week intensive sampling campaign was conducted from September 11, 2012 to September 21, 2012 at the Elms Road Observatory Site (EROS) and the A38 Queensway Tunnel, Birmingham (QT).

PM_{10} road dust samples were collected in September 2012 at QT and June-July 2013 at campus site and BROS.

2.5.2 New Delhi, India

---

[4] Queensway Tunnel

Two sampling campaigns were undertaken in New Delhi, India in summer (June 15-30, 2013) and winter (December 15, 2013- January 15, 2014). PM_{10} road dust samples were also collected in June 2013 at the same site using the dust sampler. A summary is provided in Table 6.

Table 6: Overview of the sampling campaigns

City	**Site**	**Sampler**	**Sample type**	**Size Fraction**	**Chemical Analysis**			
					EC/ OC	**Trace Metals**	**Ions**	**Organic Markers**
Birmingham (UK)	QT and EROS	High volume sampler	Quartz	$PM_{2.5}$	x	x		x
		MOUDI	PTFE	Various		x		
		Road Dust Sampler	PTFE	PM_{10}		x		
	BROS and University Ring Road (South)	Road Dust Sampler	Quartz	PM_{10}	x			x
			PTFE	PM_{10}		x		
New Delhi (India)	CRRI	Minivol	Quartz	$PM_{2.5}$	x	x		x
			PTFE	$PM_{2.5}$		x	x	
		MOUDI	PTFE	Various		x		
		Road Dust Sampler	PTFE & quartz		x	x		x

2.6 Analytical Procedures

Chemical analysis of the samples collected during the campaigns was conducted at the University of Birmingham (UK) and Desert Research Institute (USA). Table 7 summarizes the type of analysis conducted for each set of samples.

Samples collected in New Delhi using Minivol samplers were shipped to USA for chemical analysis.

Table 7: Summary of laboratory analysis of PM samples

Site	Sample type	Sampler	Gravimetric Analysis	Elemental Analysis	Carbon Analysis	Molecular Marker Analysis
Birmingham (UK)	$PM_{2.5}$	High Volume Sampler	UoB	UoB	UoB	UoB
	Size-segregated aerosol	MOUDI	UoB	UoB	N/A	N/A
	Road Dust	Dust Sampler	UoB	UoB	UoB	UoB
New Delhi (India)	$PM_{2.5}$	Low Volume Sampler	DRI	DRI	DRI	DRI
	Size-segregated aerosol	MOUDI	UoB	UoB	N/A	N/A
	Road Dust	Dust Sampler	UoB	UoB	UoB	UoB

2.6.1 Filter Preparation

The quartz fibre filters were heated in a box furnace at 500° Celsius for 6 hours to remove any carbon impurity and then packed in aluminium foil, sealed in bags and stored in a freezer at -20° Celsius until sampling.

The PTFE filters used for collecting MOUDI samples at the QT site were washed with 3M HCl followed by ultra high purity (UHP) water and dried in a laminar flow cabinet before sampling.

All exposed filters were wrapped in aluminium foil (quartz filters) or stored in clean petri dishes (PTFE filters), sealed in polyethylene bags and stored in a designated freezer where no other chemicals or standards were stored.

2.6.2 Gravimetric Analysis

The PTFE filters were weighed before and after sampling to determine the mass of PM collected during the sampling. A Sartorius Model MC5 microbalance (sensitivity- 1 μg) was used for weighing the filters. Before weighing, all filters were equilibrated in humidity (35-45% relative humidity) and temperature (25° Celsius) controlled windowless room for 24 hours. An ionizing blower and an α-particle source (^{210}Po) were used to reduce the effects of static electricity on the filter. Each filter was weighed three times and both positive and negative weights were recorded. Average weights were calculated using the arithmetic mean of the six recorded values. Sampled mass was calculated as the difference between the mass of the filter before and after sampling.

2.6.3 Clean-up Procedures

2.6.3.1 Element/Ion Analysis

All the glass/plastic ware used for the extraction procedure were soaked in 2% high purity HNO_3 (Aristar Grade) for 24 hours and thereafter rinsed with deionised water three times. Afterwards, all the glassware/ plastic ware was dried in the oven at 20-25° Celsius.

The plastic bottles and the LDPE tubes used for extraction of MOUDI samples were cleaned with 10% HCl, 10 % HNO_3 and 0.1 M HCl (clean) in sequential order. The bottles were thereafter rinsed with deionised water and dried in a laminar flow cabinet. Between extractions, the Teflon bombs were filled with aqua regia (made with HPLC [high purity] grade HCl and HNO_3) and sealed with acrylic caps and stored in a fume hood for 24 hours. Thereafter, the bombs were washed with MΩ water and filled with 0.1 N HCl (HPLC grade) and heated for 24 hours. The bombs were then washed with MΩ water, dried in the laminar flow cabinet and used again.

Unless otherwise mentioned, 18.2 MΩ distilled deionised water [DDW] (Elga filtration system) was used for cleaning as well as extraction procedures.

2.6.3.2 Analysis of Organic Species

All the glassware were soaked in a mild soap solution for 24 hours and thereafter washed with deionised water 3 times. Afterwards, all the glassware was dried in the oven at 100° Celsius. Before starting the extraction process, all glassware was rinsed with acetone and dichloromethane (DCM) three times. All the syringes were rinsed with hexane, DCM and methanol before and after use. The CERTAN vials used for storage of standards and preparation of standard mixtures were cleaned with DCM, methanol and hexane before use. The vials and inserts (Agilent vial insert 250μl glass with polymer feet, 5181-1270) used for storage of samples were cleaned with acetone and DCM before use.

Unless otherwise mentioned, laboratory grade hexane and HPLC grade acetone, DCM and methanol were used for all the analyses.

2.6.4 Limit of Detection

Blank filters were analysed with the analytical techniques as described in the sections 5.5-5.8 to calculate limit of detection (LoD) using the formula 3*standard deviation.

2.6.5 Analysis of Elements

Two different procedures were used for extraction of trace metals: reverse aqua regia (RAR) for total metal concentration and chemical fractionation for one set of samples where both total and soluble fractions of metals were determined. Only total metal methods and results are reported here. In addition, Si, Al, Fe and S were analysed using XRF since the RAR extraction method is not very efficient for these elements.

Extraction of the trace metals was performed in 4 ml Nalgene polypropylene bottles using reverse aqua regia solution prepared using 2 ml of 189 cm^3/L high purity (Aristar Grade) hydrochloric acid (HCl) and 66 cm^3/L high purity (Aristar Grade) nitric acid (HNO_3) per sample (Allen et al., 2001). The polypropylene bottles were heated to 100º Celsius for 30 minutes in the hot water bath (Grant Y14) followed by mild sonication at 50º Celsius for 30 minutes in an ultrasonic bath (Decon F510006 Ultrasonic Bath). The process was repeated once, and the extracts were transferred to 15 ml polypropylene bottles. In the case of quartz filters, the samples were filtered using 0.45 µm Acrodisc syringe filters (Pall Acrodisc, 0.45 µm with Supor Membrane). The extracts were stored at 4º Celsius until analysis. In some cases, further dilution was performed before analysis with the ICP-MS. Good recovery has been reported for most elements based on this method (Allen et al., 2001).

The MOUDI samples collected at QT and EROS were extracted using the chemical fractionation methodology to calculate total and soluble concentrations of various elements. To extract the total element fraction, exposed filters were placed in Teflon bombs and 1 ml of HF and 3 ml of HNO_3 were added to each sample. The bombs were heated for 24 hours at 150ºC and then the caps were removed to allow the HF to dry. Once the samples were dry, 5 ml of 2 M HNO_3 and 5 ml of DDW were added and the bombs were heated for 24 hours at 150ºC. The samples were then transferred into pre-cleaned and labelled LDPE tubes and stored at - 20ºC until analysis. This method has previously been used by Shi et al. (2011).

The samples were analysed for Al, Fe, S and Si using a Wavelength Dispersive X-Ray Fluorescence (WD-XRF) instrument (Tiger Bruker S8) prior to chemical extraction and metals such as Cu, Zn, Ba, Ti, Sb, Ni, Mn and Ca were analysed using Inductively Coupled Plasma Mass Spectrometry (ICP-MS, Agilent 7500ce with an Octopole Reaction System). Internal standards for the ICP-MS analysis include Sc (45), Ge (72), Y (89), In (115) and Bi (209). Calibration curves were prepared using a range of standard solutions (0-100 ppb, and 0-10 ppm). Filter blanks were analysed with the sample batches and the samples were blank corrected.

The samples from Delhi were analysed for elements from Na to U at DRI using ED-XRF (PANalytical Epsilon 5) and calibration was performed using μMatter thin film standards.

2.6.6 Analysis of Ions

10 ml deionised water was added to each sample and the mixture was shaken for 45 minutes using a mechanical shaker. The samples were filtered using 0.45 μm Acrodisc syringe filters, transferred to IC vials and stored in the refrigerator at 4ºC until analysis. Analysis was performed using a Dionex ICS 3000. Calibrations were performed using standards of known concentration in the range of 0.05-10 ppm. Filter blanks were analysed with the sample batches and the samples were blank corrected.

The samples from Delhi were analysed for elements for sulphate (SO_4^{2-}), nitrate (NO_3^-), chloride (Cl^-). Ammonium (NH_4^+), sodium (Na^+) and potassium (K^+). These samples were also analysed for carbohydrates (mono- and disaccharides and anhydrosaccharides).

2.6.7 Analysis of Organic Species

Before the extraction, each sample was spiked with 25 μl of the isotopically-labeled internal standard mixture including ααα -20R-cholestane-d4 (for hopanes), dibenz(ah)anthracene-d14 (for PAHs) and octacosane-d58 (for alkanes). The samples were then extracted using 10-20 ml of DCM under mild sonication at 25º Celsius using an ultrasonic bath. The extracts were then filtered through pre-cleaned glass wool and sodium sulphate (Na_2SO_4) columns and collected in pre-cleaned 30 ml bottles. The samples were then concentrated to 250 μl under a gentle stream of oxygen-free nitrogen and transferred to pre-cleaned GC vials. The samples were transferred to amber teflon-lid lined vials, sealed using Parafilm (Laboratory Film M) and stored in the freezer at -20º Celsius until analysis. Analysis was undertaken by direct injection of the sample into the GC-MS system (Agilent GC- 6890N plus MSD-5973N) fitted with an HP-5MS (30 m, 0.25 mm diameter, 0.25 μm thickness) column. A number of different classes of compounds including n-alkanes (11), PAHs (8) and hopanes (9) were analysed using different selective ion monitoring (SIM) programs (Table 8). Instrument detection limits are provided in Table 9.

Quantification of the different compounds was performed using deuterated (internal) standards. Six to eight point calibration curves were prepared using pure natural compound standards in the concentration range of 1-2000 pg/μl for each class of compounds ($r^2>0.994$ for all compounds). Chromatograms were analysed using the Agilent Chemstation software.

The ion source in the GC-MS system was regularly cleaned and the instrument was tuned with perfluorotributylamine (PFTBA) to calibrate the mass analyser and optimize peak (m/z) identification. Filter blanks were analysed with the sample batches and the samples were blank corrected.

At DRI, the samples from Delhi were analysed for straight chain alkanes, PAHs, hopanes and steranes using Thermal Desorption-Gas Chromatography-Mass Spectrometry (TD-GC-MS; Agilent 6890 GC with Model 5973) with an HP-5MS capillary column (Table 10). Internal standards used in the analysis include $nC_{16}D_{34}$ and $nC_{24}D_{50}$ for alkanes and phenanthrene-d_{10} and chrysene-d_{12} for PAHs. No internal standards were used for hopane and sterane analysis.

Filter punches were taken from the filter sample and injected with the internal standards. Next, the punches were cut into smaller pieces and loaded into a Pyrex glass tube and the tube was then placed into the injection port. The septum cap was subsequently closed and the sample was analysed in SCAN mode using the method described in Table 11. Details about the TD-GC-MS methodology are provided in Ho and Yu (2004).

Table 8: GC-MS SIM programs for the different compound classes

GC Condition	Compound class	
	Alkanes, Hopanes	**PAHs**
Injector temperature (ºC)	300	300
Initial Oven Temperature (ºC)	60	45
Initial Oven Hold Time (min)	0	2
Initial Oven Temperature Ramp Rate (ºC/min)	10	20
Second Oven Temperature (ºC)	250	150
Second Oven Hold Time (min)	5	-
Second Oven Temperature Ramp Rate (ºC/min)	5	4
Final Oven Temperature (ºC)	300	300
Final Oven Hold Time (min)	15	10
Carrier Gas	He	
Carrier Gas flow rate	1mL/min	
Injector Mode	Splitless	

MS Condition	Compound class	
	Alkanes and Hopanes	**PAHs**
Solvent delay (mins)	20	5
Data Collection Mode (SIM)	Alkanes: 57, 71, 82, 85, 98 Hopanes: 191 Octacosane-d58: 66 [internal standard- alkanes] aaa-20R-cholestane-d4: 221 [internal standard- hopanes] Dwell time: 50-100 millisecond	Benzo(b,k)fluoranthene, Benzo(a,e)pyrene, Perylene: 252 Indeno (123-cd)pyrene, Benzo(ghi)perylene: 276 Picene, Dibenz(ah)anthracene: 278 Coronene: 300 Dibenz(ah)anthracene- d14: 292 [internal standard- PAHs] Dwell time: 50-100 millisecond

Table 9: Instrument limits of detection

Compound	Instrument LoD (µg/filter)
Ions	
Chloride	1.5005
Nitrate	1.5005
Sulphate	1.5005
Ammonium	1.5005
Na^+	0.2362
K^+	0.1498
Elements	
Sodium (Na)	3.754
Magnesium (Mg)	1.134

Aluminum (Al)	0.448
Silicon (Si)	0.361
Phosphorus (P)	0.118
Sulfur (S)	0.051
Chlorine (Cl)	0.049
Patassium (K)	0.046
Calcium (Ca)	0.073
Scandium (Sc)	0.194
Titanium (Ti)	0.035
Vanadium (V)	0.008
Chromium (Cr)	0.038
Manganese (Mn)	0.083
Iron (Fe)	0.076
Cobalt (Co)	0.004
Nickel (Ni)	0.013
Copper (Cu)	0.044
Zinc (Zn)	0.039
Gallium (Ga)	0.128
Arsenic (As)	0.015
Selenium (Se)	0.029
Bromine (Br)	0.041
Rubidium (Rb)	0.027
Strontium (Sr)	0.063
Yttrium (Y)	0.038
Zirconium (Zr)	0.101
Niobium (Nb)	0.067
Molybdenum (Mo)	0.064
Palladium (Pd)	0.155
Silver (Ag)	0.147
Cadmium (Cd)	0.115
Indium (In)	0.127
Tin (Sn)	0.137
Antimony (Sb)	0.206
Cesium (Cs)	0.058
Barium (Ba)	0.063
Lanthanum (La)	0.043
Cerium (Ce)	0.042
Samarium (Sm)	0.086
Europium (Eu)	0.133
Terbium (Tb)	0.098
Hafnium (Hf)	0.395
Tantalum (Ta)	0.258
Wolfram (W)	0.361

Iridium (Ir)	0.119
Gold (Au)	0.196
Mercury (Hg)	0.097
Thallium (Tl)	0.065
Lead (Pb)	0.094
Uranium (U)	0.165
Carbon	
OC Fraction 1	0.052
OC Fraction 2	1.29
OC Fraction 3	3.87
OC Fraction 4	0.129
PC via transmittance	0.129
PC via reflectance	0.129
EC Fraction 1	0.039
EC Fraction 2	0.039
EC Fraction 3	0.039

Species	**Instrument LoD (µg/filter)**
Sugars	
Glycerol (C_3H_8O)	0.410
Erythritol ($C_4H_{10}O_4$)	0.015
Arabinose ($C_5H_{10}O_5$)	1.773
Xylose ($C_5H_{10}O_5$)	0.066
Arabitol ($C_5H_{12}O_5$)	0.525
Xylitol ($C_5H_{12}O_5$)	0.963
Levoglucosan ($C_6H_{10}O_5$)	1.008
Mannosan ($C_6H_{10}O_5$)	0.410
Galactose ($C_6H_{12}O_6$)	1.602
Fructose ($C_6H_{12}O_6$)	0.782
Glucose ($C_6H_{12}O_6$)	0.840
Inositol ($C_6H_{12}O_6$)	0.030
Sorbitol ($C_6H_{14}O_6$)	3.293
Mannitol ($C_6H_{14}O_6$)	0.974
Trehalose ($C_{12}H_{22}O_{11}$)	1.148
Maltitol ($C_{12}H_{24}O_{11}$)	0.645
Organic Acids	
Formic acid (CH_2O_2)	2.152
Acetic acid (CH_4O_2)	0.167
Oxalic acid ($C_2H_2O_4$)	0.661
Lactic acid ($C_3H_6O_3$)	1.774
Methanesulfonic acid (CH_4O_3S)	0.672

Malonic acid ($C_3H_4O_4$)	0.193
Maleic acid ($C_4H_4O_4$)	6.597
Succinic acid ($C_4H_6O_4$)	0.015
Glutaric acid ($C_5H_8O_4$)	2.400

Species	**Instrument LoD (µg/filter)**
Hopanes	
22,29,30-trisnorneophopane (Ts) (C27)	0.002
22,29,30-trisnorphopane (C27)	0.002
αβ-norhopane (C29αβ-hopane)	0.001
22,29,30-norhopane (29Ts)	0.003
αα- + βα-norhopane (C29αα- + βα -hopane)	0.003
αβ-hopane (C30αβ -hopane)	0.002
αα-hopane (30αα-hopane)	0.002
βα-hopane (C30βα -hopane)	0.002
αβS-homohopane (C31αβS-hopane)	0.004
αβR-homohopane (C31αβR-hopane)	0.004
αβS-bishomohopane (C32αβS-hopane)	0.004
αβR-bishomohopane (C32αβR-hopane)	0.004
22S-trishomohopane (C33)	0.004
22R-trishomohopane (C33)	0.004
22S-tretrahomohopane (C34)	0.004
22R-tetrashomohopane (C34)	0.004
22S-pentashomohopane(C35)	0.004
22R-pentashomohopane(C35)	0.004
Steranes	
ααα 20S-Cholestane (C27)	0.003
αββ 20R-Cholestane (C27)	0.003
αββ 20s-Cholestane (C27)	0.003
ααα 20R-Cholestane (C27)	0.001
ααα 20S 24S-Methylcholestane (C28)	0.002
αββ 20R 24S-Methylcholestane (C28)	0.002
αββ 20S 24S-Methylcholestane (C28)	0.002
ααα 20R 24R-Methylcholestane (C28)	0.003
ααα 20S 24R/S-Ethylcholestane (C29)	0.004
αββ 20R 24R-Ethylcholestane (C29)	0.002
αββ 20S 24R-Ethylcholestane (C29)	0.002
ααα 20R 24R-Ethylcholestane (C29)	0.002
Alkanes	
Pentadecane (*n*-C15)	0.004
Hexadecane (*n*-C16)	0.004
Heptadecane (*n*-C17)	0.003
Octadecane (*n*-C18)	0.003
Nonadecane (*n*-C19)	0.002
Eicosane (*n*-C20)	0.002

Heneicosane (*n*-C21)	0.004
Docosane (*n*-C22)	0.003
Tricosane (*n*-C23)	0.003
Tetracosane (*n*-C24)	0.003
Pentacosane (*n*-C25)	0.003
Hexacosane (*n*-C26)	0.003
Heptacosane (*n*-C27)	0.001
Octacosane (*n*-C28)	0.003
Nonacosane (*n*-C29)	0.004
Triacontane (*n*-C30)	0.004
Hentriacotane (*n*-C31)	0.004
Dotriacontane (*n*-C32)	0.004
Tritriactotane (*n*-C33)	0.003
Tetratriactoane (*n*-C34)	0.003
Pentatriacontane (*n*-C35)	0.003
Hexatriacontane (*n*-C36)	0.004
Heptatriacontane (*n*-C37)	0.004
Octatriacontane (*n*-C38)	0.004
Nonatriacontane (*n*-C39)	0.004
Tetracontane (*n*-C40)	0.004
PAHs	
Acenaphthylene (C12)	0.011
Acenaphthene (C12)	0.006
Fluorene (C13)	0.004
Phenanthrene (C14)	0.002
Anthracene (C14)	0.001
Fluoranthene (C16)	0.001
Pyrene (C16)	0.002
Benzo[a]anthracene (C18)	0.003
Chrysene (C18)	0.002
Benzo[b]fluoranthene (C20)	0.004
Benzo[j+k]fluoranthene (C20)	0.001
Benzo[a]fluoranthene (C20)	0.002
Benzo[e]pyrene (C20)	0.004
Benzo[a]pyrene (C20)	0.004
Perylene (C20)	0.004
Indeno[1,2,3-cd]pyrene (C22)	0.002
Dibenzo[a,h]anthracene (C22)	0.004
Benzo[ghi]perylene (C22)	0.003
Coronene (C24)	0.003
Dibenzo[a,e]pyrene (C24)	0.001
Dibenzothiophene (C12)	0.005
9-Fluorenone (C13)	0.005

1-Methylphenanthrene (C15)	0.004
2-Methylphenanthrene (C15)	0.005
9-Methylanthracene (C15)	0.004
3,6-Dimethyl phenanthrene (C16)	0.005
Methylfluoranthene (C17)	0.006
11H-Benzo(a)Fluorene (C17)	0.005
Retene (C18)	0.006
Benzo[ghi]fluoranthene (C18)	0.002
Benzo(c)phenanthrene (C18)	0.004
Benzo[b]naphtho[1,2-d]thiophene (C16)	0.005
Cyclopenta[cd]pyrene (C18)	0.001
Benz[a]anthracene-7,12-dione (C18)	0.005
Methylchrysene (C19)	0.002
Benzo(b)chrysene (C22)	0.004
Picene (C22)	0.005

Table 10: Organic species analysed in samples from Delhi using TD-GC-MS

Species Class	**Compounds analysed**
N-alkanes	C18- C40
PAHs	Acenaphthylene (Acy), Acenaphthene (Ace), Fluorene (Flu), Phenanthrene (Phe), Anthracene (Ant), Fluoranthene (FluA), Pyrene (Pyr), Chrysene (Chr), Benzo[a]anthracene (B[a]A), Benzo(c)phenanthrene (BcPhe), Benzo[b]fluoranthene (BbF), Benzo[j,k]fluoranthene (BjkF), Benzo[e]pyrene (BeP), Benzo[a]pyrene (BaP), Dibenzo[a,h]anthracene (DahA), Perylene (Per), Picene (Pic), Benzo(b)chrysene (BbC), Indeno[1,2,3-cd]pyrene (IcdP), Benzo(ghi)perylene (BghiPe), Dibenzo(ae)pyrene (DaeP), Coronene (Cor), Retene (Ret), Benz[a]anthracene-7,12-dione (B(a)AQ), Benzo(ghi)fluoranthene (B(ghi)F), 9-Methylanthracene (9MA), 1 Methyl phenanthrene (1MPhe), 2 Methyl phenanthrene (2MPhe), Benzo(a)fluoranthene (BaF), Methylfluoranthene (MFluA), Benzo(b)naphtho[1,2-d]thiophene (BN21T), Cyclopenta[cd]pyrene (CcdP), Dibenzothiophene (Dbt) and Methylchrysene (MChr), 11H-Benzo(a)fluorene (11H-BaF), 9-Fluorenone (FluO) and 3, 6-Dimethylphenanthrene (DMPhe)
Hopanes	22,29,30-trisnorneophopane (TNOHO), 22,29,30-trisnorphopane, C29αβ-hopane, 22,29,30-norhopane , C29αα- + βα –hopane, C30αβ–hopane 30αα-hopane, C30βα –hopane, C31αβS-hopane (SHHO), C31αβR-hopane (RHHO), C32αβS-hopane (SBHHO), C32αβR-hopane (RBHHO), 22S-trishomohopane (STHHO), 22R-trishomohopane (RTHHO), 22S-tretrahomohopane (STEHHO), 22R-tretrahomohopane (RTEHHO), 22S-pentahomohopane (SPHHO) and 22R-pentahomohopane (RPHHO).
Steranes	ααα 20S-Cholestane (ααα 20SC), αββ 20R-Cholestane (αββ 20RC), αββ 20S-Cholestane (αββ 20SC), ααα 20R-Cholestane (ααα 20RC), ααα 20S 24S-Methylcholestane (ααα 20S24S MC), αββ 20R 24S-Methylcholestane (αββ 20R24S MC), αββ 20S 24S-Methylcholestane (αββ 20S24S MC), ααα 20R 24R-Methylcholestane (ααα 20R24RMC), ααα 20S 24R/S-Ethylcholestane (ααα 20S 24R/S EC), αββ 20R 24R-Ethylcholestane (αββ 20R24R EC), αββ 20S 24R-Ethylcholestane (αββ 20S24R EC), ααα 20R 24R-Ethylcholestane (ααα 20R24R EC)
Sugars	Saccharides: Fructose, Glycerol, Mannitol, Inositol, Erythritol, Xylitol, Arabitol, Sorbitol, Trehalose, Arabinose, Glucose + Xylose, Fructose, Galactose + Maltitol Anhydrosaccharides: Levoglucosan, Mannosan

Table 11: GC-MS SIM programs for the different compound classes using TD-GC-MS

Parameter	**Condition**
Injector temperature (°C)	50 (increased to 275 over 11 minutes to desorb the organic species)
Initial Oven Temperature (°C)	30
Initial Oven Hold Time (min)	11 min (during desorption) + 2 minutes
Initial Oven Temperature Ramp Rate (°C/min)	10
Second Oven Temperature (°C)	120
Second Oven Hold Time (min)	-
Second Oven Temperature Ramp Rate (°C/min)	8
Final Oven Temperature (°C)	310
Final Oven Hold Time (min)	20
Carrier Gas	He
Carrier Gas flow rate	
Injector Mode	Splitless

2.6.8 Carbon Analysis

Elemental, organic and total carbon were analysed using a 1cm^2 punch from the quartz filter sample using the Sunset Laboratory Thermo-Optical Carbon Aerosol Analyzer. The EUSAAR2 (European Supersites for Atmospheric Aerosol Research) protocol was used for the measurement of carbon (Cavalli et al., 2010). The instrument uses methane (CH_4) gas as an internal standard and multi-point external sucrose solution standards were used for quality control. The carbon fractions (organic and elemental) are operationally defined; elemental carbon (EC) refers to "*the thermally refractory carbon fraction released in oxidising conditions*" (He/O_2) while the rest of carbon is designated as organic carbon (OC) which is released in non-oxidising (He) conditions. In the first phase, the sample (filter punch of 1 or 1.5 cm^2) was heated in step-wise temperature ramps to 650°C (200, 300, 450 and 650) and using a MnO_2 catalyst, the adsorbed vapours were converted into CO_2 which was subsequently reduced to CH_4 in a methanator oven (hydrogen enriched nickel catalyst). The concentration of the CH_4 was measured using a flame ionization detector (FID). After cooling the filter for a short period, the same process was repeated in the second phase with step-wise increase in temperature (500, 550, 700 and 850) but under oxidizing conditions (He/O_2). The filter sample was continuously measured for light transmission at 678 nm, and the filter transmission value (point at which the filter transmission is equal to transmission at the beginning) was used to derive the split point. Typically, carbon measured before the split point is referred to as OC and carbon measured after the split point is referred to as EC. However, during the temperature ramps, some of the organic carbon can undergo charring and form pyrolytic carbon (PC) which is then detected as EC. Based on the filter transmission values, the endpoint of PC evolution can be determined. At the point where the laser transmission is equal to the transmission value at the beginning, all PC is expected to be evolved completely. Internal calibration was performed using a fixed amount of CH_4 at the end of every sample.

Instrument detection limits were calculated to be 0.83 ± 0.04 $\mu g/cm^2$ for OC, 0.0002 ± 0.0000 $\mu g/cm^2$ for EC and 0.83 ± 0.04 $\mu g/cm^2$ for TC.

Filter blanks were analysed with the sample batches and the samples were blank corrected.

Samples from Delhi were analysed using the DRI Model 2001 Thermal/Optical Carbon analyser with the IMPROVE_A protocol (Chow et al., 2007b). Eight carbon fractions (OC1, OC2, OC3, OC4, OP, EC1, EC2, EC3) were analysed for each sample. The temperature profile for the measurement corresponds with the different fractions- OC1 (140°C), OC2 (280°C), OC3 (480°C), OC4 (580°C), OP (580°C), EC1 (580°C), EC2 (740°C) and EC3 (840°C). OC is defined as the sum of OC1-4 and OP and EC is defined as the sum of EC1-3 minus any OP.

Measurements conducted using EUSAAR2 and IMPROVE_A protocols can vary, partly due to differences in the measurement principle (reflectance/transmittance), as well as differences in temperature ramps (Chow et al., 2004). Querol et al. (2013) highlighted the underestimation of EC with EUSAAR2 protocol.

2.6.9 Quantification of Ambient Concentration

The following formula was used for calculation of ambient air concentrations:

$$Concentration\ in\ air = \frac{(M \times V)}{v_t} \qquad (4)$$

Where
M is concentration value obtained from the instrument (GC-MS/ICP-MS/IC)
V is final volume of the sample extract (µl/ml)
v_t is sampling time *flow rate (calculated based on the instrument)

2.6.10 Data Analysis

Microsoft Excel and SPSS 21.0 were used for data analysis. Receptor modelling was performed using the USEPA CMB Model 8.2. Details of the CMB model are described elsewhere (Chapters 1 and 3).

CHAPTER 3- SENSITIVITY OF THE CMB MODEL TO $PM_{2.5}$ TRAFFIC PROFILES

This chapter reports results for a chemical mass balance (CMB) model from a comparison of road traffic source profiles derived from dynamometer studies and ambient measurement-based profiles. Secondary data generated as part of a DEFRA project (Harrison and Yin, 2013) was utilized for preparation of a composite $PM_{2.5}$ traffic profile, and subsequently tested with the CMB model.

This chapter is adapted from the following research paper:

Pant, P., Yin, J. and Harrison, R.M. (2014) Sensitivity of a chemical mass balance model to different molecular marker traffic source profiles. **Atmospheric Environment**, 82: 238-249.

Graphical Abstract

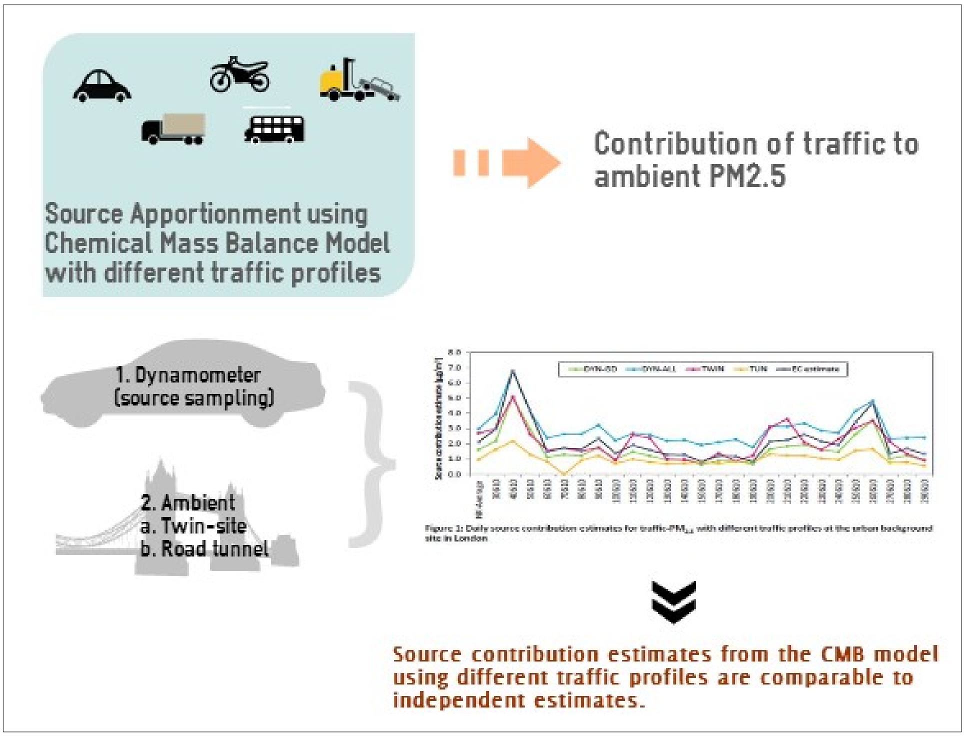

3.1 Introduction

Road traffic is one of the key urban air pollution sources, and in the last few decades a significant amount of research has been undertaken in order to understand the emission characteristics as well as processes that govern vehicular emissions (Shi and Harrison, 1999; Charron and Harrison, 2003; Phuleria et al., 2007; El Haddad et al., 2009).

In the UK, road traffic emissions contribute nearly 30% of the total $PM_{2.5}$ and constitute 30-50% of the urban and roadside increments of PM (AQEG, 2012). However, there has not been much analysis focused on the chemical characterization of traffic PM in the country, and the only published receptor modelling study using CMB (Yin et al., 2010) used non-local source profiles. AQEG (2012) recommended detailed analysis of exhaust emissions in order to improve the understanding of emission characteristics and their potential contribution to ambient PM.

The objectives of this study include:

- preparation of an ambient data-based composite traffic emissions profile ($PM_{2.5}$)
- assessment of the sensitivity of the CMB model to traffic profiles created using different techniques

To the best of our knowledge, this is the first study in the UK (and Europe) to prepare a traffic emissions profile based on ambient data.

3.1.1 Chemical Mass Balance Model

As described in Chapter 1, receptor models utilize the PM composition data to determine its sources, and quantify their contributions. Such models assume that the concentrations of chemical species are preserved between sources and receptors, and use the principle of mass conservation for apportionment of PM mass to various air pollution sources. The CMB model uses the ambient measurement data for chemical species together with the associated uncertainty and source profiles for different sources as inputs, and the output consists of estimates of the contribution of each source to the total mass. The model has several assumptions including non-reactivity of the chemical species and non-co-linearity of the source profiles (Watson et al., 2002). In addition, the number of species should be greater than the number of sources in order to derive results from the model. General principles underlying the model and the assumptions in the models are described in Chapter 1. A large number of markers can be used for source apportionment including EC, trace metals and organic species. In the case of traffic emissions, EC, PAHs, hopanes and several elements including Fe, Cu, Ba and Zn have been used as source markers.

3.2 Methods

$PM_{2.5}$ samples were collected in Birmingham in 2007-2008 and London (UK) in the years 2010 (summer) and 2011 (winter) respectively. Both sets of data were collected by Dr. Jianxin Yin and Dr. Johanna Gietl under a DEFRA project.

3.2.1 Sampling Locations

3.2.1.1 Urban Background (Birmingham)

The urban background site in Birmingham, Elms Road Observatory Site (EROS), was located in an open field within the University of Birmingham campus (further description in Chapter 4).

3.2.1.2 Rural (Birmingham)

The rural site was located about 20 kilometres west of Birmingham at a distance of about 200 metres from the A451, a moderate to heavily-trafficked road. The site is surrounded by unused land/grass.

3.2.1.3 Urban Background (London)

This site was located in a cabin within a school campus in a residential area in west London (7 kilometres from central London) at a distance of 10 metres from the road. Equipment from the national Automatic Urban and Rural Network (AURN) is also hosted at this site.

3.2.1.4 Urban Roadside (London)

The roadside site was located on the kerbside of a heavily trafficked (ca. 80,000 vehicles per day) six-lane highway (A501, Marylebone Road) running through a street canyon in central London. The sampling station was located at a distance of 1 metre from the road at height of 3 metres. The site was located opposite the Madame Tussauds Museum and is surrounded by residential and commercial buildings. Equipment from the national AURN is also hosted at this site.

3.2.2 Sampling and Chemical Analysis

$PM_{2.5}$ samples were collected on 150 mm quartz fibre filters using Digitel high volume samplers (DHA-80) in summer and winter seasons for a period of 24 hours in London. In Birmingham, 24 hour PM2.5 samples were collected for the first 5 days of every month on 20 cm x 25 cm quartz fibre filters using a Tisch TE-6070 high volume sampler. In addition, 24 hour PTFE filter samples (PM_{10} and $PM_{2.5}$) were also collected at all sites using a collocated dichotomous Partisol sampler.

OC and EC were measured using the Sunset Laboratory Thermal-Optical Carbon Analyser, molecular markers including hopanes, straight-chain alkanes, PAHs and levoglucosan were measured using GC-MS (Agilent GC-6890N plus MSD5973N) and Al and Si were measured using WD-XRF (Philips® MAGIX-PRO automatic sequential wavelength dispersive X-ray Fluorescence spectrometer). Ions (SO_4^{2-}, NO_3^-, Cl^-) were measured using ion chromatography (Dionex ICS-2000).

Further site details for Birmingham and London and chemical analysis procedures are available in Yin et al. (2010), Harrison and Yin (2010) and Gietl et al. (2010) respectively. Only $PM_{2.5}$ samples were used for this study.

The source profile was prepared using collocated samples from kerbside (Marylebone Road) and urban background (North Kensington) sites in London. Samples from the Birmingham sites (n= 28 for each site) and the samples from the urban background site (n= 30) in London were used for the CMB analysis.

3.3 Model Parameters

The USEPA CMB 8.2 model was used for the estimation of source contribution to $PM_{2.5}$-OC. Six key sources were included in the model runs including vegetative detritus (Rogge et al., 1993d), wood smoke (Fine et al., 2004; Sheesley et al., 2007), natural gas (Rogge et al., 1993c), coal combustion (Zhang et al., 2008), road dust (Chow et al., 2003) and traffic (described in the next section). Species used in the data analysis include elements (Al, Si), n-alkanes (C25-C35), hopanes (trisnorhopane [TNOHO], hopane [HOP], norhopane[NHO], S- and R-homohopanes [S+R HHO], S- and R-bishomohopanes [S+R BHHO], and S- and R-trishomohopanes [S+R THHO]), PAHs (benzo(a)pyrene [BaP], benzo(b)fluoranthene [BbF], benzo(a)fluoranthene [BkF], Picene [Pic], indeno(123-cd)pyrene [IcdP], benzo(ghi)perylene[BghiPe]) and levoglucosan.

Model outputs were evaluated using several different parameters. As a first step, goodness-of-fit parameters, r^2 and chi^2 values were checked and a chi-square value less than 4 and r^2 value between 0.8-1.0 were considered acceptable. T-stat values were used to determine the significance of a particular source, and a value less than 2 indicates that the source is at or below the detection limit. Other parameters included the species' C/M ratio and R/U ratio with acceptable values ranging between 0.75-1.5 and -2 to +2 respectively. Species that did not fit within the range were removed from subsequent runs but a base number of species were always included to ensure that the number of species is more than the number of sources. The MPIN (modified pseudo-inverse normalized) matrix was used as a diagnostic tool to identify the influential species for each source type with influential species showing values between 0.5 to 1 (Chow et al., 2007a). A discussion on the parameters is provided in Chapter 1.

3.4 Source Profiles

Selection of appropriate source profiles is one of the critical steps towards obtaining a good fit with the CMB model. Source signature refers to the mix of tracer elements and/or molecular markers used for identification of sources. Profiles are created using emission samples from a range of emitters of a particular source category and conducting physical and chemical analyses to arrive at the contributions of each tracer element/compound (Watson et al., 2002). A number of studies have reported source profiles for a wide range of sources (Rogge et al., 1993a, b, c, d; Fine et al., 2004; Zhang et al., 2008; Yan et al., 2009). Sampling methodologies include hot and diluted exhaust sampling, ground-based sampling, airborne sampling, grab sampling and re-suspension in laboratory (Watson et al., 2002).

Source profiles are used for identification of source contributions to particulate matter using CMB model as well as to compare and validate results obtained from factor analysis models. The CMB model relies to a large extent on the accuracy of the source profiles used as input. However, in the absence of locally-relevant source profiles, the source contribution estimates can be prone to erroneous results. Further, in recent years, significant differences have been observed between laboratory-tested and real-world mixed source traffic emissions (Ancelet et al., 2011; Yan et al., 2009).

The typical components of any source profiles are found to be more-or-less similar although the mass abundances vary depending on location and emitter characteristics. For example, soil/road dust is often found to contain elements such as Al, Si, Ca and Fe. Thus, different combinations of source profiles can provide statistically valid yet completely different solutions (Robinson et al., 2006a). The selection of source profiles is thus critical to obtaining a good solution from the CMB model.

Traffic emission profiles can be generated using several different methods including lab-based dynamometer studies, tunnel studies and twin-site studies (Rogge et al., 1993a; Lough et al., 2007; He et al., 2008; El Haddad et al., 2009; Yan et al., 2009). Since the twin site/tunnel/roadway (kerbside) measurements are carried out in the ambient environment, and for a mixed fleet, they are seen to be more representative of real-world emissions. Details about different methods for preparation of road traffic profiles are presented in Chapter 1.

A number of papers have reported the estimation of the contribution of traffic emissions to total PM or a component of PM using twin-site studies (Yan et al., 2009; Bukowiecki et al., 2010; Gietl et al., 2010; Oliveira et al., 2010; Pey et al., 2010). With the assumption that all sources other than traffic (including any local or regional sources) have the same impact at both roadside and a nearby background site, the increment at the roadside site obtained using the equation 5 is used as a local traffic increment estimate (Yan et al., 2009; Wang et al., 2010).

$$Increment(X) = Concentration(X)_{roadside} - Concentration(X)_{background} \quad (5)$$

Where
Concentration(X) refers to the concentration of species X at roadside or background sites

3.4.1 Profile derived from Twin-site data

To prepare a dimensionless profile for PM, the ratio of each of the species with respect to PM concentration for the same location needs to be calculated (Landis et al., 2007). In this study, a similar approach was used, and since it is assumed that the difference between the roadside and background site is the traffic increment (as in equation 5), the formula was modified accordingly (equation 6).

$$Source\ profile\ value\ (X) = \frac{X_{roadside} - X_{background}}{OC_{roadside} - OC_{background}} \qquad (6)$$

Where
(X) refers to the concentration of species X at roadside or background sites

Table 12 presents the source profile that was prepared using this approach derived from measurements at the heavily-trafficked Marylebone street canyon site (Galatioto and Bell, 2013) and the typical urban background site of North Kensington (Bigi and Harrison, 2010). The source profile value represents the species' mean value and standard deviation refers to the profile uncertainty. Daily winter campaign samples (n = 26) were averaged to obtain the profile and the average standard error was used as source profile uncertainty. A similar approach has been reported by Yan et al. (2009) for preparation of a traffic profile for Georgia, USA. The traffic mix on Marylebone Road is broadly representative of UK traffic (Table 13). However, since the profile was generated based on a select group of organic markers, and the unique site characteristics at the roadside site (Marylebone Road) in London might have introduced some bias in the results.

Table 12: Source composition profile for traffic based on twin sites from London (this study-TWIN), tunnel site from France (El Haddad et al., 2009-TUN) and 80% of concentration data from the roadside site in London (this study-R80) (all values in µg/µg of OC)

Compound	TWIN (mean ± s.d.)	TUN (mean ± s.d.)	R80 (mean ± s.d.)
EC	1.600±1.440	2.72±0.49	1.620±1.440
TNOHO	0.00005±0.00004	0.00010±0.00001	0.00007±0.00004
NHO	0.000200±0.00017	0.00036±0.0005	
HOP	0.00014±0.00012	0.00027±0.0005	0.00016±0.00010
(S+R) HHO	0.00020±0.00018	0.00028±0.00004	0.00026±0.00015
(S+R) BHHO	0.00030±0.00025	0.00010±0.00002	0.00036±0.00021
(S+R) THHO	0.00028±0.00022	0.00008±0.00002	0.00029±0.00018
BghiPe	0.000080±0.000055	0.000003±0.0000002	0.00011±0.00006

Table 13: Percentage of fleet for different vehicle types (in vehicle kilometres)

Road type	Cars & Taxis	Goods Vehicles	Buses & Coaches	Light Vans	Motorcycles
Motorways	75.2	11.7	0.45	12.2	0.42
Rural A roads	78.5	6.7	0.67	13.4	0.78
Urban A roads	82.1	3.23	1.51	12.1	1.10
Minor Rural Roads	78.6	2.35	0.88	17.2	0.99
Minor Urban Roads	81.7	1.29	1.82	13.7	1.50
Marylebone Road	75.4	1.80	5.81	13.6	3.36

Uncertainty for the various organic species in the profile was observed to be much higher compared to other published real-world and lab-based profiles. Similar observations of high uncertainties in ambient data have been reported by Yan et al. (2009) and Peltier et al. (2011) and may reflect in part, different traffic mixes on different days as well as higher uncertainties associated with ambient sampling. In addition, since twin-site data uses two different data points, the uncertainty is larger.

3.4.2 Tunnel Profile

This was derived from measurements in a road tunnel in France reported by El Haddad et al. (2009). The profile (Table 12) was prepared by normalizing the species concentration in $PM_{2.5}$ against OC concentration in $PM_{2.5}$ to derive the concentration in terms of μg (species)/μg of OC.

3.4.3 Dynamometer Profiles

Separate source profiles for gasoline, diesel and smoking (high-polluting) engines were taken from the work of Lough et al. (2007) derived from measurements of emission from US vehicles made using dynamometers.

3.4.4 Comparison of Source Profile with Other Published Profiles

Concentrations of most of the organic markers are broadly similar across the ambient data profiles with the exception of PAHs for which the tunnel profile from France reported lower PAH concentrations than roadside profiles from the UK and USA (Figure 6). This may be related to the very high uptake of diesel vehicles in France. However, the freeway measurements by Phuleria et al. (2007) appear to suggest higher emissions from diesel vehicles. The dynamometer gasoline profile was observed to be very similar to the profiles derived from ambient data.

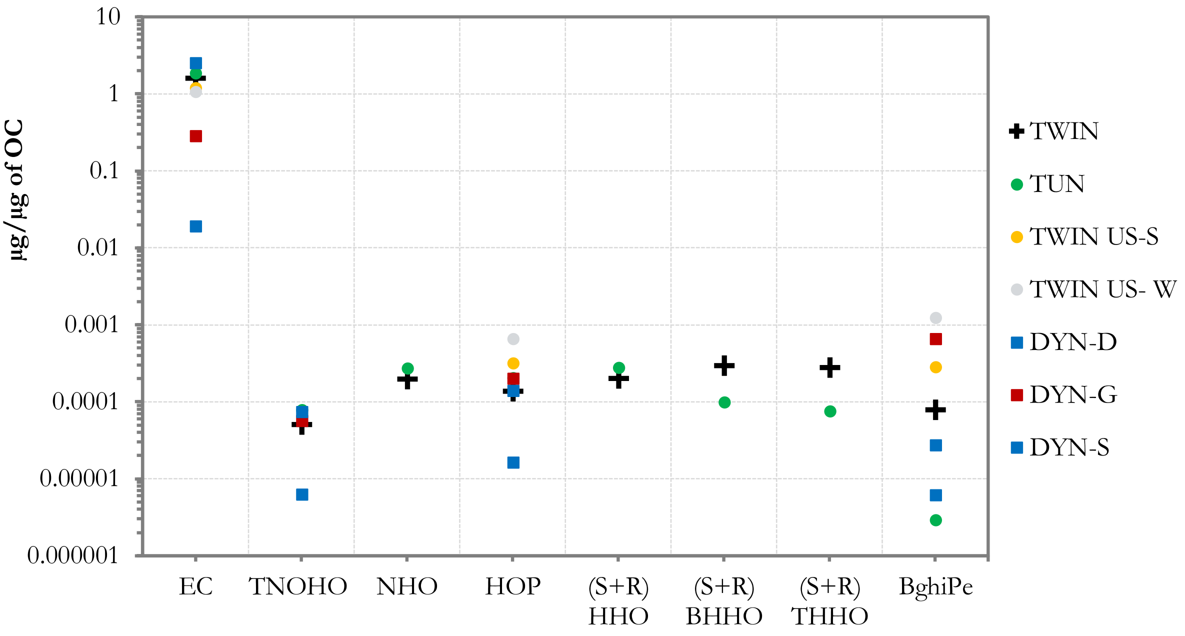

Figure 6: Comparison of London profile with other traffic and dynamometer profiles

(TWIN- profile from this study; TUN- El Haddad et al. (2009); TWIN US- S &W- Yan et al., 2009; DYN-D, G &S- Lough et al., 2007)

Ambient concentration data for hopanes from London and Birmingham were compared with a wide range of traffic profiles using ratio-ratio plots. Such plots are defined as

> "*scatter plots of ratios constructed with data from three species, i.e. two species (which are the target species) whose values are normalized using the third reference species*" (Robinson et al., 2006a).

While the aggregation of the ambient data around a point signifies that CMB can produce a good result with a single source profile, distribution of data along a diagonal line indicates the need for at least two distinct profiles for good results. Plotting the source profiles with ratio-ratio plots using specific markers can be useful for determination of the most relevant source profiles and such plots have been used previously for comparison of ambient data with source profiles (Subramanian et al., 2006; Dutton et al., 2009; Gao et al., 2011).

Ambient data for hopanes and EC from London and Birmingham were plotted together with source profiles derived from laboratory dynamometer studies, as well as real-world mixed traffic emissions collected from the literature (Schauer et al., 1999; Watson et al., 1998; Schauer et al., 2002; Lough et al., 2007; El Haddad et al., 2009; Yan et al., 2009) as illustrated in Figure 7. The composite traffic profile was found to be significantly different from lab-generated source profiles, while the comparison with other ambient traffic profiles revealed a similarity between ambient measurement data and ambient profiles, although the uncertainty (expressed as the standard deviation of daily data) is typically much higher for ambient profiles. The differences between the profiles were smaller in the case of homohopanes and bishomohopanes. Differences among the various profiles can be attributed to changes in vehicle technology over time and the dynamic fleet mix. Significant differences in the source profiles have been reported for different vehicle categories (Oanh et al., 2010). Use of different sampling and analytical protocols may also have an influence.

The ambient air data in the case of hopane-EC plots generally fit to a straight line, suggesting a variable mixture of two sources, presumably reflecting gasoline and diesel vehicles. However, the huge difference in concentrations between the ambient air data and the majority of the dynamometer profiles is unexplained. The diesel dynamometer profiles generally appear to be to the left of the gasoline profiles, but lie in a totally different region of the plot to the ambient air data. This may relate to the rapidly evolving technology of diesel vehicles, and the different vehicle types studied. In particular, the reductions in smoke emissions, and hence EC, from diesels will have led to increased hopane/EC ratios in newer vehicles.

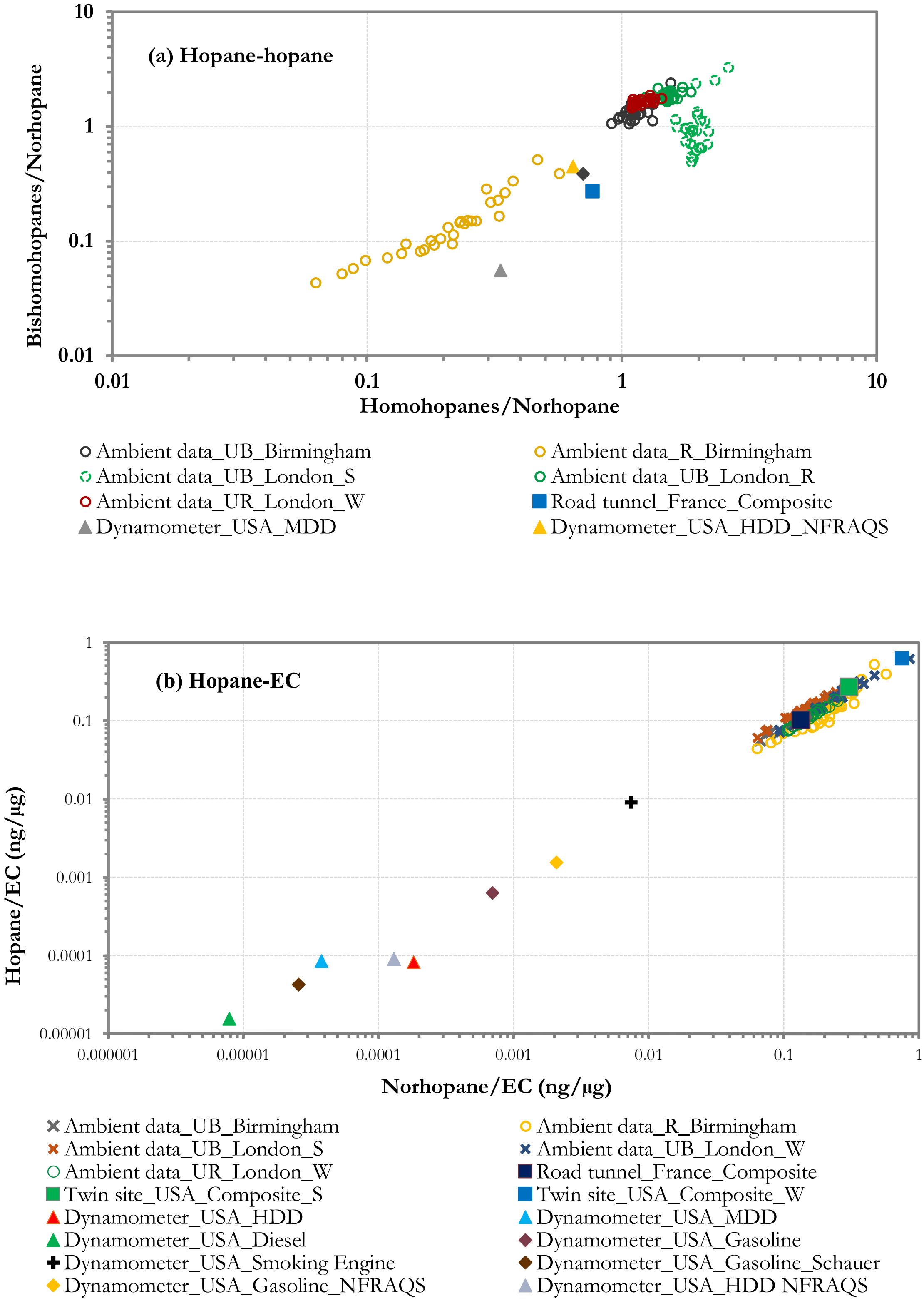

Figure 7: Comparison of source profiles derived from ambient air measurements and dynamometer studies using ratio-ratio plots

3.5 Estimation of Traffic Particle Mass and Mass Closure

Ambient concentrations measured in London (2010 summer data) and Birmingham (2007 data) were analysed using the CMB model to calculate source contributions to $PM_{2.5}$ OC with the aim of comparing the sensitivity of the model to different types of traffic profiles. Three different traffic profiles were tested, i.e. dynamometer profiles for diesel, gasoline and smoking engines (hereafter referred to as DYN) (Lough et al., 2007), a twin-site London profile (hereafter referred to as TWIN) and a France tunnel profile (hereafter referred to as TUN) (El Haddad et al., 2009). The smoking engine profile used in the analysis includes off-road engines and Lough et al. (2007) reported smoker profiles to impact the estimation of source contribution from gasoline, diesel and smoker vehicles. In order to understand the contribution from the smoking engine profile, two analyses were conducted for the DYN profile: gasoline and diesel engine only (DYN-GD) and gasoline, diesel and smoking engines (DYN-A). For comparison, the average data from each of the sites was also run with a traffic profile consisting of 80% of the concentrations of the chemical species measured at the roadside site in London (hereafter referred to as R80). For coal combustion, wood combustion and road dust, a number of source profiles were tested initially to choose the best profile for the ambient measurement data and the selected profiles were then used together with different traffic profiles to obtain final results. A number of different source profiles were run and the statistical outputs such as standard error and the C/M ratio were assessed for each profile.

Based on equation 7, "other OC" was calculated which is the OC unaccounted for by primary sources, and taken to represent secondary OC (SOC) (Yin et al., 2010).

$$Other\ OC = Measured\ OC - \sum SCEs\ (primary\ sources) \qquad (7)$$

Several other authors have also used the same approach and have also assumed the "Other OC" to be SOC (Subramanian et al., 2007; Docherty et al., 2008; Stone et al., 2009). Source contributions to $PM_{2.5}$ mass were then calculated using ratios of $PM_{2.5}$ mass/$PM_{2.5}$ OC for each source applied to the $PM_{2.5}$-OC SCEs obtained using CMB modelling as detailed in Yin et al. (2010). These were added to estimates of contributions from other sources (marine aerosol, sulphates, nitrates) using factors from the Pragmatic Mass Closure Model (Harrison et al., 2003) to test overall $PM_{2.5}$ mass closure.

In the CMB model, r^2 and χ^2 values were observed to be between 0.96-1.00 and 0.02- 2.70 respectively. As discussed in chapter 1, values lower than 4 are acceptable. Only the species with C/M ratio between 0.75-1.5 and R/U ratio between -2- +2 were used for the model runs. In addition, any profiles with a negative source contribution or a t_{stat} <1 were removed from subsequent runs and markers for the different sources were monitored using the MPIN matrix available in the CMB model runs and were cross-validated with published marker data (Table 14).

Table 14: Key markers used for the sources for both sites *(based on MPIN matrix)*

Source	*Key Marker (value of 1.00)*
Vegetative detritus	n-alkanes (A29, A31, A33)
Wood Smoke	Levoglucosan
Natural Gas	Benzo(k)fluoranthene
Coal combustion	Picene, Benzo(e)pyrene
Road dust	Si
Traffic	Benzo(ghi)perylene/ EC/Hopanes
Diesel engines	EC
Gasoline engines	Benzo(ghi)perylene
Smoking engines	Hopanes

In the case of the daily data, although overall correspondence was observed between CMB runs using DYN and TWIN and TUN in terms of identification of sources and OC mass attribution, there were variations in certain cases with higher or lower attribution of a particular source. In some cases, however, while for one model, a source was deemed insignificant (t_{stat} value < 2), the other models showed it as a significant source. It is important to note that a t_{stat} value >2 indicates 95% or more confidence in the estimates.

Results for apportionment of OC appear in Table 15. Across all scenarios, the total traffic contribution to OC varied as DYN-A> TWIN> DYN-GD> TUN. The DYN-A profile attributed more OC to vehicles (including off-road engines) than the DYN-GD, TWIN and TUN profile. However, at both the urban background and rural sites in Birmingham, the results were comparable between DYN-A and TWIN profiles and DYN-GD and TUN profiles. Interestingly, while the TWIN profile used benzo(ghi)perylene as the key marker for traffic, the TUN profile used EC as the key marker. In the case of DYN profiles, EC, hopanes and benzo(ghi)perylene were observed to be the key markers for diesel, smoking and gasoline engines respectively. In the case of the London data, the DYN-A scenario causes the primary sources in the model to account for > 100% of OC without any SOC, which is clearly implausible. In the Birmingham data, the choice of profile does not impact greatly on the outcome. The R80 profile produced very similar results to the TWIN profile (Table 15; Figure 8). The traffic SCEs using TUN and DYN-A and DYN-GD were also compared against the traffic SCE using TWIN profile, and while good correlation was observed for urban background sites (r^2>0.75), the correlation was much weaker in case of the rural site (r^2~ 0.25-0.35).

When mass closure of $PM_{2.5}$ is attempted including other major sources using the coefficients reported by Harrison et al. (2003), closure is generally good, especially for the Birmingham data (Figure 9). The DYN-A run attributes a larger $PM_{2.5}$ mass to road traffic than the other profiles, especially in the London data. Predictably, as for OC results, the total $PM_{2.5}$ mass apportioned to traffic varied as DYN-A> TWIN> DYN-GD> TUN. Overall mass closure is good for both urban and rural sites and winter and summer seasons (Table 15). Results for the R80 profile are not discussed for $PM_{2.5}$ since very similar SCEs were observed for this profile compared to the TWIN profile.

The CMB/Pragmatic Mass Closure Model resolved the PM mass reasonably well with all profiles with 89.8- 129.7% of $PM_{2.5}$ mass resolved across all data sets (Table 15, Figure 9) and the DYN-GD profile models the highest percentage mass across all sites. In general, all the CMB models (based on dynamometer profiles and the composite profiles) were able to apportion approximately similar OC mass, although dynamometer-based profiles apportioned a higher percentage of OC mass to traffic.

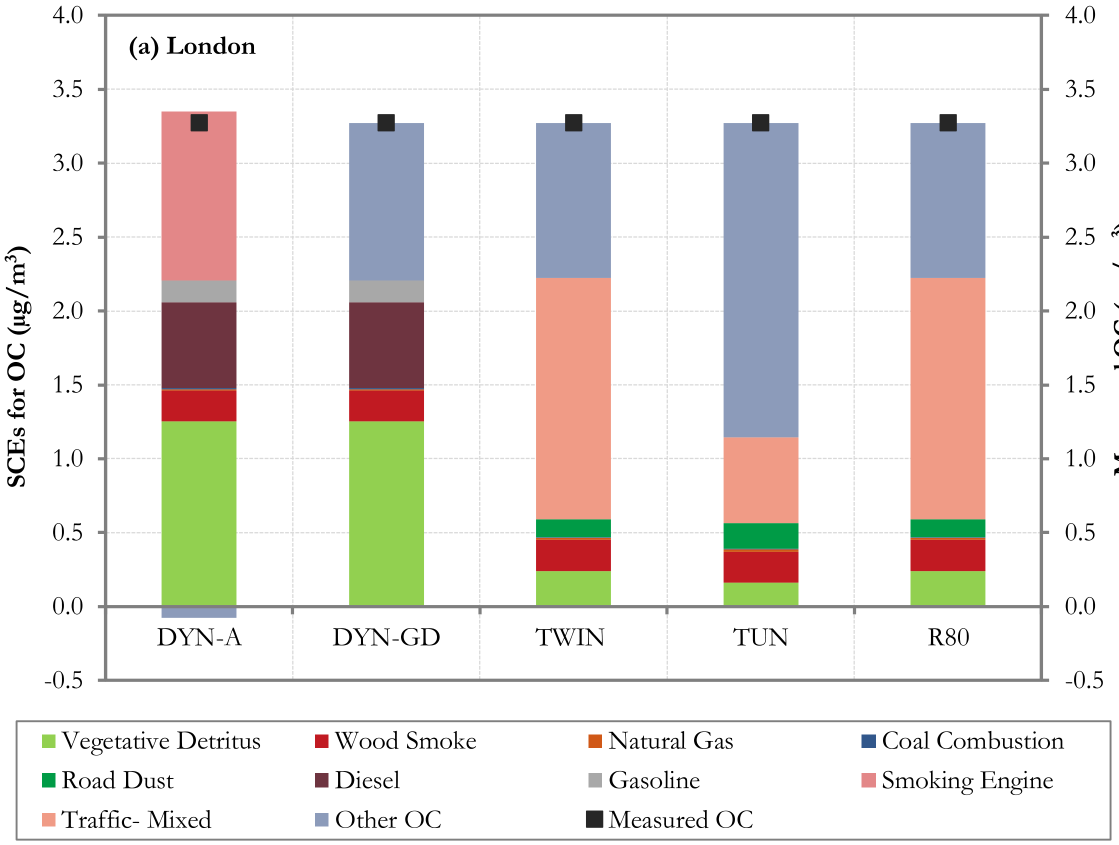

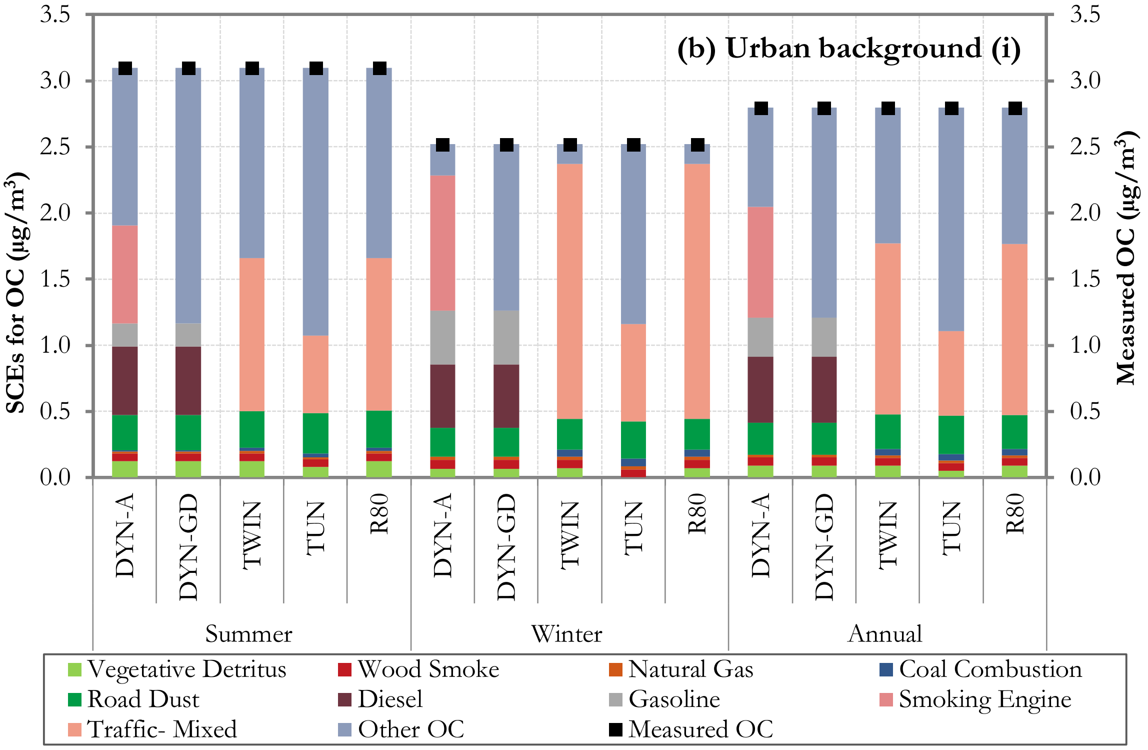

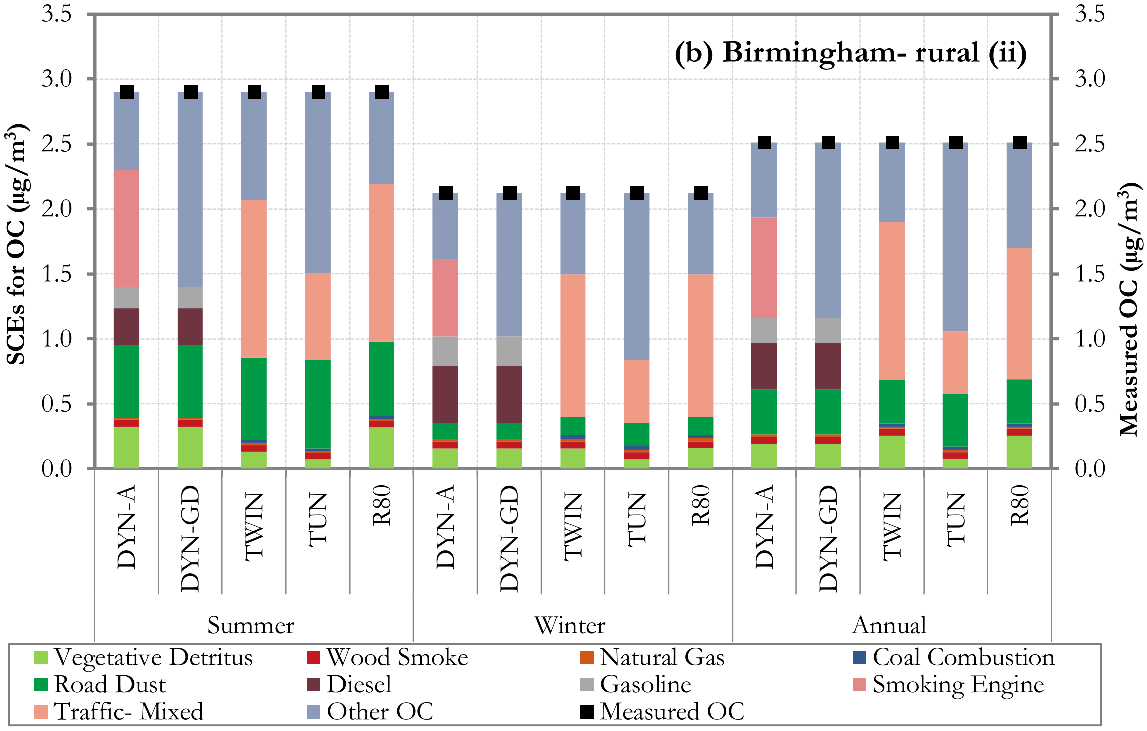

Figure 8: Source contribution estimates for OC at different sites

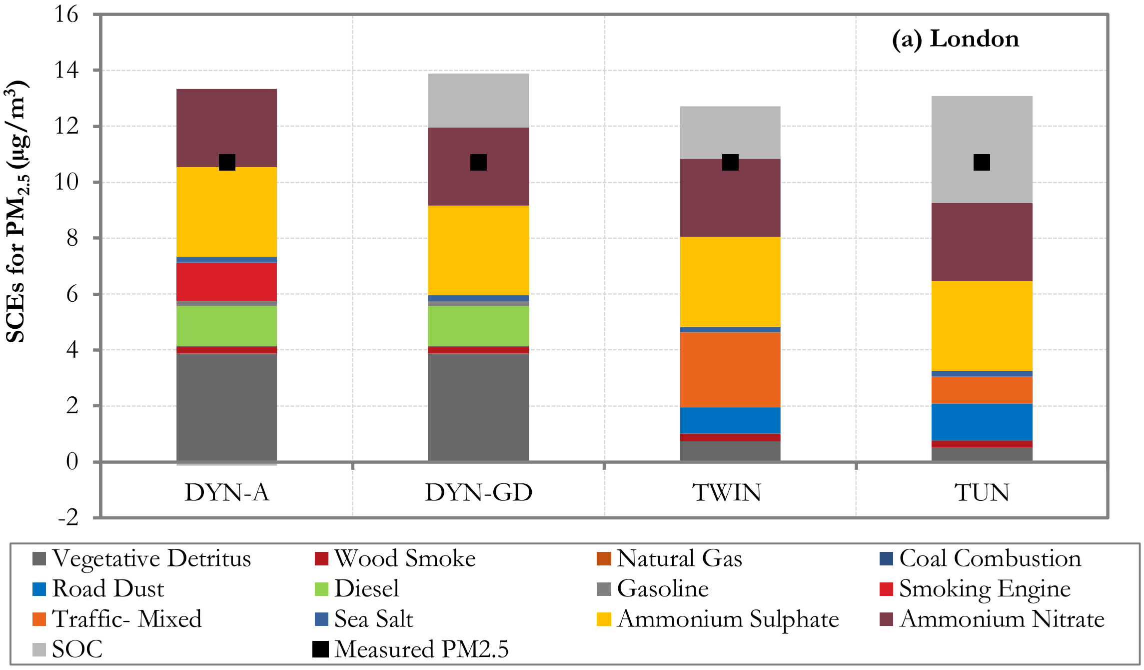
(a) London
SCEs for PM$_{2.5}$ (µg/m^3)
16
14
12
10
8
6
4
2
0
-2
DYN-A
DYN-GD
TWIN
TUN
Vegetative Detritus
Wood Smoke
Natural Gas
Coal Combustion
Road Dust
Diesel
Gasoline
Smoking Engine
Traffic- Mixed
Sea Salt
Ammonium Sulphate
Ammonium Nitrate
SOC
Measured PM2.5

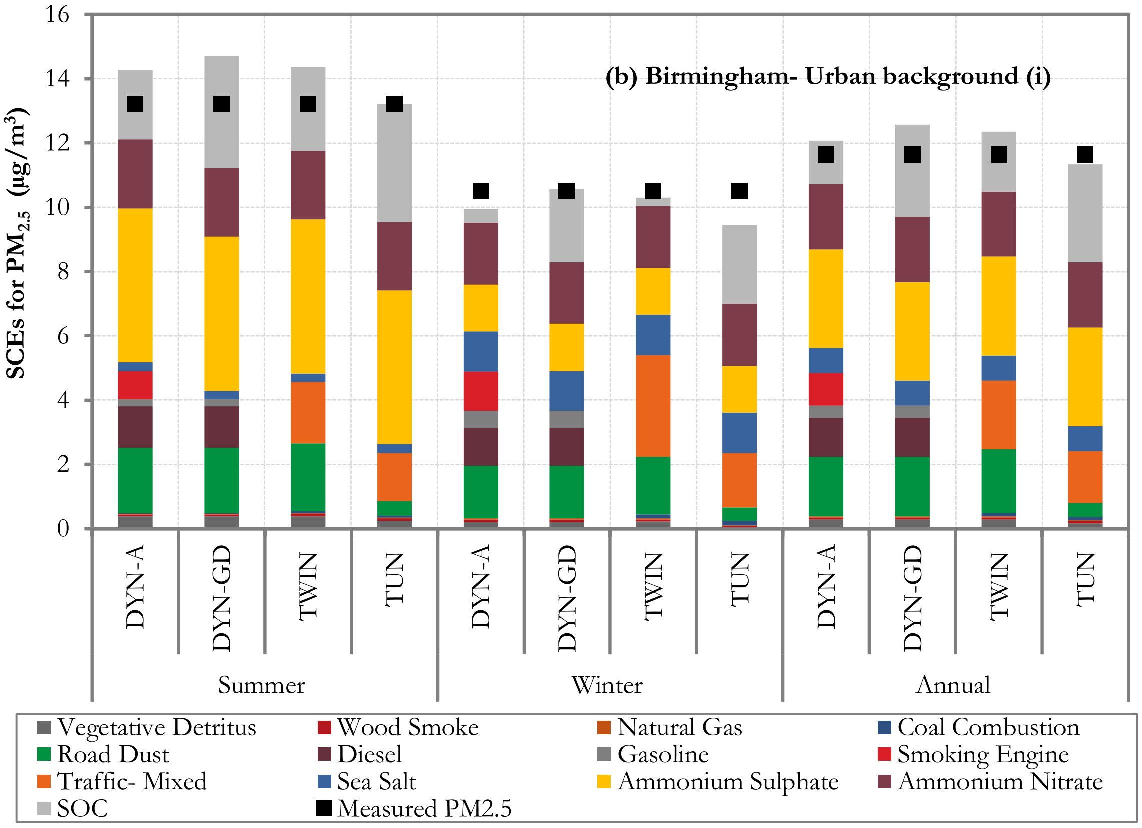
(b) Birmingham- Urban background (i)
SCEs for PM$_{2.5}$ (µg/m^3)
16
14
12
10
8
6
4
2
0
DYN-A
DYN-GD
TWIN
TUN
DYN-A
DYN-GD
TWIN
TUN
DYN-A
DYN-GD
TWIN
TUN
Summer
Winter
Annual
Vegetative Detritus
Wood Smoke
Natural Gas
Coal Combustion
Road Dust
Diesel
Gasoline
Smoking Engine
Traffic- Mixed
Sea Salt
Ammonium Sulphate
Ammonium Nitrate
SOC
Measured PM2.5

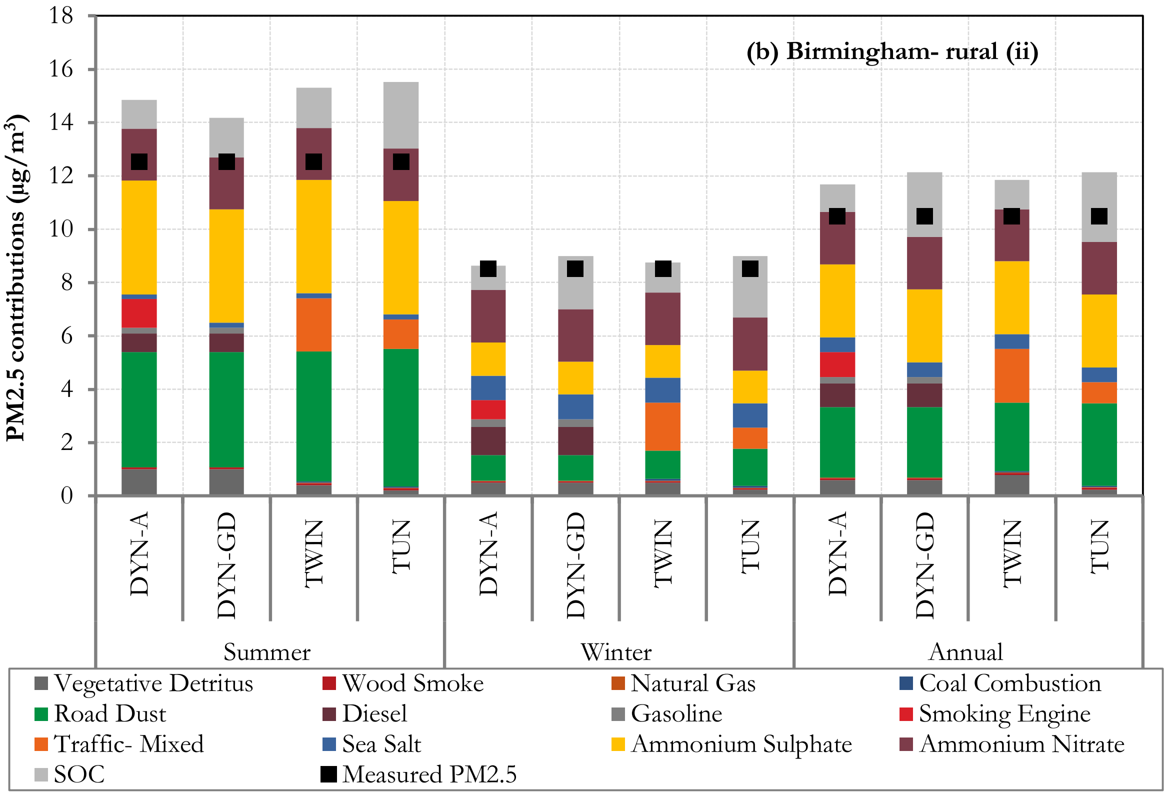

Figure 9: Source attribution of $PM_{2.5}$ mass based on CMB result

Subramanian et al. (2007) postulated that over-apportionment of OC mass can occur either due to missing primary sources or due to sampling artefacts. Between the three profiles, the lowest total OC mass was attributed by the TUN profile runs across all sites. In terms of resolution of the traffic source, CMB runs with dynamometer and composite profiles showed some differences. If only gasoline and diesel sources are considered (i.e. using DYN-GD), the TWIN profile had the maximum mass apportioned to the traffic source and the TUN profile had the minimum mass apportioned to traffic. However, with the inclusion of the smoking engine profile in DYN set of profiles, DYN-A apportioned the highest mass to the traffic source. Further, the t_{stat} values for the DYN-A ($t_{stat} > 5$ across all cases for diesel and smoking engine profiles) and TUN ($t_{stat} > 6$ across all cases) profiles were consistently higher than the TWIN model (t_{stat} between 2-3 in most cases). The lowest standard error was recorded for the DYN profiles (A & GD) which correlates with the lower uncertainties associated with these profiles. Higher uncertainties in the case of TWIN and TUN profiles can be attributed to the errors associated with ambient measurements. Between the TWIN and TUN profiles, the standard error was lower in the case of the TUN profile. In some cases, the t_{stat} for the traffic and gasoline had a value of less than 2 in the case of TWIN and DYN (A & GD) profiles respectively rendering the traffic source insignificant. No runs had t_{stat} <2 for traffic in the case of the TUN profile. The R80 profile, run as a test yielded results very similar to the TWIN profile (Table 15, Figure 8).

The MPIN matrix data for runs was also analysed to assess and cross-compare the influential species (defined as species with a value >0.7 in the matrix) for the different traffic profiles (Table 14). While in the case of DYN profiles (A & GD), the same markers (EC for diesel engine, hopanes for smoking engine and benzo(ghi)perylene for gasoline engine, value = 1 across all runs) were consistently found to be influential across all runs, different species were recorded as influential in the case of the TWIN and TUN profiles. Overall, the TWIN profile showed a value of 1 for benzo(ghi)perylene across the runs and the TUN profile showed a value of 1 for EC. In both cases, the other key sets of markers, i.e. EC and hopanes were found to be influential across most runs. Similar results were reported by Chow et al. (2007a). There were cases, however, where EC and/or trisnorhopane were over- or underestimated, and in those cases, the key marker varied. Benzo(ghi)perylene and hopane were estimated correctly in most cases. For the TUN profile, n-alkanes (A25 and 26) were also recorded as influential species in some cases. Interestingly, in the case of TUN profile runs, interference between the vegetative detritus and traffic profile was observed, and in many runs, the vegetative detritus SCE was insignificant or zero although positive SCEs were recorded using TWIN and DYN (A & GD) profiles.

In a CMB sensitivity study, Sheesley et al. (2007) observed the biomass profile to impact the contribution estimate for traffic. Test runs were then conducted with the TUN profile excluding the n-alkane data, but the SCEs for traffic were found to be more or less similar to the original runs. The other OC mass and the total mass apportioned, however, changed slightly as a result of positive SCEs for vegetative detritus. Lower percentages of mass were apportioned to traffic during the summer season by the model with both types of profile. Similar observations have been reported for the USA (Subramanian et al., 2007; Bullock et al., 2008) and Europe (El Haddad et al., 2011) where SOC has been reported to be higher in the summer season due to increased photochemical activity. Also, a higher percentage of SOC was estimated for the rural site compared to the urban background site, which is also reflected in the higher OC/EC ratio for the rural site.

3.6 Model Performance

The results obtained from the CMB model were tested against independent estimates as illustrated in Figure 10.

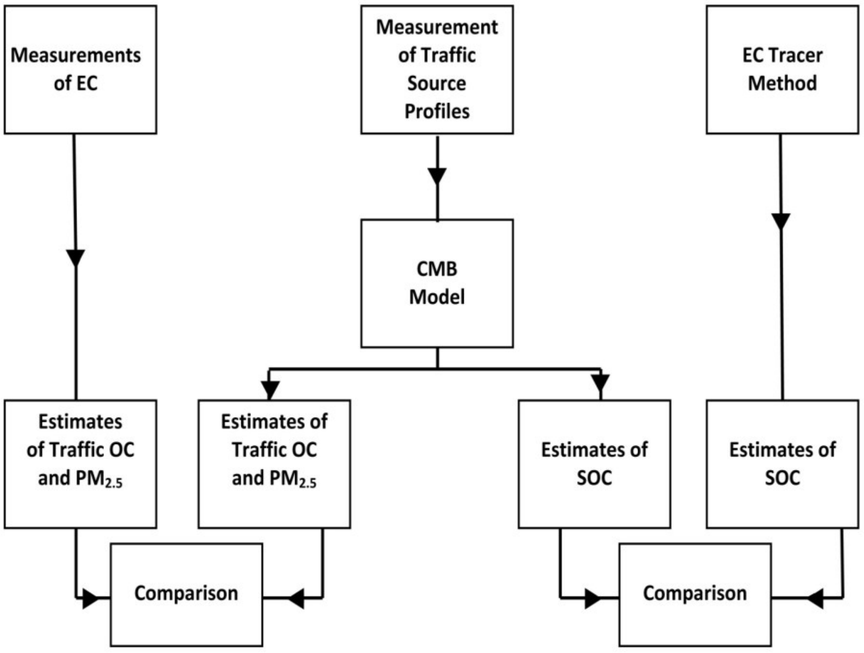

Figure 10: Assessment of model performance using different metrics

Table 15: Traffic mass estimate (μg/m³) and total percentage (%) explained using different traffic profiles for (a) OC and (b) $PM_{2.5}$

(a) OC

Site (season)	OC mass apportioned to traffic					Total % OC mass apportioned				
	DYN-A	**DYN-GD**	**TWIN**	**TUN**	**R80**	**DYN-A**	**DYN-GD**	**TWIN**	**TUN**	**R80**
Urban background site, London (Summer)	1.87	0.73	1.63	0.58	1.63	102	67.5	68.0	35.1	68.0
Urban background site, Birmingham	1.63	0.80	1.29	0.64	1.29	73.2	43.2	63.2	39.5	63.1
Urban background site, Birmingham (Summer)	1.43	0.69	1.15	0.58	1.15	61.4	37.5	53.5	34.6	53.5
Urban background site, Birmingham (Winter)	1.91	0.89	1.93	0.74	1.93	90.6	50.1	94.1	46.1	94.1
Rural site, Birmingham	1.33	0.55	1.21	0.48	1.01	77.1	46.3	75.6	42.3	67.7
Rural site, Birmingham (Summer)	1.34	0.44	1.21	0.67	1.21	79.2	48.3	71.3	52.0	75.6
Rural site, Birmingham (Winter)	1.26	0.66	1.10	0.48	1.10	76.2	48.1	70.5	39.4	70.5

(b) $PM_{2.5}$

Site (season)	**$PM_{2.5}$ mass apportioned to traffic**					**Total % $PM_{2.5}$ mass apportioned**				
	DYN-A	**DYN-GD**	**TWIN**	**TUN**	**R80**	**DYN-A**	**DYN-GD**	**TWIN**	**TUN**	**R80**
Urban background site, London (Summer)	2.98	1.61	2.69	0.96	2.69	123	130	119	122	119
Urban background site, Birmingham	2.61	1.61	2.13	1.61	2.13	104	108	106	97.5	106
Urban background site, Birmingham (Summer)	2.39	1.50	1.90	1.50	1.90	108	111	109	100	109
Urban background site, Birmingham (Winter)	2.93	1.70	3.18	1.70	3.18	94.7	101	98.1	89.9	98.1
Rural site, Birmingham	2.06	1.13	2.00	0.80	1.67	111	116	113	116	114
Rural site, Birmingham (Summer)	1.97	0.89	2.00	2.00	2.00	119	113	122	124	121
Rural site, Birmingham (Winter)	2.07	1.36	1.81	0.79	1.81	101	106	103	106	103

3.6.1 Comparison of CMB Traffic Estimates with an Estimate based upon EC

Assuming road traffic to be the dominant source of EC, traffic emission estimates were obtained for $PM_{2.5}$-OC and $PM_{2.5}$ mass using EC*0.35 and EC*1.35 respectively based on Pio et al. (2011). The traffic SCE outputs for $PM_{2.5}$-OC and $PM_{2.5}$ from the CMB model with different traffic profiles were compared against the EC traffic emission estimates (Table 16). The most similar estimates for primary vehicular emissions were observed for DYN-GD with the estimates being highly correlated ($r^2 > 0.85$) with the traffic estimates obtained using EC for the Birmingham sites. For DYN-A, the dynamometer profiles produced a much higher estimate for the traffic contribution and this was due to a high SCE for the smoking engine profile. However, not all of that SCE is necessarily derived from road traffic as the source profile for the smoking engine includes off-road vehicles which are a significant contributor to $PM_{2.5}$ in the UK (AQEG, 2012). Poor correlation was observed for all the profiles at the rural Birmingham site with correlation coefficients ranging between 0.26-0.41. The estimates obtained using the TWIN profiles showed similar correlation with the EC estimate compared to the estimates from the TUN profile.

3.6.2 Comparison of Estimates of SOC

Organic carbon can be present in the atmosphere as primary organic carbon (POC) (directly emitted) or SOC (formed by atmospheric chemistry). Generation of SOC source profiles is rendered difficult due to the complex chemistry of secondary organic aerosol formation (Bullock et al., 2008) and diversity of composition. As a result, while the CMB model works well for attribution of POC sources such as biomass combustion and traffic, it is not able to apportion SOC due to lack of availability of appropriate source profiles (Stone et al., 2009; Guo et al., 2012; Schauer and Sioutas, 2012). Consequently, as in Yin et al. (2010), the CMB model was run to account for known primary sources of OC, and the difference between the sum of POC and measured total OC was attributed to SOC.

EC is released directly into the atmosphere and can be used to estimate relative amounts of primary and secondary OC. One of the simplest approaches involves use of the ratio between OC and EC. Higher OC/EC ratios are expected in the conditions where SOC is dominant and the highest OC/EC ratios are reported in rural and remote sites (Pio et al., 2011). The EC-tracer method involves the use of EC as a tracer for POC, allowing SOC to be calculated (Turpin and Huntzicker, 1995; Castro et al., 1999; Lee and Russell, 2007; Sheesley et al., 2007; Pio et al., 2011). Minimum ratios of OC/EC are taken as representative of primary OC (although they may be an over-estimate (Pio et al., 2011) and OC above that ratio is taken to be SOC. Given that the EC tracer method is liable to under-estimate SOC (Pio et al., 2011), an excess of "other OC" over SOC might be expected, but in most cases the "other OC" is similar to, or less than the SOC.

The method as outlined by Castro et al. (1999) was used (equation 8) and estimates of daily SOC were made for each of the sites.

$$Secondary\ OC = Total\ OC - \left(EC * \left(\frac{OC}{EC}\right)_{\min}\right) \tag{8}$$

Where
Total OC refers to the concentration of OC
EC refers to the concentration of EC
(OC/EC) minimum refers to the minimum OC/EC gradient

The quality of fit between the estimates of SOC from the CMB model and the EC tracer method was evaluated by regression analysis (Table 17). In the Birmingham (urban background), London (urban background-summer) and Birmingham (rural) datasets, the three estimates are in broad agreement.

Table 16: Comparison of the traffic estimates from the CMB model with the traffic estimate obtained using EC

Site (season)	OC	$PM_{2.5}$

	r^2		r^2	
Urban background, London (Summer)				
DYN-GD	0.99	y = 1.28x + 0.01	1.00	y = 0.75x + 0.01
DYN-A	0.94	y = 1.45x + 1.04	0.98	y = 0.80x + 1.24
TWIN	0.71	y = 1.55x + 0.37	0.71	y = 0.66x + 0.60
TUN	0.84	y = 0.61x + 0.29	0.84	y = 0.26x + 0.48
Urban background, Birmingham (Summer)				
DYN-GD	0.87	y = 1.31x + 0.00	0.95	y = 0.76x - 0.03
DYN-A	0.78	y = 2.37x + 0.33	0.89	y = 1.09x + 0.37
TWIN	0.67	y = 1.93x + 0.14	0.67	y = 0.83x + 0.23
TUN	0.73	y = 0.79x + 0.14	0.73	y = 0.34x + 0.23
Rural, Birmingham (Summer)				
DYN-GD	0.97	y = 1.21x - 0.00	0.92	y = 0.73x - 0.10
DYN-A	0.41	y = 1.12x + 0.88	0.61	y = 0.71x + 0.91
TWIN	0.26	y = 1.00x + 0.55	0.26	y = 0.43x + 0.91
TUN	0.16	y = 0.32x + 0.37	0.16	y = 0.14x + 0.62

Note: y = CMB model estimate; x = estimate derived from EC concentration

Table 17: Comparison of the Other OC estimate from the CMB model with the SOC estimate obtained using EC tracer method

Site (season)	r^2	
Urban background, London (Summer)		
DYN-A	0.81	y = 0.92x - 0.69
TWIN	0.70	y = 0.83x + 0.07
TUN	0.73	y = 0.80x + 0.74
Urban background, Birmingham (Summer)		
DYN-A	0.92	y = 0.86x - 0.52
TWIN	0.91	y = 0.86x - 0.10
TUN	0.90	y = 0.90x + 0.49
Rural, Birmingham (Summer)		
DYN-A	0.76	y = 0.79x - 1.22
TWIN	0.69	y = 0.73x - 0.71
TUN	0.92	y = 0.88x - 0.67

3.7 Conclusions

It is evident from Figure 6 that $PM_{2.5}$ traffic profiles of molecular markers measured in the field show generally broad agreement. However, as Figure 7 shows, where plotted as normalised abundance (marker/EC), the field data can differ by orders of magnitude from dynamometer data, and the variation between dynamometer studies is typically greater than that between field measurements. Perhaps surprisingly, both, however, give broadly similar estimates of traffic $PM_{2.5}$ mass with the CMB model. Those from the composite $PM_{2.5}$ profile (TWIN) are probably better, as judged from the estimates from the EC tracer method, and the mass closures. Correlations of the traffic estimates using the TWIN profile against those obtained using EC were broadly similar to those obtained using the DYN (A & GD) profiles. The estimates from TUN profile, however, were much more weakly correlated, particularly at the rural site. This could be due to the interference between the traffic and vegetative detritus sources for TUN model runs as explained in the previous section. It is possible that other tunnel profiles more representative of the UK might perform better. It was also observed that selection of species for inclusion in the profile can determine the overall modelling output, both for estimation of the traffic source and the overall model output.

Based on the current analysis, it can be concluded that both the dynamometer and composite (twin-site) profiles can provide reasonable estimates of the traffic contribution. In cases where dynamometer profiles are not available, composite profiles can be used to estimate traffic contribution to OC or PM mass. However, it is important to bear in mind that the high uncertainty associated with the composite traffic profile can impact upon CMB model output since the model takes into account both the profile uncertainty and the ambient data uncertainty. Further, traffic source profiles based on ambient data can cause mis-apportionment of other sources since similar compounds are often reported from different sources, for e.g. PAHs from different combustion sources. Thus, it is important to select species for the profile in such a way that interference with other sources would be minimal. Another consideration for the use of ambient data for preparation of source profiles is the impact of oxidation of marker species in the atmosphere (Robinson et al., 2006b). This can also impact the model output as it is assumed that the species are chemically stable.

3.8 Acknowledgements

Thanks to Dr. Imad El Haddad for help in interpretation of the tunnel measurement data from France.

CHAPTER 4- PARTICULATE MATTER IN BIRMINGHAM, UK

This chapter presents results of the measurement campaign for PM_x ($PM_{2.5}$ and size-segregated PM) in Queensway Tunnel (QT) and at Elms Road Observatory Site (EROS), Birmingham in 2012. The campaign was undertaken with an aim to characterize the vehicular emissions in a tunnel environment and compare them to typical urban background values and to prepare a composite mixed fleet profile for traffic emissions.

Sampling was carried out in collaboration with Amey, UK.

Graphical Abstract

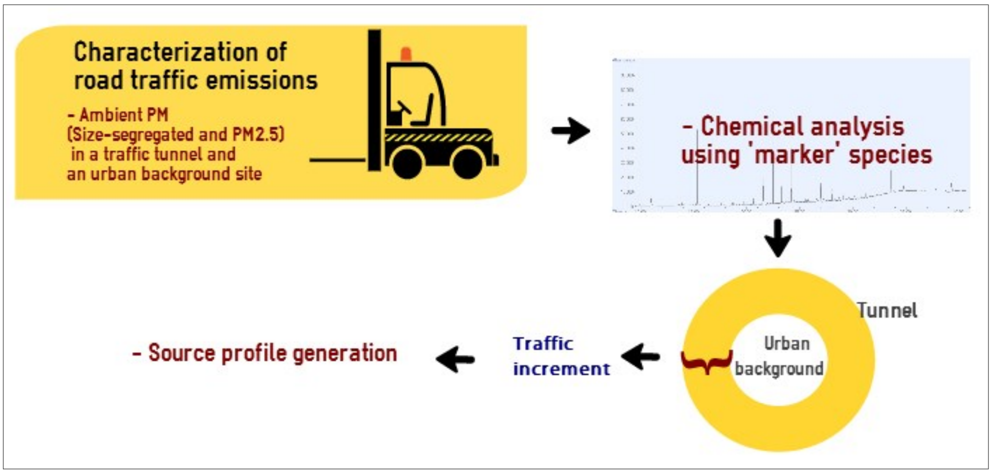

4.1 Introduction

Road transport constitutes an important source of PM emissions in urban areas, and motor vehicles are an important source for carbonaceous aerosols particularly for the particles in the fine size range (aerodynamic diameter < 2.5 μm) (Kam et al., 2012; Keuken et al., 2012). Health risk (in terms of toxicity) associated with air pollutants has been linked to concentrations of transition metals and PAHs, both of which are present in high concentrations in traffic emissions (Ayres et al., 2008). PM and diesel engine emissions have been classified as group 1 carcinogens by the IARC, and several recent studies have linked vehicular emissions to adverse health effects (HEI, 2010; Godri et al., 2011; Slezakova et al., 2013).

Only a few studies have focused on the characterization of PM emissions from road traffic in the UK. Between late 1990s and early 2000s, several papers reported on concentrations of PAHs in near-road environment (e.g. Smith and Harrison, 1996) but there are a very limited number of studies focusing on analysis of molecular markers in high traffic environments in the UK (Harrad et al., 2003; Yin et al., 2010). Recent research literature has focused on sources such as wood burning and secondary PM (Harrison et al., 2012b; Fuller et al., 2014; Charron et al., 2013) barring Lawrence et al. (2013) who reported composition of PM_{10} in a road tunnel in Hatfield (UK). The only receptor modelling study from the UK highlighted the need for generation of local representative source profiles to overcome the uncertainty introduced by profiles from North America (Yin et al., 2010). An ambient composite traffic profile was subsequently generated using existing data from UK sites and tested against dynamometer profiles with the CMB model (discussed in Chapter 3). During this study, both ambient $PM_{2.5}$ and road dust PM_{10} traffic emissions were characterized, but the data on road dust characterization in presented in Chapter 5.

As discussed in Chapter 1, traffic emissions can be characterized using a suite of methods including dynamometer analysis and ambient measurements. Source profiles prepared using ambient data offer the advantage of being representative of the on-road fleet, and they reflect emissions in the real-world conditions better than dynamometer-based profiles. However, factors such as variations in speed and fleet characteristics (i.e. proportion of HDVs and LDVs) can cause variability in the ambient measurements.

There have been studies focused on traffic emissions' characterization in tunnel environment in Europe including Austria (Laschober et al., 2004; Handler et al., 2008), Handler et al. (2008), France (El Haddad et al., 2009; Fabretti et al., 2009), Italy (Zanini et al., 2006), Portugal (Oliviera et al., 2011; Almeida-Silva et al., 2011; Pio et al., 2013; Alves et al., 2015), Sweden (Wingfors et al., 2001) and UK (Luhana et al., 2004; Lawrence et al., 2013).

The objectives of this study were:

- to characterize $PM_{2.5}$ emissions from mixed road traffic in a typical road tunnel in UK and;
- to prepare a composite road traffic (exhaust) source profile.

4.2 Methodology

Sampling was conducted at the A38 Queensway Tunnel (QT) and the Elms Road Observatory Site (EROS), Birmingham, United Kingdom between September 11 and 21, 2012.

4.2.1 Sampling Locations

4.2.1.1 A38 Queensway Tunnel, Birmingham (QT)

This tunnel is one of the major road tunnels in Birmingham and runs in the North/South direction. It is a 544 metres long twin bore tunnel with two lanes on each side and has a cross-sectional area of 25 m^2. Average vehicle speed in the tunnel is 50 kilometres/hour and the modal split is presented in Figure 11. An estimated 89000 vehicles travel through the tunnel each day (Azzi, 2012). The tunnel is ventilated naturally.

The samplers were placed in the emergency layby area directly adjacent to the road at a distance of 1.5 m in the southbound lane. At the time of the sampling, the tunnel was closed at the night for maintenance work in the northbound lane between 10 pm and 6 am. The site has been used for PM measurements previously (Birmili et al., 2006).

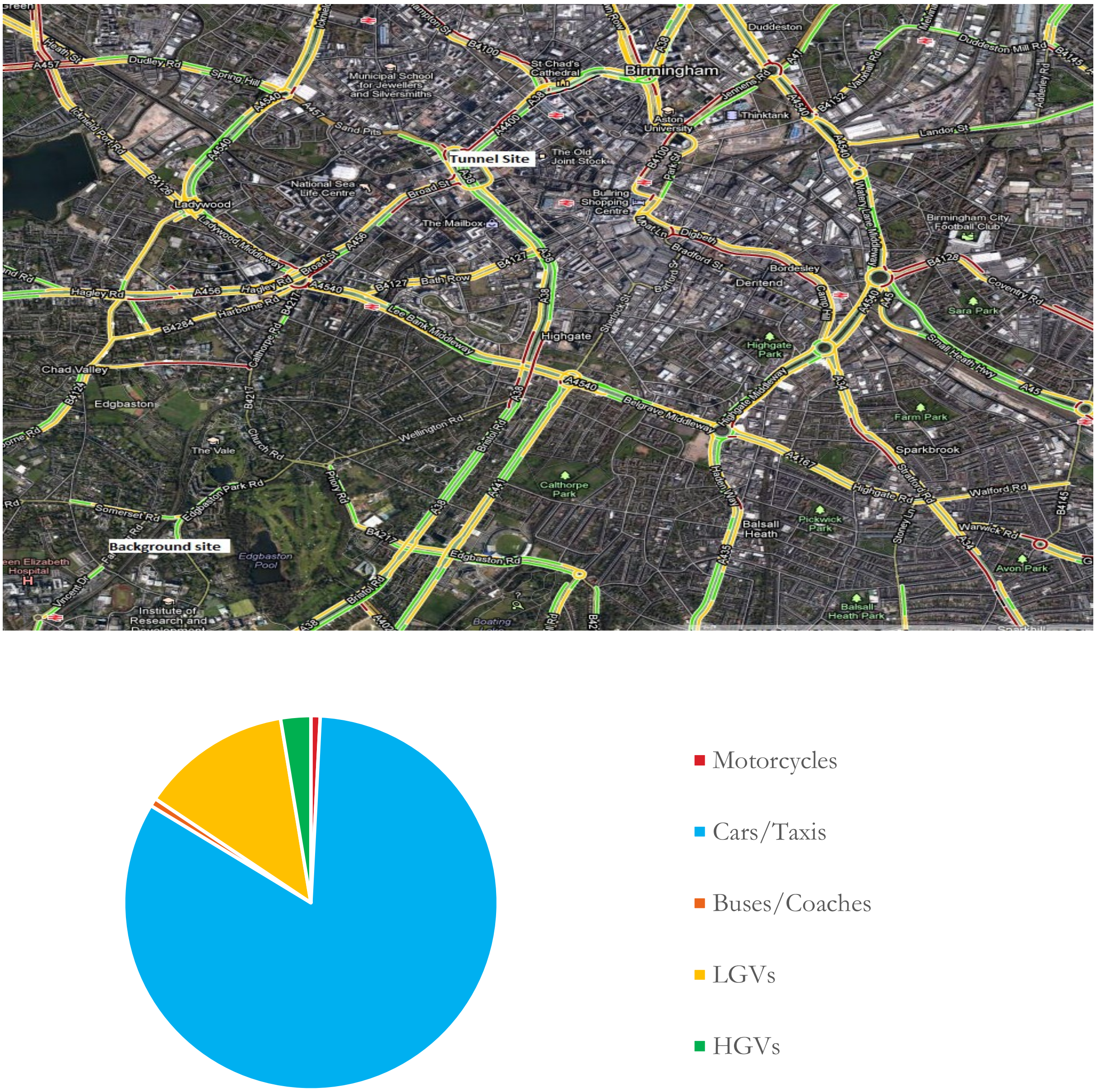

Figure 11: Site locations and modal split at A38 Queensway Tunnel *(Azzi, 2012)*

The modal split at the site (Figure 11) was found to be similar to the country average- cars and taxis (82.1%), buses and coaches (1.51%), light vehicles (12.09%), goods vehicles (3.23%) and motorcycles (1.10%) (DfT, 2013). The fuel split at the national level is nearly 70:30 for gasoline and diesel. Data on the fuel split was not available for the tunnel or the background site (DfT, 2013).

4.2.1.2 Elms Road Observatory Site (EROS)

This is an urban background site located in an open field within the University of Birmingham University (52.45° N; 1.93°W). The site is about 3.5 km southwest of the centre of Birmingham. There are no significant PM sources in the vicinity, and nearest anthropogenic sources are a nearby railway and some moderately trafficked roads. Occasionally, agricultural machinery is used in the open field. There is little residential accommodation within 300m. The site has been used as an urban background site in a number of previous research studies (Yin et al., 2010; Pant and Harrison, 2014). The samplers were placed at a height of ~1.5 m from ground level next in an open field.

4.2.2 Sampling

Ambient air samples were collected for PM using high volume sampler (n=12 at each site) and MOUDI (integrated 48 hour size-segregated aerosol, (n=4 at QT and n=3 at EROS). A description of the sampling instruments is provided in Chapter 2.

Integrated 24 hour $PM_{2.5}$ (PM with aerodynamic diameter <2.5 μm) samples were collected using the high volume samplers (Digitel DHA-80) on pre-baked quartz filters while integrated 48 hour size-segregated PM samples were collected using 8-stage rotating MOUDI (Model 100, MSP Corporation, Minneapolis, Minnesota, USA) using 47 mm PTFE and 37 mm quartz back-up filters. Both samplers were collocated at QT and EROS and measurements were conducted simultaneously.

PM mass data was obtained from collocated dichotomous samplers at both sites.

Average wind speed during the sampling period was 4.8±1.23 m/s with a predominant south, south-west direction.

4.2.3 Analytical methods

The analytical procedures are described in Chapter 2.

The quartz filter samples collected from HVS were analysed for Ti, V, Cr, Mn, Cu, Zn, Sn, Sb and Ba using ICP-MS. Size-segregate aerosol samples (PTFE filters with a quartz back-up filter) were analysed for Al, Si, Fe by WD-XRF and ICP-MS was used to analyze the digested samples for Ti, V, Cr, Mn, Cu, Zn, Sb, Pb and Ba.

The quartz filter samples were used to analyse OC and EC using the carbon analyser and GC-MS was used to analyse PAHs (BbF, BkF, BeP, BaP, IcdP, Pic, BghiPe and Cor), alkanes (C24-C35) and hopanes (TNOHO HOP, NHO, S,R- HHO, S, R-BHHO and S, R- THHO).

4.2.4 Data Analysis

Data analysis has been carried out using Microsoft Excel and SPSS (Version 21). Species with blank concentrations more than 10% were not included in the analysis (Cr was excluded). Missing or concentrations below detection limits were replaced with 0.5*detection limit. Species' correlation analysis was conducted using SPSS based on Pearson Correlation and the correlation values reported in the text are for $p<0.01$ unless otherwise mentioned.

Using the data obtained from MOUDI samples, a continuous size distribution was obtained using the numerical inversion method described in Keywood et al. (1999). This approach has previously used in several studies (Allen et al., 2001a; Gietl et al., 2010).

4.3 Results

4.3.1 Concentrations

4.3.1.1 Particulate Matter

Average 24-h $PM_{2.5}$ (fine) and $PM_{2.5-10}$ (coarse) concentrations were observed to be 56.1 and 46.9 $\mu g/m^3$ at QT and 2.38 and 2.88 $\mu g/m^3$ at EROS. Average PM_{10} and $PM_{2.5}$ concentrations at the urban background site in Birmingham (AURN Site number UKA00479) were recorded as 9.13 ± 4.46 and 8.65 ± 3.27 $\mu g/m^3$ for the same time.

A bimodal particle size distribution (PSD) was observed for PM mass at both sites with peaks in coarse and accumulation modes (Figure 12). The observation is broadly similar to previous studies across site types in the UK (Allen et al., 2001; Gietl et al., 2010; Harrison et al., 2012; Taiwo et al., 2014). At QT, 62.4% of the total PM was in the fine range ($PM_{2.5}$ and less) while at EROS, 80.2% of the PM mass was in the fine range. In comparison, Lawrence et al. (2013) reported 65% of the total PM in the fine range in the Hatfield Tunnel (UK).

Differences in the estimation of the fine fraction of PM (aerodynamic diameter < 2.5 μm) can vary due to differences in cut-points of the sampling equipment. In the case of the dichotomous sampler, a virtual impactor separates the $PM_{2.5}$ (fine) fraction from $PM_{2.5-10}$ (coarse) fraction. In the case of MOUDI, however, differences in flow rate can lead to variation in the cut-point, and hence the distribution between fine and coarse fractions.

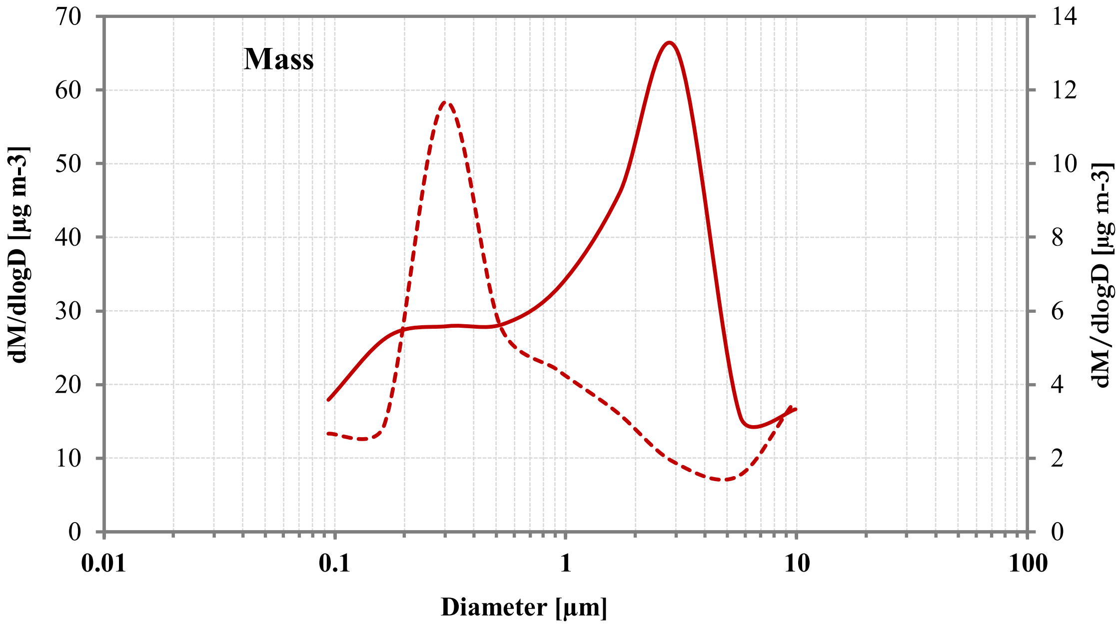

Figure 12: Average mass size distribution for PM at QT and EROS (based on MOUDI)

(solid line- QT (primary axis), dashed line-EROS (secondary axis); in µg/m^3*)*

4.3.1.2 Carbon

At QT, average 24-hour OC and EC concentrations were observed to be 16.8 and 16.9 µg/m^3 respectively while at EROS; the concentrations were 1.45 and 0.70 µg/m^3 (Table 18, Figure 13). OC and EC were strongly correlated at EROS (r^2=0.91, p<0.01) but significant correlation was not observed at QT.

Table 18: Summary of carbon concentration (PM2.5) at QT and EROS (µg/m^3)

Species	QT				EROS			
	Mean	S.D.	Minimum	Maximum	Mean	S.D.	Minimum	Maximum
OC	16.8	3.29	11.7	22.9	1.45	0.76	0.44	3.12
EC	16.9	2.38	14.1	22.0	0.70	0.55	0.16	1.89

EC is used as a marker for traffic, and is found in the atmosphere as a primary species. Previous research has utilized the ratio between OC and EC to determine the influence of traffic. A high

OC/EC ratio indicates higher contribution of OC, indicating lower traffic emissions whilst a low OC/EC ratio indicates a high contribution from traffic emissions. The OC/EC ratio was observed as 0.997±0.16 for QT and 2.72±1.45 for EROS. This is consistent with previously reported studies. He et al. (2008) observed a ratio of 0.49±0.04 for $PM_{2.5}$ emissions in a traffic tunnel (~20% HDVs) in China while Ancelet et al. (2011) observed the OC/EC ratio of 1.7 $PM_{2.5}$ emissions in a tunnel in New Zealand.

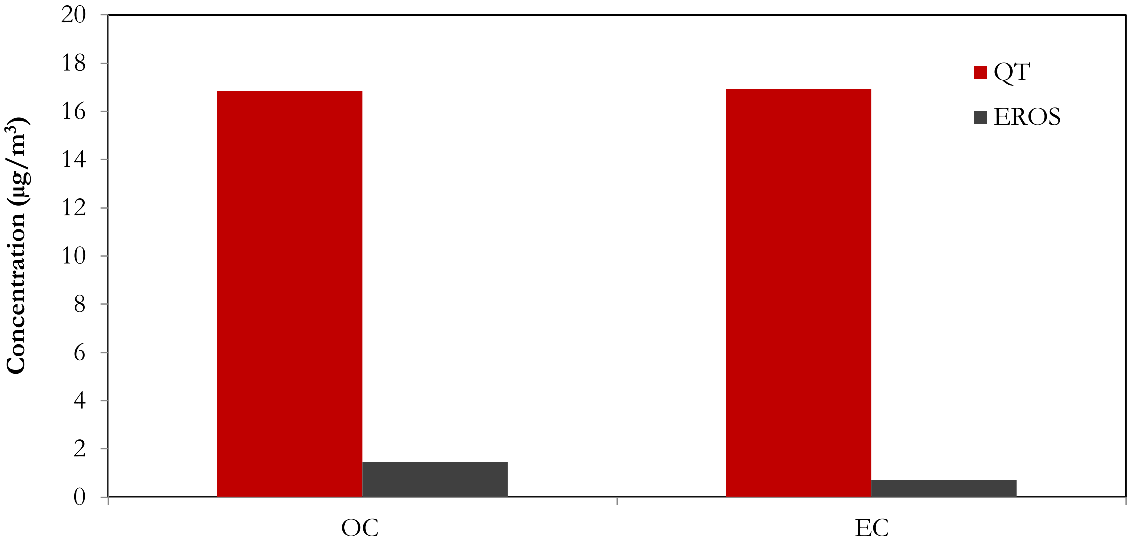

Figure 13: Concentration of OC and EC (PM2.5) at QT and EROS

4.3.1.3 Elements

Cu, Zn and Ba were found to be the most abundant metals in $PM_{2.5}$ at QT while at EROS, Mn and Zn had the highest concentrations (Figure 14). In the Hatfield Tunnel (UK), Ba followed by Zn and Cu were found to be the most abundant trace elements in PM_{10} (Lawrence et al., 2013) whereas Birmili et al. (2006) reported Zn and Cu to be the most abundant in the Queensway Tunnel in an earlier study. Concentrations in QT were similar to Hatfield Tunnel in case of Mn, V, Ca and Zn, although concentrations of Ba and Sb were higher in case of Hatfield Tunnel. This seems plausible considering that the current study focused on $PM_{2.5}$ while the measurements in Hatfield were conducted on PM_{10}, and Ba and Sb, markers for brake wear, are expected to be present in higher concentrations in the coarse fraction of PM. Concentrations observed in QT were also found to be similar to concentrations reported elsewhere in Europe with the exception of V which was found to be present in much lower concentrations in QT (Laschober et al., 2004; Fabretti et al., 2009).

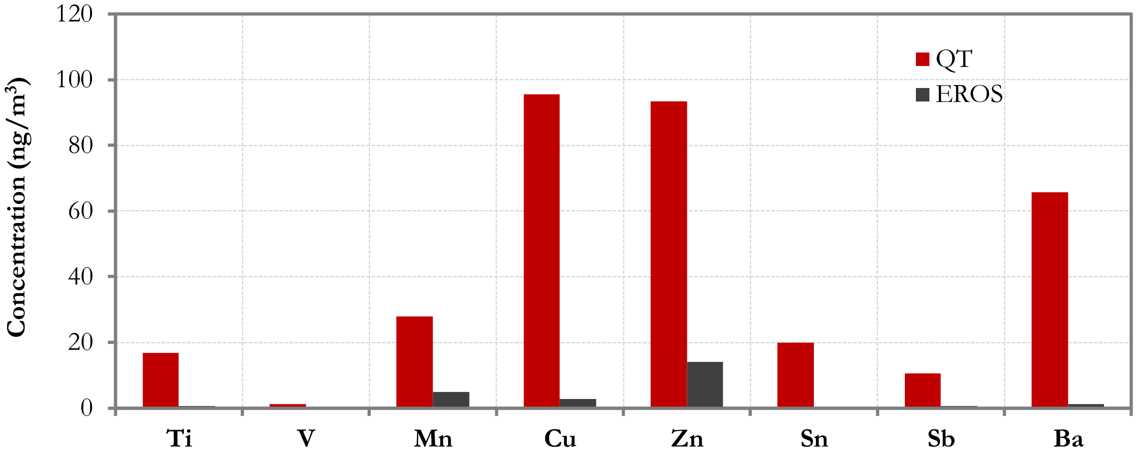

Figure 14: Concentration of the elements ($PM_{2.5}$) at QT and EROS (ng/m^3)

Significant correlations were observed between the elements at QT with the strong correlation between Cu and Sn (r^2=0.992, $p<0.01$) while at EROS, brake-wear associated elements were found to have significant correlations- Sb and Ba (r^2=0.85, $p<0.01$) and Ba and Sn (r^2=0.65, $p<0.05$). Ti and Cu were also found to be correlated at EROS (r^2=0.78, $p<0.01$) (Table 19). Weak or no correlation was observed between elements and EC, and this is generally attributed to the different sources, i.e. exhaust emissions for EC and non-exhaust emissions for trace metals. Several elements (e.g. Cu, Mn, Cr, V) were found to be moderately correlated to EC while Ti and Ca were found to have no correlation with EC. Weak or no correlation of trace elements with EC has also been observed elsewhere and it has been postulated that this could be due to the trace metal contribution from non-exhaust emissions (Funasaka et al., 1998; He et al., 2008; Ancelet et al., 2011). It should be noted, however, that this observation cannot be directly interpreted as true for all types of road traffic emissions since contributors to PM emissions in a tunnel will differ from those in a normal roadway environment and that both chemical composition and emission factors will be different.

Ratios between different elements can be used to distinguish between different sources. Various authors have proposed characteristic Cu/Sb ratio for brake wear particles including 4.6 ± 2.3 in USA (Sternbeck et al., 2002) and 7.0±1.9 in Europe (PM_{10}) (Amato et al., 2009a). In the current study, the Cu/Sb ratio was observed to be 8.95 ± 0.92 for QT and 6.84 ± 5.34 for EROS and broadly falls within the proposed ratios. Gietl et al. (2010) reported the Cu/Sb ratio of 9.1 ($PM_{2.5}$) for a heavy traffic road (Marylebone Road) in London (UK) while Lawrence et al. (2013) reported the ratio value to be 7.2 (PM_{10}) for a tunnel site in UK. In comparison, Brito et al. (2013) reported a Cu/Sb ratio of 8.2 for $PM_{2.5}$ in a road tunnel in Sao Paulo, Brazil and Amato et al. (2011a) reported a ratio of 8.0 at a roadside site in Spain. The Cu/Zn ratios were observed to be 1.05 ± 0.13 and 0.31 ± 0.28 at QT and EROS respectively. Pulles et al. (2012) reported a Cu/Zn ratio of 0.13 for gasoline and 0.35 for diesel fuel in the UK. The higher ratio value at QT indicates a source other than exhaust emissions.

Table 19: Correlation coefficients (Pearson correlation) between elemental species ($PM_{2.5}$)

(only correlations above 0.5 are reported; QT-green and EROS-yellow; *refers to significance at 0.05 and **refers to significance at 0.01)

	Ti	V	Mn	Cu	Zn	Sn	Sb	Ba	Ca
Ti	1	.987**	.976**	.965**	.992**	.937**	.916**	.900**	.980**
V		1	.967**	.946**	.980**	.928**	.928**	.895**	.957**
Mn			1	.992**	.989**	.985**	.973**	.967**	.934**
Cu	.782**			1	.981**	.992**	.958**	.975**	.940**
Zn				.544	1	.959**	.938**	.931**	.962**
Sn					.725*	1	.976**	.991**	.896**
Sb						.717*	1	.979**	.848**
Ba				.545		.679*	.862**	1	.852**

Ca	🟨	🟨	🟨	🟨	🟨	🟨	🟨	🟨	**1**

4.3.1.4 *Organic Species*

Hopanes

Hopanes are used as markers for traffic emissions, and are typically released during the combustion process. They are normally found in lubricating oil used for vehicles, and thus cannot be used to distinguish between diesel and gasoline vehicles. Total hopane concentration in $PM_{2.5}$ was observed to be 19.6±5.2 $\mu g/m^3$ at QT and 0.62±0.48 $\mu g/m^3$ at EROS. HOP and NHO were the most abundant hopane species at both sites (Table 20).

Table 20: Concentration of hopane congeners ($PM_{2.5}$) at QT and EROS (ng/m^3)

Species	QT				EROS			
	Mean	**S.D.**	**Minimum**	**Maximum**	**Mean**	**S.D.**	**Minimum**	**Maximum**
TNOHO	1.10	0.25	0.75	1.54	0.04	0.02	0.02	0.07
NHO	4.49	1.13	2.94	6.55	0.12	0.09	0.09	0.30
HOP	6.49	1.70	4.12	10.03	0.17	0.11	0.11	0.39
SHHO	1.65	0.46	1.07	2.57	0.09	0.03	0.05	0.13
RHHO	1.46	0.42	0.96	2.35	0.11	0.02	0.06	0.14
SBHHO	1.49	0.45	0.93	2.43	0.05	0.09	0.09	0.26
RBHHO	1.12	0.32	0.78	1.79	0.05	0.09	0.08	0.21
STHHO	1.01	0.31	0.70	1.68	0.02	0.05	0.04	0.12
RTHHO	0.79	0.23	0.51	1.29	*Not detected in any sample*			

Alkanes

Alkanes are emitted from natural as well as anthropogenic sources. Lower alkanes are typically associated with combustion emissions while higher alkanes, particularly the odd-numbered alkanes (C29, C31, C33) are associated with biogenic (vegetative emissions). The alkane profiles for the sites are markedly different. Traffic emissions-associated alkanes such as C24 and C25 were the most abundant in $PM_{2.5}$ at QT while C27 and C29 were the most abundant at EROS (Table 21). Higher alkanes were present in much smaller concentrations at QT.

Table 21: Concentration of alkane ($PM_{2.5}$) congeners at QT and EROS (ng/m^3)

Species	QT				EROS			
	Mean	S.D.	Minimum	Maximum	Mean	S.D.	Minimum	Maximum
C24	142	*0.34*	*95.5*	*195*	0.40	0.21	0.22	0.63
C25	127	1.11	81.9	186	0.50	0.28	0.29	0.82
C26	67.8	0.23	44.3	97.4	0.37	0.21	0.23	0.61
C27	43.8	0.56	26.2	57.4	0.54	0.22	0.40	0.80
C28	26.1	0.28	12.6	36.7	0.31	0.18	0.18	0.51
C29	48.5	1.01	32.2	62.9	0.66	0.3	0.44	0.99
C30	29.4	1.55	17.8	44.8	0.21	0.1	0.14	0.34
C31	40.7	1.66	24.9	56.6	0.50	0.28	0.29	0.82
C32	27.1	2.22	13.1	43.4	0.16	0.003	0.16	0.17
C33	28.8	3.88	15.0	47.1	0.35	0.23	0.16	0.61

PAHs

Table 22 provides a summary of PAH concentrations in $PM_{2.5}$ at both sites. BbF and BkF were found to be the most abundant PAHs. The ratio between BghiPe and IcdP (1.56 for QT and 1.42 for EROS) was similar to previously reported values. Pic and DbaA were detected in less than 20% of the samples, and this is plausible since these PAHs are typically associated with coal combustion.

Table 22: Concentration of PAH ($PM_{2.5}$) congeners at QT and EROS (ng/m^3)

Species	QT				EROS			
	Mean	S.D.	Minimum	Maximum	Mean	S.D.	Minimum	Maximum
BbF	2.16	0.54	1.27	2.97	0.07	0.07	0.03	0.21
BkF	1.55	0.31	0.80	2.00	0.07	0.05	0.04	0.14
BeP	1.75	0.28	1.28	2.02	0.08	0.07	0.05	0.22
BaP	0.95	0.29	0.41	1.36	0.06	0.04	0.05	0.14
Per	0.24	0.06	0.18	0.34	0.05	0.01	0.06	0.07
IcdP	0.32	0.06	0.22	0.46	0.05	0.04	0.04	0.13
DahA	*detected in less than 20% samples*				0.02	0.02	0.00	0.04
Pic	*detected in less than 20% samples*				0.02	0.02	0.00	0.04
BghiPe	0.50	0.08	0.39	0.65	0.07	0.03	0.06	0.14
Cor	0.14	0.02	0.11	0.18	0.05	0.01	0.05	0.07

4.3.2 Size Distributions

The size distribution of a particular element or compound not only influences the potential health impact (in terms of respiratory deposition – Harrison et al., 2010), but also influences the extent of atmospheric dispersion (Allen et al., 2001). Size distributions, measured in terms of mass, number or surface area, are helpful for determining sources of PM, and can be used to analyse the potential health impact (Harrison et al., 2000). In a traffic environment, a number of factors can influence the size distribution including, but not limited to vehicle fleet mix, road type and grade, meteorological conditions (e.g. season type) and distance from the road (Zhu et al., 2006; Beddows et al., 2009; Hays et al., 2011; Song and Gao, 2011).

For individual elements, the size distributions were observed to be markedly different. Some elements showed similar size distributions at both sites (e.g. Fe, Si) while others had distinct distributions at both sites (e.g. Al, Cu). Figure 15 presents the size distributions for the various elements at QT and EROS. Unimodal size distributions were observed for Si and Al with peaks in the coarse mode (~3-4 μm) at QT and EROS although an additional accumulation mode peak was observed for Al (~0.2 μm) at EROS. The accumulation mode peak observed in the case of Al was also observed by Taiwo et al. (2014) and could potentially be attributed to railway emissions. Fe showed bimodal size distribution at both sites, with primary (~3 μm) and secondary peaks (~0.5-0.6 μm) in coarse and accumulation modes respectively. Fe is associated both with crustal dust but brake wear is another important source. Mn also showed a bimodal size distribution although the coarse mode peaks was predominant at QT. At EROS, the primary peak was in the accumulation mode with a smaller, secondary peak in the coarse range. Zn was found to be unimodal at QT but bimodal at EROS.

At QT, primary peaks for Cu, Sb and Ba were found to be very similar (~2-3 µm) which have been associated with brake and tyre wear (Gietl et al., 2010). While Ba and Sb showed unimodal size distributions, Cu had a smaller accumulation mode peak. However, at EROS, Ba showed a bimodal size distribution with peaks in the accumulation and coarse modes. For Pb, accumulation and coarse mode peaks were observed at both sites with the primary peak in the coarse mode (~3 µm) at QT and in the accumulation mode (~0.6 µm) at EROS. Size distribution for V was very similar to Pb at EROS with the primary peak in accumulation mode.

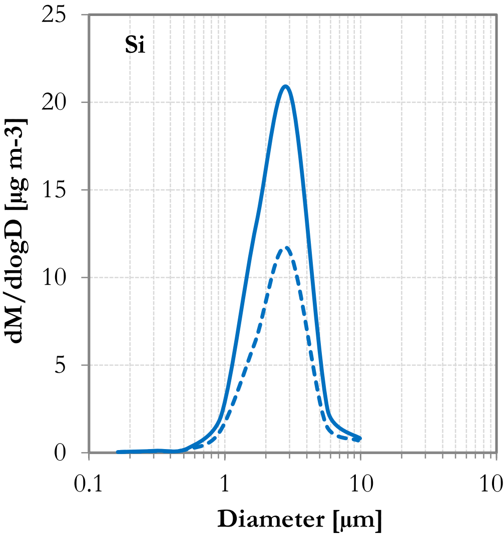

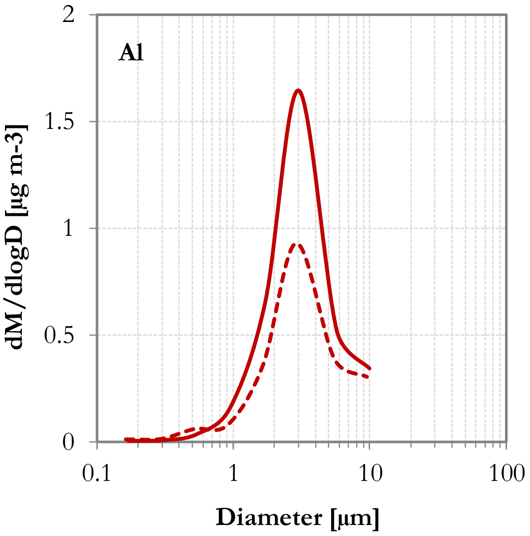

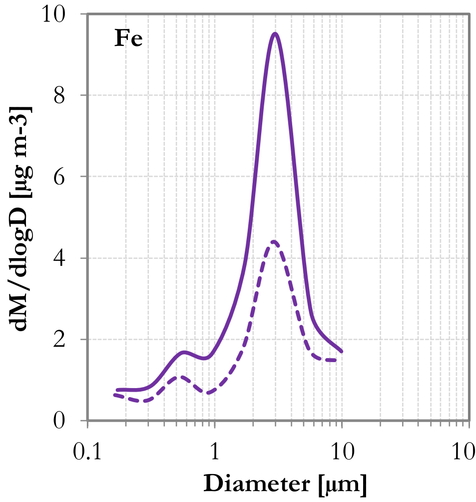

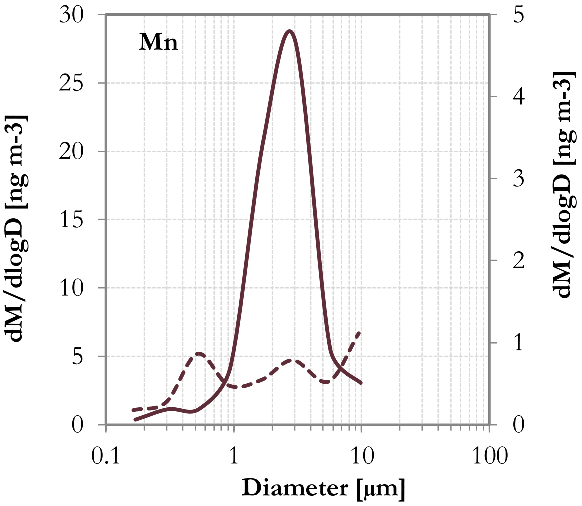

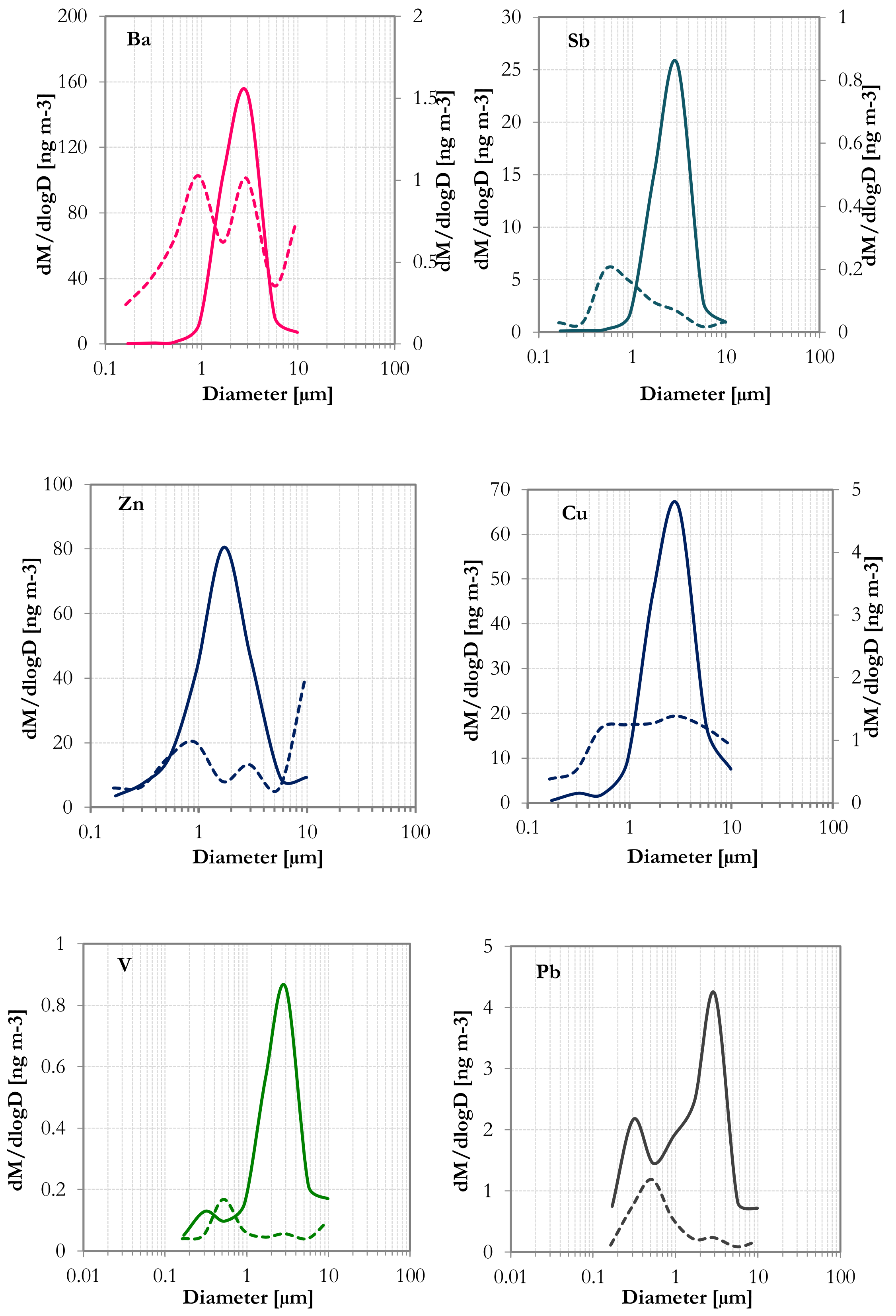

Figure 15: Size distribution for various elements at QT and EROS (based on MOUDI)

(solid line- QT, dashed line-EROS; primary axis for QT and secondary axis for EROS; Al, Si, Fe in µg/m³ and others in ng/m³)

Analyses of the fine/coarse ratios can also aid in understanding the contributions of natural and anthropogenic sources to a particular element. Soil-associated elements including Al, Si and Fe were found to have a higher fraction of coarse mass at both QT and EROS. It is important to note that Fe is also emitted from brake pads in the coarse mode, and the total Fe concentration is due to a combination of crustal and non-exhaust sources. However, all the other elements were predominantly in the fine fraction at EROS (Figure 16). At QT, on the other hand, Pb and Zn had a high fraction of fine mass while Sb, Ba and Cu had high fraction (>50%) of coarse mass. Coarse fraction of Sb and Ba can be associated with brake wear emissions. A higher percentage of elements in the fine fraction at EROS, with very similar peaks in the accumulation mode, could potentially be due to the emissions from the railway tracks in the vicinity. Elements such as Al, Fe, Cu, Zn and Ca are reported to be rich in emissions from railways (wheels, brake pads, rails etc.) with PM peaks in the fine range (0.25-0.6 µm) from brake discs used in railways (Abbasi et al., 2011). Braking action upon approach to the university and wear and tear of wheels, brakes and rail tracks can contribute to fine particle emissions in the vicinity of the site. In addition, most trains running along this route are electric, and particles can be released due to wear and tear of the power lines. However, further research is necessary to understand the possible contribution of railways to ambient PM levels in Birmingham.

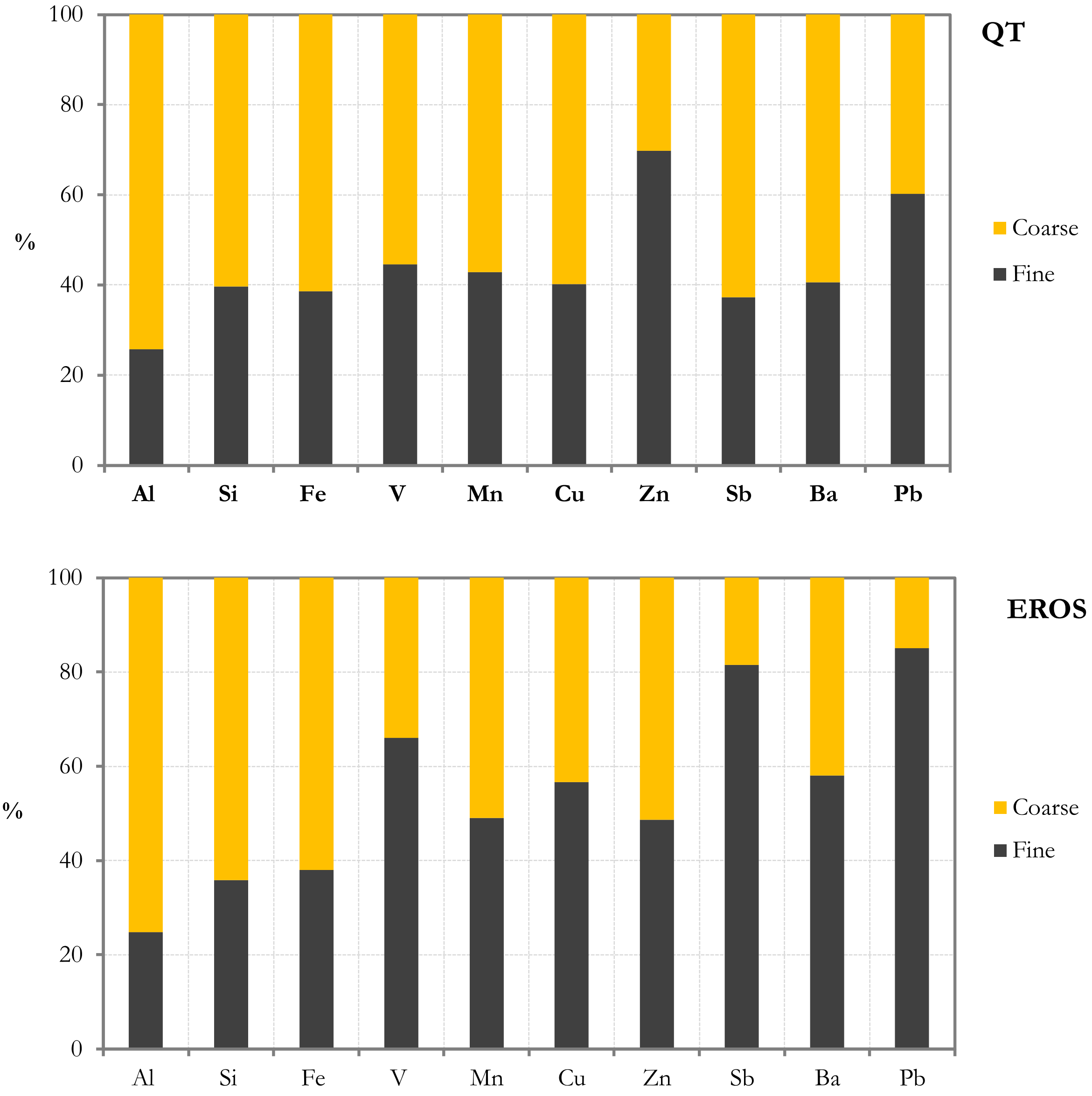

Figure 16: Fraction of fine and coarse PM for elements at QT and EROS

4.3.3 Traffic Enrichment

In order to understand the contribution of traffic on the species' concentrations, traffic enrichment was calculated for the various species based on the equation 9 (Amato et al., 2011b). $PM_{2.5}$ measurement data was used for this analysis.

$$Roadside\ enrichment = \left(\frac{C(X)_t - C(X)_{ub}}{C\ (X)_t}\right) * 100 \qquad (9)$$

Where
C_t is concentration of species X (in PM) at QT (t-tunnel)
C_{ub} is the concentration of species X (in PM) at EROS (ub-urban background)

In case of elements, more than 80% increment was observed for all the measured elements between EROS and QT with the highest increments for elements such as Sn (98.7%), Ba (98.2%) and Cu (97%) and lowest increment for Mn (82.1%) in $PM_{2.5}$. Surprisingly, the roadside enrichment for Zn in $PM_{2.5}$ was lower than the other elements.

In case of carbon ($PM_{2.5}$), enrichment of 95.9% and 91.4% was observed for EC and OC respectively. Alkanes showed the highest enrichment among the molecular marker species, with almost 100% enrichment.

This approach has been used previously to understand the enrichment due to traffic emissions in urban areas with respect to background locations by Oliviera et al. (2010) and Amato et al. (2011b) although the level of enrichment was lower compared to the results from this study.

4.3.4 Composite Traffic Source Profile

For vehicular emissions, source profiles are typically generated using dynamometer-based sampling. However, as discussed in Chapter 1, composite (i.e. mixed gasoline and diesel) profiles can also be generated using ambient measurements. Source profiles can be prepared with respect to PM as well as OC. USEPA SPECIATE 4.4 profiles are typically listed as the weight percentage of total PM mass and the related uncertainty.

Ambient profiles can be prepared using tunnel/roadway measurements, and one of the methods uses the assumption that the roadside increment (i.e. the difference in concentration between the roadside and background concentrations of PM and its constituents represent the traffic emissions', and the increment is used to prepare a source profile (µg/ µg OC). The approach is discussed in detail in Chapter 3. QT and EROS measurements for key traffic markers were used in the following equation to generate the profile (Table 23).

$$Profile\ value = \frac{Concetration\ (X)_{\mathrm{QT}} - Concentration\ (X)_{\mathrm{EROS}}}{Concentration\ (OC)_{\mathrm{QT}} - Concentration\ (OC)_{\mathrm{EROS}}} \qquad (10)$$

Where
Concentration $(X)_{\mathrm{QT/EROS}}$ refers to concentration of species X at QT/EROS
Concentration $(OC)_{\mathrm{QT}}$ refers to concentration of species OC at QT

The tunnel profile was compared against the twin-site profile reported in Chapter 3 and other traffic profiles including ambient measurement- based (France- El Haddad et al., 2009; USA- Yan et al., 2009) and dynamometer-based profiles (Lough et al., 2005). The profile was found to be broadly similar to the other ambient data-based profiles (Figure 18).

Coefficient of divergence (CoD), a self-normalizing statistic, is often used to understand the degree of similarity between PM observations across sites (Wongphatarakul al., 1998). CoD values range from 0 to 1; values closer to zero indicate a higher degree of similarity while values closer to one indicate dissimilarity. Recently, the statistic has been also used to calculate the degree of similarity between source profiles (Kong et al., 2011). For the current study, CoD was calculated using the following formula (Wongphatarakul al., 1998):

$$COD = \sqrt{\frac{1}{n}\sum_{i=1}^{k}\frac{(xij - xik)^2}{(\mathrm{xij+xik})^2}} \qquad (11)$$

Where
xij is the concentration of species i in profile j
xik is the concentration of species i in profile k
n is the number of species used in calculation

In order to understand the stability of the species, ratios of individual values to mean values were calculated, and a value of 1 represents absolute similarity. The variation within the different compound classes is presented in Figure 17. Hopane species and EC exhibit the least amount of variability, while several elements (e.g. Mn) exhibited highest degree of variability. Higher variability in case of elements can be due to the various emission sources (including soil, non-exhaust and exhaust emissions) which can lead to higher uncertainties while hopanes are emitted as exhaust emissions. The data indicates that carbonaceous species are more stable for use as markers for the exhaust emissions, and are better suited for use in receptor modelling.

Table 23: Composite $PM_{2.5}$ traffic profile based on tunnel measurements (µg/ µg OC)

Species Class	Species	Concentration	Uncertainty
Carbon	**EC**	1.0487	0.1724
Elements	**Ca**	0.1007	0.0516
	Ti	0.0011	0.0005
	V	0.0001	0.00003
	Mn	0.0015	0.0008
	Cu	0.0062	0.0019
	Zn	0.0057	0.0023
	Sn	0.0013	0.0004
	Sb	0.0007	0.0002
	Ba	0.0044	0.0011
Alkanes	**C24**	0.0093	0.0025
	C25	0.0083	0.0024
Hopanes	**TNOHO**	0.0001	0.00001
	NHO	0.0003	0.00004
	HOP	0.0004	0.0001
	HHO	0.0002	0.00003
	BHHO	0.0002	0.00002
	THHO	0.0001	0.00002
PAHs	**IcdP**	0.00002	0.00001
	BghiPe	0.00003	0.00001
	Cor	0.00001	0.00000

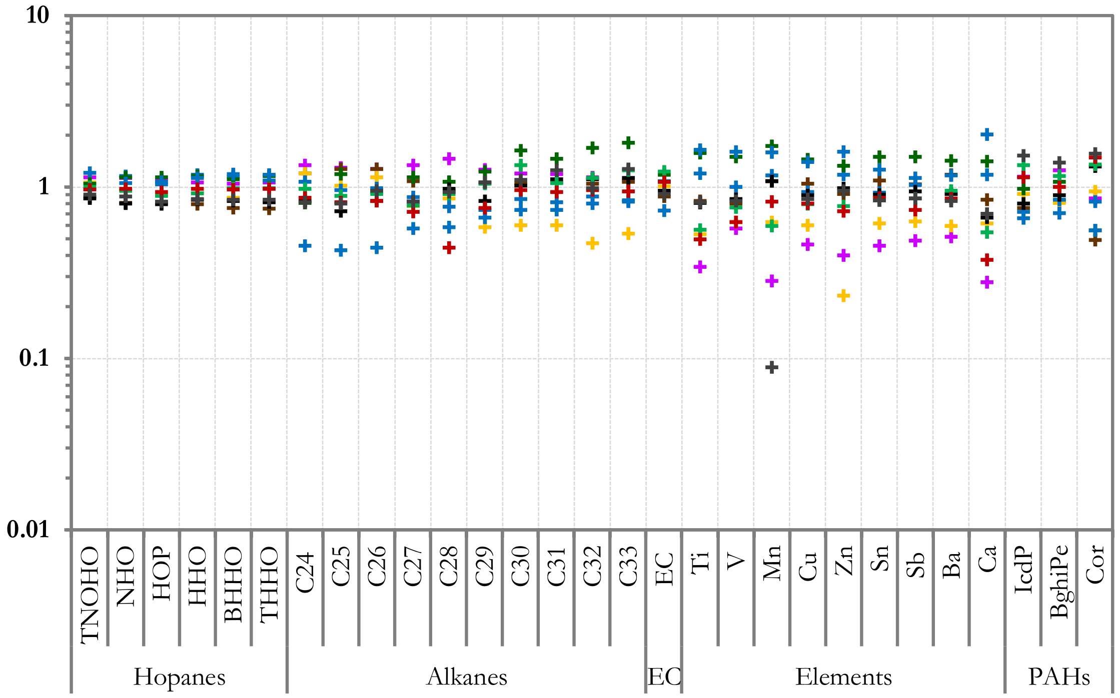

Figure 17: Variations within species classes in the tunnel profile ($PM_{2.5}$) *(individual colours represent samples)*

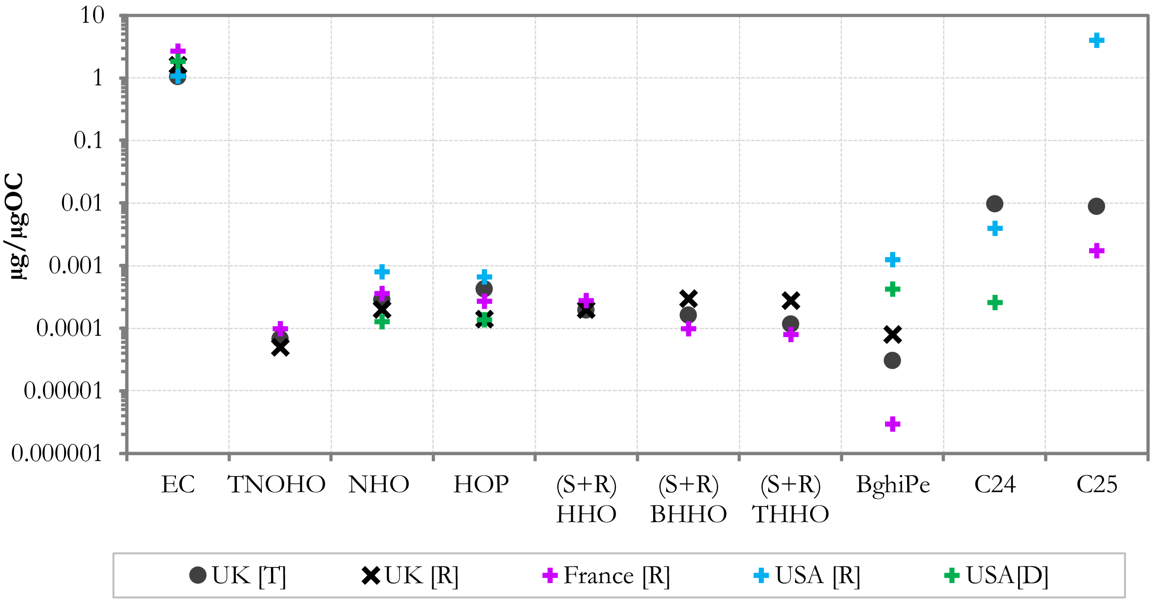

Figure 18: Comparison of tunnel profile with other ambient and dynamometer-based profiles

(all profiles for $PM_{2.5}$, R- ambient (UK [R] and USA[R]- twin-site, France[R]-tunnel) and D- dynamometer)

Highest similarity was observed for the two UK profiles (CoD= 0.32) while the highest variation was observed for the UK tunnel profile and the USA dynamometer profile (CoD= 0.65) (Figure 19). While EC and hopane congener concentrations were relatively similar across profiles, differences were observed in concentrations of BghiPe, and alkanes. Some difference in PAH concentrations is expected due to the differences in fleet composition (diesel/gasoline split) across the countries. The lowest concentration of BghiPe was observed in France, where the diesel: gasoline split is nearly 50:50. In addition, differences in concentrations can result from variations in vehicle fleet and the age of vehicles.

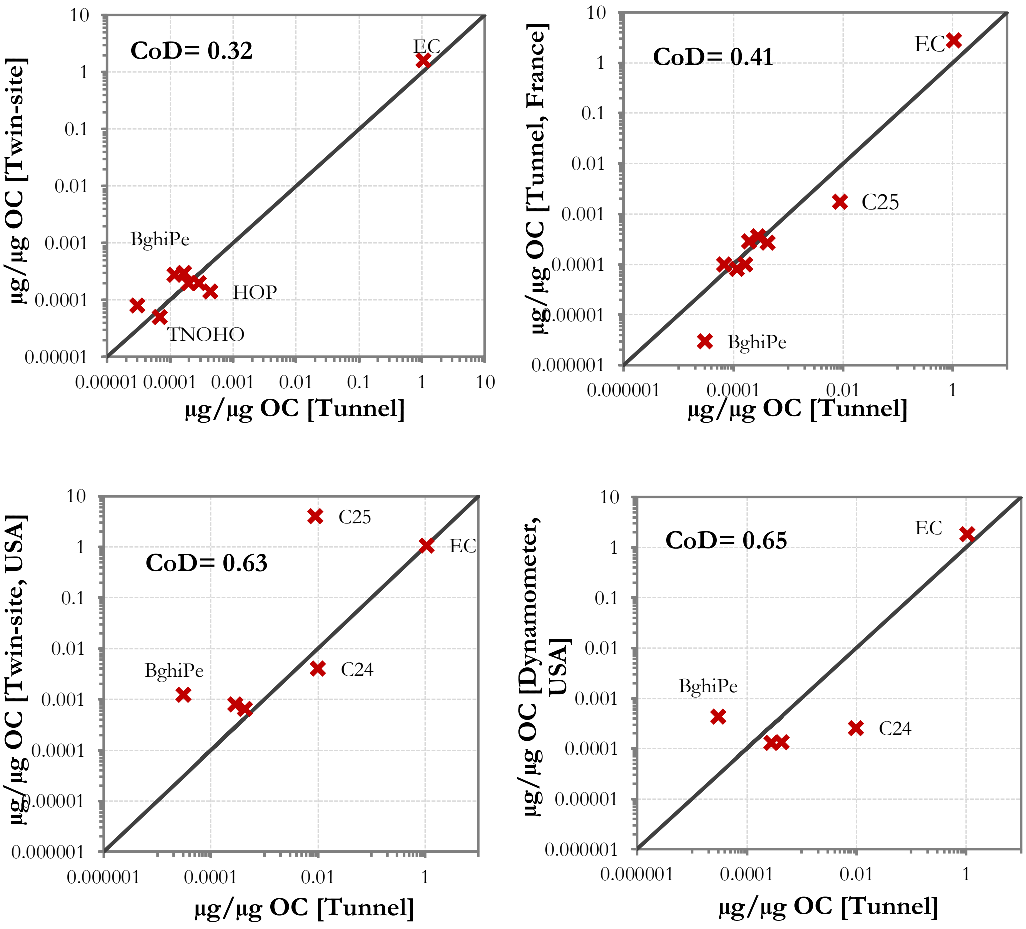

Figure 19: Comparison between the tunnel profile and other reported source profiles

4.4 Conclusions

$PM_{2.5}$ samples (total and size-segregated) were analysed at a road tunnel and an urban background site in Birmingham (UK). The samples were analysed for traffic-associated elements and molecular markers and significant enrichment was observed both for elemental and organic species at the tunnel site.

Si and Fe were found to be the most abundant elements in $PM_{2.5}$ in the tunnel, and Cu, Zn and Ba were the most abundant trace elements. Unimodal size distribution as observed for Si and Al at QT but a smaller secondary peak was also observed for Al at EROS. Analysis of size distribution data indicates the potential impact from the nearby railway tracks at EROS, but this needs to be analysed further. Characteristic coarse-mode peaks were observed for tracers of non-exhaust emissions- Cu, Sb and Ba, indicating the contribution of non-exhaust emissions. The Cu/Sb ratio was found to be broadly similar to previously reported characteristic ratio for brake –wear emissions.

A composite $PM_{2.5}$ traffic source profile was prepared using the Lenschow approach (Lenschow et al., 2001), and compared against the other profile prepared for UK (Chapter 3). Overall, the profile prepared using the tunnel measurement was similar to the other UK composite $PM_{2.5}$ profile as well as other reported profiles. However, a key difference was the lower uncertainty estimates for the individual species for this profile compared to the other profile prepared using the ambient measurements at ambient sites. High uncertainties associated with species in a source profile can introduce errors during receptor modelling with CMB, as the statistics associated with the model are dependent on the uncertainty estimates. Preparation of source profile using monitoring data from tunnels offers an advantage over monitoring data from other ambient sites (e.g. kerbside) since the influence of other sources as well as meteorology is limited. For example, Boogard et al.

(2011) reported variations in PM concentrations due to differences in wind speed and direction and/or vehicle speed in the Netherlands, particularly in street canyons.

This is the first, and one of the few studies that have focused on characterization of exhaust emissions in a road tunnel in the UK. The source profile prepared as a part of this study can be used for future receptor modelling studies as well as for improvement of emission inventories in UK and possibly in Europe.

Comparison of the profile from this study with the profile discussed in Chapter 3 indicates distinct advantage in the case of tunnel emissions' profile in the lower uncertainties associated with the individual species.

4.5 Acknowledgements

Special thanks to Mr. John Poole and Mr. Salim Azzi at Amey for access to the Queensway Tunnel and Paul and Darren for help with access to the sampling site. Help from Mr. Christopher Stark and Mr. Massimiliano Mascelloni in equipment set-up and Dr. Stephen J. Baker in elemental analysis is gratefully acknowledged. Thanks to the UoB Advanced Materials Characterization (AMC) facility for the access to XRF.

CHAPTER 5- PM_{10} ROAD DUST IN INDIA AND UK

Road dust emissions (PM_{10} fraction) were characterized and source profiles were prepared for UK and India. In addition, contributions of the key sources of PM_{10} road dust- brake wear, tyre wear and re-suspended dust were quantified using an empirical source estimation method.

Graphical Abstract

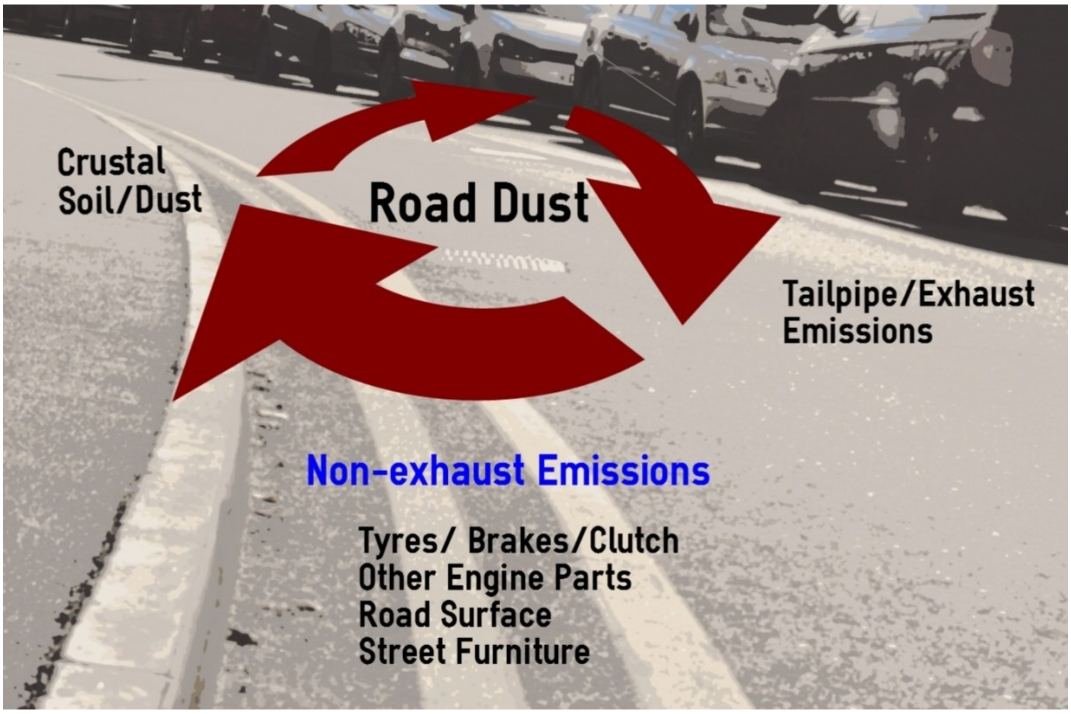

5.1 Introduction

Particulate matter (PM) emissions from road vehicles include exhaust and non-exhaust (wear and tear of vehicle parts, re-suspension of dust) emissions (Pant and Harrison, 2013). Non-exhaust emissions are more abundant in the coarse size fraction and can deposit on the roadside and can subsequently be resuspended due to vehicle activity. Road dust (RD) consists primarily of coarse-sized particles derived from sources such as wear and tear of vehicle components (brakes, tyres and clutches) and road surface, engine corrosion, tailpipe emissions, crustal dust and other emission sources. However, similarity in composition between emission sources such as brake wear and road dust and other emissions which can deposit on the road before being resuspended renders it difficult to distinguish the contribution of the various sources (Bukowiecki et al., 2010). RD can be a significant source of trace metals, particle-bound PAHs and other chemical species. Several studies on RD have reported elemental and organic marker concentrations in different size fractions (Han et al., 2007; Morillo et al., 2007; Agarwal, 2009; Amato et al., 2009a; Faiz et al., 2009; Duong and Lee, 2011; Gunawardana et al., 2011; Martuzevicius et al., 2011). Crustal dust/soil are characterized by elements such as Si, Al, Ti, Mn and Fe while non-exhaust emissions are typically characterized by trace metals such as Cu, Ba, Sb, Sn (brake wear) and Zn (tyre wear) (Wahlin et al., 2006; Gietl et al., 2010). However, several authors have also used molecular markers including PAHs, n-alkanes and benzothiazoles (Lough et al., 2005; Kwon and Castaldi, 2012). A detailed description of non-exhaust emissions is provided in Chapter 1, section 1.2.2.

Enrichment of both elements and organic species has been reported in RD samples compared to background soils worldwide (Han et al., 2007; Liu et al., 2007; Agarwal, 2009; Duong and Lee, 2011; Luo et al., 2011; Peltier et al., 2011).

It is important to note that the concentration profile for contaminated soil as well as non-exhaust emissions is unique for every region and can vary based on several parameters such as traffic (volume and pattern, fleet characteristics), road surface type and climate and geology of the region (Omstedt et al., 2005; Amato et al., 2011a; Kwak et al., 2013). Most of the research as well as policy action in the last few decades has largely focused on exhaust emissions, and with a decline in percentage contribution of vehicle exhaust emissions to ambient PM, the contribution of non-exhaust PM is becoming important (Thorpe and Harrison, 2008; Denier van der Gon et al., 2013). Detailed accounts of sources and properties of non-exhaust emissions and ambient measurements of non-exhaust components are provided elsewhere (Luhana et al., 2004; Thorpe and Harrison, 2008; Pant and Harrison, 2013; Amato et al., 2014a).

Much of the reported research so far has been conducted on suspended road dust (bulk PM fraction) with a very few studies focused on the characterization and source apportionment of the PM_{10} fraction of road dust (Wahlin et al., 2006; Amato et al., 2009a; Han et al., 2009; Amato et al., 2011a). Since RD is a significant source of PM, it is important to prepare detailed source emission profiles. Both India and UK lack detailed chemical source profiles for the road dust source. For Delhi, source profiles for PM_{10} road dust (paved, unpaved and soil) were published as part of a larger study but the molecular markers were not analysed in detail (Sethi and Patil, 2008).

The aims of this study include:

- characterization of the chemical composition of PM_{10} road dust
- preparation of PM_{10} road dust source profiles for Birmingham (UK) and New Delhi (India) and
- quantification of the contribution of the non-exhaust sources to the dust in Birmingham and New Delhi

To the best of our knowledge, this is the first study to undertake detailed elemental as well as molecular marker characterization of the PM_{10} fraction of road dust both in India and the UK.

5.2 Methodology

5.2.1 Sampling Sites

Samples were collected at three sites in Birmingham and at one site in New Delhi. Figure 20 provides the modal split at the sites B-D (DfT, 2014; Goel, 2014).

University South Road, UoB Campus, Birmingham (Site A): This site is located within the university campus.

A38 Bristol Road, Birmingham (Site B): This is one of the major arterial roads in south-west Birmingham with a dual carriageway with 32,000 vehicles/day (DfT, 2014).

A38 Queensway Tunnel (QT), Birmingham (Site C): This is one of the major road tunnels in Birmingham and runs in the North/South direction. It is a 544 metres long twin bore tunnel with two lanes on each side. Average vehicle speed in the tunnel is 50 kilometres/hour and an estimated 89000 vehicles travel through the tunnel each day (Azzi, 2012).

CRRI, New Delhi (Site D): Samples were collected adjacent to the Mathura Road/National Highway 2. Mathura Road is one of the major arterial roads in Delhi with an average traffic flow of 170,000 vehicles per day (Goel, 2014). Buses, LDVs, and two- and three-wheelers are not restricted but trucks (diesel, BS-III) are not allowed between 0730 to 1100 hours and 1700 to 2130 hours while buses (Delhi Police, 2014).

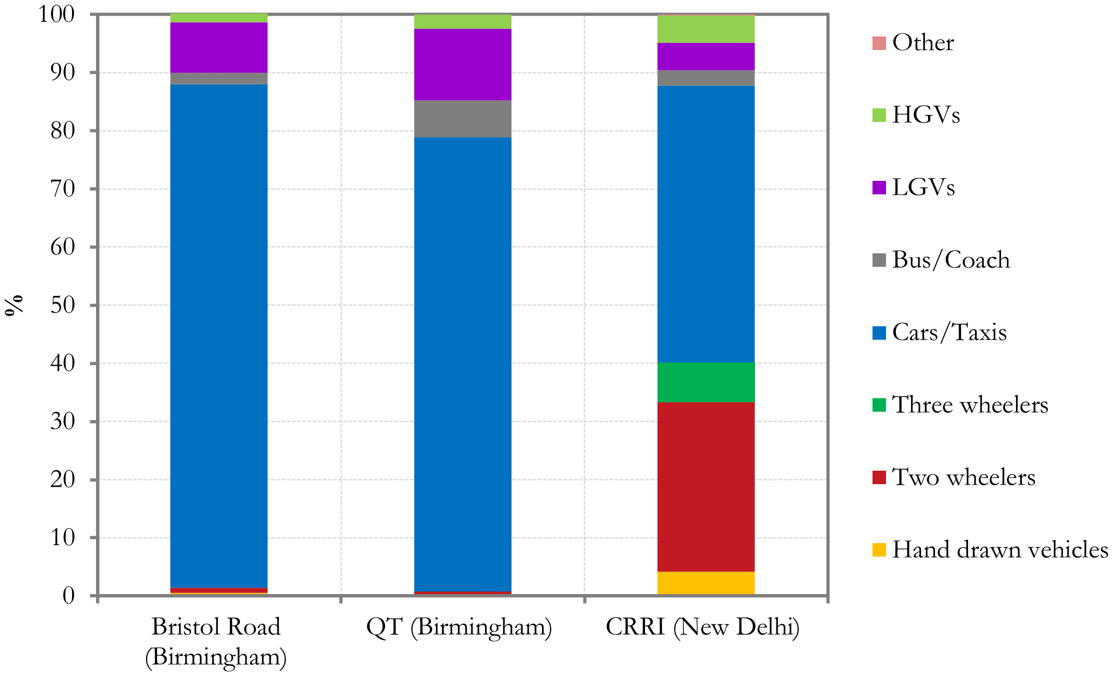

Figure 20: Modal split at the sites in Birmingham (UK) and New Delhi (India)

5.2.2 Sampling

Road dust samples were collected at Site C (QT) in September 2012 using the dust sampler (Chapter 2, Section 2.2.4). Samples were also collected at Sites A and B (University Road-South and Bristol Road) in July 2013 and at Site D (Delhi) in June 2013. At Sites A, B and D, samples were collected on quartz (QM-A Whatman 47mm) and PTFE (47mm) filters (n= 10 for each type) while at Site C, samples were collected with PTFE filters only (n=10). Samples were collected on both sites of the road close to the traffic junction, and at least two samples were taken in the middle lane (Figure 21).

Figure 21: Layout for road dust sample collection

5.2.3 Analytical Methods

Samples were analysed using methods described in Chapter 2.

The PTFE filter samples were analysed for Al, Si, Fe for sites A-D by WD-XRF and the samples from Site C were also analysed for S. ICP-MS was used to analyze the digested samples for Ti, V, Cr, Mn, Cu, Zn, Sb and Ba. In addition, samples for sites A, B and D were analysed for Sn and Ca while samples for site C were analysed for Ni, and Cd.

The quartz filter samples from Sites A, B and D were used to analyse OC and EC using the carbon analyser and GC-MS was used to analyse PAHs (BbF, BkF, BeP, BaP, IcdP, Pic, BghiPe and Cor), alkanes (C24-C35) and hopanes (TNOHO HOP, NHO, S, R- HHO, S, R-BHHO and S, R-THHO).

5.3 Results

5.3.1 Mass Loadings

Average mass loadings were observed to be 16.9 ± 12.9 mg/m^2, 9.3 ± 5.6 mg/m^2, 12.1 ± 9.3 mg/m^2 and 72.9 ± 24.3 mg/m^2 for sites A, B, C and D respectively. The mass loading for PM_{10} was found to be much higher in New Delhi (India) compared to Birmingham (UK). An average mass loading of 9 mg/m^2 has been reported for the city centre in Barcelona (Spain) while mass loadings of 2.4-21.6 mg/m^2 have been reported for different site types across Spain (Amato et al., 2009a; 2013a). In Zürich, average mass loading was observed to be 0.7 ± 0.4 mg/m^2 in a tunnel and 1.3 ± 1.3 mg/m^2 in one of the street canyons while in Utrecht, the loading was reported to be 3.6 mg/m^2 (Amato et al., 2011a; Amato et al., 2013a). Elemental concentrations are presented in Figure 22, and average mass loadings for elements and organic species are presented in Table 24.

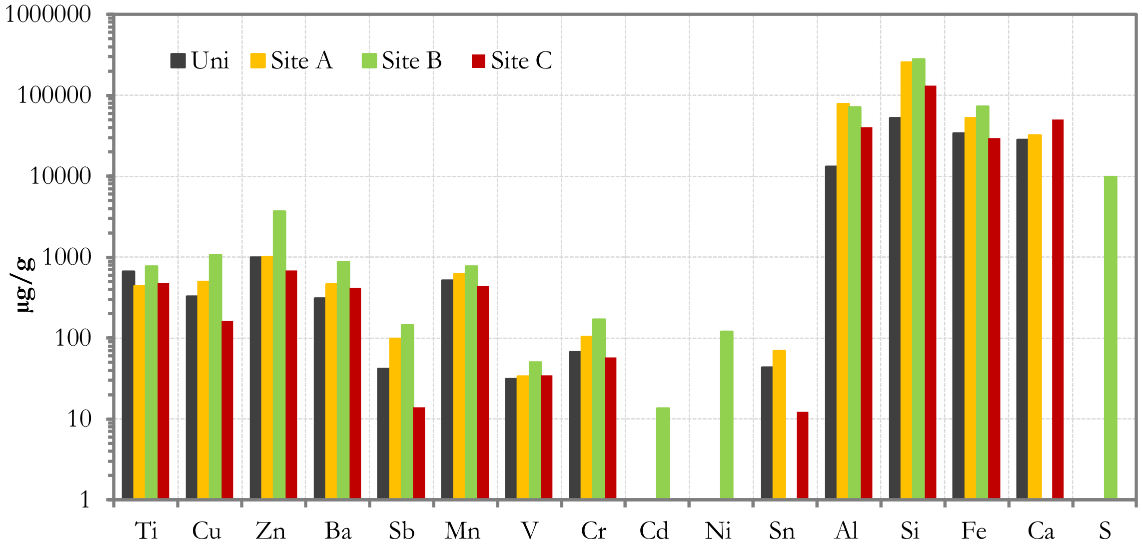

Figure 22: Concentrations of various elements in PM_{10} road dust at Sites A-D (µg/g)

Mass loadings (µg/m^2) for all the species were found to be higher in case of Site D (New Delhi) compared to the Birmingham sites (Sites A, B and C) while the concentrations (µg/g) were found to be highest in the road tunnel environment in Birmingham (Site C). Si had the highest concentration among the crustal elements, and Zn and Cu were the most abundant traffic-related elements at Sites B and C whereas Zn and Ba were the most abundant in case of Site D. Spada et al. (2012) reported similar results with higher concentrations of Cu, Zn, Pb, Ba, Sn and Sb in road dust samples from tunnel compared to roads in Houston (USA). Concentrations (µg/g) of traffic-associated elements (Cu, Zn, Ba) were lower in Birmingham as well as Delhi compared to the results reported for Barcelona and Zürich by Amato et al. (2011a) although concentrations for Mn and Fe were broadly similar. The site in Delhi had a higher proportion of HDVs as well as unpaved surfaces, and these could be contributing to the higher mass loading. Previous studies have reported higher dust loadings for areas with HDVs (Abu Allaban et al., 2003; Amato et al., 2013a). Between the road and tunnel sites in Birmingham, concentrations were consistently higher at Site C (tunnel) compared to the road site (Site B) with the exception of Al whose concentration was higher at Site B. The sampling site on campus presented an anomaly. While the site had a very low volume of traffic compared to the other Birmingham sites, the PM mass loading as well as concentrations were comparable to Site B (a high-traffic road). This could partly be explained by the higher percentage of medium duty and HDVs plying on the road and the parking lot in the vicinity, but further analysis is required.

Table 24: Average mass loadings of various species in the PM_{10} road dust (in $\mu g/m^2$)

(a) Metals

Species	*Site A*	*Site B*	*Site C*	*Site D*
PM_{10} (mg m^{-2})	16.9 ± 12.9	9.34 ± 5.56	12.1 ± 9.3	72.9 ± 24.3
Ti	12.0±10.3	3.82±2.62	8.0±4.28	33.8±9.81
Cu	5.5±4.33	4.22±2.64	11.1±5.04	12.1±4.61
Zn	15.8±11.9	8.69±5.56	37.8±19.2	50.9±22.0
Ba	5.4±4.33	3.89±2.21	8.83±4.06	31.0±11.5
Sb	0.69±0.55	0.82±0.48	1.52±0.72	1.04±0.37
Mn	8.95±7.19	5.39±3.58	7.87±3.83	31.9±11.4
V	0.53±0.43	0.29±0.18	0.52±0.27	2.53±0.88
Cr	0.92±0.60	0.85±0.44	1.69±0.86	4.10±1.33
Cd	na*	na	0.13±0.05	na
Ni	na	na	1.19±0.83	na
Sn	0.7±0.6	0.58±0.36	na	0.90±0.38
Al	201±154	696±359	712±280	2696±355
Si	814±624	2322±1250	2785±1075	8907±1468
Fe	580±459	496±339	2785±1075	2258±855
Ca	489±392	278±169	na	3632±1307
S	12.0±10.3	na	101±41	na

(b) Carbonaceous Species

Species	***Site A***	***Site B***	***Site D***
OC	218±142	570±213	1774±404
EC	0.51±0.61	88±47	317±86
TNOHO	0.09±0.05	0.95±0.31	1.20±1.25
HOP	0.36±0.31	3.29±1.29	5.75±5.98
NHO	0.67±0.57	5.88±1.66	7.00±5.95
SHHO	0.24±0.17	1.82±0.60	2.65±2.30
RHHO	0.22±0.14	1.56±0.55	2.42±2.05
SBHHO	0.28±0.16	1.77±0.37	2.65±2.24
RBHHO	0.25±0.07	1.32±0.28	1.91±1.65
STHHO	0.21±0.15	1.26±0.29	2.12±1.77
RTHHO	0.20±0.09	0.90±0.21	1.61±1.33
C24	0.03±0.01	0.18±0.08	0.31±0.27
C25	0.15±0.03	0.66±0.20	0.37±0.32
C26	0.12±0.03	0.35±0.26	0.40±0.25
C27	0.33±0.12	0.99±0.48	0.98±0.58
C28	0.39±0.19	1.42±0.85	0.95±0.62
C29	0.29±0.09	1.55±0.91	1.53±1.40
C30	0.11±0.03	0.67±0.27	0.40±0.46
C31	0.31±0.20	0.96±0.10	0.92±0.82
C32	0.23±0.08	1.01±0.21	0.31±0.26
C33	0.18±0.05	1.02±0.11	0.39±0.30
BbF	0.07±0.05	0.57±0.16	1.92±1.15
BkF	0.10±0.07	0.62±0.16	1.44±0.68
BaP	0.09±0.06	0.42±0.10	0.97±0.53
BeP	0.08±0.05	0.48±0.14	1.24±0.54
Picene	BDL**	0.03±0.04	0.18±0.14
IcdP	0.09±0.03	0.38±0.09	1.17±0.58
BghiPe	0.09±0.03	0.40±0.08	1.08±0.53
Cor	0.03±0.03	0.16±0.05	0.34±0.17

Results obtained in the current study were also compared with previously reported values of road dust from USA (Apeagyei et al., 2011), Europe (Morillo et al., 2007; Amato et al., 2009a; Sadiktis et al., 2012), China (Han et al., 2009; Wei et al., 2009; Wang et al., 2011), South Korea (Duong and Lee, 2011) and Ghana (Essumang et al., 2006) (Figure 23). Concentrations of most elements were within the reported range and corresponded with previously reported values. Concentrations for brake wear-related elements such as Sb and Ba were lower in case of New

Delhi compared to Birmingham as well as other European sites while Ca concentration in Delhi (Site D) was found to be higher than other reported studies. Ca has been used as a marker for construction activity (Chen et al., 2012). The concentration of Sn was found to be higher in Birmingham compared to New Delhi whereas concentrations of other traffic-related elements such as Cu, Ba, Zn and Sb were found to correspond with other reported datasets. However, in this study, the concentration of Ti was significantly lower across all sites compared to previously reported concentrations. For the organic species, concentrations were found to be close to the higher range of the previously reported values. In the case of Delhi, correspondence was seen between current observations and previously reported concentrations.

It is important to note that elemental concentrations can vary based on the type of tyres, brakes and pavement used at the site type. For example, summer tyres create a lower dust loading (tyre dust) compared to non-studded and studded tyres. Although both Birmingham and New Delhi use summer tyres all year round, the composition of tyres and pavement types are expected to be different. Chemical composition of brakes and tyres is expected to be different in UK and India. In addition, concentrations of elements such as Si, Al and Fe can vary based on local crustal composition. For example, Fe was found to be 3.4%, 5.3%, 7.3% and 3.1% for Sites A, B, C and D respectively while Al was found to be 1.3%, 7.8%, 7.2% and 3.98%. Chen et al. (2012) reported the abundance of Fe and Al as 2% and 3.5% in China while Amato et al. (2011a) reported Fe abundance of 4.6%, 5% and 5.8% and Al abundance of 2.8%, 8% and 13.6% for Zurich, Barcelona and Girona respectively.

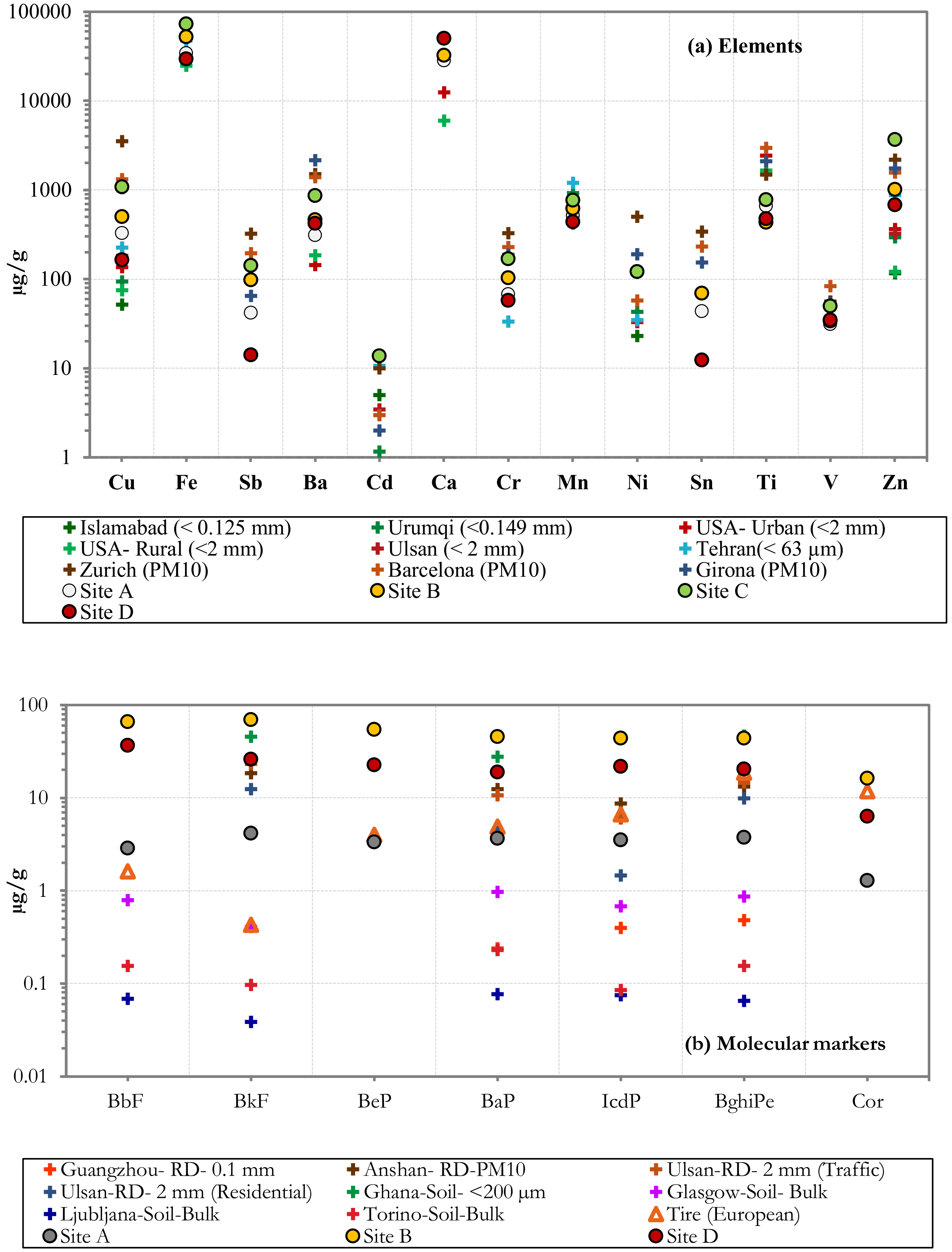

Figure 23: Comparison of (i) elemental and (ii) molecular marker concentrations found in current study with previous studies

(+ source profile;□ ambient data;□ current study)

5.3.2 Correlation Analysis

Based on Pearson correlation analyses, two major groups of elements were identified for sites B and C, each with statistically significant correlations among the elements in the group: crustal elements including Al, Si and Fe (group 1) and traffic-related elements such as Cu, Zn and Sb (group 2). In Beijing (China), Chen et al. (2012) reported four groups: crustal elements (Al, Fe, Ca, Ti), salt (K, Mg, Na), sulphur and other trace elements. At site C, Ni was not found to be correlated to either group. Nickel is typically attributed to industrial and fuel oil emissions and has also been attributed to engine metal wear and tear (Hays et al., 2011). In UK, Pulles et al. (2012) reported a high Ni concentration in gasoline.

Ca showed a high correlation with the traffic-associated elements at sites A and B. At site D, high correlation was observed between Zn, Cu and Ba but it was weaker for Sn. Antimony (Sb), on the other hand, was not found to be correlated to other traffic-associated elements. Interestingly, while Ti was found to be correlated to traffic-related elements at Sites A, B and C, a higher correlation was observed for Ti with Al and Si at Site D. The traffic-related elements could not be subdivided into tyre/brake wear categories based on correlation analysis. PAHs showed very high correlation to one another ($r^2 > 0.98$).

5.3.3 Enrichment Factor Analysis

To further understand the sources of the elements, enrichment factors (EFs) were calculated based on continental crust concentrations using Al as the reference element (Taylor and McLennan, 1995) (Figure 24). EFs above 10 imply contribution from anthropogenic emissions.

$$Enrichment\ Factor\ (X) = \frac{\left\{\frac{Concentration(X)}{Concentration(Reference)}\right\} sample}{\left\{\frac{Concentration(X)}{Concentration(Reference)}\right\} crustal} \tag{12}$$

Where
Concentration (X) refers to concentration of species X in sample/earth's crust
Concentration (Reference) refers to concentration of Al in sample/earth's crust

Use of Al as the reference element was based on previous studies in Birmingham that identified minimal traffic-associated increment for Al (Birmili et al., 2006). Corresponding to the correlations observed in the dataset, highest EFs were observed for Cu, Zn, Sb, Cr and Sn. Other studies have also reported high EFs for Ba, Cr, Cu and Sb (Birmili et al., 2006; Dongarra et al., 2009; Oliviera et al., 2011). The highest enrichment factors were observed Cd (~1000), Sb (>100) and Sn (~100), particularly at Site A. In Delhi, while Cd had a high enrichment, Sn and Ba (tracers of brake wear) were not highly enriched. Zn was not significantly enriched at any of the sites. High enrichment of Sb, Sn and Cu at Site A indicates high contribution from brake wear, and this is plausible since the site is located close to a parking area, and vehicles are also parked along the road. Si, Ti and V showed hardly any enrichment and are likely contributed by soil.

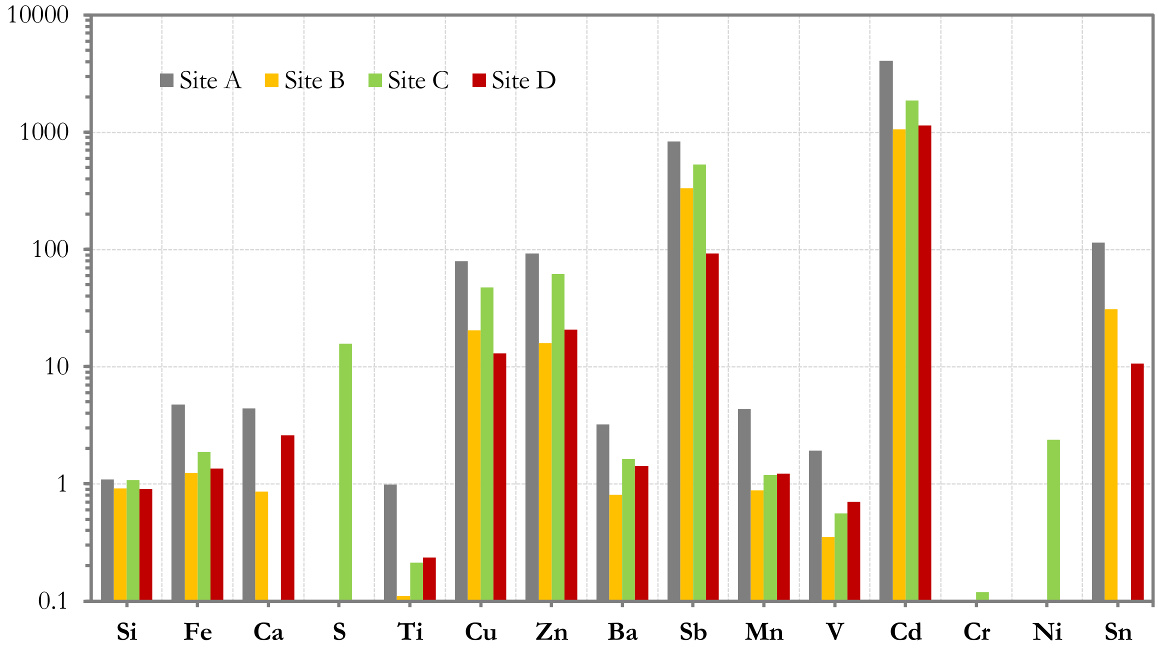

Figure 24: Enrichment factors for PM_{10} road dust for sites A-D

5.3.4 Elemental Ratios

Ratios between different elements can be used to distinguish between different sources. Various authors have proposed characteristic Cu/Sb ratio for brake wear particles including 4.6 ± 2.3 in USA (Sternbeck et al., 2002) and 7.0±1.9 in Europe (Amato et al., 2009a). In comparison, this ratio is 125 for upper continental crust (UCC) indicating much higher concentration of Cu in the crust compared to Sb. It is important to note that this ratio can vary based on the Cu content of the brakes, which differs among manufacturers (Pant and Harrison, 2013). Ratio of Cu/Sb from brake pads also varies based on the type of material used; for example, NAO brake lining material typically has a Cu/Sb ratio of 11.5 (Iijima et al., 2007) whereas the ratio is 1.33 for semi-metallic brake pad material (Schauer et al., 2006).

In the current study, the overall Cu/Sb ratio was observed to be 8.19±1.32 for Site A, 5.14±0.30 for Site B, 7.50±0.79 for Site C and 11.5±0.82 for Site D. The ratio values fall within the proposed characteristic ratio for the traffic locations (Sites B and C) in Birmingham indicating the contribution of brake wear particles to the PM_{10} fraction of road dust and are similar to the Cu/Sb ratio of 7.5 reported for low-metallic brake discs in USA (Schauer et al., 2006). However, a higher ratio was observed in the case of Site D (India) which could either be due to other sources of Cu in the area or differences in the composition of brake pads. Brake pad composition is known to vary across geographical regions (Amato et al., 2012b; Pant and Harrison, 2013).

A summary of other elemental ratios is provided in Figure 25. In order to understand the contribution of crustal material at different sites, the average Si/Al and Fe/Al at the three sites were compared to the ratios in the upper continental crust (UCC). The Si/Al ratio was found to be similar across sites (3.3-3.9) and corresponded with the average UCC composition (3.9). However, Fe was found to be enriched across all sites with maximum enrichment at Site B. In the UK, Fe is expected to be emitted from brake discs with some contribution from soil. In the case of Delhi, Fe is known to be present in high concentration in soil in Delhi due to the ferrogenous quartzite found in the Aravalli Hills (Sarin et al., 1979; Pant and Harrison, 2012). An average Fe/Al ratio of 0.55-0.63 has been reported for soil in the Indian plains (Sarin et al., 1979; Sudheer and Rengarajan, 2012). Thus, it can be concluded that crustal material is the primary source of the Si and Al concentrations across sites while Fe has both crustal and anthropogenic sources.

Pulles et al. (2012) reported a Cu/Zn ratio of 0.13 for gasoline and 0.35 for diesel fuel in the UK. Interestingly, the ratio value of 0.35 is also reported for upper continental crust (UCC) (Taylor and McLennan, 1995). This highlights the potential difficulty in ascertaining the sources of elements such as Cu in road dust on the basis of elemental ratios alone.

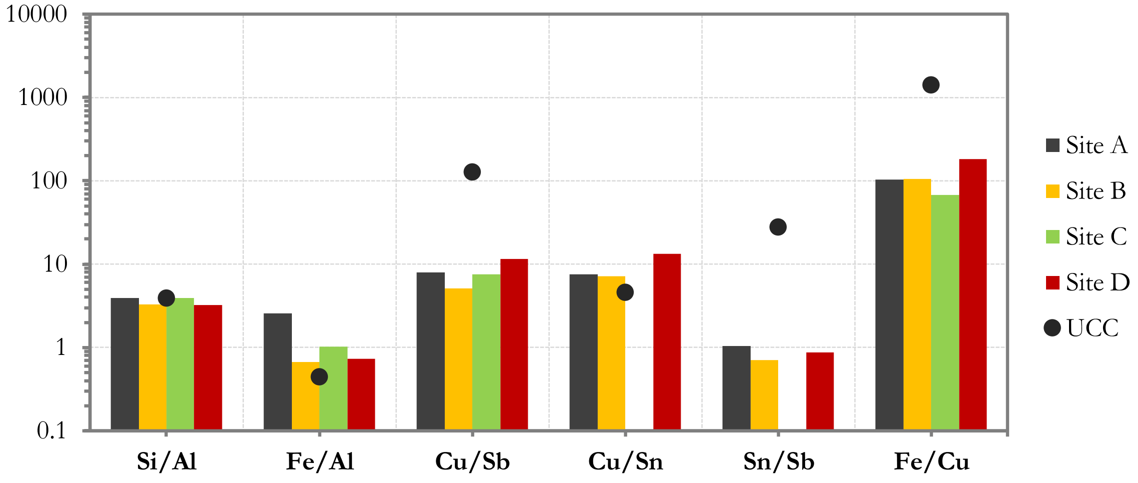

Figure 25: Elemental ratios in upper continental crust (UCC) and Sites A-D for PM_{10} road dust

5.3.5 PM_{10} Road Dust Source Profiles

Source profiles (as weight% of PM) were generated for the road traffic sites in Birmingham (Sites B and C) and New Delhi (Site D) (Table 25). Site A was not included in the preparation of the source profile since the site is not representative of a high-traffic location.

Previously reported source profiles for road dust and various non-exhaust emission sources were compared against data obtained at Sites A-D in order to get a qualitative understanding of source contributions (Figure 26). Concentrations obtained for Sites A to D were compared against a range of source profiles including tyre wear, brake wear and construction.

Table 25: Source profiles for PM_{10} road dust at heavy traffic sites in Birmingham (Sites B and C) and New Delhi (Site D) (% w/w)

Species	Site B		Site C		Site D	
	Concentration	**Uncertainty**	**Concentration**	**Uncertainty**	**Concentration**	**Uncertainty**
OC	7.91	4.80			1.82	1.69
EC	0.13	0.41			0.51	0.29
Si	25.8	2.78	28.2	8.98	13.0	3.04
Al	7.82	0.99	7.22	2.34	3.98	1.04
Ca	3.24	1.62			5.00	0.64
Fe	5.25	0.70	7.32	2.00	3.11	0.49
Ti	0.044	0.023	0.078	0.029	0.047	0.005
Mn	0.062	0.031	0.077	0.025	0.044	0.005
Cu	0.050	0.023	0.108	0.032	0.016	0.002
Sb	0.010	0.005	0.014	0.003	0.001	0.000
Ba	0.046	0.023	0.087	0.027	0.042	0.005
Sn	0.007	0.004			0.001	0.000
Cr	0.010	0.005	0.017	0.007	0.006	0.001
V	0.003	0.002	0.005	0.002	0.003	0.000
Zn	0.101	0.047	0.366	0.142	0.068	0.009
Cd			0.001	0.001		
Ni			0.012	0.009		
S			0.99	0.29		
BbF	0.004	0.002			0.004	0.003
BkF	0.004	0.002			0.003	0.002
BeP	0.003	0.002			0.002	0.001
BaP	0.002	0.001			0.002	0.002
IcdP	0.002	0.001			0.002	0.002
BghiP	0.002	0.001			0.002	0.002
Cor	0.001	0.000			0.001	0.000
C25	0.004	0.003			0.000	0.000
C26	0.003	0.003			0.001	0.001
C27	0.006	0.004			0.001	0.001

C28	0.009	0.005		0.001	0.000
C29	0.011	0.009		0.002	0.002
C30	0.005	0.004		0.000	0.001
C31	0.006	0.003		0.001	0.001
C32	0.006	0.002		0.000	0.000
C33	0.006	0.002		0.000	0.000
NHO	0.023	0.014		0.011	0.015
HOP	0.040	0.020		0.013	0.015
SHHO	0.013	0.007		0.005	0.006
RHHO	0.011	0.006		0.004	0.005
SBHHO	0.012	0.005		0.005	0.006
RBHHO	0.009	0.002		0.004	0.004

The profiles used for comparison were extracted from the USEPA SPECIATE 4.3 database and other published literature. In the case of elements, profiles included paved road dust [highway (ref. 3565), tunnel (ref. 4112410)] and road dust [Mexico] (ref. 4106) from the SPECIATE[5] database, brake and tyre wear from USA (Schauer et al., 2006), paved road dust from India (Sethi and Patil, 2008) and data from other cities including Anshan (China) (Han et al., 2009), Hong Kong (Ho et al., 2003), Barcelona (Spain) (Amato et al., 2009a) and Beijing (China) (Chen et al., 2012). Concentrations of various elements were broadly similar to other PM_{10} profiles while the brake wear and tyre wear profiles were found to vary from the road dust profiles observed in the current study, particularly for marker elements such as Cu, Sb and Ba. Previously reported PM_{10} road dust profile for Delhi was found to be different from the current profile. Detailed inferences regarding the differences could not be drawn due to unavailability of detailed sampling information for the other profile. Concentrations of several elements including Si, Al, Ca and Ba were much lower in case of the other profile, while concentrations were lower for the current profile for Sn, OC and EC and comparable for Ti, Fe and Zn. The Si/Al ratio was found to be lower than the UCC value of 3.9 for the Indian profile while Cu/Sb ratio at 21.5 was much higher compared to

---

[5] USEPA SPECIATE- http://cfpub.epa.gov/si/speciate/ehpa_speciate_browse.cfm

the profiles generated in this study. The OC/EC ratios were, however, comparable (3.6 for current study, 3.3 for the other profile).

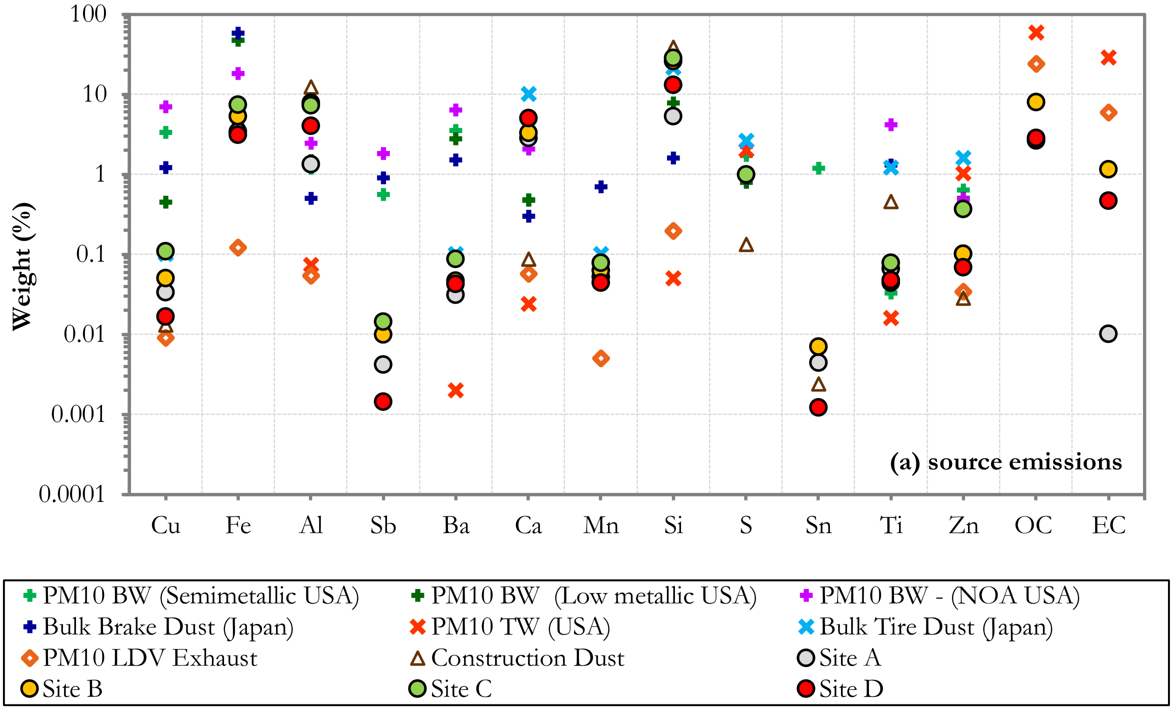

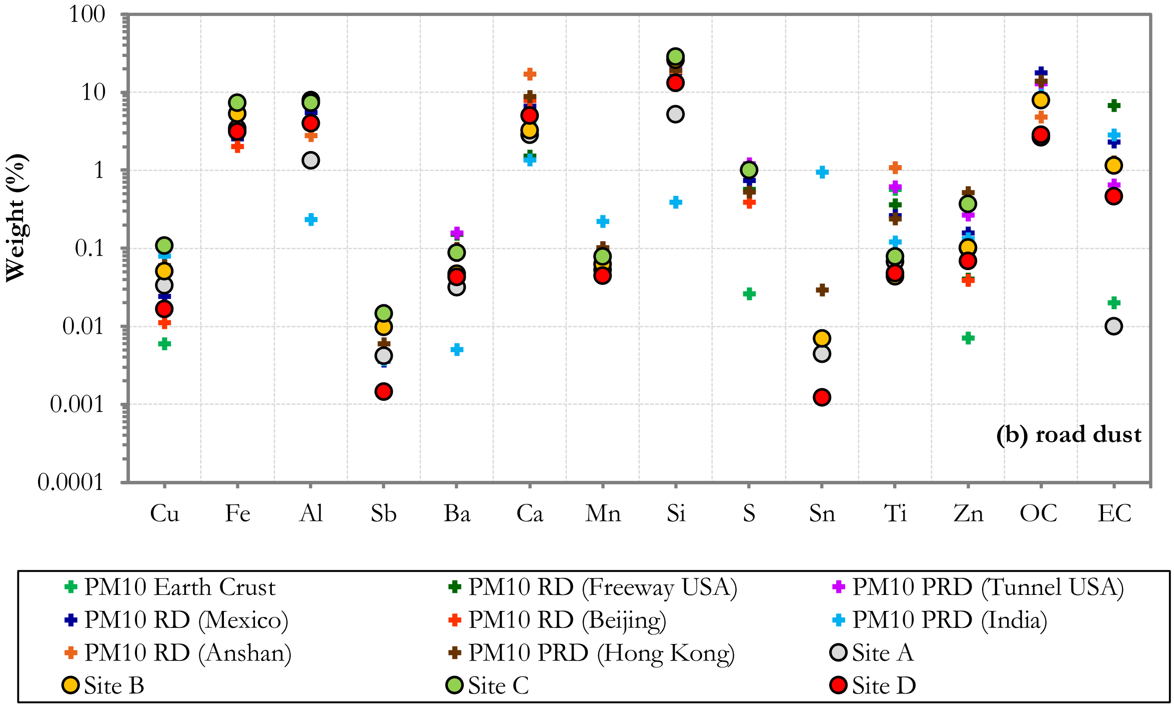

Figure 26: Comparison of species concentration (weight %) observed for PM_{10} road dust in the current study and (i) source emissions and (ii) road dust elsewhere

5.3.6 Source Apportionment of PM_{10} Road Dust

Recently, a novel method was proposed for the estimation of source contribution of non-exhaust sources using Ba, Zn and Si as source markers for brake dust, tyre dust and crustal dust respectively (Harrison et al., 2012a). The empirical factors are derived from UCC data (for Si) and ambient measurements and emission inventory data for brake and tyre wear emissions. The factors (91 for Ba, 50 for Zn and 3.6 for Si) were used to estimate the contribution of brake dust, tyre dust and crustal dust to the total PM_{10} mass. It is important to note that Zn is emitted from various sources include engine emissions and brake dust, and it is possible that using Zn as a tyre wear source results in an over-estimation of the tyre dust emissions. In Asia, Zn has also been associated with 2-stroke gasoline engine emissions and emissions from the galvanization industry (Begum et al., 2011). In the case of Delhi, Fe was used as the source marker for crustal dust due to its high abundance in crustal material. In addition, a factor of 1.35 was used for EC to estimate the contribution of vehicular exhaust (Pio et al. 2011).

Results of the source estimations are presented in Table 26. Nearly 100% of the mass is estimated using the factors for the traffic sites in Birmingham (Sites B and C). However, only 25% of the mass is explained at the low-traffic site (Site A). The site is also unique since the total traffic volume is much lower than the other sites but with a significant contribution from medium and heavy duty vehicles. The site had the lowest Si/Fe ratio, and Fe showed a significant enrichment at this site (enrichment factor of 5.90), and the use of Fe as the crustal marker increases the mass apportioned to crustal dust/soil to 79%. However, further analysis of local soil samples is required to confirm the use of Fe as a local crustal dust marker.

For site C (tunnel), the contribution of tyre wear was calculated to be 15.6% which might be an over-estimation since Zn is emitted from other sources as well. The contribution of brake wear, on the other hand, was higher for Site B where the traffic operates in a stop and go manner.

Table 26: Source contributions of various non-exhaust sources to PM_{10} road dust across sampling sites (in %)

Site ID	*Site characteristics*	*Brake Wear (Ba)*	*Tyre Wear (Zn)*	*Re-suspension (Si/Fe**)*	*Vehicle Exhaust*	*Total Mass Estimated*
Site A	Low traffic volume, mostly HDVs	2.9	4.7	17.4	0.004	**25.0**
Site B	High traffic volume, stop-and-go traffic, mixed LDVs and HDVs	3.8	4.7	89.5	1.3	**99.3**
Site C	High traffic volume, smooth traffic flow with stop-and-go during congestion, LDVs >> HDVs	6.6	15.6	82.8	*	**105**
Site D	High traffic volume, stop-and-go traffic, mixed LDVs and HDVs	3.9	3.5	71.2	0.59	**79.2**

*EC was not estimated at Site C; **Si used in case of Sites A, B and C and Fe used in case of Site D.

In the case of Delhi, 79.2% of the total mass is estimated but if Si is used as the source marker for crustal dust, only 51% of the total PM_{10} mass is estimated. This indicates that this estimation method cannot be used universally, and it is important to adjust the markers/factors according to the local soil characteristics. Other sources which could have important contributions in the case of Delhi are construction activity and deposition from other sources which are currently not included in the estimation. Vehicle exhaust was found to contribute a very small percentage to the total RD PM_{10} mass which is plausible since most of the vehicle exhaust particles are in the smaller size fraction and are less likely to deposit.

Chen et al. (2012) estimated soil dust, construction-related particles, vehicle exhaust, particle deposition and coal burning-associated particles as the key sources for road dust in Beijing while Amato et al. (2013b) estimated brake wear, tyre wear, crustal dust and vehicle exhaust to contribute 27%, 16%, 37% and 20% in Barcelona and 39%, 41%, 12%, 8% in Utrecht.

To compare the attribution of the crustal mass using Si (as described above) against an independent estimate, crustal mass was reconstructed using the concentrations of Al, Si, Fe, Ca and Ti using the equation (13) (Chan et al., 1997).

$$Crustal\ matter = 1.16\ (1.90Al + 2.15Si + 1.41Ca + 1.67Ti + 2.09Fe) \tag{13}$$

Where
Al, Si, Ca, Ti, Fe are expressed in concentration (weight %)

Results (Figure 27) indicate good correlation between measured and reconstructed mass in all cases ($r^2 > 0.85$), although a large intercept in case of Site D indicates contributions from other sources.

As with the source apportionment, it can be seen that the amount of mass apportioned as crustal matter is quite low at Sites A and D. This may be related to the varied soil composition at different locations. Hence, it is important to analyse uncontaminated soil samples (bulk and PM_{10} fraction where possible) to determine the local chemical composition which can be then be used to adjust the crustal mass factor.

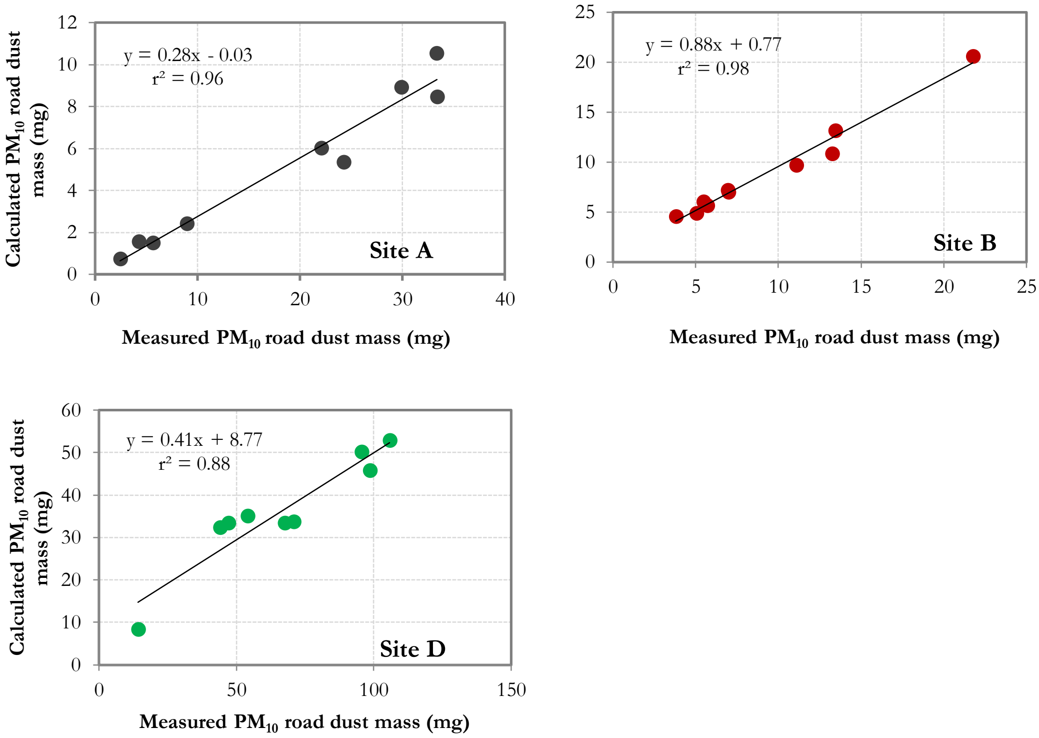

Figure 27: Correlation between observed and reconstructed PM_{10} road dust mass

5.4 Conclusions

Non-exhaust emissions constitute an important source of PM emissions in urban areas, and the chemical composition as well as contribution can vary from region to region. Since there are a number of different contributing sources, it is often difficult to estimate the contribution of different sources to the total dust levels. In this study, an attempt was made to undertake detailed characterization of PM_{10} road dust fraction and the empirical method proposed for the estimation of contribution of non-exhaust sources was applied successfully to the dataset.

Source profiles generated for sites in Birmingham and New Delhi correspond well with previously reported road dust profiles although differences were observed between elements concentrations in UK and India. This can be attributed to the difference in soil composition as well as the chemical composition of source type (tyre and brake pads) and potential influence from other sources.

Comparison carried out between elemental and PAH ratios for road dust PM and ambient PM reveal that the ratios can be quite similar between road dust and ambient PM, particularly in the case of coarse PM. Also, elemental ratios provide much better chance at segregating between road dust and ambient PM concentrations compared to PAH ratios. It seems that elemental markers are better suited to study road dust and non- exhaust emissions.

The empirical factors generated by Harrison et al. (2012a) were found to be able to generate reliable estimation of source contributions for the areas where they are empirically calculated (i.e. high-traffic areas in UK), but the apportionment was not very good for the low traffic site in Birmingham and the Indian site. Low mass closure in Delhi is perhaps due to the different sources that influence the dust concentrations in Delhi, as well as due to differences in the overall concentrations of different elements, and their sources (further discussion Chapter 6). It is therefore necessary to adjust the factors before using them for analysis in other regions. Contribution of brake wear was very similar between Sites B and D, both of which are heavily-trafficked roads with stop-and-go traffic. The low apportionment of PM mass in case of Site A is peculiar, and further analysis is required to understand the source contributions at this site.

The dataset generated in this study can also be used in receptor modelling studies. It is worth noting that the contribution of non-exhaust emissions to ambient PM concentration varies based on site characteristics, and data generated with pilot studies in specific areas/site types cannot be used to generalize the role and quantitative contribution of non-exhaust emissions to ambient air quality. An important issue which was not addressed in the current study is the variability contributed by the sampling methodology in the overall estimation of non-exhaust emission contributions since different sampling methods can provide very different results, and in the future, it is important to inter-compare various methods.

5.5 Acknowledgements

Financial support from the Rees Jeffreys Road Fund is gratefully acknowledged. Special thanks to Richard Johnson, Massimiliano Mascelloni, Barbara Macias Hernandez, Carmela Farao, Paul Darren, Jeevan Matawle and Kanika Pant for help with sampling. Thanks to Dr. Stephen J. Baker for analysis of elements and the UoB AMC facility for access to XRF.

CHAPTER 6- PARTICULATE MATTER IN INDIA

Sampling in New Delhi was carried out in collaboration with Dr. Anuradha Shukla (CRRI, New Delhi) and Professors Judith C. Chow and John G. Watson (DRI, Reno). Pre-sampling preparation, sampling and data analysis has been conducted by Pallavi Pant and chemical analysis of the Minivol filters was conducted at DRI, Reno (USA). Size-segregated samples were collected in collaboration with Dr. Anubha Goel (IIT-Kanpur, India). Sampling as well as analysis was conducted by Pallavi Pant.

Sections of this chapter are derived from:

[1] Pant, P., Harrison, R.M. (2012) Critical Review of Receptor Modelling for Particulate Matter: A Case Study of India. **Atmospheric Environment**, 49:1-12.

[2] Guttikunda, S.K., Goel, R. and Pant, P. (2014) Nature of air pollution, emission sources and management in the Indian cities. **Atmospheric Environment**, 95: 501-510.

Graphical Abstract

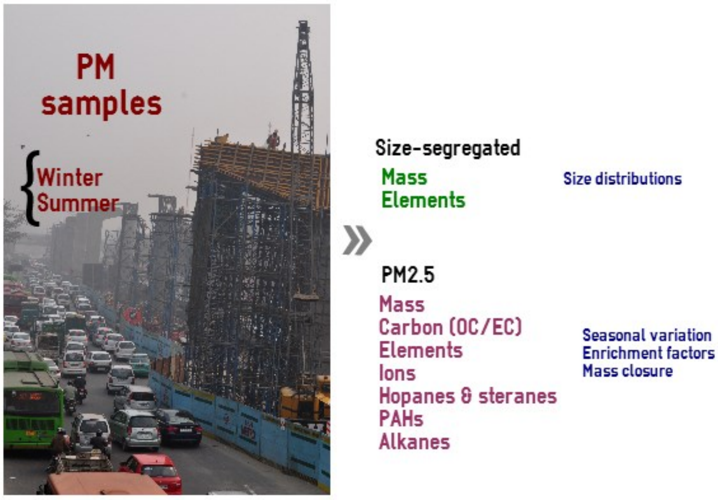

6.1 Introduction

Given the rapid rates of urbanization in Indian cities, air pollution is increasingly becoming a critical threat to the environment and to the quality of life among the urban population in India. PM concentrations are often found to exceed the National Ambient Air Quality Standards (NAAQS) and recent studies have identified PM as one of the key public health risks, particularly in urban areas (Lim et al., 2012; Guttikunda and Goel, 2013; Trivedi et al., 2014). Major sources of air pollution in India have been identified as vehicular emissions, industrial emissions, coal combustion, biomass burning, road dust, waste burning, construction, oil combustion and sea salt (Chowdhury et al., 2007; CPCB, 2010; Guttikunda and Calori, 2013; Gargava et al., 2014).

There is a growing body of literature on source apportionment of PM in India using receptor modelling with both elements and organic markers and a detailed review of source apportionment analysis in India is presented in Pant and Harrison (2012). Most studies have focused on total suspended particulate matter (TSP) and PM_{10} but there is an increasing number of studies focused on fine PM (aerodynamic diameter <2.5 μm) (Chowdhury et al., 2007; Tiwari et al., 2009; Chakrobarty and Gupta, 2010; Khare and Baruah, 2010; Gummeneni et al., 2011; Joseph et al., 2011; Kirillova et al., 2014; Sudheer et al., 2014). In terms of geographic distribution across the country, most studies focus on big cities such as Delhi (Balachandran et al., 2000; Khillare et al., 2004; Srivastava and Jain, 2007; Tiwari et al., 2009; Khillare and Sarkar, 2012; Kirillova et al., 2014; Trivedi et al., 2014), Mumbai (Kumar et al., 2001; Chelani et al., 2008; Kothai et al., 2008), Chennai (Srimuruganandam and Shiva Nagendra, 2011), Hyderabad (Gummeneni et al., 2011; Guttikunda et al., 2013) and Kolkata (Gupta et al., 2007; Kar et al., 2010). The Central Pollution Control Board (CPCB) also conducted a detailed dispersion and receptor modelling analysis in six cities across India (CPCB, 2010). In comparison, there are very few analyses in smaller cities/towns (e.g. Mouli et al., 2006; Kulshrestha et al., 2009; Chakrobarty and Gupta, 2010; Masih et al., 2010; Giri et al., 2013). Figure 28 presents a summary of receptor modelling studies from different cities in India. Some recent work has also focused on unique sources such as funeral pyres (Chakrobarty et al., 2013) and festive biomass burning (Deka and Hoque, 2014) and specific chemical components of PM such as brown carbon (Srinivas and Sarin, 2014) and WSOC (Kirillova et al., 2014).

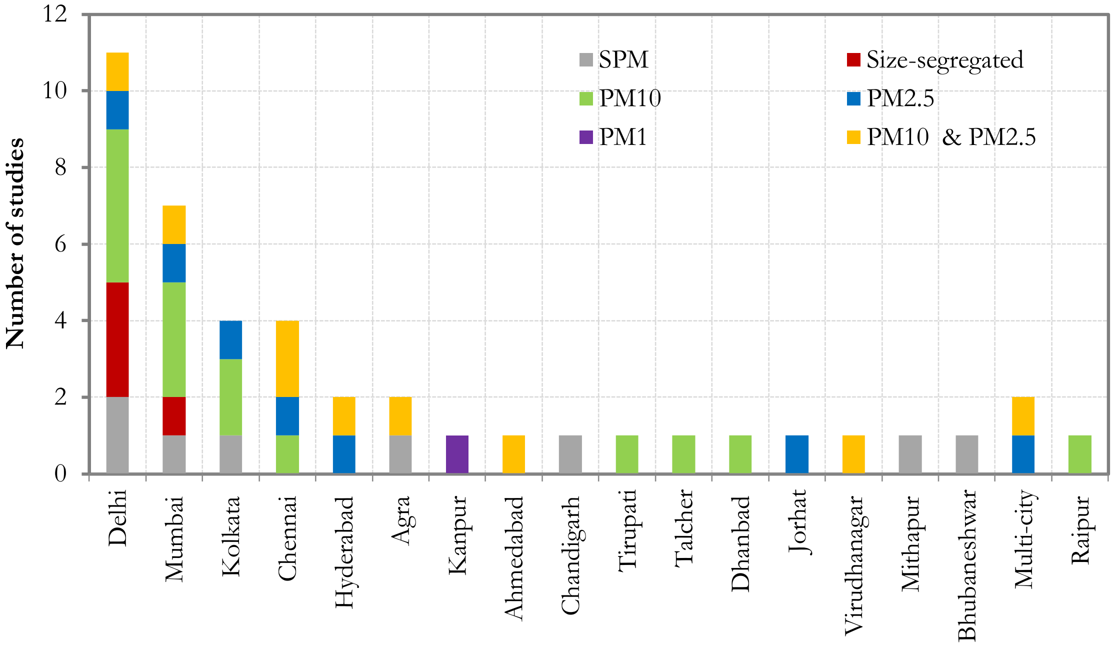

Figure 28: Summary of receptor modelling studies across India

(from Guttikunda et al., 2014)

A majority of the PM source apportionment studies have been conducted using trace element markers (Balachandran et al., 2000; Kumar et al., 2001; Kothai et al., 2008) and in some cases, inorganic tracers have been used in conjunction with OC and EC (Gupta et al., 2007; Tiwari et al., 2009; Chelani et al., 2010; Sharma et al., 2013). The use of organic molecular markers for PM source apportionment has only been reported in recent years (Chowdhury et al., 2007; Fu et al., 2010; Masih et al., 2010; Giri et al., 2013; Herlekar et al., 2012; Li et al., 2014).

India is a very large and diverse country, and unsurprisingly the receptor modelling studies have drawn widely differing conclusions. Even within individual Indian cities, different authors have come to widely varying conclusions over source attribution and apportionment, and this may to some extent be a result of using different sampling locations. Most studies have identified vehicle emissions and soil/road dust as a major contribution to the fine and coarse fractions respectively, but differentiation of these from industrial emissions and other sources such as construction activity has been poor. Based on a detailed review of SA literature from India, the following key gaps were identified:

1. Failure in most cases to distinguish vehicle exhaust from non-exhaust vehicle emissions, particularly resuspension of road dust, and/or inability to differentiate regional crustal sources (e.g. desert dust) from local wind-blown soils and from resuspended road dust. Making a distinction between road dust and local soils can be difficult under any circumstances if the soils are polluted by vehicle emissions or the road dusts contain a significant soil contribution. However, separating these sources, and in particular quantifying the vehicle exhaust contribution alone, and differentiating regional crustal sources from local soils and road dust, is crucial, as the policy response depends heavily upon these insights.
2. There has, to date, been insufficient use of organic molecular markers. While these alone will not answer all source apportionment questions, they are an important tool in receptor modelling and could help to improve both CMB and multivariate model studies.
3. There has been insufficient use of size fractionation of PM. Most studies have focused upon TSP or PM_{10}, therefore not benefiting from the additional insights to be gained from separating coarse from fine particles, and in doing so achieving a crude separation of crustal/soil/road dust/construction sources from those associated with high-temperature processes (fuel combustion, metallurgical industries, etc.) and gas-to-particle conversion of secondary pollutants.

4. Most studies pay little attention to secondary pollutants. Sulphate, which in developed countries is almost exclusively secondary, tends to be attributed to local primary sources, and regional transport processes are largely ignored. Similarly, nitrate receives little attention despite its complex atmospheric chemistry and frequent association with regional processes in developed countries (Abdalmogith and Harrison, 2005). Secondary organic aerosol may be an important contributor to PM mass in India as the conditions exist to facilitate its formation from both anthropogenic and biogenic precursors, but the literature largely ignores it.

6.1.1 Delhi

Delhi is one of the most polluted cities across the world and concentrations of air pollutants are often found to exceed the NAAQS. Delhi is reported to have 29 planned industrial areas and five factory complexes with a range of industries including food and beverages, metal and alloys, leather and leather products, chemicals, paper and others (Delhi Statistical Handbook, 2013). Delhi has two coal thermal power plants and four natural gas power plants and the sulphur content in the coal used in power plants in Delhi typically ranges between 0.35% and 0.50% (Chowdhury et al., 2007). Indian coal is typically high in ash content.

Diesel is used for both road transport (cars, utility vehicles, HDVs) and industry (power back-up, mobile phone towers, miscellaneous) while gasoline is mostly used for road transport. Public transport in the city runs on CNG (including buses, small commercial vehicles and auto-rickshaws) while private vehicles run on diesel, gasoline, CNG and LPG. A number of brick kilns are also reported to operate in areas around Delhi (Guttikunda and Calori, 2013). A range of different cooking fuels are used in Delhi including LPG, kerosene, firewood, cow dung cake, coal, crop residues, biogas and electricity with nearly 90% households using LPG (Delhi Statistical Handbook, 2013). Estimated source contributions from the different sectors are described in Figure 29. While on one hand, Sahu et al. (2011b) reported road transport as the biggest contributor to $PM_{2.5}$ emissions (30.25 Gg/yr) followed by residential emissions (18.65 Gg/yr), dust (18.35 Gg/yr) and industry (16.29 Gg/yr); Guttikunda and Calori (2013) identified transport, power plants and domestic emissions as the three biggest contributors. In South Delhi, where the sampling site is located, transport, diesel generators and road dust were identified as the biggest contributors to PM (Figure 29).

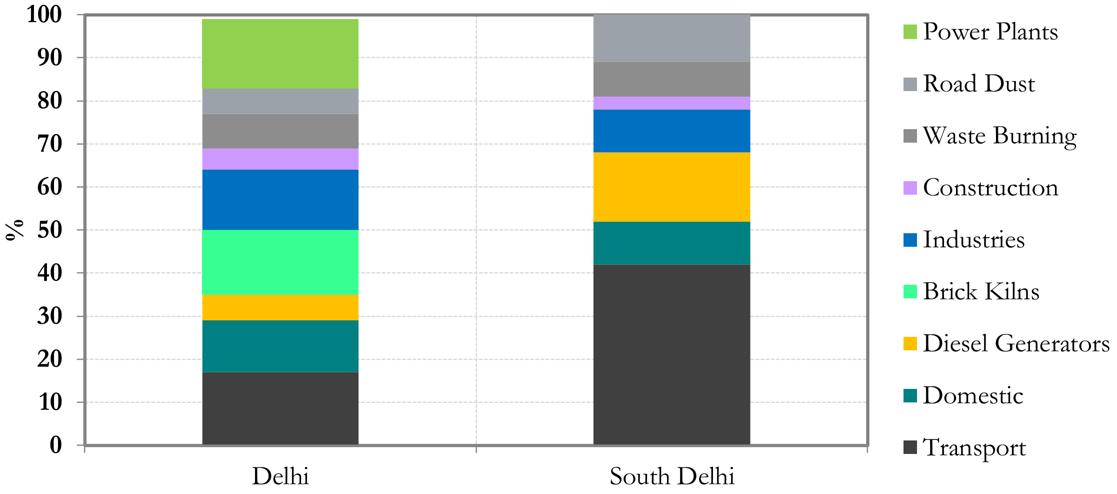

Figure 29: Emission inventory for $PM_{2.5}$ in New Delhi *(Guttikunda and Calori, 2013)*

Several studies have been undertaken for source apportionment of suspended particulate matter (SPM), PM_{10} and $PM_{2.5}$ using receptor modelling in Delhi and a majority of those have used factor analysis (PCA), PCA-MLR, diagnostic ratio, enrichment factor etc. However, several recent studies have used PMF and CMB models for source apportionment. A large percentage of the PM has been attributed to vehicular emissions, road dust, coal combustion and domestic emissions in several studies (Balachandran et al., 2000; Khillare et al., 2004; Chowdhury et al., 2007; Sharma et al., 2007; Chelani et al., 2010; Tiwari et al., 2013). Goyal et al. (2010) have reported diesel vehicles to contribute nearly 28% of the total particulate matter in Delhi. Other sources identified for PM emissions in Delhi include industrial emissions, open refuse burning and construction (Khillare et al., 2004; Mönkönnen et al., 2004; CPCB, 2010; Khillare and Sarkar, 2012; Guttikunda and Calori, 2013).

6.2 Methodology

6.2.1 Sampling Site

Mathura Road is one of the major arterial roads in Delhi with an average traffic flow of 170,000 vehicles per day (Figure 30). Other sources of PM include residential burning and an industrial hub about three kilometres from the sampling site (Okhla Industrial Area). While there are no restrictions on two- and three-wheelers, trucks (diesel, BS-III, 350 ppm sulphur) are not allowed between 0730 to 1100 hours and 1700 to 2130 hours while buses, light duty vehicles (LDVs) and are not restricted (Delhi Police, 2014, Figure 31). It is important to note that Bharat Standard IV (BS-IV, 50 ppm sulphur) standards are applicable to the vehicles within Delhi while vehicles from outside Delhi are often BS-III (equivalent of Euro III- 350 ppm sulphur).

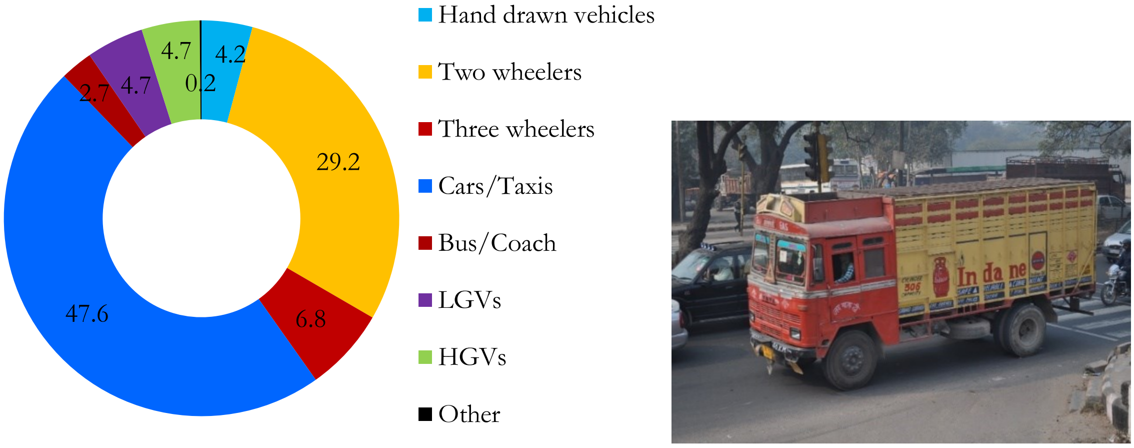

Figure 30: Modal split at the sampling location in Delhi *(Goel, 2014)*

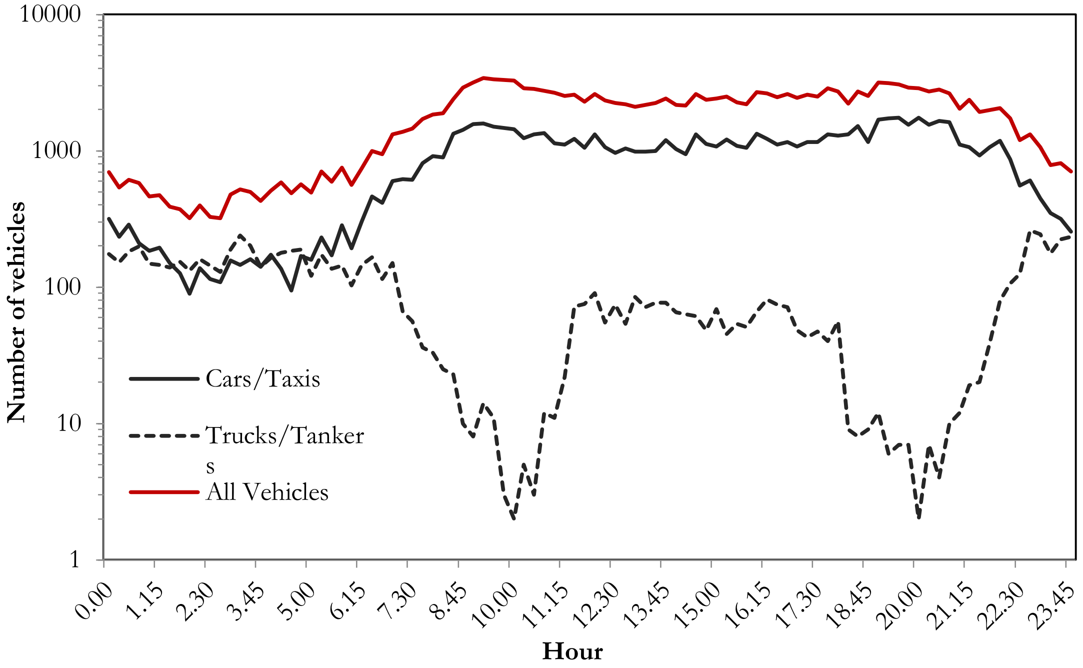

Figure 31: Temporal variation in traffic flow at the sampling location in Delhi *(Goel, 2014)*

New Delhi has sub-tropical climate with hot summers and moderately cold winter (October to January). Usually, S-SW winds are prevalent in summer and N-NW winds are prevalent in winter (Yadav and Rajamani, 2006). During the summer sampling period (June 15-30, 2014), the average temperature and relative humidity (RH) were recorded as 31.4 ± 4.02°C and 67.5 ± 20.5 respectively while during the winter sampling period (December 15, 2013-January 15, 2014), the average temperature and relative humidity (RH) were recorded as 13.4 ± 2.70°C and 80.8 ± 8.1 % respectively. During the sampling period in winter (December 15, 2013- January 14, 2014), fog/haze was reported on most days with calm wind conditions. Average rainfall in the months of June and December was recorded as 151 and 6.8 mm respectively.

6.2.2 Sampling

Two sampling campaigns were undertaken in New Delhi, India in summer (June 15-30, 2013) and winter (December 15, 2013- January 15, 2014). Collocated Minivol samplers were used to collect twelve hour $PM_{2.5}$ samples (filter change at 1200 and 2400) on quartz and PTFE filters. All samples were analysed at the Environmental Analysis Facility, Desert Research Institute (Reno, Nevada, USA). The samplers were placed at height of 2 m from ground level at a distance of 50 metres from the road.

Between 17 December and 21 December, 2013, a set of four 6-hour samples (0000- 0600, 0600-1200, 1200-1800, 1800-2400 hours) were collected on PTFE filters using an 8-stage rotating MOUDI. The instrument operated between 28-30 litres/minute. These samples were analysed at the University of Birmingham.

6.2.3 Analytical Methods

The samples were analyzed using procedures described in Chapter 2. Elements from Na to U were analysed using ED-XRF, cations and anions were analysed using ion chromatography, EC and OC were analysed using DRI carbon analyzer and carbonaceous species were quantified using TD-GC-MS.

A total of 28 samples were used in the final analysis for summer season and 15 samples were used for the winter season.

MOUDI samples were analysed using WD-XRF for Si, Al, Fe and S and extracted samples were analysed for Cu, Zn, Ca, Mn, Sb, V and Pb.

6.2.4 Data Analysis

Data analysis has been carried out using Microsoft Excel and SPSS (Version 21). Several species were detected in less than 20% of the samples and are not included in further analysis. Missing or concentrations below detection limits were replaced with 0.5*detection limit. Species' correlation analysis was conducted using SPSS based on Pearson Correlation and the correlation values reported in the text are for $p<0.01$. Reduced major axis (RMA) regression analysis has been used in most cases due to similar uncertainties of the different species.

6.3 Results

6.3.1 Concentrations

6.3.1.1 Particulate Matter

The 12-h average concentration in summer was observed to be 58.2±35.0 μg/m^3 with a maximum PM$_{2.5}$ concentration of 179.5 μg/m^3 while in winter; the average concentration was 262±99.9 μg/m^3 with a maximum of 424.9 μg/m^3 (details in Table 27). Comparative concentrations were reported by Chowdhury et al. (2007) for summer (49 ± 0.6 μg/m^3) and winter (231±1.6 μg/m^3). Trivedi et al. (2013) have reported PM$_{2.5}$ concentrations of 86.4±26.8 μg/m^3 and 221.1±94.7 μg/m^3 for summer and winter respectively in Delhi while Giri et al. (2013) reported PM$_{2.5}$ concentration of 115±36 μg/m^3 for winter in Raipur. The concentrations exceeded the NAAQS PM$_{2.5}$ 24-h standard (60 μg/m^3) on several occasions during the sampling campaigns in summer and winter.

Table 27: Summary of $PM_{2.5}$ in summer and winter

Sample type	Species	Summer				Winter			
		Mean	S.D.	Minimum	Maximum	Mean	S.D.	Minimum	Maximum
12-h integrated samples	$PM_{2.5}$ (μg/m^3)	58.2	35.0	10.7	179.5	262	99.9	108.8	424.9

Concentrations in winter were consistently higher compared to summer and this can be due to the differences in meteorological parameters as well as variations in source strengths. Significant difference between PM concentrations in summer and winter have been recorded previously (Guttikunda and Gurjar, 2012; Yadav et al., 2013; Tiwari et al., 2014).

6.3.1.2 *Size Distributions*

Several studies in India have focused on the particle size distributions including mass size distributions (Khemani et al., 1982; Balachandran et al., 2000; Venkataraman et al., 2002; Reddy et al., 2007; Chelani et al., 2010), number size distributions (Mönkkönen et al., 2005), or both (Sharma and Patil, 1992; Mönkkönen et al., 2004; Baxla et al., 2009). Several authors have reported bimodal mass size distributions in Indian cities including Pune (Khemani et al., 1982; Ernest Raj et al., 2002; Venkataraman et al., 2002), Mumbai (Sharma and Patil, 1992) and Agra (Kulshrestha et al., 1998). However, Sharma and Patil (1992) also reported a trimodal mass size distribution at a mixed traffic/industrial site in Mumbai. Several authors have reported higher concentrations of particles in winter season (Khemani et al., 1982; Venkataraman et al., 2002; Mönkkönen et al., 2005; Baxla et al., 2009; Deshmukh et al., 2012).

Using the data obtained from MOUDI samples, a continuous size distribution was obtained using the numerical inversion method described in Keywood et al. (1999). This approach has previously used in several studies (Allen et al., 2001a; Gietl et al., 2010).

Based on MOUDI samples, a trimodal size distribution was observed across all four 6-h periods with two modes in the accumulation range (0.15 μm and ~0.55 μm) and one mode in the coarse range (3.0 μm) (Figure 32). The overall pattern of the size distribution was found to be similar across all sampling times and overall, lowest concentrations were observed during early morning hours (0600-1200) which correspond with the lowest traffic volume along Mathura Road while highest concentrations were observed during the afternoon (Figure 31).

A majority of PM mass was found to be in the fine range (75.5%) compared to the coarse range (24.5%). Other studies have reported similar results in Delhi (82.9%- fine and 17.1% coarse) and Raipur (60.6%- fine and 39.4% coarse) (Balachandran et al., 2000; Deshmukh et al., 2012).

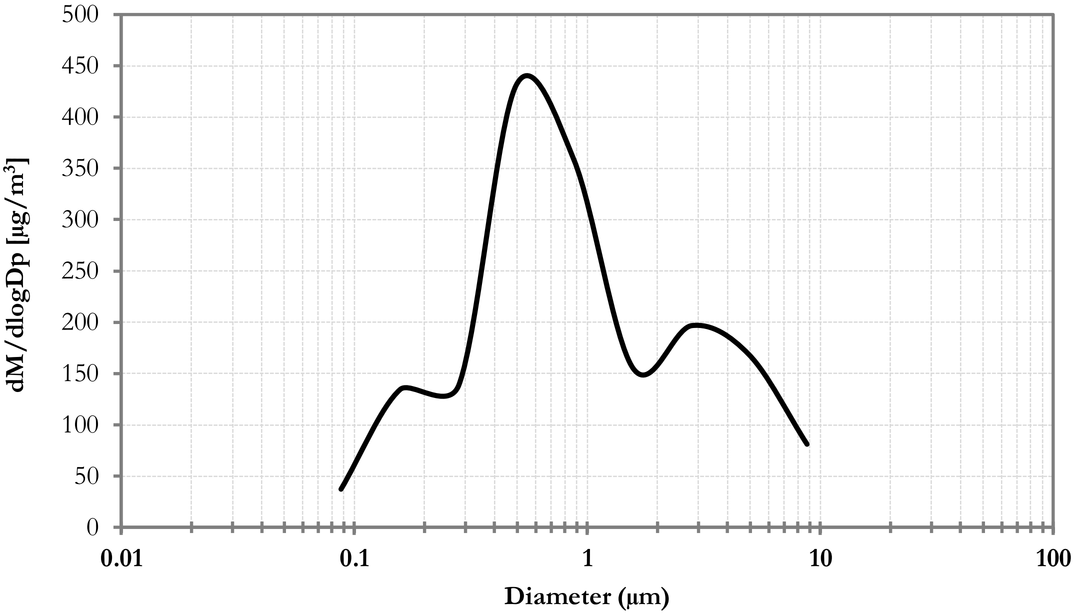

Figure 32: Average mass size distribution (based on MOUDI) for PM in New Delhi

Elemental size distributions show an interesting pattern (Figure 33).Species associated with crustal matter such as Si, Al and Fe were observed to have a unimodal mass size distribution with the primary (and only) peak (~3.0-4.0 μm) in the coarse range while Ca showed a primary peak in the coarse mode and a secondary peak in the accumulation mode (0.9 μm) (Figure 33). Cu was found to be unimodal with the primary peak in the accumulation mode (~0.5 μm). Other species associated with anthropogenic emissions such as Zn and Pb showed a bimodal size distribution with primary and secondary peaks in the accumulation mode (~0.7 µm for Zn and ~0.55 µm for Pb {primary}; ~0.15 µm {secondary}). Mn showed a bimodal size distribution with the primary peak in the accumulation mode and a secondary peak in the coarse mode (~3.0 µm) and S had a bimodal distribution with both the primary and secondary peaks in the accumulation mode. V, interestingly, showed the primary peak in the coarse mode (3.0 µm) and two secondary peaks in the accumulation mode (~0.18 and 0.55 µm). Based on an emission inventory analysis, sources of V in PM_{10} include power plants and industries (Gargava et al., 2014). This could explain the primary peak of V as coming from coal fly ash, with smaller contributions from industrial and traffic emissions in the fine range. In the case of Sb, a majority of the Sb concentration was found to be in the accumulation range. A summary is provided in Table 28.

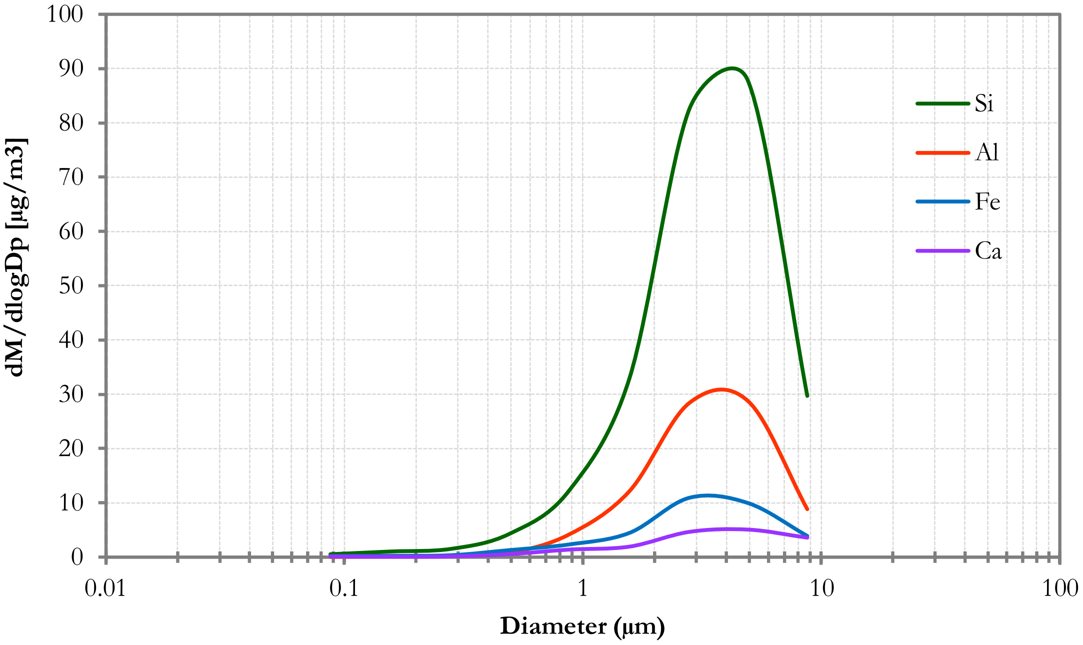

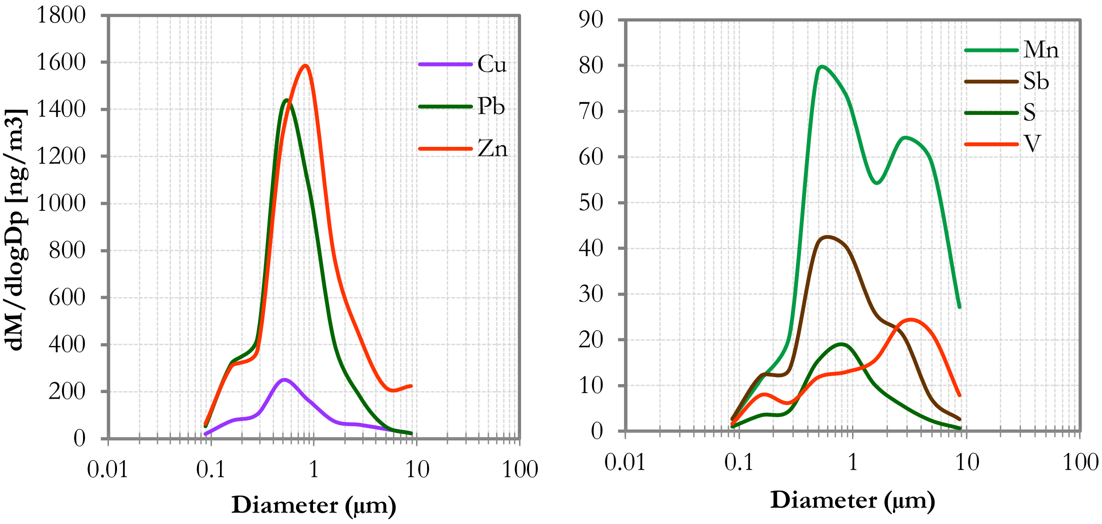

Figure 33: Average mass size distributions for elements based on MOUDI samples

Table 28: Summary of mass size distributions for elements in New Delhi

Element	**Size distribution**	**Primary Peak**	**Secondary Peak**
Si	Unimodal	Coarse (4 µm)	
Al	Unimodal	Coarse (~3.5 µm)	
Fe	Unimodal	Coarse (~3.5 µm)	
Ca	Bimodal	Coarse (4 µm)	Accumulation (0.9 µm)
Cu	Bimodal	Accumulation (~0.55 µm)	Accumulation (0.15 µm)
Zn	Bimodal	Accumulation (0.7 µm)	Accumulation (0.15 µm)
Pb	Bimodal	Accumulation (~0.55 µm)	Accumulation (0.15 µm)
Mn	Bimodal	Accumulation (~0.65 µm)	Coarse (3 µm)
S	Bimodal	Accumulation (0.9 µm)	Accumulation (~0.15 µm)
V	Trimodal	Coarse (3 µm)	Accumulation (~0.15,0.55 µm)
Sb	Bimodal	Accumulation (0.7 µm)	Accumulation (~0.15 µm)

In the current study, the fine/coarse ratios (fine refers to <2.5 µm and coarse >2.5 µm) for size-segregated aerosols were observed to be less than 1 for Al, Si, Fe, Ca, V and Mn while the ratio was greater than 1 for the other elements (Figure 34). Coarse particles are typically generated due to mechanical processes (Pant and Harrison, 2013). In this case, elements typically associated with soil/crustal material such as Si, Al, Ca and Fe were found to be dominant in the coarse range, indicating their predominant soil origin. Two other elements, Mn and V were also found to have a lower fine/coarse ratio compared to other elements associated with anthropogenic activities which indicates dominance of the soil source compared to other anthropogenic sources. Elements such as Cu, Zn, Pb and S were predominantly found in the fine range, and can be associated with traffic and industrial emissions as well as emissions due to waste burning. Interestingly, Gargava et al. (2014) reported wood combustion as the dominant source for Pb. Both intrastate and interstate traffic is allowed on Mathura Road, and some of the interstate vehicles, particularly HDVs run on high-sulphur fuel. In addition, there is an industrial zone at a distance of about 3 kilometres from the sampling site (Okhla Industrial Area). Pb was found to be present in very high concentrations, and possible sources include industrial emissions and small-scale Pb-battery recycling units. An interesting difference is the absence of peaks for elements such as Cu and Sb in the coarse range which have been associated with non-exhaust emissions (Iijima et al., 2007; Gietl et al., 2010).

It is important to note that the sample size for this analysis was very small and only represent winter aerosol composition. Fine and coarse partitioning of the individual elements can be different in case of other seasons.

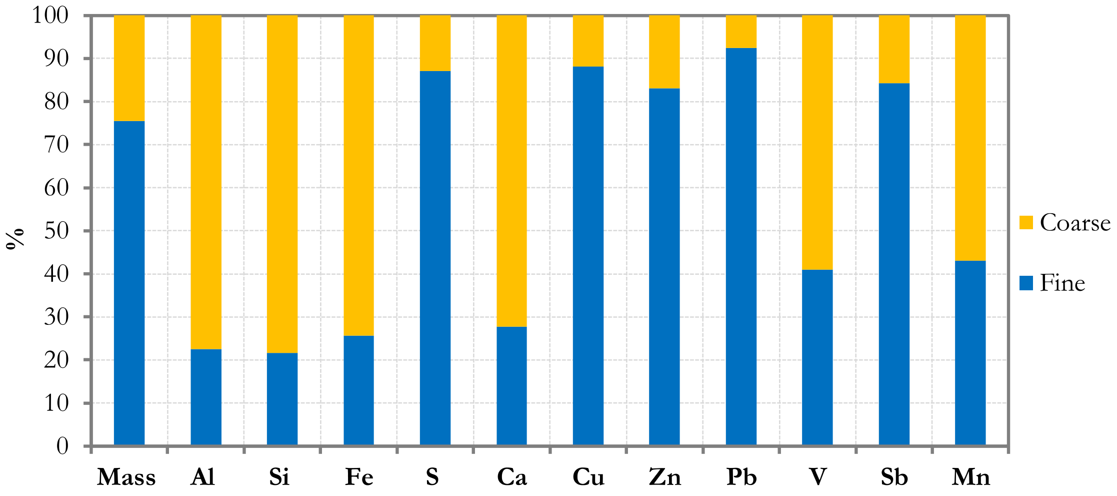

Figure 34: Percentage of elements in fine (<2.5 µm) and coarse (>2.5 µm) ranges

6.3.1.3 *Carbon*

As described in Chapter 2, all samples were analysed for eight carbon fractions with the IMPROVE_A protocol including OC1, OC2, OC3, OC4, OP, EC1, EC2 and EC3.

Both in summer and winter, OC3 and OP had the highest concentrations among the organic carbon fractions while EC1 had the highest concentration among the elemental carbon fractions (Figure 35). EC3 was detected in less than 20% samples in both seasons. A summary is presented in Table 29. Typically, EC2 and OC1 are associated with diesel vehicles while EC1, OC2 and OC3 are dominant in gasoline vehicles (Watson et al., 1994).

OC and EC were found to be reasonably correlated both in summer (r^2= 0.76) and winter (r^2= 0.72) indicating common sources such as road traffic and biomass burning. Both OC and EC were also correlated well with $PM_{2.5}$ mass in summer although no correlation was observed in winter. Both OC and EC were correlated well with the other carbon fractions.

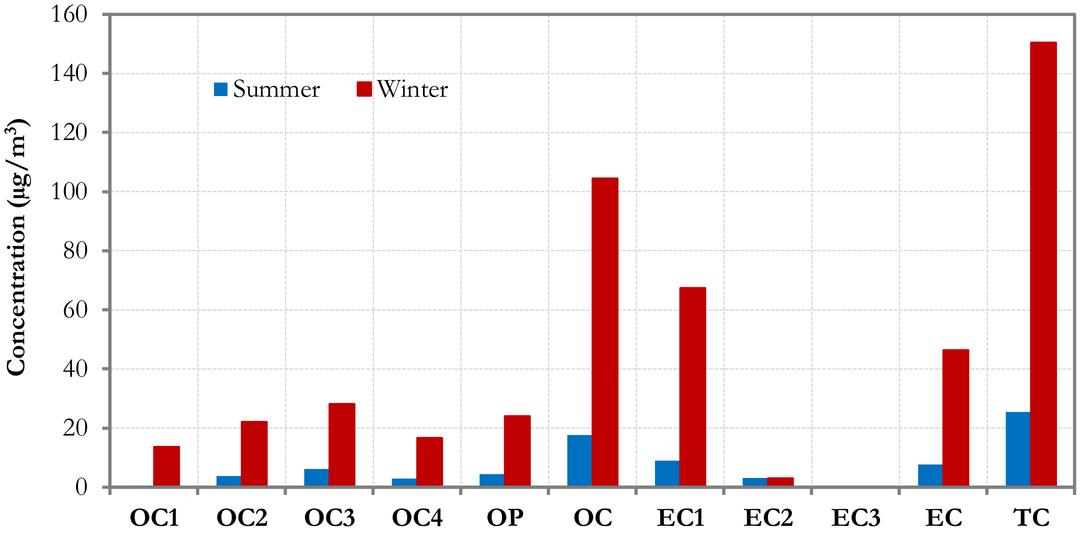

Figure 35: Seasonal variation of $PM_{2.5}$ carbon fraction concentrations at CRRI

In winter, however, OC was correlated with six fractions (OC1, OC2, OC3, OC4, OP, and EC1) but the correlation was not significant for EC2. In the case of EC, a higher correlation was seen for EC1 (r^2= 0.92) compared to EC2 while no correlation was observed for EC and OP.

If the concentration of OC is expressed as a function of concentration of EC using RMA regression, the OC/EC gradient is significant for both seasons (1.19 for summer and 2.15 for winter) (Figure 36). The intercept is greater than 4 μgC/m^3 in both cases indicating contributions from other sources to OC. R-square values for summer and winter are 0.58 and 0.52 respectively.

EC is released directly into the atmosphere and can be used to estimate relative amounts of primary OC (POC) and secondary OC (SOC). Higher OC/EC ratios are expected in the conditions where SOC is dominant and the EC-tracer method involves the use of EC as a tracer for POC, allowing SOC to be calculated (Turpin and Huntzicker, 1995; Castro et al., 1999; Pio et al., 2011).

Table 29: Summary of PM$_{2.5}$ carbon fractions at CRRI, New Delhi (in μg/m^3)

Species	Summer				Winter			
	Mean	S.D.	Minimum	Maximum	Mean	S.D.	Minimum	Maximum
OC1	0.57	0.85	0.01	2.91	13.6	7.98	3.80	29.4
OC2	3.70	1.62	1.42	7.14	22.1	8.73	10.3	38.2
OC3	6.05	2.48	2.20	13.1	28.2	9.95	15.2	48.3
OC4	2.94	1.56	0.62	6.62	16.6	7.22	8.37	33.4
OP	4.36	2.80	0.33	12.3	24.0	10.8	13.2	46.2
OC	17.6	8.38	5.18	36.4	104	40.6	53.3	196
EC1	8.98	8.05	0.33	39.9	67.3	26.9	19.6	101
EC2	3.14	2.14	0.60	9.99	2.93	2.65	1.02	11.2
EC3	*detected in <20% samples*				*detected in <20% samples*			
EC	7.76	7.05	0.60	31.4	46.3	18.9	12.0	78.9
TC	25.4	14.50	5.77	67.7	150	55.8	70.3	250

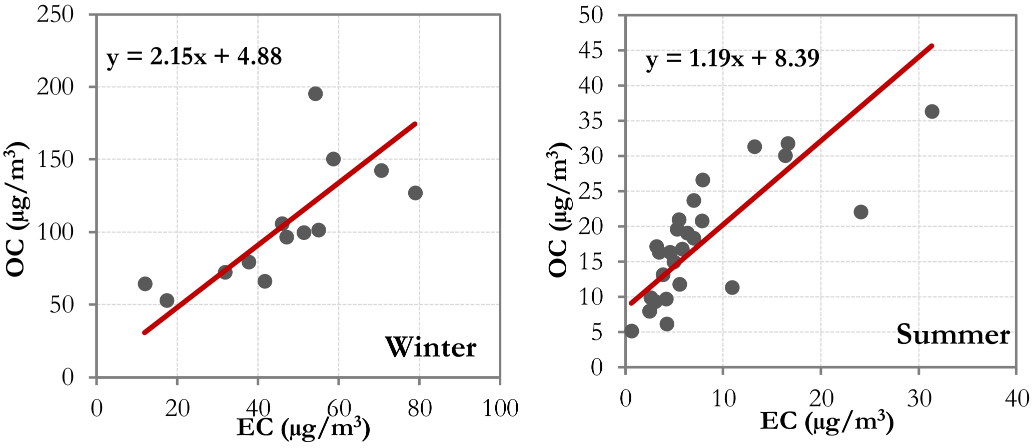

Figure 36: Relationship between PM$_{2.5}$ OC and EC in summer and winter

Minimum ratios of OC/EC are taken as representative of primary OC (although they may be an over-estimate (Pio et al., 2011) and OC above that ratio is taken to be SOC. The method as outlined by Castro et al. (1999) was used and estimates of SOC were calculated (Figure 37, discussed in Chapter 3).

$$Secondary\ OC = Total\ OC - \left(EC \times \left(\frac{OC}{EC}\right)_{minimum}\right) \qquad (14)$$

Where
Total OC refers to the concentration of OC
EC refers to the concentration of EC
(OC/EC) minimum refers to the minimum OC/EC gradient

The minimum ratios were estimated as 0.93 for summer and 1.63 for winter, and were used to calculate the contribution from primary and secondary OC for both seasons. The average contribution of POC was estimated to be 41% in summer and 72.3% in winter while the SOC was estimated to contribute 66.7% in summer, and 33.1% in winter.

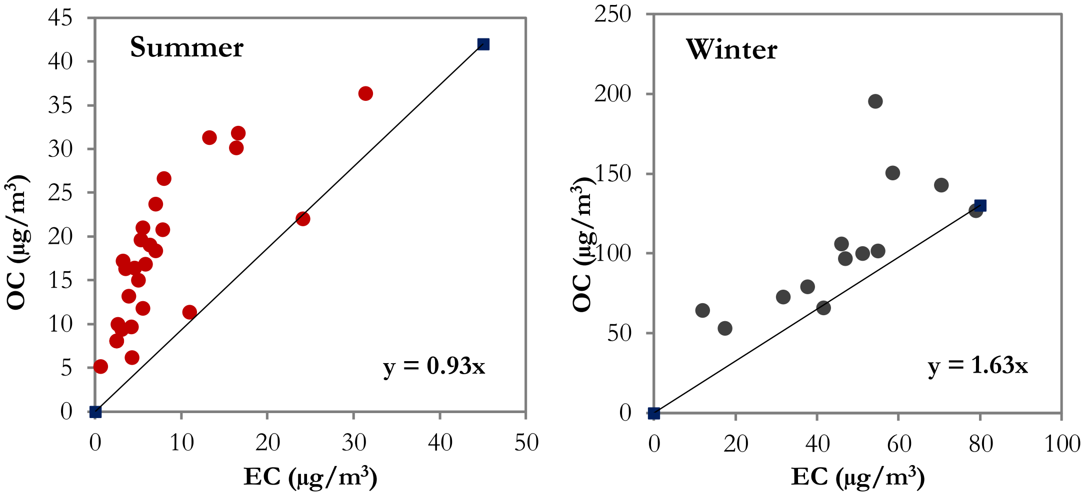

Figure 37: Estimation of minimum $PM_{2.5}$ OC/EC ratio using the EC tracer method

6.3.1.4 Ions

A summary of ion concentrations observed for $PM_{2.5}$ during the two seasons is presented in Table 30. Sulphate (SO_4^{2-}) and ammonium (NH_4^+) were found to be the most abundant ions in summer with average contributions of 17.1% and 8.5% to $PM_{2.5}$ mass (Figure 38). Higher abundance of SO_4^{2-} in summer and nitrate (NO_3^-) in winter is consistent with previous observations in the region (Satsangi et al., 2013). In winter, NH_4^+ was the most abundant ion followed by NO_3^- contributing 12.4% and 11.8% to $PM_{2.5}$ mass. NO_3^- and SO_4^{2-} were found to be correlated in summer ($r^2= 0.69$) as well as in winter ($r^2= 0.70$) and high correlation was also observed between sulphate and NH_4^+ in summer and ($r^2= 0.85$) and winter ($r^2= 0.80$). SO_4^{2-} ($r^2= 0.60$) and NO_3^- ($r^2= 0.55$) were also moderately correlated with PM mass in summer but no correlation was observed in winter. Chloride (Cl^-) was not found to be correlated with any of the other ions in summer while in winter, it was correlated with NH_4^+ ($r^2= 0.56$). Higher concentrations were observed for all ions in winter but soluble Na was present in broadly similar concentrations in both seasons with a winter/summer ratio of less than 2. On the other hand, Cl^-, NO_3^- and NH_4^+ showed the highest winter/summer ratios. It is worth noting that particulate nitrate (often present as NH_4NO_3) is semi-volatile and at high temperatures, NO_3^- might be present in volatile form, thus showing a lower particulate concentration. In winter, low temperature and high relative humidity favour the occurrence of ammonium nitrate in particle form. Further, since occurrence of NH_4NO_3 is RH dependent beyond the deliquescence point, nitrate concentrations can vary significantly across seasons. Seasonal variations in concentrations of ions have also been reported by Sudheer et al. (2014).

Cl^- and NO_3^- have been reported to be emitted during wood combustion and soluble K is widely used as a marker for biomass combustion (Kleeman et al., 1999; Simoneit et al., 2004b; Watson et al., 2008). In India, Patil et al. (2013) reported high abundance of Cl^- and K^+ in wood combustion, open burning and coal combustion while NH_4^+, NO_3^- and Cl^- are reported to be abundant in industrial emissions. The high winter concentration of Cl^- could be due to the increased burning (wood, coal, waste) in the winter season.

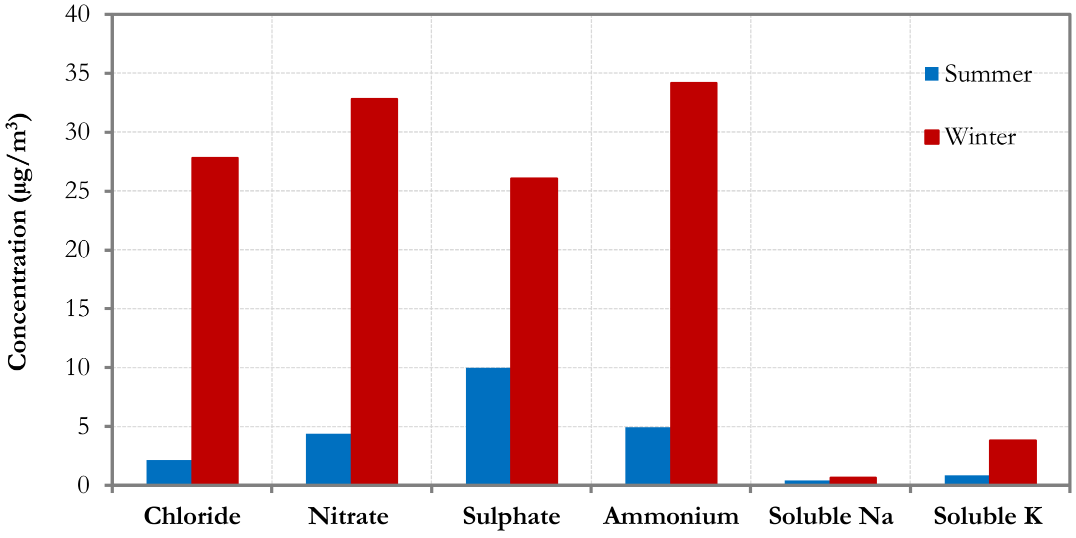

Figure 38: Seasonal variation of $PM_{2.5}$ ion concentrations at CRRI

Ion equivalency was estimated using Cl^-, SO_4^{2-}, NO_3^- (anions) and NH_4^+ (cation) for both seasons to understand the neutralization of the ions in the atmosphere (Figure 39). The anions were found to be more or less neutralized by NH_4^+ in both seasons.

Table 30: Summary of $PM_{2.5}$ ion concentrations at CRRI, New Delhi (in µg/m³)

Species	Summer				Winter			
	Mean	S.D.	Minimum	Maximum	Mean	S.D.	Minimum	Maximum
Chloride	2.14	1.54	0.56	6.70	27.8	18.1	7.21	68.1
Nitrate	4.37	2.14	1.04	8.79	32.8	20.1	0.21	76.7
Sulphate	9.97	6.25	1.74	27.5	26.1	15.3	7.66	59.1
Ammonium	4.94	2.87	0.94	12.4	34.2	17.0	13.0	64.0
Soluble Na	0.41	0.38	0.01	1.56	0.64	0.30	0.20	1.18
Soluble K	0.86	0.49	0.13	2.40	3.83	1.63	1.51	6.50

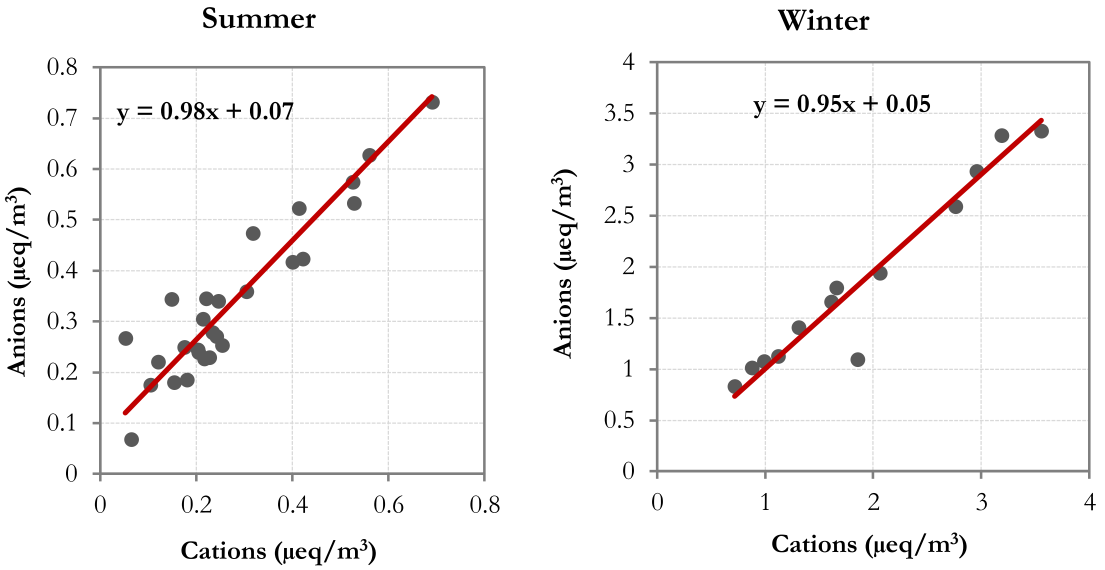

Figure 39: RMA regression between ammonium and sum (nitrate, sulphate, chloride) in $PM_{2.5}$

6.3.1.5 *Elements*

Sulphur (S), Na and Si were found to be most abundant elements in $PM_{2.5}$ in summer while Cl, Na and S were the most abundant in winter (Table 31, Figure 40). Concentrations of several elements including Cl, Pb, Fe and Zn were found to be more than five times higher in winter compared to summer. Elements typically associated with soil/mineral dust showed the lowest winter/summer ratios (e.g. Si- 0.95; Ca- 0.80) while several other species showed a 1.5 to 4 times increase in concentrations in winter (e.g.- Cr- 1.41; Mn- 2.69; S- 3.14; Zn- 3.27; Cu- 4.74).

Pearson correlation analysis was used to understand the correlations among different elements. Zn was found to be moderately correlated with Pb ($r^2= 0.57$) and Br ($r^2= 0.57$) in summer, while a strong correlation was observed in winter for Pb ($r^2= 0.83$). Previous studies have also reported correlation between Zn and Pb, and Tiwari et al. (2013) used these as markers for traffic source and Chen et al. (2011) reported association of Fe, Zn, Pb and Br with diesel vehicles. Pb and K^+ have also been used as markers for biomass burning (Cheng et al., 2013) but no correlation was observed between these two species in Delhi.

Al, Si, Ca, Ti, Mn and Fe have been used as markers for crustal dust/soil (Cass, 1998; Chow et al., 2003; Viana et al., 2008; Pant and Harrison, 2012). In summer, Si was strongly correlated with Al (r^2= 0.91), Fe (r^2= 0.97), Ca (r^2= 0.99), Ti (r^2= 0.96), Sr (r^2= 0.83) and moderately correlated with Mn (r^2= 0.51) and K (r^2= 0.59) and weakly correlated with Ni (r^2= 0.43). In winter, Si was strongly correlated with Fe (r^2= 0.81), Ca (r^2= 0.94), Ti (r^2= 0.88) but Al was not found to be correlated with the other soil-associated elements but with Cl (r^2= 0.96), Br (r^2= 0.94) and moderately correlated with Cu (r^2= 0.78), Zn (r^2= 0.58), K (r^2= 0.56). This is possibly due to anthropogenic sources of Al, particularly from industries.

Na was found to be strongly correlated to S (r^2= 0.88), and moderately correlated with Pb (r^2= 0.79) and K (r^2= 0.78) in summer. Mg was strongly correlated with Sn (r^2= 0.84) and moderately correlated with Na (r^2= 0.74) and Co (r^2= 0.68) in summer while in winter, it was moderately correlated with Cl (r^2= 0.68).

Pb was strongly correlated with Zn (r^2= 0.83), As (r^2= 0.82), K (r^2= 0.82) and moderately correlated with S (r^2= 0.66) and Na (r^2= 0.79). In summer, Pb was moderately correlated with S (r^2= 0.62), Br (r^2= 0.50), Zn (r^2= 0.56), Cu (r^2= 0.75) and V (r^2= 0. 57). Arsenic (As) was also correlated with Zn (r^2= 0.81) in winter though these elements were not found to be correlated in summer. As and Pb are also reported to be emitted from waste burning (Watson et al., 2008). V and Ni are associated with industrial emission as well as oil combustion (Viana et al., 2008). Pb, Fe, Zn and K have also been associated with industrial emissions (Sahu et al., 2011b; Moreno et al., 2013; Patil et al., 2013; Farao et al., 2014). K and Br have also been reported from wood smoke (Kleeman et al., 1999; Fine et al., 2001) while Zn has been associated with incineration (Harrison et al., 1997; Moreno et al., 2013) and industrial burning (Duvall et al., 2012). Pb and Mg are also reported to be rich in kerosene combustion (Patil et al., 2013).

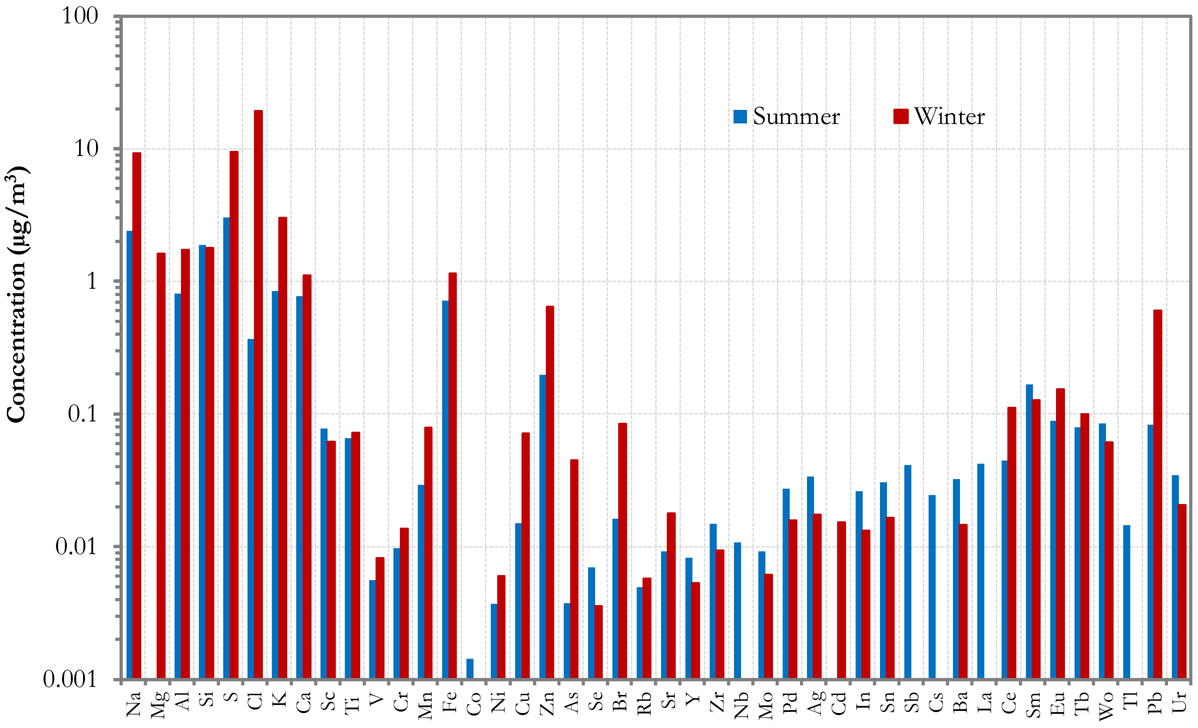

Figure 40: Seasonal variation of element concentrations in $PM_{2.5}$ at CRRI

While the correlations in the summer season are largely indicative of traffic and industrial sources, an additional source, most likely, combustion (including biomass, coal and waste) is affecting elemental concentrations in the winter season. Zn and Cl can also be emitted due to coal combustion, and waste incineration (Perrino et al., 2011).

Elements such as Cu, Ba, Sb and Sn have been associated with brake wear (Pant and Harrison, 2013) but in Delhi, these were not found to be correlated to each other in summer. Species associated with brake wear such as Cu and Ba typically exhibit a coarse mode peak at 3.2-5.6 µm (Gietl et al., 2010). However, in Delhi, these peaks were not observed. This is important for future studies, as this would imply that elements such as Cu and Ba cannot readily be used as markers for non-exhaust emissions in India.

Table 31: Summary of elemental concentrations in $PM_{2.5}$ at CRRI, New Delhi (in $\mu g/m^3$)

Species	Summer				Winter			
	Mean	S.D.	Minimum	Maximum	Mean	S.D.	Minimum	Maximum
Na	2.39	2.91	0.10	13.43	9.27	6.82	0.52	23.19
Mg	*detected in <20% samples*				1.61	1.49	0.16	5.03
Al	0.81	0.72	0.08	3.03	1.73	0.87	0.63	3.74
Si	1.88	1.87	0.02	7.80	1.79	0.67	0.77	2.94
P	*detected in <20% samples*				*detected in <20% samples*			
S	3.02	2.20	0.01	9.67	9.49	7.27	2.42	26.9
Cl	0.37	0.61	0.01	2.70	19.19	13.88	0.00	53.2
K	0.84	0.55	0.01	2.02	3.03	1.14	0.86	5.18
Ca	0.78	0.75	0.004	3.27	1.11	0.46	0.33	1.85
Sc	0.08	0.14	0.005	0.74	0.06	0.09	0.03	0.34
Ti	0.07	0.06	0.003	0.25	0.07	0.04	0.005	0.13
V	0.01	0.01	0.0004	0.02	0.01	0.01	0.001	0.03
Cr	0.01	0.01	0.0003	0.05	0.01	0.02	0.00	0.06
Mn	0.03	0.03	0.0003	0.11	0.08	0.07	0.01	0.29
Fe	0.71	0.63	0.02	2.52	1.15	0.33	0.53	1.57
Co	0.001	0.001	0.0003	0.006	*detected in <20% samples*			
Ni	0.004	0.003	0.0003	0.01	0.01	0.01	0.0003	0.02
Cu	0.02	0.01	0.001	0.05	0.07	0.07	0.01	0.28
Zn	0.20	0.19	0.01	0.75	0.64	0.38	0.23	1.47
Ga	*detected in <20% samples*				*detected in <20% samples*			
As	0.004	0.001	0.001	0.005	0.04	0.04	0.002	0.17
Se	0.007	0.003	0.001	0.01	0.00	0.00	0.001	0.00
Br	0.02	0.01	0.002	0.06	0.08	0.06	0.01	0.19
Rb	0.005	0.004	0.001	0.01	0.01	0.004	0.002	0.01
Sr	0.009	0.006	0.002	0.02	0.02	0.02	0.01	0.07
Y	0.01	0.004	0.0002	0.01	0.01	0.001	0.003	0.01
Zr	0.015	0.011	0.0003	0.03	0.01	0.01	0.002	0.01
Nb	0.01	0.008	0.0003	0.02	*detected in <20% samples*			
Mo	0.01	0.01	0.0002	0.02	0.01	0.003	0.0002	0.01
Pd	0.03	0.02	0.001	0.04	0.02	0.01	0.005	0.02
Ag	0.03	0.02	0.002	0.07	0.02	0.01	0.01	0.02
Cd	*detected in <20% samples*				0.02	0.004	0.01	0.02
In	0.03	0.01	0.001	0.04	0.01	0.01	0.002	0.02
Sn	0.03	0.02	0.01	0.10	0.02	0.01	0.005	0.03
Sb	0.041	0.023	0.0002	0.07	*detected in <20% samples*			
Cs	0.02	0.02	0.005	0.10	*detected in <20% samples*			
Ba	0.03	0.03	0.004	0.13	0.01	0.01	0.01	0.04
La	0.04	0.06	0.01	0.31	*detected in <20% samples*			

Ce	0.04	0.10	0.01	0.49	0.11	0.24	0.01	0.88
Sm	0.17	0.40	0.005	2.13	0.13	0.30	0.01	1.11
Eu	0.09	0.09	0.03	0.35	0.15	0.36	0.02	1.34
Tb	0.08	0.10	0.03	0.43	0.10	0.26	0.01	0.96
Hf	*detected in <20% samples*				*detected in <20% samples*			
Ta	*detected in <20% samples*				*detected in <20% samples*			
W	0.08	0.04	0.0003	0.12	0.06	0.06	0.01	0.25
Ir	*detected in <20% samples*				*detected in <20% samples*			
Au	*detected in <20% samples*				*detected in <20% samples*			
Hg					*detected in <20% samples*			
Tl	0.01	0.01	0.0002	0.02	*detected in <20% samples*			
Pb	0.08	0.06	0.003	0.27	0.60	0.65	0.08	2.51
U	0.034	0.018	0.002	0.05	0.02	0.01	0.003	0.03

6.3.1.6 Carbonaceous Species

A comprehensive set of organic species were measured using TD GC-MS including PAHs, hopanes, steranes and alkanes using methods described in Chapter 2. Across all species' classes, concentrations were observed to be higher in winter compared to summer. Several species were not detected in summer.

PAHs: PAHs are typically emitted as a by-product of combustion (including road traffic, solid fuel combustion, coal combustion, industries and agricultural burning) and are found both in gas- and particulate-phases (Smith and Harrison, 1996; Cass, 1998; Chow et al., 2004). Total pPAH concentration in $PM_{2.5}$ was observed to be 6.04 ng/m^3 in summer and 119.1 ng/m^3 in winter. Several species including Pic, DaeP, Cor were detected only in winter samples (Figure 41). Acy was the most abundant species in summer followed by Ace while in winter, Chr was the most abundant species followed by BaP. PAHs were strongly correlated with OC (r^2= 0.80), EC (r^2= 0.90) and hopanes (r^2= 0.83) in summer and moderately correlated with alkanes (r^2= 0.69). A summary of seasonal concentrations is presented in Table 32.

Heavy duty vehicles typically emit low molecular weight PAHs including anthracene, methyl- and dimethyl- phenanthrenes and fluoren-9-one (Rogge et al., 1993a; Sjorgen et al., 1996; Miguel et al., 1998). Species such as BN1NT, Flu, Phen have been used as markers for diesel vehicle emissions while methylphenanthrenes have been associated with evaporative emissions from fuel (Harrison et al., 1996; Jang et al., 2013). PAHs such as benzo(ghi)perylene, indeno(1,2,3-cd)pyrene and coronene have previously been used as markers for gasoline traffic emissions (Cass, 1998; Phuleria et al., 2007; Pant and Harrison, 2013). Flu, Acy, Ant, Phe, Pyr, BeP, BaP, Ret are typically used as markers for wood combustion (Cass, 1998; Fine et al., 2001; Simoneit, 2002; Jang et al., 2013) while Ant, Phe, BaA and Chr are used as markers for coal combustion (Harrison et al., 1996). Several species such as Ant, CcdP and BN1NT have been attributed to different sources in different studies. For example, Larsen and Baker (2003) reported the use of CcdP as a tracer for gasoline emissions while Jang et al. (2013) used it as a marker for coal combustion. Previous studies from India have associated pyrene with domestic fuel emissions (kerosene, dung etc.) and coal combustion, BaP with wood combustion and BghiPe and IcdP with traffic emissions (Kulkarni and Venkataraman, 2000; Sharma et al., 2007) while BaAQ has been associated with residential natural gas emissions (Cass, 1998).

If the summer and winter concentrations are compared, species such as Phe (11.6), BaA (54.7) associated with coal and biomass combustion show very high winter/summer ratios while others associated with traffic such as BghiPe (6.86) and 2MPhe (2.50) have comparatively lower winter/summer ratios. This indicates additional sources in proximity of the sampling site during winter season which is consistent with emission inventory analyses. High winter/summer ratios have been reported previously by Sharma et al. (2007) for Delhi. In addition to source types, the different temperature regimes across seasons can also influence the partitioning of the species in the gas- and particle- phases for PAHs (Smith and Harrison, 1996).

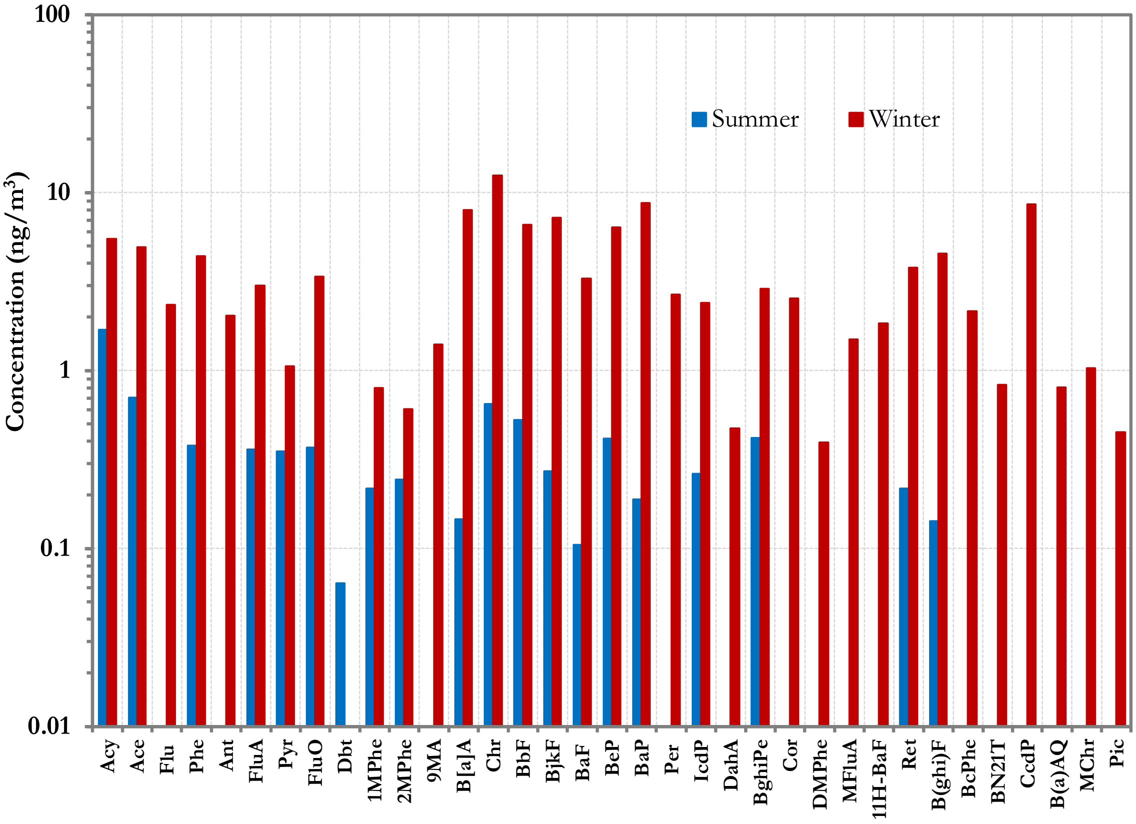

Figure 41: Seasonal variation of PAH congener concentrations in $PM_{2.5}$ at CRRI

One of the qualitative approaches for assessment of PAH source is the diagnostic ratio (DR) analysis where ratios of different PAHs are used for identification of contributing sources. Ratio of IcdP/IcdP+BghiPe is used as an indicator for diesel/gasoline or coal emissions (Ravindra et al., 2008). The ratio was observed to be 0.38 in summer and 0.46 in winter indicating the contribution from vehicular emissions. Ratio of BaA/BaA+Chr can also be used to distinguish between diesel/gasoline/wood combustion and in the present case, the ratio was observed to be 0.18 for summer and 0.39 for winter which corresponds with diesel emissions (Kavouras et al., 2001).

Table 32: Summary of PAH congener concentrations in $PM_{2.5}$ at CRRI (in ng/m^3)

Species	Summer				Winter			
	Mean	S.D.	Minimum	Maximum	Mean	S.D.	Minimum	Maximum
PAHs								
Acy	1.69	1.71	0.001	5.25	5.51	2.14	0.001	7.62
Ace	0.71	0.52	0.18	1.91	4.94	3.53	0.40	9.80
Flu	*detected in <20% samples*				2.34	1.93	0.001	4.91
Phe	0.38	0.34	0.000	1.71	4.39	1.68	2.20	7.30
Ant	*detected in <20% samples*				2.04	0.75	1.00	3.10
FluA	0.36	0.25	0.0002	1.33	3.01	3.82	0.30	10.1
Pyr	0.35	0.32	0.0003	1.53	1.06	1.20	0.30	3.30
FluO	0.37	0.10	0.29	0.75	3.36	1.26	2.00	5.80
Dbt	0.06	0.11	0.001	0.29	*detected in <20% samples*			
1MPhe	0.22	0.09	0.001	0.41	0.80	0.25	0.50	1.30
2MPhe	0.24	0.09	0.001	0.48	0.61	0.11	0.50	0.90
9MA	*detected in <20% samples*				1.40	1.40	0.001	3.23
B[a]A	0.15	0.25	0.0005	1.04	8.01	3.20	3.90	13.2
Chr	0.65	0.61	0.0003	2.95	12.5	4.18	6.50	18.6
BbF	0.53	0.32	0.001	1.69	6.61	4.62	1.50	16.0
BjkF	0.27	0.36	0.0002	0.93	7.22	2.13	3.10	12.0
BaF	0.10	0.16	0.0003	0.55	3.29	1.51	1.50	5.10
BeP	0.42	0.39	0.0006	1.61	6.40	2.06	3.40	9.6
BaP	0.19	0.27	0.0006	0.91	8.73	3.34	5.10	14.3
Per	*detected in <20% samples*				2.68	0.80	1.90	4.00
IcdP	0.26	0.22	0.0003	0.94	2.39	1.59	0.0003	4.79
DahA	*detected in <20% samples*				0.47	0.47	0.001	1.13
BghiPe	0.42	0.27	0.000	1.05	2.88	2.42	0.0004	6.19
Cor	*detected in <20% samples*				2.54	2.06	0.0005	5.52
DaeP	*detected in <20% samples*				*detected in <20% samples*			
DMPhe	*detected in <20% samples*				0.39	0.41	0.001	1.08
MFluA	*detected in <20% samples*				1.49	1.88	0.001	6.88
11H-BaF	*detected in <20% samples*				1.84	1.73	0.70	6.80
Ret	0.22	0.19	0.001	0.65	3.80	2.28	0.4	8.10
B(ghi)F	0.14	0.31	0.0003	1.27	4.53	1.44	2.5	7.10
BcPhe	*detected in <20% samples*				2.16	0.78	1.1	3.40
BN21T	*detected in <20% samples*				0.83	0.26	0.4	1.20
CcdP	*detected in <20% samples*				8.59	2.37	4.7	13.2
B(a)AQ	*detected in <20% samples*				0.81	0.93	0.001	2.80
MChr	*detected in <20% samples*				1.04	0.41	0.4	1.60
BbC	*detected in <20% samples*				*detected in <20% samples*			
Pic	*detected in <20% samples*				0.45	0.53	0.001	1.22

Hopanes and steranes: Total hopane concentration in $PM_{2.5}$ was observed to be 2.54 ng/m^3 in summer and 30.2 ng/m^3 in winter. RHHO (C31αβR-hopane) was the most abundant species in both seasons (Figure 42). A summary is presented in Table 33.

Hopanes were found to be strongly correlated to alkanes (r^2= 0.88) and PAHs (r^2= 0.88) in winter although no correlation was observed with OC and EC. In summer, hopanes were strongly correlated with EC (r^2= 0.88) and PAHs (r^2= 0.83) and moderately correlated with OC (r^2= 0.78) and alkanes (r^2= 0.74). While hopanes are typically used as markers for traffic exhaust emissions (as discussed in Chapter 1), several hopane species are also found to be abundant in coal burning emissions (Oros and Simoneit, 2000; Zhang et al., 2008). The ratio between S/S+R homohopanes was identified as 0.05 for lignite and 0.08 for brown coal (Oros and Simoneit, 2000). In Delhi, the values for this ratio were calculated as 0.11 for summer and 0.05 for winter, indicating the potential contribution from coal/lignite burning as an additional hopane source. Lignite is used for electricity generation in thermal power plants in India, and coal can also be used for cooking and/or heating, particularly in poorer areas and slums.

In the case of steranes, ααα20RC was the abundant sterane in summer while αββ20S24REC was the most abundant species in winter. Total sterane concentrations in summer and winter were 0.57 and 3.95 ng/m^3 respectively. αββ20S24SMC showed a very high winter/summer ratio (15.2) while ααα20RC and ααα20R24REC showed winter/summer ratios less than 2. Steranes were strongly correlated with hopanes (r^2= 0.81) and EC (r^2= 0.86) in summer and in winter, the correlation was moderate both in case of hopanes and steranes at $p<0.05$.

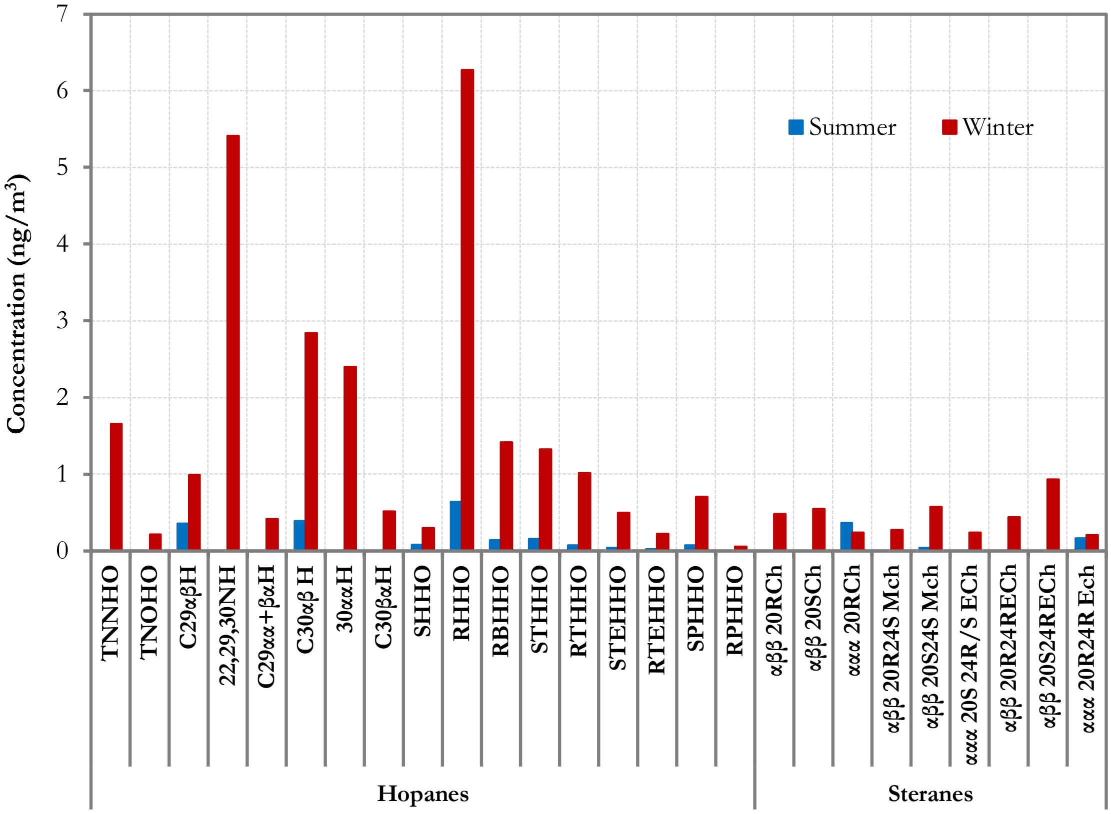

Figure 42: Seasonal concentrations of hopane and sterane congeners in $PM_{2.5}$ at CRRI

Table 33: Summary of hopane and sterane congener concentrations in $PM_{2.5}$ at CRRI (in ng/m^3)

Species	Summer				Winter			
	Mean	S.D.	Minimum	Maximum	Mean	S.D.	Minimum	Maximum
Hopanes								
TNNHO		*detected in <20% samples*			1.66	0.64	0.66	2.39
TNOHO		*detected in <20% samples*			0.22	0.32	0.0003	0.76
C29αβ-hopane	0.36	0.57	0.0002	1.93	0.99	1.82	0.0002	4.65
22,29,30-norhopane		*detected in <20% samples*			5.41	2.95	0.80	9.48
C29αα- + βα -hopane		*detected in <20% samples*			0.42	0.27	0.0004	0.73
C30αβ -hopane	0.39	0.50	0.0003	1.86	2.84	2.13	0.24	5.74
30αα-hopane		*detected in <20% samples*			2.40	2.11	0.44	6.58
C30βα -hopane		*detected in <20% samples*			0.52	0.39	0.0003	1.23
SHHO	0.08	0.19	0.0005	0.74	0.30	0.62	0.0005	1.55
RHHO	0.64	0.68	0.0005	2.72	6.27	1.65	4.16	9.22
SBHHO		*detected in <20% samples*				*detected in <20% samples*		
RBHHO	0.14	0.15	0.0005	0.59	1.42	0.40	0.80	1.98
STHHO	0.16	0.15	0.0005	0.53	1.32	0.41	0.84	2.09

RTHHO	0.07	0.10	0.0006	0.33	1.02	0.53	0.45	2.18
STEHHO	0.04	0.09	0.0005	0.34	0.50	0.65	0.001	1.97
RTEHHO	0.02	0.04	0.0005	0.14	0.22	0.18	0.001	0.49
SPHHO	0.07	0.09	0.0005	0.35	0.71	0.31	0.38	1.45
RPHHO	*detected in <20% samples*				0.06	0.07	0.001	0.16
Steranes								
ααα 20SC	*detected in <20% samples*				*detected in <20% samples*			
αββ 20RC	*detected in <20% samples*				0.48	0.31	0.0004	0.88
αββ 20SC	*detected in <20% samples*				0.55	0.26	0.21	0.96
ααα 20RC	0.36	0.79	0.0002	3.09	0.24	0.21	0.0002	0.55
ααα 20S24S MC	*detected in <20% samples*				*detected in <20% samples*			
αββ 20R24S MC	*detected in <20% samples*				0.28	0.28	0.0003	0.63
αββ 20S24S MC	0.04	0.08	0.0003	0.25	0.58	0.15	0.26	0.72
ααα 20R24RMC	*detected in <20% samples*				*detected in <20% samples*			
ααα 20S 24R/S EC	*detected in <20% samples*				0.24	0.34	0.0005	0.78
αββ 20R24REC	*detected in <20% samples*				0.44	0.14	0.22	0.64
αββ 20S24REC	*detected in <20% samples*				0.94	0.34	0.53	1.37
ααα 20R24R EC	0.17	0.40	0.0002	1.49	0.21	0.37	0.0002	1.25

Alkanes: Alkanes were the most abundant class among the organic species in PM$_{2.5}$ and the 12-h average alkane concentration was observed to be 48.2 ng/m^3 in summer and 382.3 ng/m^3 in winter. C20-31 homologues were the most abundant while C39 and C40 were not detected in either season (Table 34).

Fu et al. (2010) also did not detect C36-40 homologues in winter and C39-40 in summer in Chennai (India) in PM$_{10}$. The dominant homologues were C26, C27 and C25 in summer and C29, C22 and C31 in winter (Figure 43). The winter/summer ratios were highest for the lower homologues (C18-C23) and C34-35.

Wood and biomass combustion is quite common in Delhi during the winter period when wood is used not only as a cooking fuel but also for heating (Fu et al., 2010; Yadav et al., 2013). In addition, old tyres, furniture (often plastic) and other waste materials are often burnt in the open. Long chain alkanes (e.g. C36) are also reported to be emitted from open waste burning (Fu et al., 2010; Alves et al., 2012). Alkane emissions (n<25) from the vehicles can be attributed to unburnt engine oil in case of gasoline vehicles and fuel as well as lubricating oil in case of diesel vehicles and older vehicles are often high emitters of n-alkanes (Rogge et al., 1993a).

Alkanes were found to be correlated well with OC (r^2= 0.79), and hopanes (r^2= 0.74) and moderately correlated with PAHs (r^2= 0.69) and EC (r^2= 0.60) in summer. In winter, however, no correlation was observed with OC and EC although strong correlation was observed with hopanes as well as PAHs (r^2= 0.88 in both cases).

Carbon Preference Index (CPI), the ratio of odd to even numbered homologues, can be used to estimate the relative contribution of anthropogenic and biogenic sources. Due to the odd carbon number preference in case of vegetative material, higher ratio values are associated with biogenic contribution. In this case, the index value was 1.09 for summer and 1.22 for winter indicating a significant contribution from anthropogenic sources in both seasons.

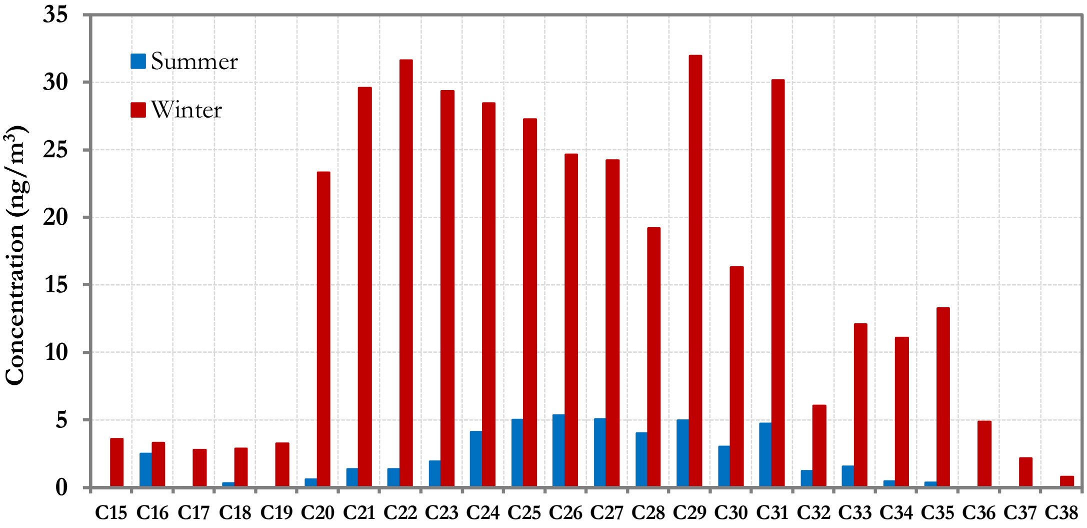

Figure 43: Seasonal concentrations of straight chain alkane species in $PM_{2.5}$ at CRRI

Table 34: Summary of alkane concentrations (C15-C40) in $PM_{2.5}$ at CRRI (in ng/m^3)

Species	Summer				Winter			
	Mean	S.D.	Minimum	Maximum	Mean	S.D.	Minimum	Maximum
C15	*detected in <20% samples*				3.60	1.82	0.001	6.5
C16	2.49	1.11	1.44	6.21	3.31	0.99	2.05	4.9
C17	0.05	0.23	0.000	1.22	2.78	1.56	0.0005	5.7
C18	0.32	0.56	0.003	1.83	2.90	1.55	0.0004	5.7
C19	0.05	0.28	0.000	1.46	3.25	1.89	0.0003	6.5
C20	0.63	1.01	0.002	3.39	23.3	15.3	1.83	54.8
C21	1.35	1.55	0.004	4.70	29.6	17.1	4.22	62.5
C22	1.39	1.66	0.003	5.56	31.6	9.66	21.6	50.9
C23	1.93	2.22	0.003	6.61	29.4	8.50	19.6	44.2
C24	4.14	3.88	0.003	14.4	28.5	9.85	17.9	49.1
C25	5.00	5.00	0.003	18.2	27.3	9.90	16.3	47.3
C26	5.35	5.02	0.003	20.2	24.7	7.98	14.5	37.5
C27	5.08	4.15	0.001	17.0	24.2	8.03	14.8	39.4
C28	4.03	3.44	0.003	13.1	19.2	8.56	0.0005	29.7
C29	4.96	4.28	0.004	17.6	31.9	19.0	0.0005	58.8
C30	3.05	2.31	0.004	9.15	16.3	11.7	0.0006	33.7
C31	4.76	2.81	0.004	12.3	30.1	18.7	0.0005	62.7
C32	1.24	1.39	0.004	4.60	6.06	7.65	0.0006	26.5
C33	1.55	1.27	0.003	4.21	12.1	10.7	0.0004	35.8
C34	0.45	0.83	0.000	2.64	11.1	7.54	0.0004	21.3
C35	0.38	0.70	0.003	2.24	13.3	7.33	6.94	28.7
C36	*detected in <20% samples*				4.87	7.91	0.001	23.4
C37	*detected in <20% samples*				2.19	3.19	0.001	9.4
C38	*detected in <20% samples*				0.79	1.10	0.001	2.3
C39	*detected in <20% samples*				*detected in <20% samples*			
C40	*detected in <20% samples*				*detected in <20% samples*			

Sugars: In ambient air, saccharides are typically associated with biological material (e.g. soil organic matter) and arabitol and mannitol have been proposed as markers for fungal spores (Simoneit et al., 2004a; Buaer et al., 2008). Glycerol, a polyol, was the only saccharide species detected in both summer and winter with a winter/summer ratio of 26.5. Most of the other saccharides were detected in less than 20% of the samples and not discussed in detail (Table 35, Figure 44).

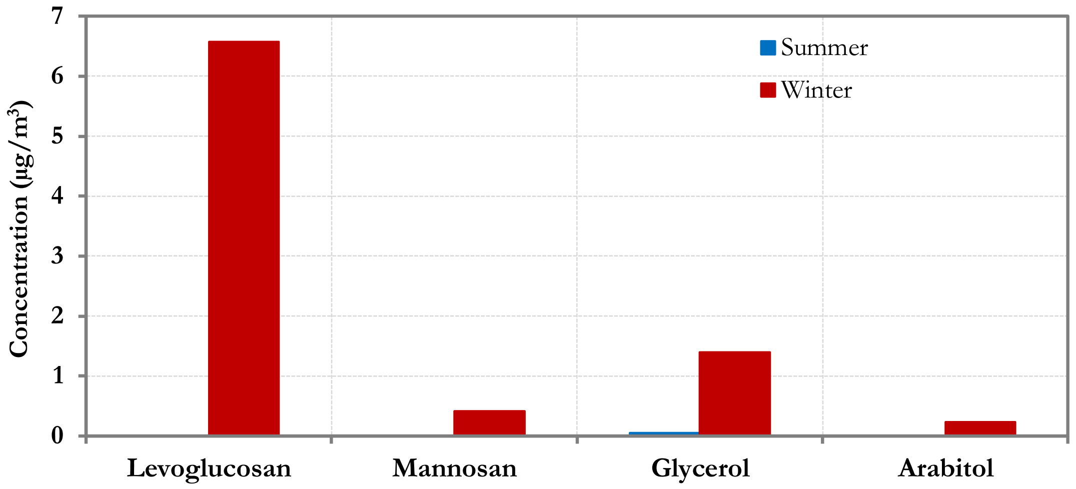

Figure 44: Seasonal concentrations of sugar species in $PM_{2.5}$ at CRRI (µg/m³)

Anhydrosaccharides such as levoglucosan and mannosan are typically associated with wood/biomass combustion (Simoneit et al., 2004b; Alves et al., 2012). Both levoglucosan and mannosan were only detected in the winter season and had a strong correlation (r^2= 0.84) (Figure 44). Fu et al. (2010) reported a levoglucosan/mannosan ratio of 16.4 which is comparable to the ratio observed in the current study (16.07). Levoglucosan was also strongly correlated with OC (r^2= 0.91) and Cl^- (r^2= 0.87). Correlation with K^+ was comparatively weaker, and not significant at $p<0.01$. Cow dung burning has also been identified as a source of levoglucosan in India, but K is typically not released from cow dung combustion (Fu et al., 2010). A recent study focused on water-soluble organic carbon (WSOC) has also highlighted the important of biomass combustion as a source of OC in Delhi (Kirillova et al., 2014).

Diacids: Several organic acids including oxalic acid, lactic acid and glutaric acid were found to be present in both seasons (Figure 45). While oxalic acid was found to be the abundant species in both seasons, formic acid had the highest winter/summer ratio of 3.14. Biogenic sources have been reported to contribute to malic acid precursors, and the absence of the compound in this sample set is consistent with the absence or low concentrations of other biogenic material-related molecular markers.

Table 35: Concentrations of sugar species in $PM_{2.5}$ at CRRI (in µg/m^3)

Species	**Summer**				**Winter**			
	Mean	**S.D.**	**Minimum**	**Maximum**	**Mean**	**S.D.**	**Minimum**	**Maximum**
Sugars								
Levoglucosan	*detected in <20% samples*				6.57	3.23	2.15	12.0
Mannosan	*detected in <20% samples*				0.42	0.27	0.06	1.04
Glycerol	0.05	0.01	0.03	0.08	1.39	1.78	0.46	7.13
Inositol	*detected in <20% samples*				*detected in <20% samples*			
Erythritol	*detected in <20% samples*				*detected in <20% samples*			
Xylitol	*detected in <20% samples*				*detected in <20% samples*			
Arabitol	*detected in <20% samples*				0.23	0.31	0.07	1.14
Sorbitol	*detected in <20% samples*				*detected in <20% samples*			
Trehalose	*detected in <20% samples*				*detected in <20% samples*			
Mannitol	*detected in <20% samples*				*detected in <20% samples*			
Arabinose	*detected in <20% samples*				*detected in <20% samples*			
Glucose + Xylose	*detected in <20% samples*				*detected in <20% samples*			
Galactose +Maltitol	*detected in <20% samples*				*detected in <20% samples*			
Fructose	*detected in <20% samples*				*detected in <20% samples*			

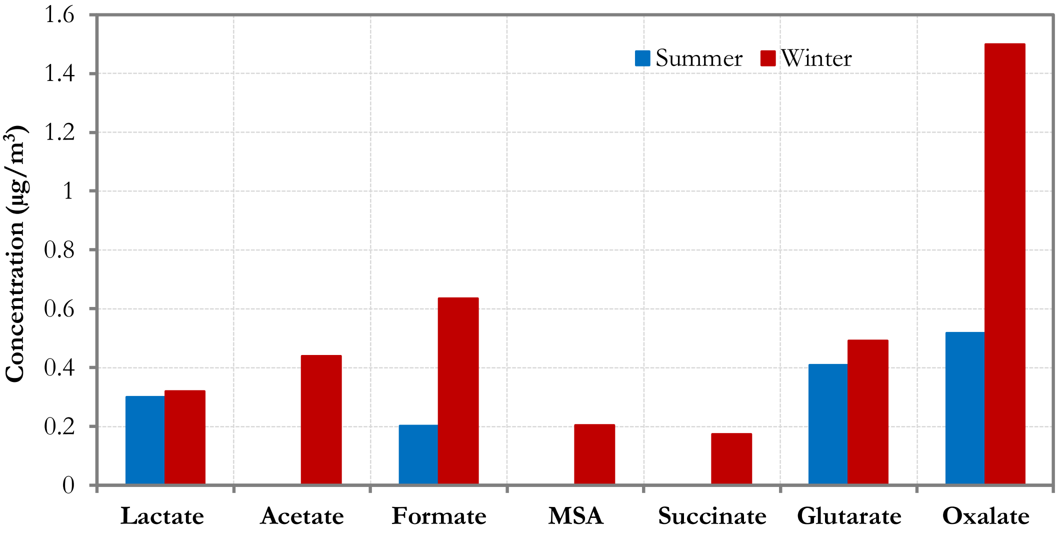

Figure 45: Seasonal variation in concentrations of organic acids in $PM_{2.5}$ at CRRI

Table 36: Summary of organic acid concentrations in $PM_{2.5}$ in summer and winter (in $\mu g/m^3$)

Species	Summer				Winter			
	Mean	S.D.	Minimum	Maximum	Mean	S.D.	Minimum	Maximum
Diacids								
Lactate	0.30	0.22	0.06	0.89		0.32	0.03	1.23
Acetate	*detected in <20% samples*					0.33	0.02	0.97
Formate	0.20	0.09	0.06	0.30		0.37	0.26	1.34
MSA	*detected in <20% samples*					0.31	0.09	1.23
Succinate	*detected in <20% samples*					0.27	0.002	0.66
Glutarate	0.41	0.15	0.33	0.83		0.26	0.33	1.02
Malonate	*detected in <20% samples*				*detected in <20% samples*			
Maleate	*detected in <20% samples*				*detected in <20% samples*			
Oxalate	0.52	0.28	0.09	1.13	1.50	1.49	0.00	4.33

6.3.2 Enrichment Factor Analysis

In order to further understand the sources of the elements (crustal vs. anthropogenic), enrichment factors (EFs) were calculated based on continental crust concentrations using Al as the reference element (Taylor and McLennan, 1995) (Figure 46).

$$\boldsymbol{EF\ (X)} = \frac{\left\{\dfrac{\boldsymbol{Concentration(X)}}{\boldsymbol{Concentration(Reference)}}\right\}\boldsymbol{sample}}{\left\{\dfrac{\boldsymbol{Concentration(X)}}{\boldsymbol{Concentration(Reference)}}\right\}\boldsymbol{crustal}} \qquad \boldsymbol{(15)}$$

Where
Concentration (X) refers to the concentration of species X in sample/crust
Concentration (reference) refers to the concentration of Al in sample/crust

EF values of 10 or higher are considered to indicate significant anthropogenic contribution. In this case, high enrichment factors (>100) were observed for elements such as Cu, Zn, Sb, Cd, Sn, As and Pb both in summer and winter, with higher enrichment observed in winter. On the other hand, Si, Sr, Se, Ba, Ca, Fe, Mn, Mg and V were found to have low EFs indicating crustal contribution.

This correlates with the size distributions for Mn and V where coarse mode was found to be dominant. Ti, typically associated with crustal matter, was also found to be enriched in both seasons although contrary to most of the other elements, the enrichment was higher in summer. Cd, As, Pb, Sb and Ti were found to be highly enriched in both seasons. Cd is primarily emitted from industries (smelting), waste incineration and recycling of electronic waste but is also associated with traffic emissions (Amato et al., 2011b). Arsenic (As) is used as a marker for coal combustion, and Pb and Zn are also emitted from waste incineration.

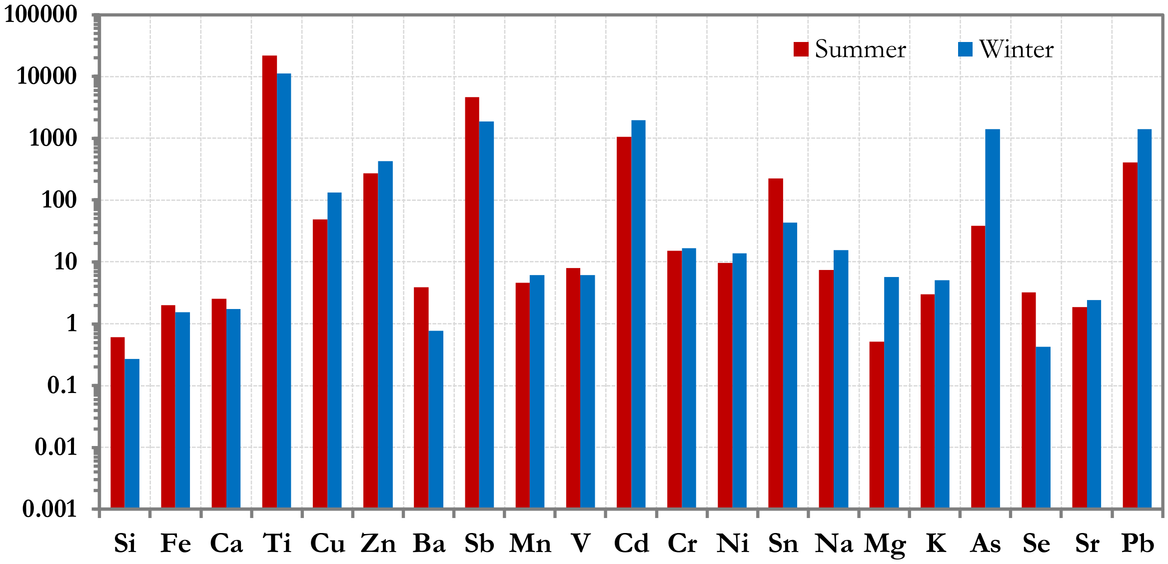

Figure 46: Enrichment factors for select elements in $PM_{2.5}$

6.3.3 Mass Closure

In order to understand the relative contribution of the different species, mass closure was attempted for $PM_{2.5}$ mass with seven components including woodsmoke, traffic, other OM, secondary aerosol (ammonium chloride, ammonium nitrate and ammonium sulphate) and mineral dust/soil. Crustal material was estimated using concentrations of elements- Si, Al, Ca, Fe and Ti, based on Chan et al. (1997) [discussed in Chapter 5, equation 15]. Organic matter (OM) was estimated from OC using a factor of 1.2 in case of traffic OM, and 1.5 in case of other OM. The factors used in the mass closure equation are listed in Table 37.

Nearly 100% of the mass was estimated in both cases [94.2% in summer and 114.7% in winter] and the results are described in Figure 47.

Sulphate (25.1%) and crustal material (17.5%) had higher contributions in summer while nitrate (12.8%) had a higher contribution to $PM_{2.5}$ in winter. Lower concentration of nitrate in summer can be explained by the volatility at higher temperatures while higher crustal matter in summer is attributed to desert dust as well as local dust sources which are frequently resuspended in dry and windy conditions. Traffic was found to contribute 23% to $PM_{2.5}$ in summer and 16% in winter, while woodsmoke was found to contribute 23% in winter.

Table 37: Estimation factors used for $PM_{2.5}$ mass closure

Source	Component	Estimation factor	Reference
Woodsmoke	OM ($PM_{2.5}$)	11.2*levoglucosan	Harrison et al. (2012)
	OC	7.35*levoglucosan	Puxbaum et al. (2007)
	EC	0.2*woodsmoke $PM_{2.5}$	Harrison et al. (2012)
Traffic	OC	0.35*EC	Pio et al. (2011)
	$PM_{2.5}$	1.35*EC	
	OM ($PM_{2.5}$)	Traffic $PM_{2.5}$*1.2	Chow et al. (2002)
Secondary Ions	$(NH_4)_2SO_4$	1.38*Sulphate	Harrison et al. (2003); molar ratios
	$(NH_4)NO_3$	1.33*Nitrate	
	$(NH_4)Cl$	1.51*Chloride	
Dust	Crustal Mass	1.16(1.90Al+ 2.15Si+ 1.41Ca+1.67Ti+ 2.09Fe)	Chan et al. (1997)

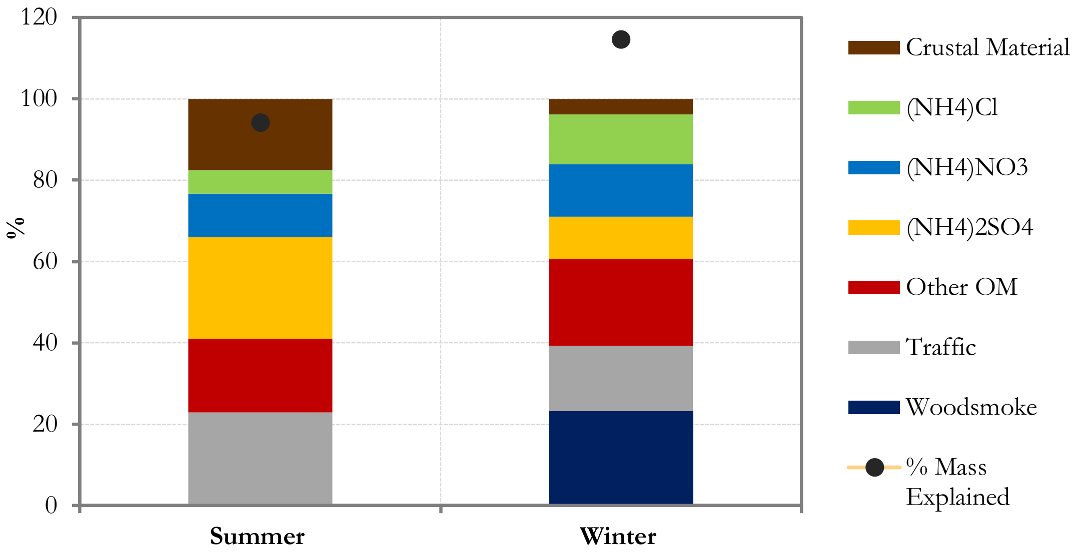

Figure 47: Mass closure for $PM_{2.5}$ at CRRI

6.4 Conclusions

$PM_{2.5}$ samples were analysed for a heavy traffic site in New Delhi, and detailed chemical characterization was conducted including analyses of metals, ions and molecular markers. PM concentrations were found to exceed the NAAQS on several occasions in summer and on most days in winter. Several elements including Cu, Zn, Sb, Pb, Cd and As were found to be significantly enriched in $PM_{2.5}$ and complex correlations were observed between elemental species. In the case of molecular markers, several species were detected only in winter. Alkanes were found to be the most abundant class of organic species followed by PAHs and hopanes.

Concentrations were found to be significantly higher in winter compared to summer. Pollutant concentrations can be affected both by meteorology and source strength. There is a significant difference in the average temperature between summer and winter seasons in Delhi, and this could be driving some of the differences between species' concentrations in the two seasons. At higher temperatures, several species can be easily volatilized and reactive species can often undergo chemical reactions in the presence of sunlight (e.g. photodegradation of PAHs) (Venkataraman and Friedlander, 1994; Smith and Harrison, 1996; Alves et al., 2012). In combination with higher wind speeds, and inversion layer; this can lead to better dispersion of pollutants in the summer season. However, in winter, there is much less solar radiation, and the weather conditions are often 'calm' in Delhi indicated by zero or very low wind speeds. Further, the inversion layer height is typically much lower in winter. A combination of such meteorological factors can thus contribute to a build-up of pollutants, leading to higher concentrations. Another important aspect is the role of additional sources in the winter season. During the winter season, biomass/waste combustion is often used as a source of heating across the city, a lot of which occurs under uncontrolled conditions in the open areas. Increase in species associated with waste combustion (Pb, Zn, C35, C36) indicates the potential contribution from this seasonal source at the sampling site. However, in the absence of detailed emission inventories, it is difficult to attribute the elemental concentrations to specific sources.

The dataset can be used to generate quantitative source contribution estimates for summer and winter seasons. A small set of $PM_{2.5}$ source profiles is available for India (Patil et al., 2013). However, the profiles only include inorganic and carbon data and it is important to assess the sensitivity of the species as well as profiles before the modelling exercise is conducted. This activity could not be carried out due to limited time, but will be conducted in the future.

6.5 Acknowledgements

This study was conducted under a UKIERI trilateral project, and financial support from UKIERI is gratefully acknowledged. Special thanks to Professors Judith C. Chow and John G. Watson (DRI-Reno) for guidance and encouragement and Mr. Steve Kohl and his team for chemical analysis. Dr. Anuradha Shukla and field staff at CRRI (New Delhi) and Dr. Anubha Goel (IIT-Kanpur, India) are thanked for logistics' support during the sampling. Thanks to Dr. Sarath Guttikunda (IIT-New Delhi and DRI-Reno) for useful inputs.

CHAPTER 7- CONCLUSIONS

This thesis presents results from characterization and source estimation of PMx in New Delhi (India) and Birmingham (UK).

In Birmingham (UK), $PM_{2.5}$ was measured in a high-traffic environment (tunnel) and an urban background site while in New Delhi (India); $PM_{2.5}$ measurements were made at a high-traffic site. PM_{10} road dust was analysed in both cities. Chemical composition data was used to prepare source profiles for $PM_{2.5}$ composite traffic in the UK and PM_{10} road dust in UK and India.

PM (size-segregated and $PM_{2.5}$) was characterized at a traffic tunnel (QT) and an urban background site (EROS) in Birmingham, UK. Significant enrichment was observed at QT across various species' classes compared to EROS for $PM_{2.5}$. A bimodal mass size distribution (derived from MOUDI) was observed at both sites, with differences in the split among coarse and fine fractions. Analysis of the elemental size distributions indicated potential influence from the railways (wear and tear, braking) at EROS.

Two different ambient monitoring-based datasets (discussed in Chapters 3 and 4) were used for preparation of composite traffic $PM_{2.5}$ profiles (e.g. tunnel profile- Figure 48). The underlying principle is the same in both cases, i.e. calculation of a traffic increment for individual species followed by the normalization of the increments with respect to traffic increment for OC, resulting in a profile (μg/μg OC). The two UK profiles (tunnel-based and kerbside-based) were found to be similar (CoD= 0.32), and the highest dissimilarity was observed for the USA dynamometer profiles.

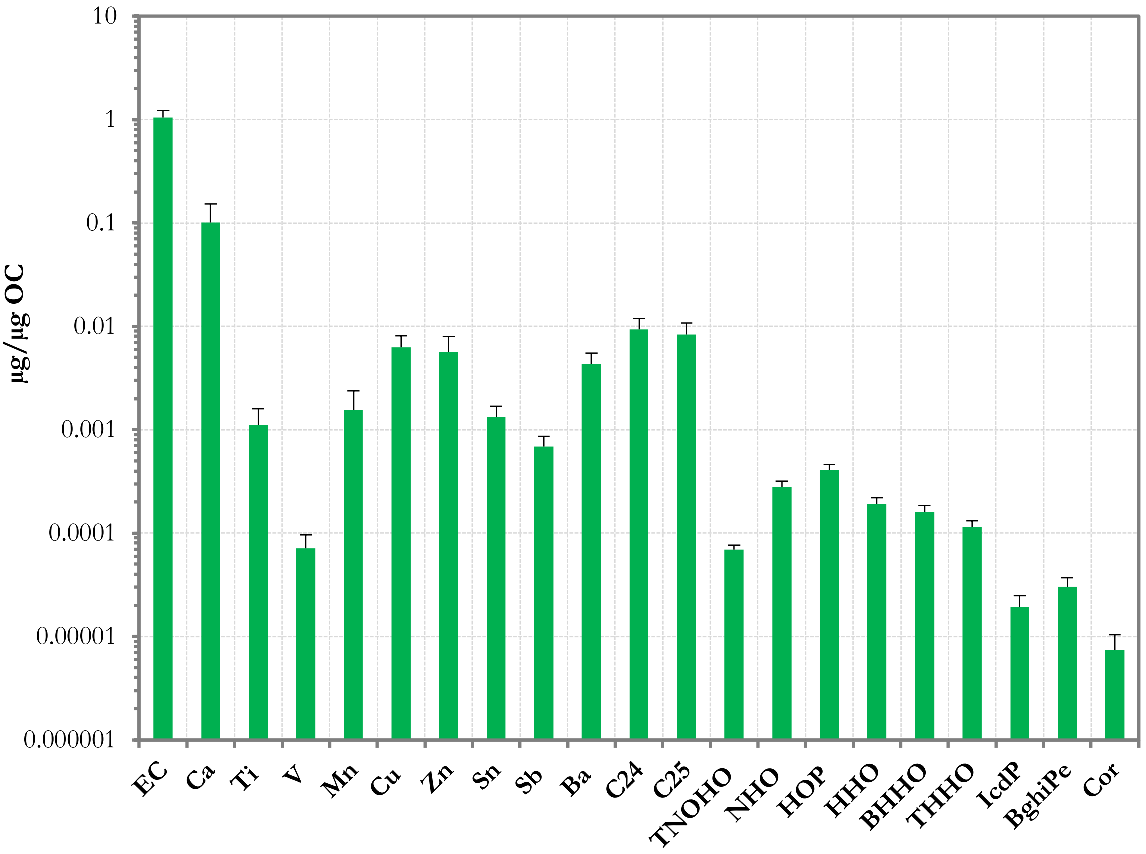

Figure 48: Source profile (μg/ μg OC) for composite traffic emissions for UK

CMB modelling was conducted for $PM_{2.5}$ at three different sites in the UK (two in Birmingham, one in London), and results were cross-compared with independent estimates for traffic contribution to PM (EC*1.35, Pio et al., 2011) and SOC contribution (EC tracer method, Turpin & Huntzicker, 1995). Overall correlation was similar for the twin-site and dynamometer profiles, with the twin-site profile performing better in some cases (results summarized in Table 38. Thus, it can be concluded that composite traffic profiles can be used to generate reliable SCEs, and offer a reliable alternative to dynamometer profiles.

Table 38: Traffic mass estimate (µg/m^3) using different traffic profiles

(values in parentheses refer to the total % PM$_{2.5}$ explained with each profile run)

Site (season)	PM$_{2.5}$ mass apportioned to traffic				
	DYN-A	**DYN-GD**	**TWIN**	**TUN**	**R80**
UB site, London (S)	2.98 *(123)*	1.61 *(130)*	2.69 *(119)*	0.96 *(122)*	2.69 *(119)*
UB site, Birmingham (A)	2.61 *(104)*	1.61 *(108)*	2.13 *(106)*	1.61 *(97.5)*	2.13 *(106)*
UB site, Birmingham (S)	2.39 *(108)*	1.50 *(111)*	1.90 *(109)*	1.50 *(100)*	1.90 *(100)*
UB site, Birmingham (W)	2.93 *(94.7)*	1.70 *(101)*	3.18 *(98.1)*	1.70 *(89.8)*	3.18 *(98.1)*
Rural site, Birmingham (A)	2.06 *(111)*	1.13 *(116)*	2.00 *(113)*	0.80 *(116)*	1.67 *(114)*
Rural site, Birmingham (S)	1.97 *(119)*	0.89 *(113)*	2.00 *(122)*	2.00 *(124)*	2.00 *(121)*
Rural site, Birmingham (W)	2.07 *(101)*	1.36 *(106)*	1.81 *(103)*	0.79 *(106)*	1.81 *(103)*

Note: S- summer, W- winter, UB- urban background, A- annual

While a number of studies have undertaken analysis of road dust in the UK and India, there is no data on the PM$_{10}$ (thoracic) fraction which is the health-relevant fraction for the non-exhaust emissions. Understanding the chemical composition of the PM$_{10}$ road dust is the first step towards improving the understanding of this source. PM$_{10}$ road dust fraction was characterized at different traffic locations in Birmingham, UK and at one location in New Delhi. Highest dust loading (µg/m^2) was observed for New Delhi (72.9 ± 24.3 mg/m^2) while the highest concentrations (µg/g) were observed for the tunnel site in the UK. PM$_{10}$ road dust source profiles were prepared for Birmingham and New Delhi (Figure 49).

The PM$_{10}$ road dust dataset was subsequently used for estimation of source contributions using an empirical method proposed by Harrison et al. (2012a). While the method was successfully applied to high-traffic locations in the UK (nearly 100% mass reconstruction), the results were not satisfactory for the low-traffic site in Birmingham and the site in New Delhi (Figure 50).

Overall, the crustal/soil contribution was the largest across sites while brake and tyre wear contributions were found to vary based on site type. The Si/Fe ratio was found to be the lowest at the low-traffic site in Birmingham, and peculiar site characteristics, as well as possible variations in the local soil composition could be the cause for the low apportionment at this site. High Cu/Sb ratios and low enrichment of Ba at the site in New Delhi indicated that the markers used for non-exhaust brake wear emissions in Europe may not be suitable for use in India. Analysis of the ambient size-segregated PM in New Delhi seemed to confirm this observation; since the characteristic peak (3.2.-5.6 μm) associated with brake wear was not observed in New Delhi. In addition, there might be other contributing sources, including construction dust which are not accounted for in the current estimation.

Since the source estimation is empirical, it can potentially be used in any city and can serve as a useful method for estimation of non-exhaust emissions in urban area. However, it is important to assess the local soil chemistry (contribution of key crustal elements such as Si/Al) to use the correct factors and analysis of bulk brake pad dust and tyre dust can be used to derive locally-relevant ratios for improved quantification.

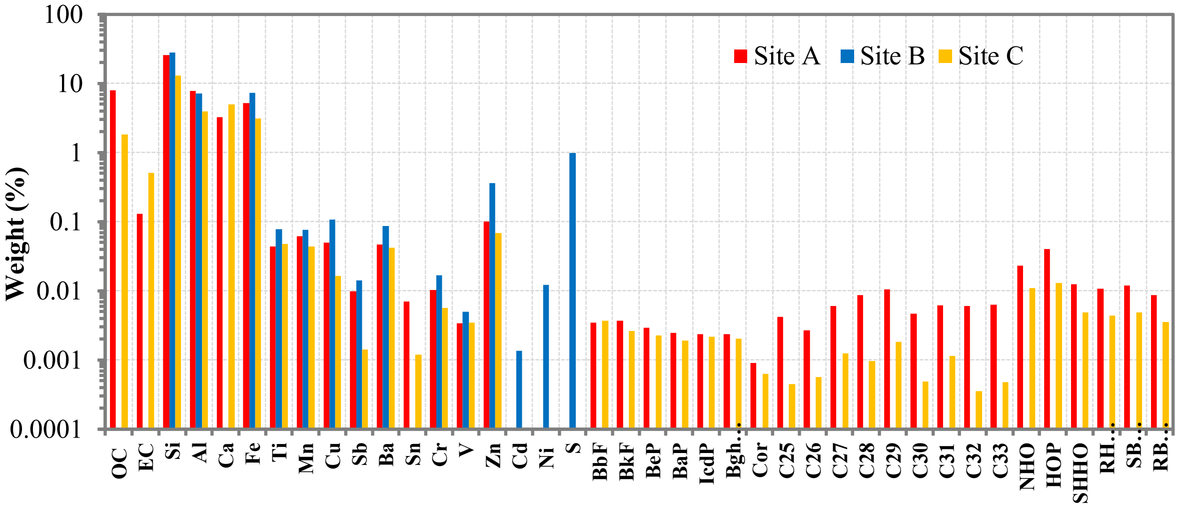

Figure 49: Source profiles for PM_{10} road dust in Birmingham (UK) and New Delhi (India)

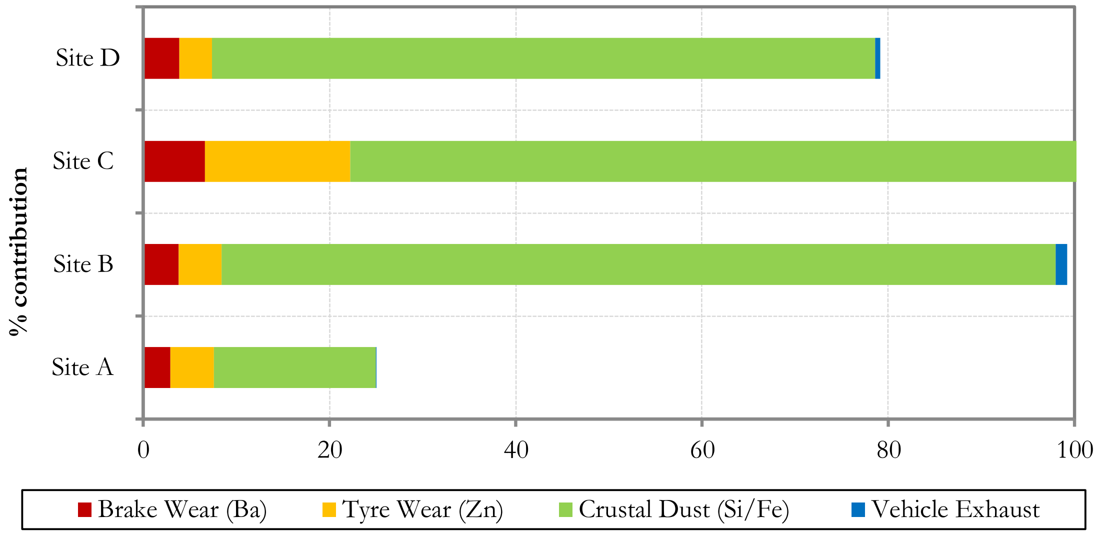

Figure 50: Source contributions of various non-exhaust sources to PM_{10} road dust across sites A-D (in %)

In New Delhi, $PM_{2.5}$ concentrations were found to exceed the NAAQS (24-h average concentration of 60 µg/m^3) on several days in summer and most days in winter. PM was found to be trimodal with a predominant contribution from fine particles (PM<2.5 µm aerodynamic diameter). Elemental size distributions were found to vary based on element type, and while soil-associated elements (Al, Si) showed primary peaks in the coarse range, most of the other elements including Cu and Zn showed primary peaks in the fine range. This is in contrast with the typical peak reported for Cu at 3.2-5.6 µm indicating the non-exhaust contribution. Other elements including Mn and V were found to be present both in coarse and fine ranges, indicating a mixed origin. Most elements were also found to have high enrichment with respect to the continental crust, indicating significant contributions from anthropogenic sources. Winter concentrations were found to be significantly higher than summer, and in some cases, winter/summer ratios were more than 10x. Mass closure was attempted for $PM_{2.5}$ for both seasons and 94.2% and 115% of the total $PM_{2.5}$ mass was estimated (Table 39). Sources such as crustal material and secondary sulphate were found to have higher contributions in the summer while nitrate and secondary OM had higher contributions in the winter.

Table 39: Mass closure for $PM_{2.5}$ in New Delhi (values in %)

Source category	Summer	Winter
Woodsmoke		23.2
Traffic	23.0	16.1
Other OM	18.0	21.3
$(NH_4)_2SO_4$	25.1	10.5
$(NH_4)NO_3$	10.6	12.8
$(NH_4)Cl$	5.88	12.3
Crustal Material	17.5	3.87

While this is one of the first studies to undertake detailed chemical composition of $PM_{2.5}$ as well as size-segregated aerosols in India, the study did have some limitations. Since the samples were collected at one site only, it was difficult to discern the influence of traffic with respect to other sources. In addition, due to time and cost constraints, sampling was conducted for a short period of time, resulting in a relatively small dataset. This renders the application of multivariate analysis tools such as PMF difficult. A larger number of sampling sites and longer sampling periods would enable analysis of the data using multiple methods including CMB and PMF. It is also clear that the knowledge of source influences and source-specific marker species from Europe and North America may not be directly applicable in Asian cities. This has also been highlighted in a recent study from Taiwan (Lin et al., 2014). Levels of PM as well as its chemical constituents are much higher in Delhi compared to European cities, and in the absence of stringent regulations, several source often go undetected.

CHAPTER 8- FUTURE DIRECTIONS

8.1 United Kingdom

This thesis has focused on development of traffic profiles ($PM_{2.5}$) for the UK based on ambient data, and the successful application of a CMB model using the composite traffic profile. Based on the traffic profiles generated in this study (traffic-$PM_{2.5}$ and road dust-PM_{10}), updated estimates for the contribution of exhaust and non-exhaust sources to ambient PM concentrations can be generated. Ambient data-based source profiles can be used as inputs for receptor modelling, and represent a cost and time-effective alternative to generate local source profiles.

While it is well known that PM causes adverse health effects, the health hazards posed by PM emitted from different sources can vary based on the characteristics of the emitted particles since toxicity varies based on the chemical composition (de Kok et al., 2006). Detailed understanding of the metal solubility (fraction of metal present in soluble form that can be absorbed across a biological membrane) and the redox activity potential (in terms of concentration of ROS) are therefore important in order to understand the health effects posed by the heavy-metal rich non-exhaust emissions. As highlighted out in Amato et al. (2014a), there is a lack of detailed evidence on the role of non-exhaust emissions in adverse health effects. Detailed analysis such as the one carried out in this study (Chapter 5) can provide relevant information to design studies focused on exposure assessment and ecotoxicology. While there are a few published studies on soluble and insoluble fraction of PM mass emitted by traffic (solubility can impact the bioavailability), there is little information on the oxidative potential of traffic PM, particularly non-exhaust PM. A recent study in London concluded that the potential to cause oxidative stress was high for tyre and brake-wear generated particles (Yanosky et al., 2012). A pilot project is currently being carried out to understand the risks of oxidative stress upon exposure to road dust in collaboration with Dr. Krystal Godri (University of Toronto).

Specific recommendations for future work include:

- Detailed analysis of metal bioavailability associated with non-exhaust emissions and health risks and impacts
- Assessment of mitigation options for non-exhaust emissions' control (following Barratt et al., 2012, Amato et al., 2014b)

8.2 India

Detailed chemical characterization and mass closure of $PM_{2.5}$ in New Delhi has highlighted the influence of local (often undocumented) sources, particularly in the winter. Several health-relevant species are present in the ambient air in very high concentrations (e.g. Pb), and warrant further analysis. As a next step, a detailed CMB-based receptor modelling analysis will be undertaken to quantify source contributions using Indian profiles (Patil et al., 2013) and other locally-relevant profiles.

As a follow-up to the project in New Delhi, Indian Institute of Technology-Delhi (IIT-Delhi) is considering setting up a state-of-the-art facility for PM speciation and analysis. Several different agencies including the Delhi Pollution Control Committee (DPCC), Central Pollution Control Board (CPCB) and the Indian Institute of Tropical Meteorology (IITM) currently conduct online measurements in New Delhi at different sites. However, access to data is often restricted. Harmonization of sampling equipment, rigorous quality assurance and quality control (QA/QC) and a central data sharing facility will help contribute towards an improved understanding of the air quality in Delhi and improve researchers' access to the data and its usability.

Specific recommendations include:

- Continuous PM sampling and speciation to determine seasonal and annual trends
- Preparation of detailed emission inventories for PM and its constituents, particularly elements
- Inter-comparison of sampling equipment used by different agencies, and establishment of common protocols for sampling and data validation
- Assessment of relevant source markers, particularly for local sources (e.g. solid waste combustion)

REFERENCES

Aatmeeyata, Kaul, D.S. and Sharma, M. (2009) Traffic generated non-exhaust particulate emissions from concrete pavement: A mass and particle size study for two-wheelers and small cars. **Atmospheric Environment**, 43(35):5691-5697.

Aatmeeyata and Sharma, M. (2010) Polycyclic aromatic hydrocarbons, elemental and organic carbon emissions from tire-wear. **Science of the Total Environment**, 408(20): 4563-4568.

Abbasi, S., Olander, L., Larsson, C., Olofsson, U., Jansson, A. and Sellgren, U. (2011) A field test study of airborne wear particles from a running regional train. **Proceedings of the Institution of Mechanical Engineers, Part F: Journal of Rail and Rapid Transit**, 226: 95-109.

Abdalmogith, S.S. and Harrison, R.M. (2005) The use of trajectory cluster analysis to examine the long-range transport of secondary inorganic aerosol in the UK. **Atmospheric Environment**, 39: 6686-6695.

Abu-Allaban, M., Coulomb, W., Gertler, A.W., Gillies, J.A., Pierson, W.A., Rogers, C.F., Sagebiel, C. and Tarnay, L. (2002) Exhaust particle size distribution measurements at the Tuscacora Mountain Tunnel. **Aerosol Science and Technology**, 36: 771-789.

Abu-Allaban, M., Gillies, J.A., Gertler, A.W., Clayton, R. and Proffitt, D. (2003) Tailpipe, resuspended road dust, and brake wear emission factors from on-road vehicles. **Atmospheric Environment**, 37: 5283-5293.

Adachi, K., and Tainosho, Y. (2004) Characterization of heavy metal particles embedded in tire dust. **Environment International**, 30(8): 1009-1017.

Agarwal, T. (2009) Concentration level, pattern and toxic potential of PAHs in traffic soil of Delhi, India. **Journal of Hazardous Materials***,* 171: 894-900.

Allen, A.G., Nemitz, E., Shi, J.P., Harrison, R.M., and Greenwood, J.C. (2001) Size distributions of trace metals in atmospheric aerosols in the United Kingdom. **Atmospheric Environment**, 35(27): 4581-4591.

Allen, J.O., Alexandrova, O. and Kaloush, K.E. (2006) **Tire wear emissions for asphalt rubber and portland cement concrete pavement surfaces**. Report submitted to Arizona Department of Transportation (Contract KR-04-0720-TRN). Available at http://www.azdot.gov/docs/default-source/planning/dp.pdf?sfvrsn=2 [Accessed July 12, 2012].

Almeida, S.M., Pio, C.A., Freitas, M.C., Reis, M.A., and Trancoso, M.A. (2006) Source apportionment of atmospheric urban aerosol based on weekdays/weekend variability: evaluation of road re-suspended dust contribution. **Atmospheric Environment**, 40(11): 2058-2067.

Almeida, S.M., Canha, N., Freitas, M.C., Dung, H.M. and Dionisio, I. (2011) Air pollution at an urban traffic tunnel in Lisbon, Portugal- an INAA study. **Applied Radiation and Isotopes,** 69: 1586-1591.

Alves, C., Vicente, A., Pio, C., Kiss, G., Hoffer, A., Decesari, S., Prevot, A.S.H., Minguillon, M.C., Querol, X., Hillamo, R., Spindler, G. and Swietlicki, E. (2012) Organic compounds in aerosols from selected European sites- Biogenic versus anthropogenic sources. **Atmospheric Environment**, 59: 243-255.

Alves, C., Gomes, J., Nunes, T., Duarte, M., Calvo, A., Custodio, D., Pio, C., Karanasiou, A. and Querol, X. (2015) Size-segregated particulate matter and gaseous emissions from motor vehicles in a road tunnel. **Atmospheric Research**, 153: 134-144.

Amato, F., Pandolfi, M., Viana, M., Querol, X., Alastuey, A. and Moreno, T. (2009a) Spatial and chemical patterns of PM_{10} in road dust deposited in urban environment. **Atmospheric Environment**, 43(9): 1650-1659.

Amato, F., Pandolfi, M., Moreno, T., Furger, M., Pey, J., Alastuey, A., Bukowiecki, N., Prevot, A.S.H., Baltensperger, U. and Querol, X. (2011a) Sources and variability of inhalable road dust particles in three European cities. **Atmospheric Environment**, 45(37): 6777-6787.

Amato, F., Viana, M., Richard, A., Furger, M., Prévôt, A. S. H., Nava, S., Lucarelli, F., Bukowiecki, N., Alastuey, A., Reche, C., Moreno, T., Pandolfi, M., Pey, J. and Querol, X. (2011b) Size and time-resolved roadside enrichment of atmospheric particulate pollutants. **Atmospheric Chemistry and Physics**, 11(6): 2917-2931.

Amato, F., Karanasiou, A., Moreno, T., Alastuey, A., Orza, J.A.G., Lumbreras, J., Borge, R., Boldo, E., Linares. C. and Querol, X. (2012a) Emission factors from road dust resuspension in a Mediterranean freeway. **Atmospheric Environment**, 61: 580-587.

Amato, F., Karanasiou, A., Font, O., Moreno, N., Alastuey, A. and Querol, X. (2012b) Mineralogy and elemental composition of brake pads of common use in Spain. **Macla**, 16: 154-155.

Amato, F., Schaap, M., Denier van der Gon, H.A.C., Pandolfi, M., Alastuey, A., Keuken, M. and Querol, X. (2013a) Short-term variability of mineral dusts, metals and carbon emission from road dust resuspension. **Atmospheric Environment**, 74: 134-140.

Amato, F., Pandolfi, M., Alastuey, A., Lozano, A., Gonzalez, J.C. and Querol, X. (2013b) Impact of traffic intensity and pavement aggregate size on road dust particles loading. **Atmospheric Environment**, 77: 711-717.

Amato, F., Cassee, F.R., Denier van der Gon, H.A.C., Gehrig, R., Gustaffson, M., Hafner, W., Harrison, R.M., Jozwicka, M., Kelly, F.J., Moreno, T., Prevot, A.H., Schaap, M., Sunyer, J. and Querol, X. (2014a) Urban air quality: The challenge of non-exhaust traffic emissions. **Journal of Hazardous Materials**, 275: 31-36.

Amato, F., Karanasiou, A., Cordoba, P., Alastuey, A., Moreno, T., Lucarelli, F., Nava, S., Calzolai, G. and Querol, X. (2014b) Effects of road dust suppressants on PM levels in a Mediterranean urban area. **Environmental Science and Technology**, 48(14): 8069-8077.

Ancelet, T., Davy, P.K., Trompetter, W.J., Markwitz, A., and Weatherburn, D.C. (2011) Carbonaceous aerosols in an urban tunnel. **Atmospheric Environment**, 45(26): 4463-4469.

Apeagyei, E., Bank, M. S. and Spengler, J. D. (2011) Distribution of heavy metals in road dust along an urban-rural gradient in Massachusetts. **Atmospheric Environment**, 45(13): 2310-2323.

Ayres, J.G., Borm, P., Cassee, F.R., Castranova, V., Donaldson, K., Ghio, A., Harrison, R.M., Hider, R., Kelly, F., Ingeborg, M.K., Marano, F., Maynard, R.L., Mudway, I., Nel, A., Sioutas, C., Smith, S., Baeza-Squiban, A., Cho, A., Duggan, S. and Froines, J. (2008) Evaluating the toxicity of airborne particulate matter and nanoparticles by measuring oxidatve stress potential- a workshop report and consensus statement. **Inhalation Toxicology**, 20: 75-99.

Ault, A.P., Peters, T.M., Sawvel, E.J., Casuccio, G.S., Willis, R.D., Norris, G.A. and Grassian, V.H. (2012) Single-particle SEM-EDX analysis of iron-containing coarse particulate matter in an urban environment: sources and distribution of iron within Cleveland, Ohio. **Environmental Science and Technology**, 46: 4331-4339.

AQEG, 2012. **Fine Particulate Matter (PM$_{2.5}$) in the United Kingdom**. Air Quality Expert Group, Department for Environment, Food and Rural Affairs, London. Available at https://www.gov.uk/government/publications/fine-particulate-matter-pm2-5-in-the-uk [Accessed February 27, 2013].

Azzi, S. (salim.azzi@amey.co.uk) (18 September 2012). **Re: Air sampling in the Queensway road tunnel, Birmingham**. E-mail to P. Pant (pxp024@bham.ac.uk)

Bahreini, R., Middlebrook, A.M., de Gouw, J.A., Warneke, C., Trainer, M., Brock, C.A., Stark, H., Brown, S.S., Dube, W.P., Gilman, J.B., Hall, K., Holloway, J.S., Kuster, W.C., Perring, A.E., Prevot, A.S.H., Schwarz, J.P., Spackman, J.R., Szidat, S., Wagner, N.L., Weber, R.J., Zotter, P., Parrish, D.D. (2012) Gasoline emissions dominate over diesel in formation of secondary organic aerosol mass. **Geophysical Research Letters**, 39, L06805, doi: 10.1029/2011GL050718.

Balachandran, S., Meena, B.R. and Khillare, P.K. (2000) Particle size distribution and its elemental composition in the ambient air of Delhi. **Environment International**, 26: 49-54.

Bardelli, F., Cattaruzza, E., Gonella, F., Rampazzo, G. and Valotto, G. (2011) Characterization of road dust collected in *Traforo del San Bernardo* highway tunnel: Fe and Mn speciation. **Atmospheric Environment**, 45: 6459-6468.

Barratt, B., Carslaw, D., Fuller, G., Green, D. and Tremper, A. (2012) **Evaluation of the impact of dust suppressant application on ambient PM_{10} concentrations in London**. Prepared for Transport for London under contract to URS Infrastructure & Environment Ltd. Available at http://www.tfl.gov.uk/cdn/static/cms/documents/evaluation-dust-suppressants-pmconcentrations.pdf [Accessed February 15, 2013].

Bauer, H., Claeys, M., Vermeylen, R., Schueller, E., Weinke, G., Berger, A. and Puxbaum, H. (2008) Arabitol and mannitol as tracers for the quantification of airborne fungal spores. **Atmospheric Environment**, 42: 588-593.

Baxla, S.P., Roy, A.A., Gupta, T., Tripathi, S.N., Bandyopadhyaya, R. (2009) Analysis of diurnal and seasonal variation of submicron outdoor aerosol mass and size distribution in a Northern Indian city and its correlation to black carbon. **Aerosol and Air Quality Research**, 9: 458-469.

Beddows, D.C.S., Dall'Osto, M., Harrison, R.M. (2009) Cluster analysis of rural, urban and curbside atmospheric particle size data. **Environmental Science and Technology**, 43: 4694-4700.

Begum, B.A., Kim, E., Biswas, S.K. and Hopke, P.K. (2004) Investigation of sources of atmospheric aerosol at urban and semi-urban areas in Bangladesh. **Atmospheric Environment**, 38: 3025-3038.

Begum, B.A., Biswas, S.K. and Hopke, P.K. (2011) Key issues in controlling air pollutants in Dhaka, Bangladesh. **Atmospheric Environment***,* 45: 7705-7713.

Belis, C.A., Karagulian, F., Larsen, B.R. and Hopke, P. K. (2013) Critical review and meta-analysis of ambient particulate matter source apportionment using receptor models in Europe. **Atmospheric Environment**, 69: 94-108.

Bell, M.L. (2012) **Assessment of the health impacts of partiuculate matter characteristics**. HEI Research Report 161. Health Effects Institute, Boston, MA.

Benbrahim-Tallaa, L., Baan, R.A., Gross, Y., Lauby-Secretan, B., El Ghissaddi, F., Bouvard, V., Guha, N., Loomis, D. and Straif, K. (2012) Carcinogenicity of diesel-engine and gasoline-engien exhausts and some nitroarenes. **The Lancet Oncology**, 13(7): 663-664.

Berger, J. and Denby, B. (2011) A generalized model for traffic induced road dust emissions. Model description and evaluation. **Atmospheric Environment**, 45: 3692-3703.

Bhaskar, V.S. and Sharma, M. (2008) Assessment of fugitive road dust emissions in Kanpur, India. **Transportation Research Part D**, 13: 400-403.

Bi, X., Feng, Y., Wu, J., Wang, Y. and Zhu, T. (2007) Source apportionment of PM_{10} in six cities of Northern China. **Atmospheric Environment**, 41: 903-912.

Bigi, A. and Harrison, R.M. (2010) Analysis of the air pollution climate at a central urban background site. **Atmospheric Environment**, 44: 2004-2012.

Birmili, W., Allen, A.G., Bary, F., and Harrison, R.M. (2006) Trace metal concentrations and water solubility in size-fractionated atmospheric particles and influence of road traffic. **Environmental Science and Technology**, 40(4): 1144-1153.

Blau, P.J. and Meyer, H.M. III (2003) Characteristics of wear particles produced during friction tests of conventional and unconventional disc brake materials. **Wear**, 255: 1261-1269.

Boogaard, H., Kos, G.P.A., Weijers, E.P., Janssen, N.A.H., Fischer, P.H., van der Zee, S.C., de Hartog, J.J. and Hoek, G. (2011) Contrast in air pollution components between major streets and background locations: Particulate matter mass, black carbon, elemental composition, nitrogen oxide and ultrafine particle number. **Atmospheric Environment**, 45(3): 650-658.

Boonyatumanond, R., Murakami, M., Wattayakorn, G. Togo, A. and Takeda, H. (2007) Sources of polycyclic aromatic hydrocarbons (PAHs) in street dust in a tropical Asian mega-city, Bangkok, Thailand. **Science of the Total Environment**, 384: 420-432.

Boulter, P.G., Thorpe, A.J., Harrison, R.M. and Allen, A.G. (2005) **Road vehicle non-exhaust particulate matter: Final report on emission modelling**. Published Project Report PPR110. Available at http://uk-air.defra.gov.uk/reports/cat15/0706061624_Report2__Emission_modelling.PDF [Accessed 10 July 2012].

Brook, J.R., Graham, L., Charland, J.P., Cheng, Y., Fan, X., Lu, G., Li, S.M., Lillyman, C., MacDonald, P., Caravaggio, G. and MacPhee, J.A. (2007) Investigation of the motor vehicle exhaust contribution to primary fine particle organic carbon in urban air. **Atmospheric Environment**, 41(1): 119-135.

Brito, J., Rizzo, L.V., Herckes, P., Vasconcellos, P.C., Caumo, S.E.S., Fornaro, A., Ynoue, R.Y., Artaxo, P. and Andrade, M.F. (2013) Physical-chemical characterization of the particulate matter inside two road tunnels in the Sao Paulo Metropolitan Area. **Atmospheric Chemistry and Physics**, 13: 12199-12213.

Brunekreef, B., Beelen, R., Hoek, G., Schouten, L., Bausch-Goldbohm, S., Fischer, P., Armstrong, B., Hughes, E., Jerrett, M. and van den Brandt, P. (2009) **Effects of long-term exposure to traffic-related air pollution on respiratory and cardiovascular mortality in the Netherlands: the NLCS- AIR study**. HEI Research Report 139, Health Effects Institute, Boston, MA .

Bullock, K.R., Duvall, R.M., Norris, G.A., McDow, S.R. and Hays, M.D. (2008) Evaluation of the CMB and PMF models using organic molecular markers in fine particulate matter collected during the Pittsburgh Air Quality Study. **Atmospheric Environment**, 42: 6897-6904.

Bukowiecki, N., Lienemann, P., Hill, M., Furger, M., Richard, A., Amato, F., Prevot, A.S.H., Baltensperger, U., Buchmann, B. and Gehrig, R. (2010) PM_{10} emission factors for non-exhaust particles generated by road traffic in an urban street canyon and along a freeway in Switzerland. **Atmospheric Environment**, 44(19): 2330-2340.

Caceres, D., Adonis, M., Gil, L., and Miguel, A.H. (1998) Exhaust PAH in Chilean vehicles: Levels, source signatures and receptor modeling. **Journal of Aerosol Science**, 29, Supplement 2(0), S741-S742.

Calvo, A.I., Alves, C., Castro, A., Pont, V., Vicente, A.M. and Fraile, R. (2013) Research on aerosol sources and chemical composition: Past, current and emerging issues. **Atmospheric Research**, 120-121: 1-28.

Camatani, M., Crosta, G.F., Dolukhanyan, T., Sung, C., Giuliani, G., Corbetta, G. M., Cencetti, S. and Regazzoni, C. (2001) Microcharacterization and identification of tire debris in heterogenous laboratory and environmental specimens. **Materials Characterization**, 46: 271-283.

Canepari, S., Perrino, C., Olivieri, F., and Astolfi, M.L. (2008) Characterisation of the traffic sources of PM through size-segregated sampling, sequential leaching and ICP analysis. **Atmospheric Environment**, 42(35): 8161-8175.

Cass, G. R. (1998) Organic molecular tracers for particulate air pollution sources. **Trends in Analytical Chemistry**, 17(6): 356-366.

Castro, L.M., Pio, C.A., Harrison, R.M. and Smith, D.J.T. (1999) Carbonaceous aerosol in urban and rural European atmospheres: estimation of secondary organic carbon concentrations. **Atmospheric Environment**, 33: 2771-2781.

Cavalli, F., Viana, M., Yttri, K.E., Genberg, J. and Putuad, J.-P. (2010) Towards a standardized thermal-optical protocol for measuring atmospheric organic and elemental carbon: the EUSAAR protocol. **Atmospheric Measurement Techniques,** 3: 79-89.

Chakrobarty, A. and Gupta, T. (2010) Chemical characterization of submicron aerosol in Kanpur region: a source apportionment study. **Aerosol and Air Quality Research**, 10: 433-445.

Chakrobarty, R.K., Pervez, S., Chow, J.C., Watson, J.G., Dewangan, S., Robles, J. and Tian, G. (2013) Funeral pyres in South Asia: Brown carbon aerosol emissions and climate impacts. **Environmental Science and Technology Letters**, 1(1): 44-48.

Chan, D. and Stachowiak, G.W. (2004) Review of automotive brake friction materials. Proceedings of the Institution of Mechanical Engineers, Part D: **Journal of Automobile Engineering**, 218 (9): 953-966.

Chan, Y.C., Simpson, R.W., Mctainsh, G.H., Vowles, P.D., Cohen, D.D. and Bailey, G.M. (1997) Characterisation of chemical species in $PM_{2.5}$ and PM_{10} aerosols in Brisbane, Australia. **Atmospheric Environment**, 31(22): 3773- 3785.

Charron, A. and Harrison, R.M. (2003) Primary particle formation from vehicle emissions during exhaust dilution in the roadside atmosphere. **Atmospheric Environment**, 37: 4109-4119.

Charron, A., Degrendele, C., Laongsri, B. and Harrison, R.M. (2013) Receptor modelling of secondary and carbonaceous particulate matter at a southern UK site. **Atmospheric Chemistry and Physics**, 13: 1879-1894.

Chellam, S., Kulkarni, P. and Fraser, M.P. (2005) Emissions of organic compounds and trace metals in fine particulate matter from motor vehicles: a tunnel study in Houston, Texas. **Journal of Air and Waste Management Association**, 55: 60-72.

Chelani, A.B., Gajghate, D.G. and Devotta, S., (2008) Source apportionment of PM_{10} in Mumbai, India using CMB model. **Bulletin of Environmental Contamination and Toxicology**, 81: 190-195.

Chelani, A.B., Gajghate, D.G., Chalapati Rao, CV., Devotta, S. (2010) Particle size distribution in ambient air of Delhi and its statistical analysis. **Bulletin of Environmental Contamination and Toxicology**, 85 (1): 22-27.

Chen, J., Zheng, H., Wang, W., Liu, H., Lu, L., Bao, L. and Ren, L. (2006) Resuspension method for road surface dust collection and aerodynamic size distribution characterization. **China Particuology**, 4(6): 300-303.

Chen, L.W.A., Watson, J.G., Chow, J.C., DuBois, D.W. and Herschberger, L. (2011) $PM_{2.5}$ source apportionment: Reconciling receptor models for U.S. nonurban and urban long-term networks**. Journal of Air and Waste Management Association**, 61(11): 1204-1217.

Chen, J., Wang, W., Liu, H. and Ren, L. (2012) Determination of road dust loadings and chemical characteristics using resuspension. **Environmental Monitoring and Assessment***,* 184: 1693-1709.

Chen, F., Hu, W. and Zhong, Q. (2013) Emissions of particle-phase polycyclic aromatic hydrocarbons (PAHs) in the Fu Gui-Shan Tunnel of Nanjing, China. **Atmospheric Research**, 124: 53-60.

Cheng, H., Deng, Z., Chakraborty, P., Liu, D., Zhang, R., Xu, Y., Luo, C., Zhang, G. and Li, J. (2013) A comparison study of atmospheric polycyclic aromatic hydrocarbons in three Indian cities using PUF disk passive air samplers. **Atmospheric Environment**, 73: 16-21.

Chow, J.C., Bachmann, J.D., Wierman, S.S.G., Mathai, C.V., Malm, W.C., White, W.H., Mueller, P.K., Kumar, N. and Watson, J.G. (2002) Visibility: Science and Regulation. **Journal of Air and Waste Management Association**, 52(9): 973-999.

Chow, J.C., Watson, J.G., Ashbaugh, L.L. and Magliano, K.L. (2003) Similarities and differences in PM_{10} chemcial source profiles for geological dust from the San Joaquin Valley, California. **Atmospheric Environment**, 37: 1317-1340.

Chow, J.C., Watson, J.G., Kuhns, H., Etyemezian, V., Lowenthal, D.H., Crow, D., Kohl, S.D., Engelbrecht, J.P. and Green, M.C. (2004) Source profiles for industrial, mobile and area sources in the Big Bend Regional Aerosol Visibility and Observational Study**. Chemosphere**, 54: 185-208.

Chow, J.C., Watson, Antony Chen, L.-W., Arnott, W.P. and Moosmüller, H. (2004) Equivalence of elemental carbon by thermal/optical reflectance and transmittance with different temperature protocols**. Environmental Science and Technology**, 38: 4414-4422.

Chow, J.C., Watson, J.G., Lowenthal, D.H., Chen, L.W.A., Zielinska, B., Mazzoleni, L.R. and Magliano, K.L. (2007a) Evaluation of organic markers for chemical mass balance source apportionment at the Fresno Supersite. **Atmospheric Chemistry and Physics**, 7: 1741-1754.

Chow, J.C., Watson, J.G., Chen, L.W.A., Oliver Chang, M.C., Robinson, N.F., Trimble, D. and Kohl, S. (2007b) The IMPROVE_A temperature protocol for thermal/optical carbon analysis: mainitaining consistency with a long-term database. **Atmospheric Environment Part A: General Topics** 27(8): 1185-1201.

Chow, J.C. and Watson, J.G. (2012) Chemical analyses of particle filter deposits. In **Aerosols Handbook: Measurement, Dosimetry, and Health Effects**, 2; Ruzer, L., Harley, N. H., Eds.; CRC Press/Taylor & Francis: New York, NY, 179-204.

Chowdhury, Z., Zheng, M., Schauer, J.J., Sheesley, R.J., Salmon, L.G., Cass, G.R., Russell, A.G. (2007) Speciation of fine organic carbon particles and source apportionment of $PM_{2.5}$ in Indian cities. **Journal of Geophysical Research**, 112, D15303, doi:10.1029/2007JD008386.

Clements, N., Eav, J., Xie, M., Hannigan, M.P., Miller, S.L., Navidi, W., Peel, J.L., Schauer, J.J., Shafer, M.M. and Milford, J.B. (2014) Concentrations and source insights for trace elements in fine and coarse particulate matter. **Atmospheric Environment**, 89: 373-381.

Colbeck, Ian. and Lazardis, M. (2010) Aerosols and environmental pollution. **Naturwissenschaften**, 97: 117-131.

Colville, R.N., Hutchinson, E.J., Mindell, J.S. and Warren, R.F. (2001) The transport sector as a source of air pollution. **Atmospheric Environment**, 35: 1537-1565.

Cooper, J.A. and Watson, J.G. (1980) Receptor oriented methods of air particulate source apportionment. **Journal of Air Pollution Control Association**, 30 (10): 1116-1125.

Councell, T.B., Duckenfield, K.U., Landa, E.R. and Callender, E. (2004) Tire wear particles as a source of Zn to the environment. **Environmental Science and Technology**, 38(15): 4206-4214.

CPCB (2010). **Air quality monitoring, emission inventory and source apportionment study for Indian cities**. Central Pollution Control Board, February 2010. Available at http://www.cpcb.nic.in/Source_Apportionment_Studies.php [Accessed 28 February 2011].

Cusack, M., Perez, N., Pey, J., Alastuey, A. and Querol, X. (2013) Source apportionment of fine PM and sub-micron particle number concentrations at a regional background site in the western Mediterranean: a 2.5 year study. **Atmospheric Chemistry and Physics**, 13: 5173-5187.

Daher, N., Ruprecht, A., Invernizzi, G., De Marco, C., Miller-Schulze, J., Heo, J.B., Shafer, M.M., Shelton, B.R., Schauer, J.J. and Sioutas, C. (2012) Characterization, sources and redox activity of fine and coarse particulate matter in Milan, Italy. **Atmospheric Environment**, 49: 130-141.

Dahl, A., Gharibi, A., Swietlicki, E., Gudmundsson, A., Bohgard, M., Ljungman, A., Blomqvist, G. and Gustafsson, M. (2006) Traffic-generated emissions of ultrafine particles from pavement–tire interface. **Atmospheric Environment**, 40(7): 1314-1323.

Dall'Osto, M., Beddows, D.C.S, Gietl, J.K., Olatunbosun, O.A., Yang, X. and Harrison R.M. (2014) Characteristics of tyre dust in polluted air: studies by single particle mass spectrometry (ATOFMS). **Atmospheric Environment**, 94: 224-230.

Davy, P.K., Gunchin, G., Markwitz, A., Trompetter, W.J., Barry, B.J., Shagjjamba, D. and Lodoysamba, S. (2011) Air particulate matter pollution in Ulaanbaatar, Mongolia: determination of composition, source contributions and source locations. **Atmospheric Pollution Research**, 2: 126-137.

de Kok, T.M.C.M., Driece, H.A.L., Hogervorst, J.G.F. and Briede, J.J (2006) Toxicological assessment of ambient and traffic-related particulate matter: A review of recent studies. **Mutation Research**, 613: 103-122.

Delhi Police (2014) Restriction on the movement of LGV and HGV/MGV vehicles. Available at http://www.delhitrafficpolice.nic.in/restri-lgv-hgv.aspx [Accessed on February 08, 2014].

Delhi Statistical Handbook (2013) Available at http://www.delhi.gov.in/wps/wcm/connect/doit_des/DES/Our+Services/Statistical+Hand+Book/ [Accessed February 20, 2014].

Deka, P. and Hoque, R.R. (2014) Incremental effect of festive biomass burning on wintertime PM_{10} in Brahmaputra Valley of Northeast India. **Atmospheric Research**, 143: 380-391.

Denier van der Gon, H., Gerlofs-Nijland, M.E., Gehrig, R., Gustafsson, M., Janssen, N., Harrison, R.M., Hulskotte, J., Johansson, C., Jozwicka, M., Keuken, M., Krijgsheld, K., Ntziachristos, L., Riediker, M. and Cassee, F.R. (2013) The Policy Relevance of Wear Emissions from Road Transport, Now and in the Future- An International Workshop Report and Consensus Statement. **Journal of the Air and Waste Management Association**, 63(2): 136-149.

Department for Transport (2013) **Department for Transport Statistics 2012**. Available at http://www.dft.gov.uk/statistics/series/traffic/ [Accessed on 12 September 2013].

Department for Transport (2014) **Traffic Counts Birmingham**. Accessed at http://www.dft.gov.uk/traffic-counts/cp.php?la=Birmingham#81577.

Derwent, R.G. and Malcolm, A.L. (2000) Photochemical generation of secondary particles in the United Kingdom. **Philosophical Transactions of the Royal Society A**, 358 (1775): 2643-2657.

Deshmukh, D.K., Deb, M.K. and Mkoma, S.L. (2012) Size distribution and seasonal variation of size-segregated particulate matter in the ambient air of Raipur city, India. **Air Quality, Atmosphere and Health**, 6: 259-276.

Docherty, K.S., Stone, E.A., Ulbrich, I.M., DeCarlo, P.F., Snyder, D.C., Schauer, J.J., Peltier, R. E., Weber, R.J., Murphy, S.M., Seinfeld, J.H., Grover, B.T., Eatough, D.J. and Jimenez J.L. (2008) Apportionment of Primary and Secondary Organic Aerosols in Southern California during the 2005 Study of Organic Aerosols in Riverside (SOAR-1). **Environmental Science and Technology**, 42 (20): 7655-7662.

Donahue, N.M., Robinson, A.L. and Pandis, S.N. (2009) Atmospheric organic particulate matter: From smoke to secondary organic aerosol. **Atmospheric Environment**, 43: 94-106.

Dongarra, G., Manno, E. and Varrica, D. (2009) Possible markers of traffic-related emissions. **Environmental Monitoring and Assessment**, 154 (1-4): 117-125.

Duong, T. T. and Lee, B. K. (2011) Determining contamination level of heavy metals in road dust from busy traffic areas with different characteristics. **Journal of Environmental Management**, 92(3): 554-562.

Dutton, S.J., Williams, D.E., Garcia, J.K., Vedal, S. and Hannigan, M.P. (2009) $PM_{2.5}$ Characterization for Time Series Studies: Organic Molecular Marker Speciation Methods and Observations from Daily Measurements in Denver. **Atmospheric Environment**, 43(12): 2018-2030.

Duvall, R.M., Norris, G.A., Burke, J.M., Olson, D.A., Vedantham, R. and Williams, R. (2012) Determining spatial variability in $PM_{2.5}$ source impacts across Detroit, MI. **Atmospheric Environment**, 47: 491-498.

El Haddad, I., Marchand, N., Dron, J., Temime-Roussel, B., Quivet, E., Wortham, H., Jaffrezo, J.L., Baduel, C., Voisin, D., Besombes, J.L. and Gille, G. (2009) Comprehensive primary particulate organic characterization of vehicular exhaust emissions in France. **Atmospheric Environment**, 43(39): 6190-6198.

El Haddad, I., Marchand, N., Wortham, H., Piot, C., Besombes, J.-L., Cozic, J., Chauvel, C., Armengaud, A., Robin, D. and Jaffrezo, J.-L. (2011) Primary sources of $PM_{2.5}$ organic aerosol in an industrial Mediterranean city, Marseille. **Atmospheric Chemistry and Physics**, 11: 2039- 2058.

El-Fadel, M. and Hashisho, Z. (2000) Vehicular emissions and air quality assessment in roadway tunnels: the Salim Slam tunnel. **Transportation Research Part D**, 5: 355-372.

Enviro Technology Services plc.(n.d.) Digitel DHA-80- High volume aerosol sampler (HVS). Available at http://www.et.co.uk/docs/Digitel%20DHA-80%20Product%20Datasheet.pdf [Accessed 12 July 2012].

Ernest Raj, P., Maheshkumar, R.S., Devara, P.C.S., Sonbawne, S.M., Saha, S.K. and Dani, K.K.(2002) Aerosol Size distributions and their temporal variations in relation to urban activity. **Indian Journal of Radio and Space Physics**, 31: 140-150.

Essumang, D.K., Dodoo, D.K., Obiri, S. and Oduro, A.K. (2006) Analysis of polycyclic aromatic hydrocarbons in street soil dust in Kumasi metropolis of Ghana. **Environmental Monitoring and Assessment**, 121: 401-408.

Etyemezian, V., Kuhns, H., Gillies, J., Chow, J., Hendrickson, K., McGown, M. and Pitchford, M. (2003) Vehicle-based road dust emissions measurement (III): effect of speed, traffic volume, location, and season on PM_{10} road dust emissions in the Treasure Valley, ID. **Atmospheric Environment**, 37: 4583-4593.

Fang, G.-C., Chang, C.-N., Wu, Y.-S., Fu, P.P.-C., Yang, I.-L. and Chen, M.-S. (2004) Characterization, identification of ambient air and road dust polycyclic aromatic hydrocarbons in central Taiwan, Taichung. **Science of the Total Environment**, 327: 135-146.

Fabretti, J.-F., Sauret, N., Gal, J.-F., Maria, P.-C. and Schärer, U. (2009) Elemental characterization and source identification of $PM_{2.5}$ using Positive Matrix Factorization: The Malraux road tunnel, Nice, France. **Atmospheric Research**, 94(2): 320-329.

Faiz, Y., Tufail, M., Javed, M.T., Chaudry, M.M. and Siddique, N. (2009) Road dust pollution of Cd, Cu, Ni, Pb and Zn along Islamabad Expressway, Pakistan. **Microchemical Journal***,* 92: 186-192.

Farao, C., Canepari, S., Perrino, C. and Harrison, R.M. (2014) Sources of PM in an industrial area: comparison between receptor model results and semiempirical calculations of source contributions. **Aerosol and Air Quality Research**, doi: 10.4209/aaqr.201308.0281.

Fernandes, M.B., Skjemstad, J.O., Johnson, B.B., Wells, J.D. and Brooks, P. (2000) Characterization of carbonaceous combustion residues. I. Morphological, elemental and spectroscopic features. **Chemosphere**, 51: 785-795.

Fine, P.M., Cass, G.R. and Simoneit, B.R.T. (2001) Chemical characterization of fine particle emissions from fireplace combustion of woods grown in the northeastern United States. **Environmental Science and Technology**, 35(13): 2665-2675.

Fine, P.M., Cass, G.R. and Simoneit, B.R.T. (2004) Chemical characterization of fine particle emissions from the wood stove combustion of prevalent United States tree species. **Environmental Engineering Science**, 21(3): 705-721.

Fine, P.M, Sioutas, C. and Solomon, P.A. (2008) Secondary particulate matter in the United States: Insights from the particulate matter supersites program and related studies. **Journal of Air and Waste Management Association**, 58(2): 234-253.

Franco, V., Kousoulidou, M., Muntean, M., Ntziachristos, L., Hausberger, S. and Dilara, P. (2013) Road vehicle emission factors development: a review. **Atmospheric Environment**, 70: 84-97.

Fraser, M.P., Cass, G.R. and Simoneit, B.R. (1998) Gas-phase and particle-phase organic compounds emitted from motor vehicle traffic in a Los Angeles Roadway Tunnel. **Environmental Science and Technology**, 32: 2051-2060.

Friedlander, S.K. (1973) Chemical element balances and identification of air pollution sources. **Environmental Science and Technology**, 7(3): 235-240.

Fu, P.Q., Kawamura, K., Pavuluri, C.M., Swaminathan, T. and Chen, J. (2010) Molecular characterization of urban organic aerosol in tropical India: contributions of primary emissions and secondary photooxidation. **Atmospheric Chemistry and Physics**, 10: 2663-2689.

Fujita, E.M., Campbell, D.E. and Zielinska, B. (2006) **Chemical analysis of lubrication oil samples from a study to characterize exhaust emissions from light-duty gasoline vehicles in the Kansas City metropolitan area**. CRC Report 69 (Final Report). Available at http://www.crcao.org/publications/emissions/ [Accessed 24 August 2013].

Fujita, E.M., Campbell, D.E., Arnott, W.P., Chow, J.C. and Zielinska, B. (2007) Evaluations of the chemical mass balance method for determining contributions of gasoline and diesel exhaust to ambient carbonaceous aerosols. **Journal of Air and Waste Management Association**, 57: 721-740.

Fulper, C.R., Kishan, S., Baldauf, R.W., Sabisch, R., Warila, J., Fujita, E.M., Scarbro, C., Crews, W.S., Snow, R., Gabele, P., Sanots, R., Tierney, E. and Cantrell, B. (2010) Methods of characterizing the distribution of exhaust emissions from light-duty, gasoline-powered motor vehicles in the U.S. fleet. **Journal of Air and Waste Management Association**, 60: 1376-1387.

Fuller, G.W., Tremper, A.H., Baker, T.D., Yttri, K.S. and Butterfield, D. (2014) Contribution of wood burning to PM_{10} in London. **Atmospheric Environment**, 87: 87-94.

Funasaka, K., Miyazaki, T., Kawaraya, T., Tsuruho, K. and Mizuno, T. (1998) Characteristics of particulates and gaseous pollutants in a highway tunnel. **Environmental Pollution**, 102(2–3): 171-176.

Fujiwara, F.G., Gomez, D.R., Dawidowski, L., Perelman, P. and Faggi, A. (2011) Metals associated with airborne particulate matter in road dust and tree bark collected in a megacity (Buenos Aires, Argentina). **Ecological Indicators**, 11: 240-247.

Galatioto, F. and Bell, M.C. (2013) Exploring the processes governing roadside pollutant concentrations in urban street canyon. **Environmental Science and Pollution Research**, 20(7): 4750-4765.

Gao, B., Yu, J.-Z., Li, S.-X., Ding, X., He, Q.-F. and Wang, X.-M. (2011) Roadside and rooftop measurements of polycyclic aromatic hydrocarbons in PM2.5 in urban Guangzhou: Evaluation of vehicular and regional combustion source contributions. **Atmospheric Environment**, 45(39): 7184-7191.

Garg, B.D., Cadle, S.H., Mulawa, P.A., Groblicki, P.J., Laroo, C. and Parr, G.A. (2000) Brake wear particulate matter emissions. **Environmental Science and Technology**, 34(21): 4463-4469.

Gargava, P., Chow, J.C., Watson, J.G. and Lowenthal, D.H. (2014) Speciated PM_{10} emission inventory for Delhi, India. **Aerosol and Air Quality Research**, 14: 1515-1526.

Gehrig, R., Hill, M., Buchmann, B., Imhof, D., Weingartner, E. and Baltensperger, U. (2004) Separate determination of PM_{10} emission factors of road traffic for tailpipe emissions and emissions from abrasion and resuspension processes. **International Journal of Environment and Pollution**, 22(3): 312-325.

Gertler, A.W. and Pierson, W.R. (1996) Recent measurements of mobile source emission factors in North American Tunnels. **Science of the Total Environment**, 189/190: 107-116.

Gertler, A.W., Gillies, J.A., Pierson, W.R., Rogers, C.F., Sagebiel, J.C., Abu-Allaban, M., Coulombe, W., Tarnay, L. and Cahill, T.A. (2002) **Real-World Particulate Matter and Gaseous Emissions from Motor Vehicles in a Highway Tunnel**. Research Report 107. Health Effects Institute, Boston, MA.

Gertler, A., Kuhns, H., Abu-Allaban, M., Damm, C., Gilies, J., Etyemezian, V., Clayton, R. and Proffitt, D. (2006) A case study of the impact of winter road sand/salt and street sweeping on road dust re-entrainment. **Atmospheric Environment**, 40: 5976-5985.

Giechaskiel, B., Maricq, M., Ntziachristos, L., Dardiotis, C., Wang, X., Axmann, H., Bergmann, A. and Schindler, W. (2014) Review of motor vehicle particulate emissions sampling and measurement: From smoke and filter mass to particle number. **Journal of Aerosol Science**, 67: 48-86.

Gietl, J.K., Lawrence, R., Thorpe, A.J. and Harrison, R.M. (2010) Identification of brake wear particles and derivation of a quantitative tracer for brake dust at a major road. **Atmospheric Environment**, 44(2): 141-146.

Giri, B., Patel, K.S., Jaiswal, N.K., Sharma, S., Ambade, B., Wang, W., Simonich, S.L.M., Simoneit, B.R.T. (2013) Composition and sources of organic tracers in aerosol particles of industrial central India. **Atmospheric Research**, 120-121: 312-324.

Godri, K.J., Harrison, R.M., Evans, T., Baker, T., Dunster, C., Mudway, I.S. and Kelly, F.J. (2011) Increased oxidative burden associated with traffic component of ambient particulate matter at roadside and urban background school sites in London. **PloS ONE**, 6(7), e21961, doi:10.1371/journal.pone.0021961.

Goel, R. (rahulatiid@gmail.com) (12 February 2014). **Re: Query**. E-mail to P. Pant (pxp024@bham.ac.uk)

Gordon, G.E. (1980) Receptor Models. **Environmental Science and Technology** 14: 792-800.

Gordon, G.E. (1988) Receptor Models. **Environmental Science and Technology**, 22: 1132-1142.

Goyal, P., Jaiswal, N., Kumar A., Dadoo, J.K. and Dwarakanath, M. (2010) Air quality impact assessment of NOx and PM due to diesel vehicles in India. **Transportation Research Part D**, 15: 298-303.

Green, M.C., Chow, J.C., Oliver Chang, M.-C., Chen, L.W.A., Kuhns, H.D, Etyemezian, V.R. and Watson, J.G. (2013) Source apportionment of atmospheric particulate carbon in Las Vegas, Nevada, USA. **Particuology**, 11: 110-118.

Grieshop, A.P., Lipsky, E. M., Pekney, N.J., Takahama, S. and Robinson, A.L. (2006) Fine particle emission factors from vehicles in a highway tunnel: Effects of fleet composition and season. **Atmospheric Environment**, 40: 287-298.

Gu, J., Pitz, M., Schenlle-Kreis, J., Diemer, J., Reller, A., Zimmermann, R., Soentgen, J., Stoelzel, M., Wichmann, H.E., Peters, A. and Cyrys, J. (2011) Source apportionment of ambient particles: Comparison of positive matrix factorization analysis applied to particle size distribution and chemical composition data. **Atmospheric Environment**, 45: 1849-1857.

Gummeneni, S., Yusup, Y.B., Chavali, M. and Samadi, S.Z. (2011) Source apportionment of particulate matter in the ambient air of Hyderabad city, India. **Atmospheric Research**, 101(3): 752-764.

Gunawardana, C., Goonetilleke, A., Egodawatta, P., Dawes, L. and Kokot, S. (2011) Source characterisation of road dust based on chemical and mineralogical composition. **Chemosphere**, 87(2): 163-170.

Guo, H., Ding, A.J., So, K.L., Ayoko, G., Li, Y.S. and Hung, W.T. (2009) Receptor modelling of source apportionment of Hong Kong aerosols and the implication of urban and regional contribution. **Atmospheric Environment**, 43: 1159-1169.

Guo, S., Hu, M., Guo, Q., Zhang, X., Zhang, M., Zheng, J., Chang, C.C., Schauer, J.J. and Zhang, R., (2012) Primary Sources and Secondary Formation of Organic Aerosols in Beijing, China. **Environmental Science and Technology**, 46: 9846-9853.

Gupta, A.K., Karar, K. and Srivastava, A. (2007) Chemical mass balance source apportionment of PM_{10} and TSP in residential and industrial sites of an urban region of Kolkata, India. **Journal of Hazardous Materials**, 142: 279-287.

Gustafsson, M., Blomqvist, G., Gudmundsson, A., Dahl, A., Swietlicki, E., Bohgard, M., Lindbom, J. and Ljungman, A. (2008) Properties and toxicological effects of particles from the interaction between tyres, road pavement and winter traction material. **Science of the Total Environment**, 393(2-3): 226-240.

Gustafsson, M., Blomqvist, A., Gudmundsson, A., Dahl, A., Jonsson, P. and Swietlicki, E. (2009) Factors influencing PM_{10} emissions from road pavement wear. **Atmospheric Environment**, 49: 226-240.

Guttikunda, S.K. and Gurjar, B. R. (2012) Role of meteorology in seasonality of air pollution in megacity Delhi, India. **Environmental Monitoring and Assessment**, 184(5): 3199-3211.

Guttikunda, S., Kopakka, R.V., Dasari, P. and Gertler, A.W. (2013) Receptor model-based source apportionment of particulate pollution in Hyderabad, India. **Environmental Monitoring and Assessment**, 185: 5585-5593.

Guttikunda, S. and Goel, R. (2013) Health impacts of particulate pollution in a megacity- Delhi, India. **Environmental Development**, 6: 8-20.

Guttikunda, S. and Calori, G. (2013) A GIS based emissions inventory at 1 km x 1 km spatial resolution for air pollution analysis in Delhi, India. **Atmospheric Environment**, 67: 101-111.

Han, L., Zhuang, G., Cheng, S., Wang, Y. and Li, J. (2007) Characteristics of re-suspended road dust and its impact on the atmospheric environment in Beijing. **Atmospheric Environment**, 41(35): 7485-7499.

Han, B., Bai, Z., Guo, G., Wang, F., Li, F., Liu, Q., Ji, Y., Li, X. and Hu, Y. (2009): Characterization of PM(10) fraction of road dust for polycyclic aromatic hydrocarbons (PAHs) from Anshan, China. **Journal of Hazardous Materials**, 170(2-3), 934-940.

Han, S., Youn, J.-S. and Jung, Y.-W. (2011) Characterization of PM_{10} and $PM_{2.5}$ source profiles for resuspended road dust collected using mobile sampling methodology. **Atmospheric Environment**, 45: 3343-3351.

Handler, M., Puls, C., Zbiral, J., Marr, I., Puxbaum, H. and Limbeck, A. (2008) Size and composition of particulate emissions from motor vehicles in the Kaisermühlen-Tunnel, Vienna. **Atmospheric Environment**, 42: 2173-2186.

Hanedar, A., Alp, K., Kaynak, B., Baek, J., Avsar, E. and Odman, M.T. (2008) Concentrations and sources of PAHs at three stations in Istanbul, Turkey. **Atmospheric Research**, 99: 391-399.

Harrad, S., Hassoun, S., Romero, M.S.C. and Harrison, R.M. (2003) Characterisation and source attribution of the semi-volatile organic content of atmospheric particles and associated vapour phase in Birmingham, U.K.. **Atmospheric Environment**, 37: 4985-4991.

Harrison, R.M., Smith, D.J.T. and Luhana, L. (1996) Source apportionment of atmospheric polycyclic aromatic hydrocarbons collected from an urban location in Birmingham, U.K.. **Environmental Science and Technology**, 30: 825-832.

Harrison, R.M., Smith, D.J.T., Pio, C.A. and Castro, L.M. (1997) Comparative receptor modelling study of airborne particulate pollutants in Birmingham (United Kingdom), Coimbra (Portugal) and Lahore (Pakistan). **Atmospheric Environment**, 31: 3309-3321.

Harrison, R.M., Shi, J.P., Xi, S., Khan, A., Mark, D., Kinnersley, R. and Yin, J. (2000) Measurement of number, mass and size distribution of particles in the atmosphere. **Philosophical Transactions of the Royal Society A**, 358: 2567-2580.

Harrison, R.M., Tilling, R., Romero, M.S.C., Harrad, S. and Jarvis, K. (2003) A study of trace metals and polycyclic aromatic hydrocarbons in the roadside environment. **Atmospheric Environment**, 37: 2391-2402.

Harrison, R.M., Jones, A.M. and Lawrence, R.G. (2003) A pragmatic mass closure model for airborne particulate matter at urban background and roadside sites. **Atmospheric Environment**, 37: 4927-4933.

Harrison, R.M., Giorio, C., Beddows, D.C.S. and Dall'Osto, M., (2010) Size distribution of airborne particles controls outcome of epidemiological studies. **Science of the Total Environment**, 409: 289-293.

Harrison, R.M. and Yin, J. (2010) Chemical speciation of $PM_{2.5}$ particles at urban background and rural sites in the UK atmosphere. **Journal of Environmental Monitoring**, 12, 1404-1414.

Harrison, R.M., Beddows, D.C.S. and Dall'Osto, M., (2011) PMF analysis of wide-range particle size spectra collected on a major highway. **Environmental Science and Technology**, 45: 5522-5528.

Harrison, R.M., Jones, A.M., Gietl, J., Yin, J. and Green, D.C. (2012a) Estimation of the contributions of brake dust, tire wear, and resuspension to nonexhaust traffic particles derived from atmospheric measurements. **Environmental Science and Technology**, 46: 6523-6529.

Harrison, R.M., Beddows, D.C.S, Hu, L. and Yin, J. (2012b) Comparison of methods for evaluation of wood smoke and estimation of UK ambient concentrations. **Atmospheric Chemistry and Physics**, 12: 8271-8283.

Harrison, R.M. and Yin, J. (2013) **Use of chemical composition and molecular markers to infer the sources of airborne particulate matter**. Final project report No. 1 for DEFRA (Ref. AQ0707).

Hassanien, M.A. and Abdel-Latif, N.M. (2008) Polycyclic aromatic hydrocarbons in road dust over Greater Cairo, Egypt. **Journal of Hazardous Materials**, 151: 247-254.

Hays, M.D., Cho, S.-H., Baldauf, R., Schauer, J.J. and Shafer, M. (2011) Particle size distributions of metal and non-metal elements in an urban near-highway environment. **Atmospheric Environment**, 45(4): 925-934.

He, L.-Y., Hu, M., Huang, X.-F., Zhang, Y.-H., Yu, B.-D. and Liu, D.-Q. (2006) Chemical characterization of fine particles from on-road vehicles in the Wutong tunnel in Shenzhen, China. **Chemosphere**, 62(12): 1565-1573.

He, L.-Y., Hu, M., Zhang, Y.-H., Huang, X.-F. and Yao, T.-T. (2008) Fine particle emissions from on-road vehicles in the Zhujiang tunnel, China. **Environmental Science and Technology**, 42(12): 4461-4466.

HEI Panel on the Health Effects of Traffic-Related Air Pollution (2010) **Traffic-Related Air Pollution: A Critical Review of the Literature on Emissions, Exposure, and Health Effects**. HEI Special Report 17. Health Effects Institute, Boston, MA.

Henry, R.C., Lewis, C.W., Hopke, P.K. and Williamson, H.J. (1984) Review of receptor model fundamentals. **Atmospheric Environment**, 18: 1507-1515.

Heo, J., Dulger, M., Olson, M.R., McGinnis, J.E., Shelton, B.R., Matsunga, A., Sioutas, C. and Schauer, J.J. (2013) Source apportionment of $PM_{2.5}$ organic carbon using molecular marker positive matrix factorization and comparison of results from different receptor models. **Atmospheric Environment**, 73: 51-61.

Herlekar, M., Joseph, A.E., Kumar, R. and Gupta, I. (2012) Chemical speciation and source assignment of particulate (PM_{10}) phase molecular markers in Mumbai. **Aerosol and Air Quality Research**, 12: 1247-1260.

Hien, T.T., Thanh, L.T., Kameda, T., Takenaka, N. and Bandow, H. (2007) Distribution characteristics of polycyclic aromatic hydrocarbons with particle size in urban aerosols at the roadside in Ho Chi Minh City, Vietnam. **Atmospheric Environment**, 41(8): 1575-1586.

Hildemann, L.M., Markowski, G.R. and Cass, G.R. (1991) Chemical composition of emissions from urban sources of fine organic aerosol. **Environmental Science and Technology**, 25(4): 744-759.

Hinds, W. C. (1982) **Aerosol Technology: Propoerties, Behaviour, and Measurement of Airborne Particles**. First Edition. Wiley- Interscience: New York.

Hjortenkrans, D.S.T., Bergbäck, B.G. and Häggerud, A.V. (2007) Metal emissions from brake linings and tires: Case studies of Stockholm, Sweden 1995/1998 and 2005. **Environmental Science and Technology**, 41(15): 5224-5230.

Ho, K.F., Lee, S.C., Chow, J.C. and Watson, J.G. (2003) Characterization of PM_{10} and $PM_{2.5}$ source profiles for fugitive dust in Hong Kong. **Atmospheric Environment**, 37: 1023-1032.

Ho, S.S.H. and Yu, J.Z. (2004) In-injection port thermal desorption and subsequent gas chromatography-mass spectrometric analysis of polycyclic aromatic hydrocarbons and n-alkanes in the atmospheric aerosol samples**. Journal of Chromatography A**, 1059: 121-129.

Hopke P.K. (1991) An introduction to receptor modelling. **Chemometrics and Intelligent Laboratory Systems**, 10: 21-43.

Hopke P.K. (2003) Recent developments in receptor modelling. **Journal of Chemometrics**, 17: 255-265.

Hussein, T., Johansson, C., Karlsson, H. and Hansson, H.-C. (2008) Factors affecting non-tailpipe aerosol particle emissions from paved roads: On-road measurements in Stockholm, Sweden. **Atmospheric Environment**, 42(4): 688-702.

Iijima, A., Sato, K., Yano, K., Tago, H., Kato, M., Kimura, H. and Furuta, N. (2007) Particle size and composition distribution analysis of automotive brake abrasion dusts for the evaluation of antimony sources of airborne particulate matter. **Atmospheric Environment**, 41(23): 4908-4919.

Imhof, D., Weingartner, E., Prevot, A.S.H., Ordonez, C., Kurtenbach, R., Weisen, P., Rodler, J., Sturm, P., McCrae, I., Sjodin, A. and Baltensperger, U. (2005) Aerosol and NOx emissions factors and submicron particle size distributions in two road tunnels with different traffic regimes. **Atmospheric Chemistry and Physics**, 5: 5127-5166.

Ingo, G.M., D'Uffizi, M., Falso, G., Bultrini, G. and Padeletti, G. (2004) Thermal and microchemical investigation of automotive brake pad wear residues. **Thermochimica Acta**, 418: 61-68.

Jang, E., Alam, M.S. and Harrison, R.M. (2013) Source apportionment of polycyclic aromatic hydrocarbons in urban air using positive matrix factorization and spatial distribution analysis. **Atmospheric Environment**, 79: 271-285.

Johansson, C., Norman, M. and Burman, L. (2009) Road traffic emission factors for heavy metals. **Atmospheric Environment**, 43(31): 4681-4688.

Joseph, A.E., Unnikrishnan, S. and Kumar, R. (2011) Chemical characterization and mass closure of fine aerosol for different land use patterns in Mumbai city. **Aerosol and Air Quality Research**, 12: 61-72.

Kam, W., Liacos, J.W., Schauer, J.J., Delfino, R.J. and Sioutas, C. (2012) Size-segregated composition of particulate matter (PM) in major roadways and surface streets. **Atmospheric Environment**, 55: 90-97.

Kappos, A.D., Bruckmann, P., Eikmann, T., Englert, N., Heinrich, U., Hoppe, P., Koch, E., Krause, G.H.M., Kreyling, W.G., Rauchfuss, K., Rombout, P., Schulz-Klemp, V., Thiel, W.R. and Wichmann, H.-R. (2004) Health effects of particles in ambient air. **International Journal of Hygeine and Environmental Health**. 207(4): 399- 407.

Kar, S., Maity, J.P., Samal, A.C. and Santra, S.C. (2010) Metallic components of traffic-induced urban aerosol, their spatial variation, and source apportionment. **Environmental Monitoring and Assessment**, 168: 561–574.

Karanasiou, A., Moreno, T., Amato, F., Tobias, A., Boldo, E., Linares, C., Lumbreras, J., Borge, R., Alastuey, A. and Querol, X. (2012) Variation of $PM_{2.5}$ concentrations in relation to street washing activities. **Atmospheric Environment**, 54: 465- 469.

Karanasiou, A., Amato, F., Moreno, T., Lumbreras, J., Borge, R., Linares, C., Boldo, E., Alastuey, A. and Querol, X. (2014) Road dust emission sources and assessement of street washing effect. **Aerosol and Air Quality Research**, 14: 734- 743.

Kaunhaniemi, M., Kukkonen, J., Harkonen, J., Nikmo, J., Kangas, L., Omstedt, G., Ketzel, M., Kousa, A., Haakana, M. and Karppinen, A. (2011) Evalaution of a road dust suspension model for predicting the concentrations of PM10 in a street canyon. **Atmospheric Environment**, 45: 3646-3654.

Kavouras, I.G., Koutrakis, P., Tsapakis, M., Lagoudaki, E., Stephahou, E.G., von Baer, D. and Oyola, P. (2001) Source apportionment of urban particulate aliphatic and polynuclear aromatic hydrocarbons (PAHs) using multivariate methods. **Environmental Science and Technology**, 35: 2288-2294.

Ke, H., Ondov, J.M. and Rogge, W.F. (2013) Detailed emission profiles for on-road vehicles derived from ambient measurements during a windless traffic episode in Baltimore using a multi-model approach. **Atmospheric Environment**, 81: 280-287.

Kelly, F.J. (2003) Oxidative stress: its role in air pollution and adverse health effects. **Occupational and Environmental Medicine**, 60: 612- 616.

Ketzel, M.G., Omstedt, G., Johansson, C., During, I., Pohjola, M., Oettl, D., Gidhagen, L., Wahlin, P., Lohmeyer, A. and Berkowicz, R. (2007) Estimation and validation of $PM_{2.5}/PM_{10}$ exhaust and non-exhaust emission factors for practical street pollution modelling. **Atmospheric Environment**, 41(40): 9370-9385.

Keuken, M., Denier van der Gon, H. and van der Valk, K. (2010) Non-exhaust emissions of PM and the efficiency of emission reduction by road sweeping and washing in the Netherlands. **Science of the Total Environment**, 408(20): 4591-4599.

Keuken, M., Henzing, B., Zandveld, P., van den Elshout, S. and Karl, M. (2012) Dispersion of particle numbers and elemental carbon from road traffic, a harbour and an airstrip in the Netherlands. **Atmospheric Environment**, 54: 320-327.

Khare, P. and Baruah, B.P. (2010) Elemental characterization and source identification of $PM_{2.5}$ using multivariate analysis at the suburban site of North-East India. **Atmospheric Research**, 98: 148-162.

Khemani, L.T., Momin, G.A., Naik, M.S., Vijayakumar, R. and Ramana Murty, B.H.V. (1982) Chemical composition and size distribution of atmospheric aerosols over the Deccan Plateau, India. **Tellus**, 34: 151-158.

Khillare, P.K., Balachandran, S. and Meena, B.R. (2004) Spatial and temporal variation of heavy metals in atmospheric aerosol in India. **Environmental Monitoring and Assessment**, 90: 1-21.

Khillare, P.S. and Sarkar, S. (2012) Airborne inhalable metals in residential areas of Delhi, India: distribution, source apportionment and health risks. **Atmospheric Pollution Research**, 3: 46-54.

Kim, J. Y., Lee, J. Y., Kim, Y. P., Lee, S. B., Jin, H. C. and Bae, G. N. (2012) Seasonal characteristics of the gaseous and particulate PAHs at a roadside station in Seoul, Korea. **Atmospheric Research**, 116: 142-150.

Kirillova, E.N., Andersson, A., Tiwari, S., Srivastava, A.K., Bisht, D.S. and Gustafsson, O. (2014) Water-soluble organic carbon aerosols during a full New Delhi winter: Isotope-based source apportionment and optical properties. **Journal of Geophysical Research**: Atmospheres, doi: 101.1002/2013JD020041.

Kleeman, M.J., Schauer, J.J. and Cass, G.R. (1999) Size and composition distribution of fine particulate matter emitted from wood burning, meat charboiling, and cigarettes. **Environmental Science and Technology**, 33: 3516-3523.

Kong, S., Han, B., Bai, Z., Chen, L., Shi, J. and Xu, Z. (2010) Receptor modelling of $PM_{2.5}$, PM_{10} and TSP in different seasons and long-range transport analysis at a coastal site of Tianjin, China. **Science of The Total Environment**, 408: 4681-4694.

Kong, S., Ji, Y., Lu, Chen, L., B., Han, B., Li, Z. and Bai, Z. (2011) Characterization of PM_{10} source profiles for fugitive dust in Fushun- a city famous for coal. **Atmospheric Environment**, 45: 5351- 5365.

Kothai, P., Saradhi, I.V., Prathibha, P., Pandit, G.G. and Puranik, V.D. (2008) Source apportionment of coarse and fine particulate matter at Navi Mumbai, India. **Aerosol and Air Quality Research**, 8: 423-436.

Kreider, M.L., Panko, J.M., McAtee, B.L., Sweet, L.I. and Finley, B.L. (2010) Physical and chemical characterization of tire-related particles: Comparison of particles generated using different methodologies. **Science of The Total Environment**, 408: 652-659.

Kukutschova, J., Roubicek, V., Maslan, M., Jancik, D., Slovak, V., Malachova, K., Pavlickova, Z. and Filip, P. (2010) Wear performance and wear debris of semimetallic automotive brake materials. **Wear**, 268: 86-93.

Kukutschova, J., Moravec, P., Tomasek, V., Matejka, V., Smolik, J., Schwarz, J., Seidlerova, J., Safarova, K. and Filip, P. (2011) On airborne nano/micro-sized wear particles released from low-metallic automotive brakes. **Environmental Pollution**, 159: 998-1006.

Kulkarni, P. and Venkataraman, C. (2001) Atmospheric polycyclic aromatic hydrocarbons in Mumbai, India. **Atmospheric Environment**, 34: 2785-2790.

Kulshrestha, U.C., Saxena, A., Kumar, N., Kumari, K.M. and Srivastava, S.S. (1998). Chemical composition and association of size-differentiated aerosols at a suburban site in a semi-arid tract of India. **Journal of Atmospheric Chemistry**, 29: 109-118.

Kulshrestha, A., Satsangi, P.G., Masih, J. and Taneja, A. (2009) Metal concentration of $PM_{2.5}$ and PM_{10} particles and seasonal variations in urban and rural environment of Agra, India. **Science of The Total Environment**, 407, 6196-6204.

Kumar, A.V., Patil, R.S. and Nambi, K.S.V. (2001) Source apportionment of suspended particulate matter at two traffic junctions in Mumbai, India. **Atmospheric Environment**, 35: 4245-4251.

Kumar, P., Pirjola, L., Ketzel, M. and Harrison, R.M. (2013) Nanoparticle emissions from 11 non-vehicle exhaust sources- A review. **Atmospheric Environment**, 67: 252-277.

Kumata, H., Yamada, J., Masuda, K., Takada, H., Sato, Y., Sakural, T. and Fujiwara, K. (2002) Benzothiazolamines as tire-derived molecular markers: sorptive behaviours in street runoff and application to source apportioning. **Environmental Science and Technology**, 36(4): 702-708.

Kupiainen, K.J., Tervahattu, H., Räisänen, M., Mäkelä, T., Aurela, M. and Hillamo, R. (2005) Size and composition of airborne particles from pavement wear, tires, and traction sanding. **Environmental Science and Technology**, 39(3): 699-706.

Kwak, J., Kim, H., Lee, J. and Lee, S. (2013) Characterization of non-exhaust coarse and fine particles from on-road driving and laboratory measurements. **Science of the Total Environment**, 458-460: 273-282.

Kwon, E.E. and Castaldi, M.J. (2012) Mechanistic understanding of polycyclic aromatic hydrocarbons (PAHs) from the therman degradation of tires under various oxygen concentration atmospheres. **Environmental Science and Technology**, 46(23): 12921- 6.

Laidlaw, M.A.S., Zahran, S., Mielke, H.W., Taylor, M.P. and Filippelli, G.M. (2012) Re-suspension of lead contaminated urban soil as a dominant source of atmospheric lead in Birmingham, Chicago, Detroit and Pittsburgh, USA. **Atmospheric Environment**, 49: 302-310.

Lambe, A.T., Logue, J.M., Kreisberg, N.M., Hering, S.V., Worton, D.R., Goldstein, A.H., Donahue, N.M. and Robinson, A.L. (2009) Apportioning black carbon to sources using highly time-resoled ambient measurements of organic molecular markers in Pittsburgh. **Atmospheric Environmen**t, 43: 3941-3950.

Landis, M.S., Lewis, C.W., Stevens, R.K., Keeler, G.J., Dvonch, J.T. and Tremblay, R.T. (2007) Ft. McHenry tunnel study: Source profiles and mercury emissions from diesel and gasoline powered vehicles. **Atmospheric Environment**, 41: 8711-8724.

Larsen, R.K. and Baker, J.E. (2003) Source apportionment of polycyclic aromatic hydrocarbons in the urban atmosphere: a comparison of three methods. **Environmental Science and Technology**, 37: 1873-1881.

Laschober, C., Limbeck, A., Rendl, J. and Puxbaum, H. (2004) Particulate emissions from on-road vehicles in the Kaisermühlen-tunnel (Vienna, Austria). **Atmospheric Environment**, 38: 2187-2195.

Lawrence, S., Sokhi, R., Ravindra, K., Mao, H., Prain, H.D. and Bull, I.D. (2013) Source apportionment of traffic emissions of particulate matter using tunnel measurements. **Atmospheric Environment**, 77: 548-557.

Lee, W.-J., Wang, Y.-F., Lin, T.-C., Chen, Y.-Y., Lin, W.-C., Ku, C.-C. and Cheng, J.-T. (1995) PAH characteristics in the ambient air of traffic-source. **Science of the Total Environment**, 159: 185-200.

Lee, S. and Russell, A.G. (2007) Estimating uncertainities and uncertainty contributors of CMB $PM_{2.5}$ source apportionment results. **Atmospheric Environment**, 41: 9616-9624.

Lee, S., Kwak, J., Kim, H. and Lee, J. (2013) Properties of roadway particles from interaction between the tire and road pavement. **International Journal of Automotive Technology**, 14(1): 163-173.

Lenschow, P., Abraham, H.-J., Kutzner, K., Lutz, M., Preuss, J.-D. and Reichenbacher, W. (2001) Some ideas about the sources of PM10. **Atmospheric Environment**, 35(1): S23-S33.

Lewandowski, M., Jaoui, M., Offenberg, J.H., Kleindienst, T.E., Edney, E.O., Sheesley, R.J. and Schauer, J.J. (2008) Primary and secondary contributions to ambient PM in the Midwestern United States. **Environmental Science and Technology**, 42: 3303-3309.

Li, C.K. and Kamens, R.M. (1993) The use of polycyclic aromatic hydrocarbons as source signatures in receptor modeling. **Atmospheric Environment**, 27A (4): 523-532.

Li, J., Wang, G., Aggarwal, S.G., Huang, Y., Ren. Y., Zhou, B., Singh, K., Gupta, P.K., Cao, J. and Zhang, R. (2014) Comparison of abundances, compositions and sources of elements, inorganic ions and organic compounds in atmospheric aerosols from Xi'an and New Delhi, two megacities in China and India. **Science of the Total Environment**, 476-477: 485-495.

Liati, A., Schreiber, D., Eggenschwiler, P.D. and Dasilva, Y.A.R. (2013) Metal particle emissions in the exhaust stream of diesel engines: An electron microscope study. **Environmental Science and Technology**, 47: 14495-14501.

Lighty, J.S., Veranth, J.M. and Sarofim, A.F. (2000) Combustion aerosols: Factors governing their size and composition and implications to human health. **Journal of Air and Waste Management Association**, 50(9): 1565-1618.

Lim, L.H., Harrison, R.M. and Harrad, S. (1999) The contribution of traffic to atmospheric concentrations of polyaromatic hydrocarbons. **Environmental Science and Technology**, 33: 3538-3542.

Lim, H.-J., and Turpin, B.J. (2002) Origins of primary and secondary organic aerosl in Atlanta: Results of time resolved measurements during the Atlanta supersite experiment. **Environmental Science and Technology**, 36: 4489-4496.

Lim, S.S., Vos, T., Flaxman, A.D., Danaei, G., Shibuya, K., Adair-Rohani, H., et al. (2012) A comparative risk assessment of burden of disease and injury attributable to 67 risk factors and risk factor clusters in 21 regions, 1990–2010: a systematic analysis for the Global Burden of Disease study 2010. **Lancet**, 380: 2224–2260.

Lin, C.-C., Chen, S.-J., Huang, K.-L., Hwang, W.-I., Chang-Chien, G.-P. and Lin, W.-Y. (2005) Characteristics of metals in nano/ultrafine/fine/coarse particles collected beside a heavily trafficked road. **Environmental Science and Technology**, 39(21): 8113-8122.

Liu, M., Cheng, S.B., Ou, D.N., Hou, L.J., Gao, L., Wang, L.L., Xie, Y.S., Yang, Y. and Xu, S.Y. (2007) Characterization, identification of road dust PAHs in central Shanghai areas, China. **Atmospheric Environment**, 41: 8785-8795.

Lin, L., Lee, M.L. and Eatough, D.J. (2010) Review of recent advances in detection of organic markers in fine particulate matter and their use for source apportionment. **Journal of Air and Waste Management Association**, 60: 3-25.

Lin, Y.-C., Tsai, C.-J., Wu, Y.C., Zhang, R., Chi, K.-H., Huang, Y.-T., Lin, S.-H. and Hsu, S.-C. (2014) Characteristics of trace metals in traffic-derived particles in Hsuehshan Tunnel, Taiwan: size distribution, fingerprinting metal ratio, and emission factor. **Atmospheric Chemistry and Physics Discussions**, 14: 13963-14004.

Liu, M., Cheng, S.B., Ou, D.N., Hou, L.J., Gao, L., Wang, L.L., Xie, Y.S., Yang, Y. and Xu, S.Y. (2007) Characterization, identification of road dust PAHs in central Shanghai areas, China. **Atmospheric Environment**, 41: 8785-8795.

Lloyd, A.C. and Cackette, T.A. (2001) Diesel engines: Environmental impact and control. **Journal of Air and Waste Management Association**, 51 (6): 809-847.

Loomis, D., Grosse, Y., Lauby-Secretan, B., El Ghissassi, F., Bouvard, V., et al. (2013) The carcinogenicity of outdoor air pollution. **The Lancet Oncology**, 14(13): 1262-1263.

Lough, G.C., Schauer, J.J., Park, J.-S., Shafer, M.M., DeMinter, J.T. and Weinstein, J.P. (2005) Emissions of metals associated with motor vehicle roadways. **Environmental Science and Technology**, 39(3): 826-836.

Lough, G.C., Christensen, C.G., Schauer, J. J., Tortorelli, J., Mani, E., Lawson, D.R., Clark, N.N. and Gabela, P.A. (2007) Development of molecular marker source profiles for emissions from on-road gasoline and diesel vehicle fleets. **Journal of the Air and Waste Management Association**, 57: 1190-1199.

Lowenthal, D.H., Chow, J.C., Watson, J.G., Neuroth, GR., Robbins, R.B., Shafritz, B.P. and Countess, R.J. (1992) The effects of collinearity on the ability to determine aerosol contributions from diesel- and gasoline-powered vehicles using the chemical mass balance model. **Atmospheric Environment**, 26A(13): 2341-2351.

Luhana, L., Sokhi, R., Warner, L., Mao, H., Boulter, P., McCrae, I., Wright, J. and Osborn, D. (2004) **Characterisation of Exhaust Particulate Emissions from Road Vehicles (PARTICULATES), Deliverable 8: Measurement of non-exhaust particulate matter**. Contract Number 2000-RD.11091, European Commission – DG TrEn, 5th

Framework Programme Competitive and Sustainable Growth Sustainable Mobility and Intermodality. Available at http://ec.europa.eu/transport/roadsafety_library/publications/particulates_d8.pdf [Accessed 12 February 2012].

Luo, X. S., Yu, S., Zhu, Y. G. and Li, X. D. (2011) Trace metal contamination in urban soils of China. **Science of the Total Environment**, 421-422: 17-30.

Majumdar, D., Rajaram, B., Meshram, S. and Chalapati Rao, C.V. (2012) PAHs in road dust: Ubiquity, fate, and summary of available data. **Critical Reviews in Environmental Science and Technology**, 42(12): 1191-1232.

Mancilla, Y. and Mendoza, A. (2012) A tunnel study to characterize $PM_{2.5}$ emissions from gasoline-powered vehicles in Monterrey, Mexico. **Atmospheric Environment**, 59: 449-460.

Mari, M., Harrison, R.M., Schuhmacher, M., Domingo, J.L. and Pongpiachan S. (2010) Inferences over the sources and processes affecting polycyclic aromatic hydrocarbons in the atmosphere derived from measured data. **Science of the Total Environment**, 408: 2387-2393.

Maricq, M. M. (2007) Chemical characterization of particulate emissions from diesel engines: A review. **Journal of Aerosol Science**, 38(11): 1079-1118.

Marple, V.A., Rubow, K.L. and Behm, S.M. (1991) A microorifice uniform deposit impactor (MOUDI): Description, calibration, and use. **Aerosol Science and Technology**, 14(4): 434-446.

Martuzevicius, D., Kliucininkas, L., Prasauskas, T., Krugly, E., Kauneliene, V. and Strandberg, B. (2011) Resuspension of particulate matter and PAHs from street dust. **Atmospheric Environment**, 45(2): 310-317.

Masih, A., Saini, R., Singhvi, R. and Taneja, A. (2010) Concentrations, sources, and exposure profiles of polycyclic aromatic hydrocarbons (PAHs) in particulate matter (PM_{10}) in the north central part of India. **Environmental Monitoring and Assessment**, 163(1-4): 421–431.

Mathissen, M., Scheer, V., Vogt, R. and Benter, T. (2011) Investigation on the potential generation of ultrafine particles from the tire–road interface. **Atmospheric Environment**, 45(34): 6172-6179.

Maynard, R. (2004) Key airborne pollutants- the impact on health. **Science of the Total Environment**, 334-335: 9-13.

Mclaren, R., Gertler, A.W., Wittorff, D.N., Belzer, W., Dann, T. and Singleton, D.L. (1996) Real-world measurements of exhaust and evaporative emissions in the Cassiar tunnel predicted by chemical mass balance modeling. **Environmental Science and Technology**, 30: 3001-3009.

Miguel, A.H., Kirchstetter, T.W., Harley, R.A. and Hering, S.V. (1998) On-road emissions of particulate polycyclic aromatic hydrocarbons and black carbon from gasoline and diesel vehicles. **Environmental Science and Technology**, 32(4): 450-455.

Milani, M., Pucillo, F.P., Ballerini, M., Camatani, M., Gualtieri, M. and Martino, S. (2004) First evidence of tyre debris characterization at the nanoscale by focused ion beam. **Materials Characterization**, 52: 283-288.

Miller, M.S., Friedlander, S.K. and Hidy, G.M. (1972) A chemical element balance for the Pasadena aerosol. **Journal of Colloid and Interface Science**, 39(1): 165-176.

Mönkkönen, P., Uma, R., Srinivasan, D., Koponen, I.K., Lehtinen, K.E.J., Hameri, Suresh, R., Sharma, V.P. and Kulmala, M. (2004) Relationship and variations of aerosol number and PM_{10} mass concentrations in a highly polluted urban environment- New Delhi, India. **Atmospheric Environment**, 38: 57-66.

Mönkkönen, P., Koponen, I.K., Lehtinen, K.E.J., Hameri, K., Uma, R. and Kulmala, M. (2005) Measurements in a highly polluted Asian mega city: observations of aerosol number size distribution, modal parameters and nucleation events. **Atmospheric Chemistry and Physics**, 5: 57-66.

Moreno, T., Karanasiou, A., Amato, F., Lucarelli, F., Nava, S., Calzolai, G., Chiari, M., Coz, E., Artinano, B., Lumbreras, J., Borge, R., Boldo, E., Linares, C., Alastuey, A., Querol, X. and Gibbons, W. (2013) Daily and hourly sourcing of metallic and mineral dust in urban air contaminated by traffic and coal-burning emissions. **Atmospheric Environment**, 68: 33-33.

Morillo, C., Romero, A.S., Maqueda, C., Madrid, L., Ajmone-Marsan, F., Grcman, H., Davidson, C.M., Hursthouse, A.S. and Villaverde, J. (2007) Soil pollution by PAHs in urban soils: a comparison of three European cities. **Journal of Environmental Monitoring**, 9: 1001-1008.

Mouli, P.C., Mohan, S.V., Balaram, V., Praveen Kumar, M. and Reddy, S.J. (2006) A study on trace elemental composition of atmospheric aerosols at a semi-arid urban site using ICP-MS technique. **Atmospheric Environment**, 40: 136-146.

MSP Corporation (n.d.) Models 100, 110, 115 and 116-MOUDI™ Impactors (Product Information). Available at http://www.mspcorp.com/images/products/MSP-PI100_Rev%20A%20(PI)%20Moudi%20Impactors-000.pdf [Accessed 11 June 2012].

Narvaez, R.F., Hoepner, L., Chillrud, S.N., Yan, B., Garfinkel, R., Whyatt, R., Camann, D., Perera, F.P., Kinney, P. L. and Miller, R.L. (2008) Spatial and temporal trends of polycyclic aromatic hydrocarbons and other traffic-related airborne pollutants in New York City. **Environmental Science and Technology**, 42: 7330-7335.

NARSTO (2004) **Particulate Matter Science for Policy Makers: A NARSTO Assessment**. McMurry, P.H., Shepherd, M. F. And Vickery, J.S., eds. Cambridge University Press, Cambridge, England.

Nicholson, K.W. (1988) A review of particle resuspension. **Atmospheric Environment** (1967), 22(12): 2639-2651.

Nielsen, T. (1996) Traffic contribution of polycyclic aromatic hydrocarbons in the centre of a large city. **Atmospheric Environment**, 30(20): 3481-3490.

Ntziachristos, L., Ning, Z., Geller, M.D., Sheesley, R.J., Schauer, J.J. and Sioutas, C. (2007) Fine, ultrafine and nanoparticle trace element compositions near a major freeway with a high heavy-duty diesel fraction. **Atmospheric Environment**, 41: 5864-5696.

Oliveira, C., Pio, C., Caseiro, A., Santos, P., Nunes, T., Mao, H., Luahana, L. and Sokhi, R.S. (2010) Road traffic impact on urban atmospheric aerosol loading at Oporto, Portugal. **Atmospheric Environment**, 44: 3147-3158.

Oliveira, C., Martins, N., Tavares, J., Pio, C., Cerqueira, M., Matos, M., Silva, H., Oliviera, S. and Camoes, F. (2011) Size distribution of polycyclic aromatic hydrocarbons in a roadway tunnel in Lisbon, Portugal. **Chemosphere**, 83(11): 1588-1596.

Omar, N.Y.M.J., Abas, M.R.B., Rahman, N.A., Tahir, N.M., Rushdi, A.I. and Simoneit, B.R.T. (2007) Levels and distributions of organic source tracers in air and roadside dust particles of Kuala Lumpur, Malaysia. **Environmental Geology**, 52: 1485-1500.

Omstedt, G., Bringfelt, B. and Johansson, C. (2005) A model for vehicle-induced non-tailpipe emissions of particles along Swedish roads. **Atmospheric Environment**, 39: 6088-6097.

Oanh, K.N.T., Thiansathit, W., Bond, T.C., Subramanian, R., Winijkul, E. and Paw-Armart, I. (2010) Compositional characterization of $PM_{2.5}$ emitted from in-used diesel vehicles. **Atmospheric Environment**, 44: 15-22.

Ondráček, J., Schwarz, J., Ždímal, V., Andělová, L., Vodička, P., Bízek, V., Tsai, C.-J., Chen, S.-C. and Smolik, J. (2011) Contribution of the road traffic to air pollution in the Prague city (busy speedway and suburban crossroads). **Atmospheric Environment**, 45(29): 5090-5100.

Ondov, J.M., Zoller, W.H. and Gordon, G. E. (1982) Trace element emissions on aerosols from motor vehicles. **Environmental Science and Technology**, 16: 318-328.

Oros, D.S. and Simoneit, B.R.T. (2000) Identification and emission rates of molecular tracers in coal smoke particulate matter. **Fuel**, 79: 515-536.

Pant, P. and Harrison, R. M. (2012) Critical review of receptor modelling for particulate matter: A case study of India. **Atmospheric Environment**, 49: 1-12.

Pant, P. and Harrison, R.M. (2013) Estimation of the contribution of road traffic emissions to particulate matter concentrations from field measurements: A review. **Atmospheric Environment**, 77:78-97.

Pant, P., Yin, J. and Harrison, R.M. (2014) Sensitivity of a chemical mass balance model to different molecular marker traffic source profiles. **Atmospheric Environment**, 82: 238-249.

Pascal, M., Corso, M., Chanel, O., Declercq, C., Badaloni, C., Cesaroni, G., Neschel, S., Meister, K., Haluza, D., Martin-Olmedo, P. and Medina, S. (2013) Assessing the public health impacts of urban air pollution in 25 European cities: Results of the Aphekom project. **Science of the Total Environment**, 449: 390- 400.

Patil, R.S., Kumar, R., Menon, R., Shah, M.K. and Sethi, V. (2013) Development of particulate matter speciation profiles for major sources in six cities in India. **Atmospheric Research**, 132-133: 1-11.

Peltier, R.E., Cromar, K.R., Ma, Y., Fan, Z.-H. and Lippmann, M. (2011) Spatial and seasonal distribution of aerosol chemical components in New York City: (2) Road dust and other tracers of traffic-generated air pollution. **Journal of Exposure Science and Environmental Epidemiology**, 21(5): 484-494.

Perez, N., Pey, J., Cusack, M., Reche, C., Querol, X., Alastuey, A. and Viana, M. (2010) Variability of particle number, black carbon and PM_{10}, $PM_{2.5}$ and PM_1 levels and speciation: Influence of road traffic emissions on urban air quality. **Aerosol Science and Technology**, 44(7): 487-499.

Perrino, C., Tiwari, S., Catrambone, M., Torre, S.D., Rantica, E. and Canepari, S. (2011) Chemical characterization of atmospheric PM in Delhi, India, during different periods of the year including Diwali festival. **Atmospheric Pollution Research**, 2: 418-427.

Perrone, M.G., Larsen, B.R., Ferrero, L., Sangiorgi, G., De Gennaro, G., Udisti, R., Zangranado, R., Gambaro, A. and Bolzacchini, E. (2012) Sources of high $PM_{2.5}$ concentrations in Milan, Northern Italy: Molecular marker data and CMB modelling. **Science of the Total Environment**, 414: 343-355.

Pey, J., Querol, X. and Alastuey, A. (2010) Discriminating the regional and urban contributions in the North-Western Mediterranean: PM levels and composition. **Atmospheric Environment**, 44(13): 1587-1596.

Phuleria, H.C., Geller, M.D., Fine, P.M. and Sioutas, C. (2006) Size-resolved emissions of organic tracers from light- and heavy-duty vehicles measured in a California roadway tunnel. **Environmental Science and Technology**, 40(13): 4109-4118.

Phuleria, H.C., Sheesley, R.J., Schauer, J.J., Fine, P.M. and Sioutas, C. (2007) Roadside measurements of size-segregated particulate organic compounds near gasoline and diesel-dominated freeways in Los Angeles, CA. **Atmospheric Environment**, 41(22): 4653-4671.

Pio, C., Cerqueira, M., Harrison, R.M., Nunes, T., Mirante, F., Alves, C., Oliviera, C., Sanchez de la Campa, A., Artinano, B. and Matos, M. (2011) OC/EC ratio observations in Europe: Re-thinking the approach for apportionment between primary and secondary organic carbon. **Atmospheric Environment**, 45: 6121-6132.

Pio, C., Mirante, F., Oliviera, C., Matos, M., Caseiro, A., Oliviera, C., Querol, X., Alves, C., Martins, N, Cerqueira, M., Camoes, F., Silva, H. and Plana, F. (2013) Size-segregated chemical composition of aerosol emisisons in an urban road tunnel in Portugal. **Atmospheric Environment**, 71: 15-25.

Pirjola, L., Johansson, C., Kupiainen, K., Stojiljkovic, A., Karlsson and Hussein, T. (2010) Road dust emisisons from paved road measured using different mobile systems. **Journal of Air and Waste Management Association**, 60: 1422-1433.

Pope, C.A., Burnett, R.T., Thurston, G.D., Thun, M.J., Calle, E.E., Krewski, D. and Godleski, J.J. (2004) Cardiovascular mortality and long-term exposure to particulate air pollution: Epidemiological evidence of general pathophysiological pathways of disease. **Circulation**, 109: 71-77.

Prather, K.A., Hatch, C.D. and Grassian, V.H. (2008) Analysis of atmospheric aerosols. **Annual Review of Analytical Chemistry**, 1: 485-514.

Prichard, H.M. and Fisher, P.C. (2012) Identification of platinum and palladium particles emitted from vehicles and dispersed into the surface environment. **Environmental Science and Technology**, 46(6): 3149-3154.

Pulles, T., Denier van der Gon, H., Appelman, W. and Verheul, M. (2012) Emission factors for heavy metals from diesel and petrol used in European vehicles. **Atmospheric Environment**, 61: 641- 651.

Pye, H.O.T. and Pouliot, G.A. (2012) Modeling the role of alkanes, polycyclic aromatic hydrocarbons, and their oligomers in secondary organic aerosol formation. **Environmental Science and Technology**, 46: 6041-6047.

Querol, X., Alastuey, A., Viana, M., Moreno, T., Reche, C., Minguillon, M.C., Ripoll, A., et al. (2013) Variability of carbonaceous aerosols in remote, rural, urban and industrial environments in Spain: implication for air quality policy. **Atmospheric Chemistry and Physics**, 13: 6185-6206.

Ramanathan, V. and Carmichael, G. (2008) Global and regional climate changes due to black carbon. **Nature Geoscience**, 1: 221-227.

Ravindra, K., Sokhi, R. and van Greiken, R. (2008) Atmospheric polycyclic aromatic hydrocarbons: source attribution, emission factors and regulation. **Atmospheric Environment**, 42: 2895-2921.

Reddy, C.M. and Quinn, J.G. (1997) Environmental Chemistry of Benzothiazoles Derived from Rubber. **Environmental Science and Technology**, 31: 2847-2853.

Reddy, R.R., Rama Gopal, K., Narasimhulu, K., Siva Sankara Reddy, L. and Raghavendra Kumar, K. (2007) Aerosol size distribution variation in Anantapur (14.62°N, 77.65°E) Semi Arid Zone and its Impact on Aerosol Effective Radius. **Aerosol and Air Quality Research**, 7(4): 550-562.

Riddle, S.G., Robert, M.A., Jakober, C.A., Hannigan, M.P. and Kleeman, M.J. (2007) Size distribution of trace organic species emitted from light-duty gasoline vehicles. **Environmental Science and Technology**, 41(21): 7464-7471.

Robert, M.A., VanBergen, S., Kleeman, M.J. and Jakober, C.A. (2007a) Size and composition distributions of particulate matter emisisons: Part 1- Light-duty diesel vehicles. **Journal of Air and Waste Management Association**, 57: 1414-1428.

Robert, M.A., Kleeman, M.J. and Jakober, C.A. (2007b) Size and composition distributions of particulate matter emisisons: Part 2- Heavy-duty diesel vehicles. **Journal of Air and Waste Management Association**, 57: 1429-1438.

Robinson, A.L., Subramanian, R., Donahue, N.M., and Rogge, W.F. (2006a) Source apportionment of molecular markers and organic aerosol. 1.Polycyclic aromatic hydrocarbons and Methodology for Data Visualization. **Environmental Science and Technology,** 40: 7803-7810.

Robinson, A.L., Donahue, N.M., and Rogge, W.F. (2006b) Photochemical oxidation and changes in molecular composition of organic aerosol in the regional context. **Journal of Geophysical Research** 111, D03302, doi: 10.1029/2005JD006265.

Rogak, S.N., Green, S.I. and Pott, U. (1998) Use of Tracer Gas for Direct Calibration of Emission-Factor Measurements in a Traffic Tunnel. **Journal of the Air and Waste Management Association**, 48(6): 545-552.

Rogge, W.F., Hildemann, L.M., Mazurek, M.A. and Cass, G.R. (1993a) Sources of fine organic aerosol. 2. Noncatalyst and catalyst equipped automobiles and heavy duty diesel trucks. **Environmental Science and Technology**, 27: 636-651.

Rogge, W.F., Hildemann, L.M., Mazurek, M.A., Cass, G.R. and Simoneit, B. R. T. (1993b) Sources of fine organic aerosol. 3. Road dust, tire debris, and organometallic brake lining dust: roads as sources and sinks. **Environmental Science and Technology**, 27(9): 1892-1904.

Rogge, W.F., Hildemann, L.M., Mazurek, M.A., Cass, G.R. and Simoneit, B.R.T. (1993c) Sources of fine organic aerosol. 5. Natural-gas home appliances. **Environmental Science and Technology**, 27: 2736-2744.

Rogge, W.F., Hildemann, L.M., Mazurek, M.A., Cass, G.R. and Simoneit, B.R.T. (1993d) Sources of fine organic aerosol. 4. Particulate abrasion products from leaf surfaces of urban plants. **Environmental Science and Technology**, 27(13): 2700-2711.

Rose, D., Wehner, B., Ketzel, M., Engler, C., Voigtlander, J., Tuch, T. and Wiedensohler, A. (2006) Atmospheric number size distributions of soot particles and estimation of emission factors. **Atmospheric Chemistry and Physics**, 6(4): 1021-1031.

Roy, A.A., Wagstrom, K.M., Adams, P.J., Pandis, S.N. and Robinson, A.L. (2011) Quantification of the effects of molecular marker oxidation on source apportionment estimates for motor vehicles. **Atmospheric Environment**, 45: 3132-3140.

Rutter, A.P., Snyder, D.C., Schauer, J.J., Sheesley, R.J., Olson, M.R. and DeMinter, J. (2011) Contributions of resuspended soil and road dust to organic carbon in fine particulate matter in the Midwestern US. **Atmospheric Environment**, 45(2): 514-518.

Sadiktsis, I., Bergvall, C., Johansson, C. and Westerholm, R. (2012) Automobile Tires—A potential source of highly carcinogenic dibenzopyrenes to the environment. **Environmental Science and Technology**, 46(6): 3326-3334.

Sahu, M., Hu, S., Ryan, P. H., Le Masters, G., Grinshpun, S. A., Chow, J. C. and Biswas, P. (2011a) Chemical compositions and source identification of $PM_{2.5}$ aerosols for estimation of a diesel source surrogate. **Science of the Total Environment**, 409(13): 2642-2651.

Sahu, S.S., Beig, G. and Parkhi, N.S. (2011b) Emissions inventory of anthropogenic $PM_{2.5}$ and PM_{10} in Delhi during Commonwealth Games 2010. **Atmospheric Environment**, 45(34): 6180-6190.

Sanchez-Ccoyllo, O.R., Ynoue, R.Y., Martins, L.D., Astolfo, R., Miranda, R.M., Freitas, E.D., Borges, A.S., Fornaro, A., Freitas, H., Moreira, A. and Andrade, M.F. (2009) Vehicular particulate matter emissions in road tunnels in Sao Paulo, Brazil. **Environmental Monitoring and Assessment**, 149(1-4): 241-249.

Sanders, P.G., Xu, N., Dalka, T.M. and Maricq, M.M. (2003) Airborne brake wear debirs: Size distributions, composition, and a comparison of dynamometer and vehicle tests. **Environmental Science and Technology**, 37(4): 4060-4069.

Sarin, M.M., Borole, D.V. and Krishnaswami, S. (1979) Geochemistry and geochronology of sediments from the Bay of Bengal and the Equatorial Indian Ocean. **Proceedings of the Indian Academy of Science**, 88: 131- 154.

Satsangi, A., Pachauri, T., Singla, V., Lakhani, A. and Kumari, K.M. (2013) Water soluble ionic species in atmospheric aerosols: Concentrations and sources at Agra in the Indo-Gangetic Plain (IGP). **Aerosol and Air Quality Research**, 13: 1877-1889.

Schaap, M., Manders, A.M.M., Hendriks, E.C.J., Cnossen, J.M., Segers, A.J.S., Denier van der Gon, H.A.C., Jozwicka, M., Sauter, F., Velders, G., Matthijsen, J. and Builtjes, P.J.H. (2009) **Regional modelling of PM_{10} over the Netherlands**. Technical Report 500099008. Available at http://www.rivm.nl/bibliotheek/rapporten/500099008.pdf [Accessed September 9, 2012].

Schauer, J.J., Rogge, W. F., Hildemann, L.M., Mazurek, M.A. and Cass, G.R. (1996) Source apportionment of airborne particulate matter using organic compounds as tracers. **Atmospheric Environment**, 30: 3837-3855.

Schauer, J.J., Kleeman, M.J., Cass, G.R. and Simoneit, B.R.T. (1999) Measurement of emissions from air pollution sources. 2. C_1 through C_{30} organic compounds from medium duty diesel trucks. **Environmental Science and Technology**, 33: 1578-1587.

Schauer, J.J., Kleeman, M.J., Cass, G.R. and Simoneit, B.R.T. (2002) Measurement of emissions from air pollution sources. 5. C_1-C_{32} organic compounds from gasoline-powered motor vehicles. **Environmental Science and Technology**, 36: 1169-1180.

Schauer, J. J., Lough, G.C., Shafer, M.M., Christensen, W.C., Arndt, M.F., DeMinter, J.T. and Park, J.-S. (2006) **Characterization of Emissions of Metals Emitted from Motor Vehicles**. Research Report 133, Health Effects Institute, Boston, MA.

Schauer, J.J. and Sioutas, C. (2012) **Source apportionment of carbonaceous aerosols using integrated multi-variant and source tracer techniques and a unique molecular marker data set**. Report Version 3.0, Contract Number 07-333. Prepared for California Air Resources Board and California Environment Protection Agency. Available at http://www.arb.ca.gov/research/rsc/05-11-12/item7dfr07-333.pdf [Accessed 5 October 2013].

Sehlstedt, M., Forsberg, B., Westerholm, R., Boman, C. and Sandtrom, T. (2012) **The role of particle size and chemical composition for health risks of exposure to traffic related aerosols- a review of the current literature**. Final Report 071212. Available at http://www20.vv.se/fud-resultat/Publikationer_000301_000400/Publikation_000310/EMFO%20litteraturstudie%20-Trafikrelaterade%20partiklar%20och%20h%C3%A4lsoeffekter%20-%20Final%20report%20071212.pdf [Accessed 15 February, 2014].

Seinfeld, J.H. and Pandis, S.N. (1998) **Atmospheric Chemistry and Physics: From Air Pollution to Climate Change**. 2nd Edition. New York: Wiley Blackwell.

Seinfeld, J.H. and Pankow, J.F. (2003) Organic atmospheric particulate matter. **Annual Reviews of Physical Chemistry**, 54: 121-140.

Sethi, V. and Patil, R. S. (2008) **Development of Air Pollution Source Profiles- Stationary Sources- Volumes I &2**. Available at *http://www.cpcb.nic.in/Source_Emission_%20Profiles_NVS_Volume%20One.pdf* [Accessed April 21, 2011].

Shafer, M.M., Perkins, D.A., Antkiewicz, D.S., Stone, E.A., Quraishi, T.A. and Schauer, J.J. (2010) Reactive oxygen species activity and chemical speciation of size-fractionated atmospheric particulate matter from Lahore, Pakistan: an important role for transition metals. **Journal of Environmental Monitoring**, 12: 704-715.

Shafer, M.M., Toner, B.M., Overdier, J.T., Schauer, J.J., Fakra, S.C., Hu, S., Herner, J.D. and Ayala, A. (2012) Chemical speciation of vanadium in particulate matter emitted from diesel vehicles and urban atmospheric aerosol. **Environmental Science and Technology**, 184: 1693-1709.

Sharma, V.K. and Patil, R.S. (1992) Size distribution of atmospheric aerosols and their source identification using factor analysis in Bombay, India. **Atmospheric Environment**, 26B(1): 135-140.

Sharma, H., Jain, V.K. and Khan, Z.H. (2007) Characterization and source identification of polycyclic aromatic hydrocarbons (PAHs) in the urban environment of Delhi. **Chemosphere**, 66: 302-310.

Sharma, S.K., Mandal, T.K., Saxena, M., Rohtash, R., Sharma, A. and Gautam, R. (2013) Source apportionment of PM10 by using positive matrix factorization at an urban site of Delhi, India. **Urban Climate**, doi: http://dx.doi.org/10.1016/j.uclim.2013.11.002.

Sheesley, R.J., Schauer, J.J., Zheng, M. and Wang, B. (2007). Sensitivity of molecular marker-based CMB models to biomass burning source profiles. **Atmospheric Environment**, 41: 9050-9063.

Shi, J.P. and Harrison, R.M. (1999) Investigation of ultrafine particle formation during diesel exhaust dilution. **Environmental Science and Technology**, 31: 3730-3736.

Shi, Z., Woodhouse, M.T., Carslaw, K.S., Krom, M.D., Mann, G.W., Baker, A.R., Savov, I., Fones, G.R., Brooks, B., Drake, N., Jickells, T.D. and Benning, L.G. (2011) Minor effect of physical size sorting on iron solubility of transported mineral dust. **Atmospheric Chemistry and Physics**, 11: 8459-8469.

Shrivastava, M.K., Subramanian, R., Rogge, W.F. and Robinson, A.L. (2007) Sources of organic aerosol: Positive matrix factorization of molecular marker data and comparison of results from different source apportionment models. **Atmospheric Environment**, 41: 9353-9369.

Simoneit, B.R.T. (2002) Biomass burning-a review of organic tracers for smoke from incomplete combustion. **Applied Geochemistry**, 17: 129-162.

Simoneit, B.R.T., Elias, V.O., Kobayashi, M., Kawamura, M., Rushdi, A.I., Medeiros, P.M., Rogge, W.F. and Didyk, B.M. (2004a) Sugars- Dominant water-soluble organic compounds in soils and characterisation as tracers in atmospheric particulate matter. **Environmental Science and Technology**, 38: 5939-5949.

Simoneit, B.R.T., Kobayashi, M., Mochida, M., Kawamura, K., Lee, M., Lim, H.-J., Turpin, B.J and Komazaki, Y. (2004b) Composition and major sources of organic compounds of aerosols particulate matter sampled during the ACE-Asia campaign. **Journal of Geophysical Research**, Vol. 109, D19S10, doi: 10.1019/2004JD004598.

Sjodin, A., Ferm, M., Bjork, A., Rahmberg, M., Gudmundsson, A., Swietlickli, E., Johansson, C., Gustafsson, M. and Blomqvist, G. (2010). Wear particles from road traffic: a field, laboratory and modelling study. **IVL Report B1830**. Availabe at: http://www.ivl.se/webdav/files/B-rapporter/B1830.pdf.

Sjorgen, M., Li, H., Rannug, W. and Westerholm, R. (1996) Multivariate analysis of exhaust emissions from heavy-duty diesel fuels. **Environmental Science and Technology**, 30: 38-49.

Slezakova, K., Castro, D., Delerue-Matos, C., Alvim-Ferraz, M.C., Morais, S. and Pereira, M.C. (2013) Impact of vehicular traffic emissions on particulate-bound PAHs: levels and associated health risks. **Atmospheric Research**, 127: 141-147.

Smith, D.J.T. and Harrison, R.M. (1996) Concentrations, trends and vehicle source profile of polynuclear aromatic hydrocarbons in the U.K. atmosphere. **Atmospheric Environment**, 30(14): 2513-2525.

Sodeman, D.A., Toner, S.M. and Prather, K.A. (2005) Determination of single particle mass spectral signatures from light-duty vehicle emissions. **Environmental Science and Technology**, 39: 4569-4580.

Song, Y., Zhang, Y., Xie, S., Zeng, L., Zheng, M., Salmon, L.G., Shao, M. and Slanina, S. (2006) Source apportionment of $PM_{2.5}$ in Beijing by positive matrix factorization. **Atmospheric Environment**, 40: 1526-1537.

Song, F. and Gao, Y. (2011) Size distributions of trace elements associated with ambient particular matter in the affinity of a major highway in the New Jersey–New York metropolitan area. **Atmospheric Environment**, 45(37): 6714-6723.

Spada, N., Bozlaker, A. and Chellam, S. (2012) Multi-elemental characterization of tunnel and road dusts in Houston, Texas using dynamic reaction cell-quadrupole-inductively coupled plasma-mass spectrometry: Evidence for the release of platinum group and anthropogenic metals from motor vehicles. **Analytica Chimica Acta**, 735: 1-8.

Srimuruganandam, B. and Shiva Nagendra, S. M. (2011) Chemical characterization of PM (10) and PM (2.5) mass concentrations emitted by heterogeneous traffic. **Atmospheric Environment**, 45: 3091-3102.

Srinivas, B. and Sarin, M.M. (2014) Brown carbon in atmospheric outflow from the Indo-Gangetic Plain: Mass absorption efficiency and temporal variability. **Atmospheric Environment**, doi: 10.1016/j.atmosenv.2014.03.030.

Srivastava, A. and Jain, V.K. (2007) Size distribution and source identification of total suspended particulate matter and associated heavy metals in the urban atmosphere of Delhi. **Chemosphere**, 68: 579-589.

Staehelin, J., Schlapfer, K., Burgin, T., Steinemann, U., Schneider, S., Brunner, D., Baumle, M., Meier, M., Zahner, C., Keiser, S., Stahel, W. and Keller, C. (1995) Emission factors from road traffic from a tunnel study (Gubrist tunnel, Switzerland). Part I: concept and first results. **Science of the Total Environment**, 169: 141-147.

Stanek, L.W., Sacks, J.D., Dutton, S.J. and Dubois, J.-J. B. (2011) Attributing health effects to apportioned components and sources of particulate matter. **Atmospheric Environment,** 45(32): 5655-5663.

Stechmann, H. and Dannecker, W. (1990) Characterization and source analysis of vehicle-generated aerosols. **Journal of Aerosol Science**, 21(1): S287-S290.

Steenhof, M., Gosens, I., Strak, M., Godri, K.J., Hoek, G., Cassee, F.R., Mudway, I.S., Kelly, F.J., Harrison, R.M., Lebret, E., Brunekreef, B., Janssen, N.A.H. and Pieters, R.H.H. (2011) In vitro toxicity of particulate matter (PM) collected at different sites in the Netherlands is associated with PM composition, size fraction and oxidative potential- the RAPTES project. **Particle and Fibre Toxicology**, 8:26. doi: 10.1186/1743-8977-8-26.

Sternbeck, J., Sjödin, Å. and Andréasson, K. (2002) Metal emissions from road traffic and the influence of resuspension—results from two tunnel studies. **Atmospheric Environment**, 36(30): 4735-4744.

Stone, E.A., Zhou, J., Snyder, D.C., Rutter, A.P., Mieritz, M. and Schauer, J.J. (2009) A comparison of summertime secondary organic aerosol source contributions at contrasting urban locations. **Environmental Science and Technology**, 43: 3448-3454.

Stone, E., Schauer, J.J., Quraishi, T.A. and Mahmood, A. (2010) Chemical characterization and source apportionment of fine and coarse particulate matter in Lahore, Pakistan. **Atmospheric Environment**, 44: 1062-1070.

Subramanian, R., Donahue, N.M., Bernardo-Bricker, A., Rogge, W.F. and Robinson, A.L. (2006) Contribution of motor vehicle emissions to organic carbon and fine particle mass in Pittsburgh, Pennsylvania: Effects of varying source profiles and seasonal trends in ambient marker concentrations. **Atmospheric Environment**, 40: 8002-8019.

Subramanian, R., Donahue, N.M., Bernardo-Bricker, A., Rogge, W.F. and Robinson, A. (2007) Insights into the primary-secondary and regional-local contributions to organic aerosol and $PM_{2.5}$ mass in Pittsburg, Pennsylvania. **Atmospheric Environment**, 41: 7414-7433.

Sudheer, A.K. and Rengarajan, R. (2012) Atmospheric mineral dust and trace metals over urban environment in Western India during winter. **Aerosol and Air Quality Research**, 12: 923- 933.

Sudheer, A.K., Rengarajan, R., Deka, D., Bhushan, R., Singh, S.K. and Aslam, M.Y. (2014) Diurnal and seasonal characteristics of aerosol ionic constituents over an urban location in Western India: Secondary aerosol formation and meteorological influence. **Aerosol and Air Quality Research**, doi: 10.4209/aaqr.2013.09.0288.

Sysalova, J., Sykorova, I., Havelcova, M., Szakova, J., Trejtnarova, H. and Kotlik, B. (2012) Toxicologically important trace elements and organic compounds investigated in size –fractionated urban particulate matter collected near the Prague highway. **Science of the Total Environment**, 437: 127- 136.

Taylor, S.R. and McLennan, S.M. (1995) The geochemical evolution of the continental crust. **Reviews of Geophysics**, 33: 241-265.

Taiwo, A.M., Beddows, D.C.S., Shi, Z. and Harrison, R.M. (2014) Mass and number size distributions of particulate matter components: Comparison of an industrial site and an urban background site. **Science of the Total Environment**, 475: 29-38.

Tanner, P.A., Hoi-Ling, M. and Yu, P.K.N. (2008) Fingerprinting metals in street dust in Beijing, Shanghai and Hong Kong. **Environmental Science and Technology**, 42: 7111-7117.

Tervahattu, H., Kupiainen, K.J., Raisanen, M., Makela, T. and Hillamo, R. (2006) Generation of urban road dust from anti-skid and asphalt concrete aggregates. **Journal of Hazardous Materials**, 132: 39-46.

Thorpe, A.J., Harrison, R.M., Boulter, P.G. and McCrae, I.S. (2007) Estimation of particle resuspension source strength on a major London Road. **Atmospheric Environment**, 41: 8007-8020.

Thorpe, A. and Harrison, R.M. (2008) Sources and properties of non-exhaust particulate matter from road traffic: a review. **Science of the Total Environment**, 400(1-3): 270-282.

Thurston, G.D. and Lioy, P.J. (1987) Receptor modelling and aerosol transport. **Atmospheric Environment**, 21: 687-698.

Tiwari, S., Srivastava, A.K., Bisht, D.S., Bano, T., Singh, S., Behura, S., Srivastava, M.K., Chate, D.M. and Padmanabhamurthy, B. (2009) Black carbon and chemical characteristics of PM_{10} and $PM_{2.5}$ at an urban site of North India. **Journal of Atmospheric Chemistry**, 62: 193- 209.

Tiwari, S., Pervez, S., Perrino, C., Bisht, D.S., Srivastava, A.K. and Chate, D. (2013) Chemical characterization of atmospheric particulate matter in Delhi, India, Part II: source apportionment studies using PMF 3.0. **Atmospheric Research**, 145-146: 45-56.

Tiwari, S., Bisht, D.S., Srivastava, A.K., Pipal, A.S., Taneja, A., Srivastava, M.K. and Attri, S.D. (2014) Variability in atmospheric particulates and meteorological effects on their mass concentrations over Delhi, India. **Atmospheric Research**, 145-146: 45-56.

Trivedi, D.K., Ali, K. and Beig, G. (2013) Impact of meteorological parameters on the development of fine and coarse particles over Delhi. **Science of The Total Environment**, 478: 175-183.

Turpin, B. & Huntzicker, J.J. (1995) Identification of secondary organic aerosol episodes and quantification of primary and secondary organic aerosol concentrations during SCAQS. **Atmospheric Environment**, 29(23): 3527-3544.

USEPA (1997) Chemical mass balance receptor model version 8(CMB8), User manual, Research Triangle Park, NC, Desert Research Institute, Reno, NV.

USEPA SPECIATE 4.3 Database. Available at http://cfpub.epa.gov/si/speciate/

Valavadinis, A., Fiotakis, K. and Vlachogianni, T. (2008) Airborne particulate matter and human health: toxicological assessment and important of size and composition of particles for oxidative damage and carcinogenic mechanism. **Journal of Environmental Science and Health Part C**, 26: 339-362.

Varrica, D., Bardelli, F., Dongarra, G. and Tamburro, E. (2012) Speciation of Sb in airborne particulate matter, vehicle brake linings and brake pad wear residues. **Atmospheric Environment**, 64: 18-24.

Venkataraman, C. and Friedlander, S.K. (1994) Source resolution of fine particulate polycyclic aromatic hydrocarbons using a receptor model modified for reactivity. **Journal of Air and Waste Management Association**, 44: 1103-1108.

Venkataraman, C., Konda Reddy, C., Josson, S. and Shekar Reddy, M. (2002) Aerosol size and chemical characteristics at Mumbai, India during the INDONEX-IFP (1999). **Atmospheric Environment**, 36: 1979-1991.

Viana, M., Chi, X., Maenhaut, W., Cafmeyer, J., Querol, X., Alastuey, A., Mikuška, P. and Večeřa, Z. (2006) Influence of sampling artefacts on measured PM, OC and EC levels in carbonaceous aerosols in an urban area. **Aerosol Science and Technology**,40(2): 107-117.

Viana, M., Kuhlbusch, T.A.J., Querol, X., Alastuey, A., Harrison, R.M., Hopke, P.K., Winiwarter, W., Vallius, M., Szidat, S., Prevot, A.S.H., Hueglin, C., Bloemen, H., Wahlin, P., Vecchi, R., Miranda, A.I., Kasper-Giebl, A., Maenhaut, W. and Hitzenberger, R. (2008) Source apportionment of particulate matter in Europe: A review of methods and results. **Journal of Aerosol Science**, 39: 827-849.

Viana, M., Amato, F., Alastuey, A., Querol, X., Moreno, T., Dos Santos, S.G., Herce, M.D. and Fernandez-Patier, R. (2009) Chemical tracers of particulate emissions from commercial shipping. **Environmental Science and Technology**,43(19): 7472-7477.

Wahlin, P., Berkowicz, R. and Palmgren, F. (2006) Characterisation of traffic-generated particulate matter in Copenhagen. **Atmospheric Environment**, 40(12): 2151-2159.

Wang, F., Ketzel, M., Ellermann, T., Wahlin, P., Jensen, S.S., Fang, D. and Massling, A. (2010) Particle number, particle mass and NOx emission factors at a highway and an urban steet in Copenhagen. **Atmospheric Chemistry and Physics**, 10: 2745-2764.

Wang, W., Huang, M.-J., Kang, Y., Wang, H.-S., Leung, A.O.W., Cheung, K.C. and Wong, M.H. (2011) Polycyclic aromatic hydrocarbons (PAHs) in urban surface dust of Guangzhou, China: Status, sources and human health risk assessment. **Science of the Total Environment**, 409: 4519-4527.

Watson, J.G., Chow, J.C., Lowenthal, D.H., Pritchett, L.C., Frazier, C.A., Neuroth, G.R. and Robbins, R. (1994) Differences in the carbon composition of source profiles for diesel- and gasoline- powered vehicles. **Atmospheric Environment**, 28(15): 2493-2505.

Watson, J.G., Fujita, E.M., Chow, J.C. and Zielinska, B. (1998) **Northern Front Range Air Quality Study: Final Report and Supplemental Volumes. Desert Research Institute**. Available at http://www.dri.edu/images/stories/editors/eafeditor/Watsonetal1998NFRAQSFinal.pdf [Accessed 16 September 2012].

Watson, J.G. (2002) Visibility: Science and Regulation. **Journal of Air and Waste Management Association**, 52: 628-713.

Watson, J.G., Zhu, T., Chow, J.C., Engelbrecht, J., Fujita, E.M. and Wilson, W.E. (2002) Receptor modeling application framework for particle source apportionment. **Chemosphere**, 49(9): 1093-1136.

Watson, J.G. and Chow, J.C. (2007) **Receptor models for source apportionment of suspended particles**.In Introduction to Environmental Forensics, 2nd Edition, 2, B. Murphy and R. Morrison (Eds.), Academic Press, New York, NY, 279-316.

Watson, J.G., Chen, L.-W. A., Chow, J.C., Doraiswamy, P. and Lowenthal, D.H. (2008) Source Apportionment: Findings from the U.S. Supersites Program. **Journal of Air and Waste Management Association**, 58: 265-288.

Watson, J.G., Chow, J.C., Wang, X.L., Kohl, S.D., Chen, L.W.A. and Etyemezian, V. (2012) **Overview of real-world emission characterization methods**. In Alberta Oil Sands: Energy, Industry, and the Environment, Percy, K. E., Ed.; Elsevier Press: Amsterdam, The Netherlands, 145-170.

Wei, B., Jiang, F., Li, X. and Mu, S. (2009) Spatial distribution and contamination assessment of heavy metals in urban road dusts from Urumqi, NW China. **Microchemical Journal***,* 93:147-152.

Wei, B. and Yang, L. (2010) A review of heavy metal contaminations in urban soils, urban road dusts and agricultural soils from China. **Microchemical Journal***,* 94: 99-107.

Weingartner, E., Keller, C., Stahel, W.A., Burtscher, H. and Baltensperger, U. (1997) Aerosol emission in a road tunnel. **Atmospheric Environment**, 31(3): 451-462.

Werkenthin, M., Kluge, B. and Wessolek, G. (2014) Metals in European roadside soils and soil solution- A review. **Environmental Pollution**,189: 98-110.

Wik, A. and Dave, G. (2009) Occurrence and effects of tire wear particles in the environment-a critical review and an initial risk assessment. **Environmental Pollution**, 157(1): 1-11.

Wingfors, H., Sjödin, A., Haglund, P. and Brorström-Lundén, U. (1997) Characteristics and determination of profiles of polycyclic aromatic hydrocarbons in a traffic tunnel in Gothenburg, Sweden. **Atmospheric Environment**, 35: 63611-6369.

Wongphatarakul, V., Friedlander, S.K. and Pinto, J.P. (1998) A comparative study of $PM_{2.5}$ ambient aerosol chemical databases. **Environmental Science and Technology**, 32: 3926-3934.

Yadav, S. and Rajamani, V. (2006) Air quality and trace metal chemistry of different size fractions of aerosols in N-NW India- implications for source diversity, India. **Atmospheric Environment**, 40: 698-712.

Yadav, S., Tandon, A. and Attri, A.K. (2013) Characterization of aerosol associated non-polar organic compounds using TD-GC-MS: A four year study from Delhi, India. **Journal of Hazardous Materials**, 252-253: 29-44.

Yan, B., Zheng, M., Hu, Y., Ding, X., Sullivan, A.P., Weber, R.J., Baek, J., Edgerton, E.S. and Russell, A.G. (2009) Roadside, Urban, and Rural Comparison of Primary and Secondary Organic Molecular Markers in Ambient $PM_{2.5}$. **Environmental Science and Technology**, 43(12): 4287-4293.

Yanowitz, J., McCormick, R.L. and Graboski, M.S. (2000) In-use emissions from heavy-duty diesel vehicles. **Environmental Science and Technology**, 34(5): 729-740.

Yanosky, J.D. Tonne, C.C., Beevers, S.D., Wilkinson, P. and Kelly, F.J. (2012) Modelling exposures to oxidative potential of PM_{10}. **Environmental Science and Technology**, 46(14): 7612-7620.

Yin, J., Harrison, R.M., Chen, Q., Rutter, A. and Schauer, J.J. (2010) Source apportionment of fine particles at urban background and rural sites in the UK atmosphere. **Atmospheric Environment**, 44: 841-851.

Zanini, G., Berico, M., Monforti, F., Vitali, L., Zambonelli, S., Chiavarini, S., Georgiadis, T. and Nardino, M. (2006) Concentration measurement in a road tunnel as a method to assess "real-world" vehicles exhaust emissions. **Atmospheric Environment**, 42: 1242-1254.

Zhang, Y.X., Schauer, J.J., Zhang, Y.H., Zeng, L., Wei, Y., Liu, Y. and Shao, M. (2008) Characterisitcs of particulate carbon emissions from real world Chinese coal combustion. **Environmental Science and Technology**, 42: 5068-5073.

Zhu, Y., Kuhn, T., Mayo, P. and Hinds, W.C. (2006) Comparison of daytime and nighttime concentration profiles and size distributions of ultrafine particles near a major highway. **Environmental Science and Technology**, 40:2531-2536.

LIST OF RESEARCH PAPERS AND PRESENTATIONS

Peer-reviewed Articles

[1] Pant, P., Baker, S.J., Shukla, S., Godri Pollitt, K.J. and Harrison, R.M. PM_{10} road dust in India and UK: Characterization, source profiles and health risks. **Environmental Pollution** [*in preparation*, invited for a special edition of Environmental Pollution based on UEP 2014]

[2] Guttikunda, S., Goel, R. and **Pant, P.** (2014) Nature of Air Pollution, Emission Sources, and Management in the Indian cities. **Atmospheric Environment,** 95: 501-510**.**

[3] **Pant, P.**, Yin, J. and Harrison, R.M. (2014) Sensitivity of a Chemical Mass Balance Model to Different Molecular Marker Traffic Source Profiles. **Atmospheric Environment**, 82: 238-249.

[4] **Pant, P.** and Harrison, R.M. (2013) Estimation of the Contribution of Road Traffic Emissions to Particulate Matter Concentrations from Field Measurements: A Review. **Atmospheric Environment**, 77: 78-97.

[5] **Pant, P.** and Harrison, R.M. (2012) Critical review of receptor modelling for particulate matter: A case study of India. **Atmospheric Environment**, 49: 1-12.

Conference Papers

[1] **Pant, P.,** Baker, S.J., Shukla, A. and Harrison, R.M. (2014) Road dust (PM_{10} fraction) source profiles for India and UK. In: *UEP 2014*. Toronto, Canada, 12-15 June, 2014. **(Poster Presentation)**

[2] **Pant, P.,** Baker, S.J., Goel, R., Guttikunda, S., Goel, A., Shukla, A. and Harrison, R.M. (2014) Particulate matter size distributions: A case study of Delhi, India. In: *UEP 2014*. Toronto, Canada, 12-15 June, 2014. **(Poster Presentation)**

[3] **Pant, P.,** Yin, J. and Harrison, R.M. (2013) Performance of the Chemical Mass Balance Model with Various Traffic Profiles. In: *AAAR 2013*. Portland, Oregon, USA, 30 September-04 October, 2013. **(Oral Presentation)**

[4] **Pant, P.,** Yin, J. and Harrison, R.M. (2013) Performance of the Chemical Mass Balance Model with Various Traffic Profiles. In: *European Aerosol Conference 2013*. Prague, Czech Republic, 01-06 September, 2013. **(Oral Presentation)**

[5] **Pant, P.,** Baker, S.J. and Harrison, R.M. (2013) Estimation of Non-Exhaust Emissions in PM10 Road Dust. In: *European Aerosol Conference 2013*. Prague, Czech Republic, 01-06 September, 2013. **(Poster Presentation)**

[6] **Pant, P.,** Yin, J. and Harrison, R.M. (2013) Performance of the Chemical Mass Balance Model with Different Molecular Marker Traffic Profiles. In: *2013 Annual UK Review Meeting on Outdoor and Indoor Air Pollution Research*. Cranfield, UK, 23-24 April, 2013. **(Poster Presentation)**

[7] **Pant, P.** and Harrison, R.M. (2012) Assessment of vehicular profiles of organic molecular markers vis-à-vis real world traffic emissions. In: *European Aerosol Conference.* Granada, Spain, 2-7 September, 2012. **(Poster Presentation)**

[8] **Pant, P.** and Harrison, R.M. (2012) Particulate Matter Receptor Modelling in India: A Critical Review. In: *Better Air Quality Conference*. Hong Kong, 5-7 December, 2012. **(Poster Presentation)**

[9] **Pant, P.** and Harrison, R.M. (2012) Assessment of vehicular profiles of organic molecular markers vis-à-vis real world traffic emissions. In: *ECG Atmospheric & Environmental Chemistry Forum 2012*. Leicester, UK, 25 June, 2012. **(Poster Presentation)**

[10] **Pant, P.**, and Harrison, R.M. (2011) Source apportionment using receptor modelling for PM_{10} in New Delhi, India. In: *From Exposure to Health Effects: Novel Approaches to find the Linkage*. Birmingham, United Kingdom, 17 May, 2011. **(Poster Presentation)**